The Role of SOX9 in Neural Progenitor Identity

Adam Charles Nunn

A thesis submitted to University College London in fulfilment of the requirements for the degree of Doctor of Philosophy.

September 2012

Division of Stem Cell Biology and Developmental Genetics

National Institute for Medical Research

The Ridgeway

Mill Hill, London NW7 1AA

Declaration

I, Adam Charles Nunn, confirm that the work presented in this thesis is my own. Where information has been derived from other sources, I confirm that this has been indicated in the thesis.

.....

Abstract

Recent evidence has shown that SOX9 is required for the proliferation and multipotentiality of neural progenitors in the developing CNS. Notably, these findings suggest that in contrast to previous studies, SOX9 is important for differentiation along the neuronal lineage, both in the adult and embryonic CNS. Here, a phenotypic analysis of the CNS-specific *Sox9*-null forebrain, including detailed analysis of cortical lamination, shows that neurons of the appropriate layer-identity are born and migrate to their destined layers. All other parameters in this analysis were normal, with the exception of the formation of glia from the ventral and dorsal telencephalons, and midline glial structures, which were absent in the mutant. Since *Sox9* is expressed long before the onset of gliogenesis in these brain regions, the possibility that *Sox9* may 'prime' the progenitors of the ventricular zone to respond to a gliogenic signal arose. To investigate this, populations of *Sox9*-deficient and wild-type dorsal telencephalon cells were enriched for progenitors and subjected to transcriptional profiling. Bioinformatic analysis revealed that 'vascular endothelial growth factor' receptors, which are important for gliogenesis, were down-regulated, in addition to two transcription factors. Previously, *Sox9*-deficient neural progenitors have been shown to generate neurospheres poorly, and so the dataset of potential targets was used to identify candidates that might mediate this reduced neurosphere-forming ability. Thirteen down-regulated targets were confirmed by qPCR, six of which were expressed in the same distribution as *Sox9* in the embryonic telencephalon; three were also expressed in neurosphere cultures. Of these, one encoded a K^+ channel (Kir4.1), and the other a modulator of the $GABA_A$ channel (DBI). In order to show that reduced expression of one of these might contribute to the *Sox9*-deficient neurosphere phenotype, pharmacological modulators were used and showed that blockade

of Kir4.1 or enhancement of $GABA_A$ channels mimicked the effect of *Sox9* loss, leaving open the possibility that Kir4.1 or DBI expression might mediate this effect.

Table of Contents

CHAPTER 1 GENERAL INTRODUCTION 19

Process of Neural Development 19

The Gliogenic 'Switch' 22

Adult Neurogenesis 23

Sox9 and *Sox* Transcription Factors 24

Multiple Developmental Roles of *Sox9* 25

Campomelic Dysplasia 26

The Role of *Sox9* in Gliogenesis 27

Sox Genes and the Progenitor State 28

The Role of SOX9 in Progenitor Identity 29

SOX9 and Neural Stem Cells 33

Functional Redundancy within the *SoxE* Group 36

SOX Proteins Tend to Bind DNA in Complexes 37

SOX Transcription Factors As Architectural Proteins 39

Background and Aims of Thesis 41

CHAPTER 2 MATERIALS AND METHODS 44

Deletion of *Sox9* in the CNS 44

Genotyping 44

Histology 45

Immunohistochemistry 45

In Situ Hybridisation 46

Obtaining RNA from FAC Sorted Cells 47

RNA-Seq 48

Affymetrix Arrays 49

Bioinformatics 49

Quantitative PCR 50

Reverse Transcription (RT)-PCR 52

Neurosphere Assay 54

CHAPTER 3 THE ROLE OF *SOX9* IN THE *IN VIVO* DEVELOPMENT OF THE FOREBRAIN 56

Introduction 58

Formation of the Embryonic Brain 58

Progenitors in the Developing CNS 58

Corticogenesis 60

Interneurons 61

Oligodendrogenesis 62

Results 66

Survival of $Sox9^{\Delta/\Delta}$ Pups 67

SOX9 Expression in the Forebrain 69

Embryonic Analysis 71

Early Neurogenesis 75

Corticogenesis 78

Generation of Interneurons in $Sox9^{\Delta/\Delta}$ Embryos 81

Formation of OPCs in *Sox9*$^{\Delta/\Delta}$ Embryos....83

Discussion....86

CHAPTER 4 TRANSCRIPTIONAL TARGETS OF SOX9 IN THE NEURAL PROGENITORS OF THE DORSAL TELENCEPHALON....89

Introduction....90

Enriching a Population of NPCs....90

Transcriptional Profiling....91

DNA Microarrays....92

Second-Generation Sequencing....93

cDNA Normalisation....95

Bridge Amplification....97

Alignment and Analysis....98

Results....100

RNA-Seq....103

Microarray....106

Gene Ontology Categories....108

Down-Regulated Gene Lists....110

KEGG Pathway Analysis....113

Up-Regulated Gene Lists....116

Discussion....121

CHAPTER 5 IDENTIFYING CANDIDATE SOX9 PRIMARY TARGETS....124

Introduction....125

Neurosphere Assay....125

Results **126**

Generating Candidate Lists 126

Validation of Candidates by qPCR 129

Spatial Expression Patterns of Candidates at Mid-Neurogenesis by *In Situ* Hybridisation 132

Expression of Candidate Genes in Neurospheres 140

Discussion **142**

Hopx and *Tnfrsf19* May Mediate the Failure of Midline Glial Populations to Form in *Sox9*$^{\Delta/\Delta}$ Embryos 143

CHAPTER 6 KCNJ10 AS A CANDIDATE SOX9 TARGET INVOLVED IN MEDIATING THE IMPAIRED NEUROSPHERE-FORMING ABILITY OF *SOX9*$^{\Delta/\Delta}$ NEURAL PROGENITORS **147**

Introduction **148**

The Resting Membrane Potential 148

Potassium Channels 149

Kcnj10 150

Kir Channels and Their Role in Glia 151

A Role for K^+ Channels in Neural Progenitors? 152

Kir Channels and the Neural Stem Cells of the Adult SVZ 153

A Potential Role for K^+ Channels in the Maturation of Oligodendrocytes 154

Results **156**

Expression of Kir Subunits in CD133^{High} Cells 158

The Effect of Kir Channel Blockade on the Proliferation of NPCs 160

Discussion **166**

Effect of Ba^{2+} and Fluoxetine on NPC Differentiation 168

A Role for *Kcnj10* in Establishing the Conditions for Gliogenesis? 168

Further Work 169

CHAPTER 7 DBI AS A CANDIDATE SOX9 TARGET INVOLVED IN MEDIATING THE IMPAIRED NEUROSPHERE-FORMING ABILITY OF *SOX9*$^{\Delta/\Delta}$ NEURAL PROGENITORS **170**

Introduction **171**

GABA and the $GABA_A$ Receptor 171

GABA Signalling in CNS development 172

How Might GABA Affect the Proliferation of NPCs? 173

Diazepam-Binding Inhibitor 175

Results **177**

Rescue 181

Discussion **182**

$GABA_A$ or $GABA_C$? 184

Potential SOX9 Binding Partners? 184

Further Work 185

CHAPTER 8 GENERAL DISCUSSION **186**

Transcriptional Profiling 189

Candidate Downstream Targets of SOX9 190

Functional Studies 191

APPENDIX A **194**

APPENDIX B 206

REFERENCES 214

Table of Figures

Figure 3-1 Diagram depicting strategy used to delete *Sox9* specifically within the CNS. 57

Figure 3-2 SOX9 immunostaining on $Sox9^{F/F}$ and $Sox9^{F/F}$;NesCre embryonic brains. 66

Figure 3-3 Survival of $Sox9^{\Delta/\Delta}$ pups at P2 and at weaning (~4 weeks of age). 68

Figure 3-4 Luxol fast blue staining of the brain of a surviving $Sox9^{\Delta/\Delta}$ adult and a wild-type littermate (P63). 68

Figure 3-5 SOX9 expression (by immunohistochemistry) at E12.5, E14.5 and E18.5. 70

Figure 3-6 A. H&E-stained sections of the anterior cortex of E18.5 embryos. CC = corpus callosum; AC = anterior commissure; HC = hippocampal commissure; BoP = bundle of Probst. B. Number of times a given commissure is present in a given number of brains of each genotype.....72

Figure 3-7 A. Midline glial populations in the $Sox9^{\Delta/\Delta}$ at E17.5 and E18.5. B. The 'glial' sling fails to form in the $Sox9^{\Delta/\Delta}$ (E17.5). IG = indusium griseum, MZG = midline zipper glia, SS = subcallosal sling. 74

Figure 3-8 A. The distribution of $PAX6^{+}$ cortical radial glia is similar between $Sox9^{\Delta/\Delta}$ and wild-type littermates at E12.5 and E14.5. B. The initial phase of neurogenesis, formation of the preplate, is normal in the $Sox9^{\Delta/\Delta}$.....76

Figure 3-9 A. Immunostaining for INSM1, which is a marker of intermediate progenitor cells (IPCs), at E12.5, E14.5 and E18.5. B. Percentage of $DAPI^{+}$ cells that are also $INSM^{+}$ at these three stages of development.....77

Figure 3-10 Immunohistochemistry showing the distribution of three antigens, each marking a particular subset of cortical plate layers. The ventricular zone is to the right of each image, and the pial surface to the left.....79

Figure 3-11 Binning on immunostainings for three markers of different cortical layers, BRN2 (marks layers II-IV of the future cortex), CTIP2 (marks layers V and VI) and

TBR1 (marks layer VI only). The bars represent the percentage of the total number of marker-positive cells in a radial segment of dorsal telencephalon that reside within the each bin, where Bin 1 is closest to the pial surface, and Bin 9 to the ventricular surface. 80

Figure 3-12 A. In situs showing the distribution of *Lhx6* transcripts at E12.5 and E14.5. B. In situs showing the distribution of another marker of interneuons (*Isl1*) at E12.5. 82

Figure 3-13 Oligodendrocyte progenitors (OPCs) in the ventral telencephalon at E12.5. 84

Figure 3-14 Fewer oligodendrocyte progenitor cells (OPCs) are found in the cortex of $Sox9^{\Delta/\Delta}$ brains versus wild-type littermates at P5. 85

Figure 4-1 CD133/SOX9 immunohistochemistry on sections of the E16.5 forebrain from $Sox9^{\Delta/\Delta}$ and wild-type littermates. All images are at 240X, except B and E, which are magnifications of A and D, respectively (at 1200X). VZ – ventricular zone, SVZ – subventricular zone, IZ – intermediate zone, CP – cortical plate. 101

Figure 4-2 FACS plots of CD133-PE- and unstained populations. 102

Figure 4-3 Alignment of reads from the sequencing of RNA extracted from $CD133^{High}$ cells to the *Sox9* locus in the $Sox9^{\Delta/\Delta}$ and wild-type situation. 105

Figure 4-4 Volcano plots for RNA-Seq (A) and microarray data (B). 107

Figure 4-5 The different Gene Ontology categories into which the genes of each gene list fall. 109

Figure 4-6 GO Term Enrichment Analysis (restricted to Molecular Function categories) on RNA-Seq Down-Regulated dataset (p-value ≤ 0.05, fold change ≥ 2 [66 genes]), using Entrez genes as a background list. Statistical test: Hypergeometric. Multiple-testing correction: Benjamini-Hochberg. Cut-off: Adjusted p-value < 0.05. 112

Figure 4-7 GO Term Enrichment Analysis on the 'Microarray Down-Regulated' dataset (p-value ≤ 0.05, fold change ≥ 1.35 [26 genes]), using the genes represented by a probe set on the Affymetrix 430 2.0 GeneChip as a background list. Statistical test:

Hypergeometric. Multiple-testing correction: Benjamini-Hochberg. Cut-off: Adjusted p-value<0.05. 114
Figure 4-8 KEGG pathways that are enriched in RNA-Seq Down-Regulated dataset (p-value < 0.05, fold change ≥ 1.4 [106 genes]), using Entrez genes as a background list. Statistical test: Hypergeometric. Multiple-testing correction: Benjamini-Hochberg. Cut-off: Adjusted p-value ≤ 0.1. 115
Figure 4-9 KEGG pathways that are enriched in Microarray Down-Regulated dataset (p-value < 0.05, fold change ≥ 1.25 [67 genes]), using the gene recognised by probe sets on the Affy GeneChip 430 2.0 array as a background list. Statistical test: Hypergeometric. Multiple-testing correction: Benjamini-Hochberg. Cut-off: Adjusted p-value ≤ 0.1. 115
Figure 4-10 GO Term Enrichment Analysis on RNA-Seq Up-Regulated dataset (p-value ≤ 0.05, fold change ≥ 2.5 [81 genes]), using Entrez genes as a background list. Statistical test: Hypergeometric. Multiple-testing correction: Benjamini-Hochberg. Cut-off: Adjusted p-value < 0.1. Categories represented by fewer than 3 genes in the gene set were ignored. 118
Figure 4-11 GO Term Enrichment Analysis on the 'Microarray Up-Regulated' dataset (p-value ≤ 0.05, fold change ≥ 1.25 [89 genes]) , using the gene represented by a probe set on the Affymetrix 430 2.0 GeneChip as a background list. Statistical test: Hypergeometric. Multiple-testing correction: Benjamini-Hochberg. Cut-off: Adjusted p-value < 0.05. Minimum: 3. 119
Figure 4-12 The members of two GO term categories enriched in our Microarray Up-Regulated dataset. 120
Figure 5-1 A – Venn diagrams showing the overlap between the RNA-Seq and microarray datasets at a variety of p-value cut-off levels (α). B – Correlation between the fold change derived from the RNA-Seq and microarrays for i) the up-regulated genes and ii) the down-regulated genes. 128

Figure 5-2 qPCR expression data for Common Down-Regulated dataset (A), Common Up-Regulated dataset (B) and *Sox9* (C). 131

Figure 5-3 Number of SOX9 binding sites identified by ChIP-Seq within 20kb of the transcriptional start sites of the candidate targets. 131

Figure 5-4 The expression patterns (by *in situ* hybridisation) of those candidates whose dominant expression was deemed to be in the subventricular zone of the dorsal telencephalon. 137

Figure 5-5 Expression (by *in situ* hybridisation) of *Hopx* (A) and *Tnfrsf19* (B). 138

Figure 5-6 Expression (by *in situ* hybridisation) of *Rlbp1*. 138

Figure 5-7 The expression patterns (by *in situ* hybridisation) of those candidates that appear to be expressed specifically within the VZ of the developing telencephalon. A *Sox9 in situ* is included for comparison. 139

Figure 5-8 The expression pattern (by *in situ* hybridisation) of *5830403L16Rik*. 140

Figure 5-9 The expression (by RT-PCR) of *Kcnj10*, *Dbi*, *Arhgef3* and *AI646023* in neurosphere cultures and embryonic brains (E14.5). 141

Figure 6-1 Both of the SOX9 binding sites in the first intron of the *Kcnj10* gene are highly conserved across mammalian species. 157

Figure 6-2 Transcription factor binding sites within 40bp of each SOX9 binding site (limited to those transcription factors expressed in the CNS). 157

Figure 6-3 The expression of Kir subunits in $CD133^{High}$ cells from the embryonic VZ. Only those subunits with >1 read aligning per 1kb of CDS were included. 159

Figure 6-4 The effect of Ba^{2+} ion concentration on the rate of neurosphere formation (assayed at 7DIV). 162

Figure 6-5 The effect of fluoxetine concentration on the rate of neurosphere formation (assayed at 9DIV). 162

Figure 6-6 The effect of two inhibitors of Kir currents on the differentiation of neural progenitor cells. Ba^{2+} ions are regarded as a general inhibitor of Kir channels; fluoxetine has been reported to be a specific inhibitor of Kir4.1. The $GABA_A$ channel antagonist, gabazine, was used as a control in this experiment. 165

Figure 7-1 The SOX9 binding site identified by ChIP-Seq is highly conserved across mammalian species. 178

Figure 7-2 Transcription factor binding sites within 40bp of the SOX9 binding site. 178

Figure 7-3 The effect of various concentrations of two antagonists, SR95531 and bicuculline, and one agonist of $GABA_A$ channels, muscimol, on the proliferation of NPCs in the neurosphere assay (N=3)..... 180

Figure 7-4 Potential model illustrating how reduced expression of DBI might contribute to the poor growth rates of *Sox9*-deficient neurospheres. ODN – octadecaneuropeptide. 183

Figure 8-1 Expression of *Sox* genes in wild-type $CD133^{High}$ cells. Those genes with <1 read mapping per kilobase of CDS were omitted. 187

Abbreviations

$[Ca^{2+}]_i$	Intracellular Ca^{2+} concentration
5-HT	Serotonin
ACC	Agenesis of the corpus callosum
AEP	Anterior entopeduncular area
bFGF	Basic fibroblast growth factor
bHLH	Basic helix-loop-helix
BMP	Bone morphogenetic protein
CalM	Calmodulin
CD	Campomelic dysplasia
cDNA	Complementary DNA
CDS	Coding sequence
CGE	Caudal ganglionic eminence
ChIP	Chromatin immunoprecipitation
CP	Cortical plate
DIG	Digoxigenin
DMEM	Dulbecco's modified eagle medium
dNTP	Deoxyribonucleotide triphosphate
DPBS	Dulbecco's phosphate-buffered saline
DSN	Duplex-specific nuclease
EGF	Epidermal growth factor
E_K	Potassium equilibrium potential
EST	Expressed sequence tag
FACS	Fluorescence-activated cell sorting

GABA	Gamma aminobutyric acid
GSEA	Gene set enrichment analyses
HMG	High mobility group
IHC	Immunohistochemistry
IPC	Intermediate progenitor cell
IZ	Intermediate zone
Kir	Inwardly-rectifying K^+
LGE	Lateral ganglionic eminence
MGE	Medial ganglionic eminence
NesCre	Nestin-Cre
NPC	Neural progenitor cell
NSC	Neural stem cell
O-2A	Oligodendrocyte-type-2 astrocyte
OPC	Oligodendrocyte progenitor cell
PBS	Phosphate-buffered saline
PCR	Polymerase chain reaction
PFA	Paraformaldehyde
pH_i	Intracellular pH
qPCR	Quantitative PCR
RMP	Resting membrane potential
RMS	Rostral migratory stream
RNAi	RNA interference
RT-PCR	Reverse transcription-PCR
shRNA	Short hairpin RNA
SSC	Saline-sodium citrate
SVZ	Subventricular zone

TEA	Tetra-ethyl-ammonium
TNF	Tumour necrosis factor
TSS	Transcriptional start sites
TTN	Triakontatetraneuropeptide
UTR	Untranslated region
VEGF	Vascular endothelial growth factor
VZ	Ventricular zone

Chapter 1 General Introduction

Process of Neural Development

The vertebrate brain and spinal cord arise from a neural plate, which is a region of ectoderm (the outer layer of the embryo), that has obtained a neural fate through signalling from the underlying mesoderm layer (Harland, 2000). Once induced, the neural plate folds up and fuses in the midline to give a neural tube (beginning at embryonic day [E] 8.5), and from this structure, all the components of the mature central nervous system (CNS) are laid down over the remaining 10 days of development (Copp et al., 2003). The walls of the neural tube are composed of specialised epithelial cells, called neuroepithelial (or NE) cells, which divide symmetrically (forming two NE cells with each division) for a number of days prior to the onset of differentiative divisions, which give rise to the mature cell types of the CNS, neurons and glia (reviewed in Zhong and Chia, 2008). This 'neuroepithelium' is later termed the ventricular zone (VZ). Neurons are the cells that will eventually convey information in the nervous system through the co-ordinated firing of action potentials, whereas glia are conventionally thought not to be involved in this process, and are divided into two categories, astrocytes and oligodendrocytes. Astrocytes eventually vastly outnumber any other cell type in the mature CNS, and have a variety of functions, including providing physical support and nutrition to neurons, as well as buffering of substances that would otherwise interfere with the proper functioning of neuronal circuits, such as potassium ions (Kandel et al., 2000). They also form the blood-brain barrier that protects the brain from potentially toxic substances in the blood. Oligodendrocytes are responsible for the laying down of an insulating substance, myelin, on the axons of neurons, which allow fast, 'saltatory' conduction through the setting up of

circuits that ‘jump’ between gaps in the myelin sheath, called the nodes of Ranvier (Kandel et al., 2000).

Following a period of symmetrical division during which the total surface area of the neuroepithelium expands, most prominently at the rostral end, which will become the brain, various ‘hinge points’ develop that define the mid- and forebrain. At the onset of neurogenesis, the neuroepithelium begins to undergo asymmetrical divisions that give rise to a progenitor and a lineage-committed cell, in this case, a neuron. At the onset of ‘asymmetrical’ divisions, the metaphase plate is no longer perpendicular to the plane of the neuroepithelium, resulting in a neuronal-lineage committed cell, which is destined to migrate and differentiate (Zhong and Chia, 2008). This transition from symmetrical to asymmetrical division is thought to result in daughter cells inheriting less of a protein (such as the suppressor of Notch signalling ‘Numb’) that resides on the apical side of the original mother cell, prompting its differentiation along a neuronal lineage. Following this, direct cell-to-cell signalling, such as Notch signalling, where cell-surface ligands on one daughter cell stimulate Notch receptors on the other, reinforces differences between the cells. Alongside this transition from symmetrical to asymmetrical division, the neuroepithelial cells also begin to adopt a number of characteristics suggestive of a glial identity, such as cytoplasmic glycogen granules (Choi and Lapham, 1978), and expression of Brain Lipid-Binding Protein (Feng et al., 1994), the glutamate transporter, GLAST (Shibata et al., 1997), and Tenascin (Yuasa, 2001). The adoption of these markers signifies the transformation of NE cells into radial glia, which occurs at the onset of neurogenesis (Doetsch, 2003).

It was initially thought that radial glia, with their vast projections extending from the apical to the basal sides of the ventricular wall, simply provided a scaffold over which

newly-formed neurons could migrate; however, work in the late 1980s challenged this dogma, and genetic lineage tracing has put the progenitor status of radial glia beyond doubt (Misson et al., 1988, Malatesta et al., 2003, Anthony et al., 2004). This was demonstrated with a system involving a 'Cre recombinase', which is an enzyme capable of excising the intervening DNA between two 'LoxP' sites. The gene encoding Cre recombinase was placed under the control of the regulatory region of a gene normally expressed in radial glia, and the LoxP sites flanked a STOP cassette in a reporter transgene, such that when the Cre was expressed (specifically in the radial glia), the STOP cassette was excised and all future progeny expressed the reporter, in this case, green fluorescent protein (GFP). The result was that all the cells of the mature CNS were shown to be GFP^+, and hence had originated from radial glia (Anthony et al., 2004).

Aside from radial glia, recent work has shown that neurons are not the only progenitors in the CNS. In the context of the dorsal telencephalon, the result of an asymmetrical division of a neural progenitor was thought to always be one neuron and one radial glial cell. However, elegant retroviral lineage tracing studies have shown that a different type of asymmetrical division commonly occurs from the peak of neurogenesis, where a transit-amplifying cell is formed instead of a neuron, and this cell, termed an intermediate progenitor cell (IPC), then migrates to a second progenitor layer, overlying the VZ, called the subventricular zone (SVZ; Noctor et al., 2004). These IPCs usually divide only once to give rise to two neurons, but have been shown occasionally to generate pairs of progenitors (Noctor et al., 2004). It has been suggested that the development of IPCs produced an amplification step essential for the expansion of cortical surface area throughout mammalian evolution (Pontious et al., 2008). This is underlined by the human phenotype that results from homozygous loss of genes important for IPC generation (such as *PAX6* or *TBR2*), which produces microcephaly (a small brain), polymicrogyria (an

increased number of small gyri) and cortical thinning (Glaser et al., 1994, Baala et al., 2007).

Following the onset of neurogenesis in the dorsal telencephalon, the layers of the future cortex are laid down by divisions of both radial glial cells and IPCs. An initial wave of neurogenesis, occurring at around E11.5, generates neurons that migrate to form the preplate, a layer just superficial to the VZ, then a later wave, at ~E12.5, produces the first layer of the cortical plate (the future cortex), splitting the preplate into a deep 'subplate' and a superficial 'marginal zone'. Subsequent waves of neurogenesis generate cohorts of neurons that migrate along the basal endfeet of the radial glia, past the preceding layer of the cortical plate, to establish the next most superficial layer; in this way, the cortex is often describe as being formed in an 'inside-out' fashion (reviewed in Gupta et al., 2002). The final cortex is a six-layered structure.

The Gliogenic 'Switch'

It is a general principle in the developing CNS that neurogenesis (the production of neurons from radial glia) precedes gliogenesis (the production of glia). A good example of this is the ventral half of the developing spinal cord. The VZ of the spinal cord (the region where progenitors reside) is divided into discrete domains by the expression of homeodomain transcription factors in the dorso-ventral axis. These domains are initially established by a concentration gradient of a morphogen secreted from the floorplate, Sonic Hedgehog (SHH), and then refined and reinforced by cross-inhibitory effects of the transcription factors induced by this morphogen (reviewed in Briscoe and Ericson, 2001). One of these domains, the pMN domain, produces first motoneurons, and then, at around E14.5, oligodendrocyte precursors (Sun et al., 1998, Lu et al., 2002, Takebayashi et al.,

2002). Astrocytes arise from other parts of the spinal cord, but only after neurons have been produced from these domains (Pringle et al., 2003). The same principle holds true in the dorsal telencephalon, where the neurons of the cortical plate are formed initially, but thereafter, oligodendrocyte precursors are generated, as well as astrocytes (Kessaris et al., 2008).

Adult Neurogenesis

Until very recently, it was believed that once the brain and spinal cord were formed in their entirety, no new neurons were born. Work over the last twenty years challenged this long-held belief, and an important part of this was the finding that neurospheres could be formed from various parts of the adult brain and spinal cord (Reynolds and Weiss, 1992). The neurosphere assay was in fact developed by these authors, and provides a means of retrospectively identifying neural stem cells, by demonstrating that cells are present within a cellular population that have the potential to undergo self-renewing divisions to generate spheres (in the presence of epidermal growth factor and also basic fibroblast growth factor in some protocols), and also to generate all the lineages of the CNS when growth factors are withdrawn. This is achieved by seeding plates of media with the cell population of interest at very low density and seeing if they give rise to spherical aggregates of cells (the 'neurospheres'), and if these aggregates, once dissociated, will generate neurospheres themselves. These neurospheres can also be transferred to an artificial matrix, called *Matrigel*, and allowed to differentiate in media that lacks growth factors, before immunohistochemistry is used to determine what cell types are formed. The major criticism of this method of identifying neural stem cells is that it only demonstrates the potential of cells to proliferate and acquire multipotency, not necessarily that they had these properties *in vivo* (Pastrana et al., 2011). It is also possible that other

transit-amplifying cells, such as oligodendrocyte progenitors, might give rise to neurospheres, but these should not form neurons or astrocytes upon differentiation.

Once it was accepted that neurogenesis did indeed occur within the adult brain, it was initially proposed that it might be the ependymal cells that line the ventricles that had the properties of neural stem cells (Johansson et al., 1999). However, it is now established that it is the subventricular zone $GFAP^+$ cells, known as 'Type B cells' that possess these properties (Doetsch et al., 1999). These are very slowly dividing cells that give rise to transit-amplifying cells, known as 'Type C cells', which go on to form migratory neuroblasts called 'Type A cells'. These Type A cells migrate along the walls of the lateral ventricles through tunnels formed by the processes of Type B cells, and eventually join the rostral migratory stream that leads to the olfactory bulbs, where they differentiate as interneurons (Pastrana et al., 2011).

***Sox9* and *Sox* Transcription Factors**

Sox9 is a member of the family of *Sry*-related box genes (or *Sox* genes), so-called because of the homology they share with the mammalian sex-determination gene, *Sry*, within their high mobility group (HMG) box. Around 20 *Sox* genes have been described to date in mammals, and these have been implicated in diverse processes within development. The common feature of the *Sox* genes is the presence of an HMG box, which is the domain in the proteins they encode that mediates DNA binding (reviewed in Wilson and Koopman, 2002). The HMG box forms an L-shaped complex in the minor groove of DNA, and induces a significant bend in the helix (Ma et al., 1998b). All SOX proteins have been shown to recognise a common binding site (A/T A/T CAA A/T G), and must share at least 50% homology with SRY in their HMG box to be defined as a SOX protein (Denny

et al., 1992, Harley et al., 1994, Pevny and Lovell-Badge, 1997). SOX proteins (and genes) are further categorised on the basis of structural homology outside their HMG boxes, for example, the SOXE family, of which SOX9 is a member (along with SOX8 and SOX10). All SOXE proteins have the same three functional domains, arranged in the same pattern within the protein. At their N-terminus, they have a dimerisation domain and contiguous HMG box, and toward the C-terminus, they have a transactivation domain.

Multiple Developmental Roles of *Sox9*

Sox9 is expressed strongly in a number of tissues during development, such as mesenchyme destined to become cartilage and bone, the gonads, and the CNS, as well as other sites such as the heart and gastrointestinal tract (Ng et al., 1997). During chondrogenesis, *Sox9* is expressed in mesenchymal condensations prior to their differentiation as hyaline cartilage, and it is known to transactivate a number of genes essential for this process, such as *Col2a1* (Bell et al., 1997). During gonadal development, expression of *Sox9* begins at ~E10.5 in cells that have migrated from the coelomic epithelium, and which subsequently differentiate as Sertoli cells (Morais da Silva et al., 1996, Sekido et al., 2004). These cells express SRY for a short period, during which *Sox9* is strongly up-regulated. Recent work has established that *Sox9* is required for the maintenance of Sertoli cell identity, and this may be achieved by the synergistic action of SF1 and SOX9 on a region of the testis-specific regulatory element of *Sox9* (Sekido and Lovell-Badge, 2008). In the CNS, *Sox9* is expressed from E9.5 in the ventricular zone (VZ) of the developing spinal cord, and maintained in astrocytes and oligodendrocyte progenitor cells (OPCs) migrating out of the progenitor zone (Stolt et al., 2003). In the adult brain, SOX9 expression continues in the limited number of radial glia maintained

into adulthood, such as the Bergmann glia in the cerebellum (Pompolo and Harley, 2001), and also in the $GFAP^+$ NSCs of the adult SVZ (Scott et al., 2010).

Campomelic Dysplasia

In humans, infants with CD display a variety of skeletal defects and male-to-female sex reversal, although some authors have also reported mild mental retardation in the few children with this condition who survive early childhood (Maroteaux et al., 1971). The condition was first described (as a distinct clinical entity) by Lee and colleagues in 1972, and subsequently found to be caused by deletions or mutations in or around the *Sox9* gene (Foster et al., 1994, Wagner et al., 1994). The authors of the original paper describe three babies with severe skeletal deformities, all of whom failed to breathe spontaneously at birth, and died within the first few weeks of life. The skeletal deformities were wide, but the characteristic features were bowing of the long bones of the arms and legs, a small, bell-shaped thoracic cage and hypoplastic scapulae. In each case, radiographs showed poor bone mineralisation. The defects of chondrogenic tissue were not limited to the skeletal system, and affected the cartilaginous rings of the trachea, essential for its patency, which may have contributed to their respiratory distress at birth, and subsequent death. In addition to the defects of the tracheobronchial tree, all three children had severe cleft palates, which further complicated their breathing, and 'peculiar facies', the consistent features of which being hypertelorism of the eyes, a flat nose and low-set ears (both lacking normal cartilage structure), and a hypoplastic mandible. Interestingly, these babies had a number of neurological findings, including hypotonia (reduced muscle tone), and hyporeflexia (reduced tendon reflexes), which are usually associated with a defect of lower motoneurons, as opposed to the upper motoneurons that reside in the CNS. Bi and colleagues (2001) were the first to produce a null allele of *Sox9*, and found that in the

heterozygous state this mutation appeared to phenocopy CD in humans: The mice had bowing of the long bones, and these were of smaller than usual size. They also had cleft palates, and they died perinatally, as has been the case with CD neonates until recently.

The Role of *Sox9* in Gliogenesis

Since the deletion of *Sox9* in the germline results in embryonic lethality at E11.5 due to morphogenetic defects of the heart (Akiyama et al., 2004), Stolt and colleagues (2003) studied the effects of *Sox9* deletion on the development of the CNS using the Cre/LoxP system, and discovered that their spinal cords were profoundly deficient in astrocytes and OPCs. They noted that the defect of oligodendrogenesis recovered at later stages of development whereas astrogliogenesis did not. Further to this, they describe a prolonged phase of motoneuron generation from the pMN domain of the spinal cord, which is also the site from which oligodendrocyte progenitors arise, and hence proposed that there was a delay in the progression from neuro- to gliogenesis. Recent evidence has shown that a key driver of the 'gliogenic switch', as it is called, is the up-regulation of *Nfia* by SOX9, and that a heterodimer formed from SOX9 and NFIA activates gliogenic gene targets, which are themselves capable of restoring gliogenesis in the absence of either factor (Kang et al., 2012).

These observations raised a number of questions: Firstly, if *Sox9* is crucial for the timely onset of gliogenesis in the spinal cord, why is it that *Sox9* is expressed from the earliest point of neurogenesis (~E10.5)? Later we see a similar phenomenon in the dorsal telencephalon in my own analysis of the $Sox9^{Flox/Flox}$;NesCre mutants (Chapter 3). Two potential solutions seem most prominent: Either SOX9 may 'prime' the progenitors of the CNS to respond to a gliogenic signal, such as ciliary neurotrophic factor (CNTF), or

alternatively, SOX9 might perform some other function within the VZ prior to gliogenesis, for instance in neurogenesis.

Sox Genes and the Progenitor State

A number of *Sox* genes have established roles in stem cell behaviour. The first and most notable example of this is *Sox2*, which is known to be required for the pluripotency of embryonic stem cells within the inner cell mass (Avilion et al., 2003). Also, in the neural crest, *Sox10* has been shown to be required for maintaining both the neurogenic and gliogenic potential of neural crest stem cells (NCSCs; Kim et al., 2003). In this paper, the authors show that BMP2 and TGFβ, which normally extinguish glial or neuronal potential, respectively, when added to cultures of NCSCs are prevented from doing so by the over-expression of *Sox10*, and hence this factor is thought to maintain the multipotency of these cells. Within the neuroepithelium, *Sox1-3* are thought to maintain progenitors in an undifferentiated state, and inhibition of these factors is sufficient to induce differentiation (Bylund et al., 2003). *Sox1*, *2* and *3*, collectively referred to as the *SoxB1* genes due to their considerable homology, are all expressed in progenitors, and over-expression of any one of them in the chick spinal cord severely disrupts neurogenesis. The authors of this study initially hypothesised that this was caused by an increase in the number of progenitors vs. differentiated progeny; however, markers of cycling cells were not up-regulated. Repression of *SoxB1* targets using a construct in which *Sox3* had been fused to an Engrailed domain led to cell cycle exit and up-regulation of some neuronal markers, a phenotype that is reminiscent of the effect of *Neurogenin2* (*Ngn2*) over-expression. This led the authors to speculate that *Ngn2* brings about neuronal differentiation by inhibiting *SoxB1* targets, and later experiments showed that *Ngn2* was able to repress *Sox3*. The authors posited that repression of *SoxB1* targets

was necessary for neuronal differentiation, and this claim was substantiated by the finding that co-electroporation with *Sox3* inhibited the ability of *Ngn2* to initiate neuronal differentiation. However, it is important to bear in mind that as with any experiment involving electroporation, both *Sox3* and *Ngn2* would have been introduced into cells that would not normally express them, and also that the level of this expression may far exceed that seen in normal physiology.

The Role of SOX9 in Progenitor Identity

Vidal and colleagues' paper (2005) on the role of *Sox9* in hair follicle development and postnatal function was one of the first to identify a central role for this transcription factor in the genesis or maintenance of a stem cell population. Hair follicles of the mouse pelage arise at E14.5 as a result of signalling from mesenchymal cells acting on overlying epidermal cells (reviewed in Fuchs et al., 2001), which induces thickening of the epidermal layer (a structure referred to as the hair placode). The cells of this placode then invade the mesenchyme, and invaginate a small group of mesenchymal cells near the basement membrane, forming the 'hair bulb'. The epidermal cells between the hair bulb and the skin surface then differentiate into the inner and outer root sheaths of the hair (IRS and ORS, respectively) and, innermost within the follicle, the hair shaft itself. Matrix cells at the base of the hair serve as a reservoir of transient-amplifying cells that give rise to the new cells of the ever-elongating hair. For some time it has been known that stem cells originating in an out-pouching of the ORS, the bulge, migrate towards the bulb to replace matrix cells that have differentiated. Vidal and colleagues found that *Sox9* is expressed in the ORS and in the CD34-expressing stem cells of the bulge, and that loss of *Sox9* through a skin-specific Cre led to transdifferentiation of the ORS towards a more epithelial character, and the complete loss of the bulge stem cells, resulting in alopecia in

adult mutants. They show, through elegant transplantation studies, that *Sox9* is not necessary for the formation of the hair follicle, only for the formation of this specialised group of stem cells required for completion of the hair cycle.

A similar observation was made in the context of the intestinal crypts (crypts of Leiberkühn), which are themselves stem cell niches (Blache et al., 2004). The villi that maximise the internal surface area of the small and large intestine are constantly subject to damage from movement of the bowel contents, resulting in the tips of the villi being sloughed off. New epithelial cells are continually generated from stem cells within the crypts (reviewed in Crosnier et al., 2006), and migrate up the walls of the intestinal villi to replace those epithelial cells being sloughed off at the tips. The fact that these stem cells are maintained in an undifferentiated state by Wnt signalling (van de Wetering et al., 2002) suggested to Blache and colleagues that a *Sox* gene may be involved in this effect since a number of *Sox* genes contain TCF/LEF response elements (which mediate the activation of Wnt target genes) in upstream regulatory regions, and have also been implicated in maintaining progenitor identity (Avilion et al., 2003, Bylund et al., 2003, Kim et al., 2003). They found that *Sox9* is robustly expressed in the proliferating cells of the crypt, presumed to be the stem cells, and regulated by the canonical Wnt pathway. Furthermore, the authors show that ectopic expression of *Sox9* is capable of repressing two genes expressed in the differentiating progeny of the crypt stem cells. However, they do not provide direct evidence that *Sox9* is required for the maintenance of stem cells in the crypts, such as loss of function data, and they concede that no intestinal defect has yet been described in the human condition associated with haploinsufficiency of *SOX9*, Campomelic Dysplasia (CD).

The same relationship of *Sox9* expression to progenitor identity is observed in the pancreas, where its expression is restricted to the $PDX1^+$ cells, found initially in the dorsal aspect of the forming gut and then maintained in a subset of cells in the pancreatic anlagen, that are known to generate all the cell lineages of the endo- and exocrine constituents of this organ (Seymour et al., 2007, Lynn et al., 2007, Gu et al., 2002). SOX9 is excluded from differentiated cell types, such as glucagon-expressing cells (Lynn et al., 2007), and its deletion using a *Pdx1*-Cre results in a severely hypoplastic pancreas (Seymour et al., 2007). Although in all cases, $Sox9^{\Delta Pdx1/\Delta Pdx1}$ pancreases were small rudiments of the wild-type organs, the authors noted that there was considerable variation in their size. Further analysis using a Cre reporter (containing the lacZ gene) revealed that some cells were escaping Cre-mediated excision and those cells that made up the hypoplastic pancreases in these mutants were over-represented by β-gal-negative cells, i.e. those that had not undergone recombination, suggesting a high degree of selection for unrecombined cells. Moreover, organ size correlated with the frequency of non-recombined cells in the $Sox9^{\Delta Pdx1/\Delta Pdx1}$. These observations suggest that loss of *Sox9* precludes proper generation of the cell lineages of the pancreas from $PDX1^+$ progenitors, emphasised by the clear selection for unrecombined cells where mosaicism exists. However, the authors of a subsequent paper (Lynn et al., 2007) found that *Sox9* was also expressed in endocrine lineage transient-amplifying cells, not only the stem cells, and challenged its position as a gene that maintains the undifferentiated state of progenitors by showing that it transactivates a number of genes required for endocrine cell fate, pointing to a role in setting up further differentiation along this lineage.

In the context of the developing CNS, Scott and colleagues (2010), whose work will be discussed in more detail in the next section, showed that the onset of neurosphere-forming ability, a retrospective means of identifying neural stem cells (NSCs), arises at the same

time as *Sox9* expression, and that in the absence of *Sox9*, radically fewer neurospheres are formed. The authors also found that ectopic expression of *Sox9* in neuroepithelial (NE) cells before the onset of neurosphere-forming ability gave rise to this property, suggesting that *Sox9* was capable of inducing an NSC-like state from symmetrically-dividing, pre-neurogenic NE cells. In the case of adult neurogenesis, deletion of *Sox9* in the cells of the SVZ that contact the ventricular lumen using a Cre adenovirus and mice carrying a floxed allele of *Sox9*, revealed a loss of GFAP expression in the cells in which *Sox9* was deleted, and a significant increase in cells carrying markers of migrating neuroblasts. This would appear to suggest that Type B cells of the SVZ niche have undergone differentiation as a result of *Sox9* loss. However, the authors assert that the increase in neuroblast number reflects a failure of their final differentiation into interneurons.

Sox9 has a similar ability to produce stem cell characteristics in cell types that do not normally possess them in the context of the adult mammary gland. In the context of this organ, *Sox9*, acting in concert with *Slug*, was found to facilitate the conversion of differentiated luminal epithelial cells of the mammary gland into mammary stem cells, capable of forming a complete ductal tree when transplanted back into mammary fat pads (referred to as 'organoids'; Guo et al., 2012). The authors of this paper found that *Slug* alone was able to convert ductal progenitors into organoid-forming cells, but was not capable of inducing organoid-forming ability in differentiated luminal cells. However, co-transfection with *Sox9* facilitated this conversion, suggesting that *Sox9* is a key regulator of stem cell identity in this context. Furthermore, *Slug* and *Sox9* are co-expressed in the putative stem cells of the adult mammary gland, and knockdown of both *Slug* and *Sox9* impairs their ability to form organoids in culture and also in gland reconstitution assays. Interestingly, only transient expression of *Slug* and *Sox9* was required for conversion of differentiated luminal cells into mammary stem cells, and once expression of these genes

was silenced (by doxycycline withdrawal in a Tet-O system), the downstream gene regulatory changes were maintained.

In summary, *Sox9* has been shown to be necessary for the acquisition of a stem cell state in the development of the hair follicle and the pancreatic anlagen *in vivo* (Vidal et al., 2005, Seymour et al., 2007), and the NSC populations of the developing CNS *in vitro* (Scott et al., 2010). Further to this, in the developing CNS and mammary gland, ectopic expression can induce stem cell properties in cells that would otherwise not exhibit these properties (Scott et al., 2010, Guo et al., 2012), emphasising an important role in stem cell identity.

SOX9 and Neural Stem Cells

As outlined in the previous section, work by Scott and colleagues (2010) has implicated SOX9 in the identity of NSCs. These authors first observed that SHH protein could transform non-neurosphere-forming, pre-neurogenic NE cells into cells capable of producing primary and secondary neurospheres. Treatment with recombinant SHH also conferred the ability to form all three lineages of the CNS in differentiation assays. Together these observations suggested that SHH could induce the two properties required by the definition of NSCs, namely self-renewal and multipotency. Using transcriptional profiling, the authors identified *Sox9* as a potential target of SHH signalling that might mediate the ability of SHH to transform NE cells into an NSC-like state. Subsequently, they found that *Sox9* expression coincided with the onset of neurosphere-forming ability in both the mouse and the chick, and that over-expression of this transcription factor had the same ability to transform NE cells. Experiments showing that a dominant negative *Sox9* construct could ablate the transformative effects of SHH, and that expression of

Sox9 in the presence of an inhibitor of SHH signalling could recapitulate its effects, established the epistasis of a pathway in which SHH induces *Sox9*, thus bestowing the properties of NSCs. This raises a number of questions about the mechanism by which *Sox9* is able to achieve this, such as what are its downstream targets in NE cells? This is an interesting question, but one that is not addressed in this thesis (attempts were made, but were frustrated by the difficulties of over-expressing *Sox9* in very early NE cells).

Having demonstrated through gain of function that *Sox9* is sufficient for NSC identity *in vitro*, the authors use a germline Cre approach to delete *Sox9* before it is expressed in the CNS. This strategy has the disadvantage that *Sox9* is lost from all tissues of the developing embryo, and by the time the neuroepithelium was assessed (at E11.5), these embryos would already have developed severe defects of their hearts (Akiyama et al., 2004). A significant reduction in neurosphere numbers is indeed seen, but this may be secondary to poor perfusion as a result of the cardiac abnormalities. In addition to the use of a germline Cre, a LoxP strategy involving the NesCre, intended to deleted *Sox9* specifically within NPCs, was used. Using this strategy, the authors again see a loss of neurosphere-forming ability, and surprisingly, loss not only of glial potential but also impaired ability to form neurons in neurosphere differentiation assays. This defect of neurogenesis was also seen *in vivo* in the developing $Sox9^{Flox/Flox}$;NesCre embryos in Scott and colleagues' analysis. This raised a new possibility that *Sox9* might be important in some way for the generation of neurons from neural progenitors and prompted us to investigate this in the region of the developing brain that gives rise to the cortex (the dorsal telencephalon). Although an interesting finding, in my own analysis, I found no difference in the onset of neurogenesis between $Sox9^{Flox/Flox}$;NesCre and wild-type embryos (Figure 3-8), and when I looked in some detail at the generation of the cortical layers using markers for each layer, I see no difference in the process of corticogenesis

(Figures 3–10 and 3–11). Two potential reasons for the differences between my findings and those of Scott and colleagues (with regards to impaired neurogenesis in *Sox9*$^{Flox/Flox}$;NesCre embryos) have been raised; one is that there may have been some mistake in genotyping, although the phenotype that I do observe is seen consistently, and never in embryos genotyped as wild-type. Another is that the NesCre transgene may have become dysfunctional, as a result perhaps of mutations. However, immunohistochemistry (Figure 3-2), *in situ* (Figure 5-7), qPCR (Figure 5-2), RNA-Seq (Figure 4-3) and microarray data have confirmed loss of SOX9/*Sox9* in the *Sox9*$^{Flox/Flox}$;NesCre embryos analysed in this thesis.

The impaired neurosphere-forming ability that Scott and colleagues observe persists throughout neurogenesis and is seen at the latest stages of embryogenesis. This suggests that whatever change in the cellular physiology of *Sox9*$^{Flox/Flox}$;NesCre neural progenitors that results from loss of *Sox9* is persistent in the NPCs at mid-neurogenesis and beyond. In Chapters 5-7 of this thesis, I use transcriptional profiling data obtained to investigate the impaired gliogenesis in *Sox9*$^{Flox/Flox}$;NesCre embryos, to find potential *Sox9* downstream targets that might mediate this deficient ability to form neurospheres. Although this data came from dorsal telencephalons towards the end of embryogenesis (E16.5), it was still a time-point at which deficient neurosphere formation would have been seen.

Aside from its role in the developing telencephalon, Scott and colleagues also investigated a role for *Sox9* in the NSCs of the adult SVZ niche. In order to do this, they inject a Cre adenovirus into the lateral ventricles of *Sox9*$^{Flox/Flox}$ embryos, deleting *Sox9* from all cells that contact the ventricle (Type B cells as well as ependymal cells). The inclusion of a ROSA26 reporter transgene in their crosses permits the progeny of *Sox9*-

deleted cells to be traced, and a dramatic increase in migratory neuroblasts is seen. They also find that these neuroblasts fail to form fully-differentiated interneurons in the olfactory bulbs, which is the final destination of neuroblasts migrating along the rostral migratory stream. These observations imply either that *Sox9* loss induces the Type B cells (or ependymal cells) to undergo differentiation into neuroblasts, or as the authors suggest, that *Sox9* loss has prevented the neuroblasts formed from *Sox9*-deleted NSCs from undergoing terminal differentiation into interneurons.

Functional Redundancy within the *SoxE* Group

One important observation that has to be borne in mind when attempting to tease out the function of individual *Sox* genes is the significant redundancy within the *Sox* family. As mentioned, virtually all SOX proteins have been shown to bind to the same sequence. The high degree of functional redundancy within the SOXE family is revealed by the fact that individual mutants often have a starkly less severe phenotype than double mutants. For instance, in developing OPCs, deletion of *Sox9* following their initial specification produces no defect in oligodendrogenesis. Also, replacement of *Sox10* with a lacZ cassette produces no phenotype in the oligodendrocyte lineage (even in the homozygous state) until terminal differentiation, which is deficient in these mutants. Compound deletion of both *Sox9* (after OPC specification) and *Sox10* results in widespread apoptosis within the oligodendrocyte lineage (Finzsch et al., 2008), demonstrating the ability of these two factors to compensate for each other during oligodendrocyte differentiation. The same phenomenon is seen in the developing testes. *Sox9* is required for specification of the testes, and in its absence, XY sex-reversal is seen. *Sox8* is not required for testis specification, but is required in Sertoli cells for the production of sperm from the seminiferous tubules. When *Sox9* is selectively deleted in the Sertoli cells of *Sox8*$^{-/-}$

mutant mice (after sex determination), failure of the seminiferous tubules is seen earlier than in Sertoli cells deleted for either factor individually, suggesting that *Sox8* is able to compensate for *Sox9* loss during testis maturation (Barrionuevo et al., 2009). However, it is clear that this functional 'redundancy' is not universal: Kellerer and colleagues (2006) replaced the open reading frame of *Sox10* with that of *Sox8* and found that although mice homozygous for this mutant allele showed rescue of some aspects of the $Sox10^{-/-}$ phenotype such as normal specification of glia and sensory neurons in the dorsal root ganglia, other aspects, such as loss of melanocytes showed no rescue. This demonstrates that the subtle differences between these two proteins, most likely outside their HMG boxes (since they bind the same sequence), are functionally important.

SOX Proteins Tend to Bind DNA in Complexes

A number of *Sox* genes are expressed in a variety of different tissues, and play diverse roles in development. *Sox9* is a good example of this since it has been shown to have crucial roles in the development of a range of tissues. For this transcription factor to play a role in each of these settings, it must have a distinct set of target genes in each context. It is known that SOX proteins tend to bind DNA in partnership with other individual factors (Kamachi et al., 2001, Yuan et al., 1995), or even in larger complexes (Ma et al., 2000, Lefebvre et al., 1998), and this provides a mechanism by which a single transcription factor can influence the expression of different sets of genes in different tissues, depending on the repertoire of partner proteins expressed.

This synergism with other factors was elegantly demonstrated for SOX2 by the work of Kamachi and colleagues (2001), who showed that SOX2 and PAX6 stabilise each other's binding to chromatin. They demonstrated this by showing, using chromatin-

immunoprecipitation (ChIP), that both SOX2 and PAX6 bind an enhancer of the δ-crystallin gene when they are expressed together, but when they are expressed individually, neither factor binds to this enhancer, showing the binding of one depends on the other. In a different transcriptional setting, the pre-implantation embryo, SOX2 has been shown to interact with a different partner (POU5F1, more commonly known as OCT4) in activating the transcription of *Fgf4* (Yuan et al., 1995). In this case, the physical separation of the binding sites for these factors seems to be of critical importance. An increase from 3 to 6bp in their separation was sufficient to prevent transactivation (Ambrosetti et al., 1997). The authors show that this effect was not caused by the rotation of the factors relative to each other, since increasing the separation to 10bp (equivalent to one turn of the DNA helix) did not rescue the effect. Interestingly, SOX2 would still bind if the spacing between the OCT4 and SOX2 binding sites were increased, but not OCT4, suggesting that SOX2 stabilises the binding of OCT4 to DNA.

In addition to binding with individual partners, SOX proteins have also been shown to synergistically activate enhancers in concert with more than one other transcription factor, such as in the case of the activation of the *Slit* gene in the midline of the *Drosophila* CNS. *Slit* can be activated *in vitro* by the binding of a heterodimer of Single-minded (SIM) and Tango (TGO; both bHLH-PAS proteins). However, further factors are required for the strong *Slit* expression seen in the midline of the *Drosophila* brain. Ma and colleagues (2000) found that the SIM-TGO heterodimer associates with both a SOX protein, Fish-hook (FISH), and a POU domain protein, Drifter (DFR), to initiate this level of expression. The authors also identified a number of other bHLH-PAS factors that associate with FISH, suggesting that this class of transcription factor might commonly form complexes with SOX proteins. A similar phenomenon has been observed for SOX9, which has been found to activate the transcription of *Col2a1* in chondrogenic

mesenchymal condensations through synergism with two other SOX proteins, the long form of SOX5 (L-SOX5) and SOX6. In 10T1/2 cells, transfection with these three factors produces activation of a *Col2a1* regulatory region that is many fold greater than that elicited by transfection with any of the factors individually (Lefebvre et al., 1998).

Although generally regarded as transcriptional activators, a number of SOX proteins have also been shown to act as repressors in certain circumstances, such as SOX2, which aside from activating a number of downstream targets in germs cells and in the inner cell mass, can also prevent the transactivation of *Osteopontin* by OCT4 in these cell types (Botquin et al., 1998). Repressive interactions have also been described for other SOX proteins that are conventionally thought of as transcriptional activators, such as SOX6, which represses *Fgf3* transcription by recruiting CtBP2 (Murakami et al., 2001).

SOX Transcription Factors As Architectural Proteins

The idea that SOX proteins might serve as 'architectural' factors that modify the secondary structure of DNA, rather than enhancing transcription directly, stems from studies of the specific mutations of *SRY* that lead to sex-reversal in humans. The authors of one particular study (Pontiggia et al., 1994) identified a mutation of *SRY* that causes sex-reversal by altering the angle of DNA-bend induced by SRY binding, without significantly affecting its affinity for its target sequence, suggesting that this angle is important for the function of *SRY* in testis specification. The theory that SRY merely affects the structure of chromatin, perhaps by bringing two factors on either side of its binding site into apposition, is consistent with the observation that only its HMG box is conserved in different vertebrate species (Tucker and Lundrigan, 1993, Whitfield et al., 1993). However, many SOX proteins, including those of the SOXE subfamily, have

delineated transactivation domains, so are likely to interact with the basal transcriptional complex directly (Hosking et al., 1995, Sudbeck et al., 1996, van de Wetering et al., 1993). Although this potential mechanism for SOX protein action is of historical interest in the development of our understanding of how SOX factors influence transcription, it is unlikely to be a major factor in the action of SOX9 due to its well-demarcated transactivation domain and also the fact that the mutations causing CD are distributed throughout the coding region of SOX9 (not just in the HMG box; reviewed in Pevny and Lovell-Badge, 1997).

Background and Aims of Thesis

As I alluded to at the beginning of this Introduction, part of the initial impetus for this work came from studies carried out in the lab by Charlotte Scott (Scott et al., 2010). In this article, the authors show that the capacity of neuroepithelial (NE) cells to form neurospheres in culture, and to give rise to all the lineages of the mature CNS, which are the defining characteristics of NSCs, are 'induced' at a specific time-point in embryogenesis, which coincides with neurogenesis. This runs counter to the classical paradigm, which would be that from the induction of neural tissue onwards, developmental potential is progressively narrowed. Scott and colleagues (2010) note that Sonic Hedgehog (SHH) can prompt NE cells that lack the ability to form neurospheres (prior to neurogenesis; at E9.5) to become multipotent NSCs, and through transcriptional profiling techniques identified *Sox9* as a potential mediator of this transformation. *Sox9* itself was found to induce NSC properties from E9.5 NE cells, and was shown to lie downstream of SHH. These data showed that *Sox9* is necessary and sufficient for the induction of cells with NSC properties from NE cells. The authors then used the Cre/LoxP system to delete *Sox9* from neural progenitors and found that these cells also had an impaired ability to form neurospheres throughout neurogenesis. Since the Cre acts after SOX9 is first expressed, and cells with NSC properties are first induced, this suggests that *Sox9* is also required for the maintenance of NSC properties. The authors also observed that *Sox9* deletion led to a thinned cortical wall, dilated ventricles and haemorrhage into the ventricles by the time of birth. The findings of this work prompted me to gain a fuller understanding of the phenotype of the $Sox9^{Flox/Flox}$;NesCre, which appeared to have undergone defective neurogenesis, since the ventricular walls of these embryos were reported to be thinner, and their cortices disordered (Scott et al., 2010).

Therefore, the first results chapter in this thesis contains a phenotypic analysis of the development of the dorsal telencephalon in the *Sox9*$^{Flox/Flox}$;NesCre embryo, including an analysis of the developing cortex, which should represent a sensitive assay of any change in the developmental potential of neurons born from *Sox9*-deficient radial glia. Surprisingly, the only abnormalities detected can be related to abnormal or delayed gliogenesis. I expected to see a phenotype involving neurogenesis, not only because it was reported in Scott et al., but also because *Sox9* is expressed from the very earliest point of neurogenesis in both the spinal cord (Stolt et al., 2003) and the dorsal telencephalon (my own data). Earlier in this introduction, I set out two possible explanations for why *Sox9* might be expressed in radial glia long before the onset of gliogenesis: The first possibility is that *Sox9* might be performing a function unrelated to gliogenesis during this period, and perhaps has some role in endowing neurogenic radial glia with their full developmental potential, such as the ability to form all types of cortical neurons. The second possibility is that *Sox9* may be involved in 'priming' the radial glia of the VZ to respond to a gliogenic signal, such as CNTF, a platelet-derived growth factor, or a vascular endothelial growth factor. The first explanation is made less likely by the result of our phenotypic analysis in Chapter 3 which reveals neurogenesis to be normal. In order to investigate the second possible explanation, I used transcriptional profiling techniques to determine if any receptor or component of a second messenger system that might transduce gliogenic signals were down-regulated in the *Sox9*$^{Flox/Flox}$;NesCre. This work forms the second results chapter (Chapter 4).

Since Scott and colleagues (2010) note that cells from the *Sox9*$^{Flox/Flox}$;NesCre dorsal telencephalon exhibit poor neurosphere-forming ability throughout embryonic development (at both E14.5 and E18.5), I used the transcriptional profiling data, originally obtained to answer the gliogenesis question, to identify potential mediators of

the poor proliferation of *Sox9*$^{Flox/Flox}$;NesCre NSCs. This forms Chapter 5, and interestingly, identifies a number of cell-surface receptors and a modulator of a cell-surface channel. In order to establish if any of these targets might feasibly mediate the continued poor proliferation of *Sox9*$^{Flox/Flox}$;NesCre NSCs in the neurosphere assay, I employed a number of agonists/antagonists to see if any could recapitulate this phenotype, and this work forms the last two results chapters (Chapters 6 and 7).

Chapter 2 Materials and Methods

Deletion of *Sox9* in the CNS

The floxed *Sox9* mice were originally derived by Akiyama and colleagues (2002), and the Nestin-Cre (NesCre) mice were produced by Tronche et al. (1999). In order to delete *Sox9* selectively in the CNS, $Sox9^{Fl/WT;NesCre}$ mice were crossed with $Sox9^{Fl/Fl}$ mice, and the litters harvested at various stages of embryonic development. A quarter of the embryos resulting from these crosses are $Sox9^{Fl/Fl;NesCre}$, and these are referred to as $Sox9^{\Delta/\Delta}$ in subsequent chapters.

Genotyping

The following protocol was used for genotyping: First, earpieces were taken, placed in an Eppendorf tube and submerged in 200µl of Tail Lysis Buffer (recipe below; supplemented with 20mg/ml proteinase K). These tubes were left in a waterbath at 55°C for >8 hours, and then 200µl of TE was added, followed by 400µl of Phenol/Chloroform/Isoamylalcohol (mixed in the ratio 25:24:1). The tubes were then agitated, and spun in a bench-top centrifuge for 2 mins; 1µl of the upper, aqueous phase was used in each PCR reaction. The following primers were used: GGC GGA TCC GAA AAG AAA A / CAG GGC GCG AGT TGA TAG C (NesCre); GTC TTT GGT CCA GGA / AGC TCG CTC TGT TGA TCC AT (floxed *Sox9*). The 'floxed *Sox9*' primers flank one of the LoxP sites in the floxed *Sox9* allele, such that when it is present, a 375bp amplicon is generated, whereas in the wild-type allele, a 341bp amplicon is generated.

Tail Lysis Buffer:-

	For 500ml (ml)
1M Tris-HCl pH8.5	50
0.5M EDTA	5
10% SDS	10
4M NaCl	25
H_2O	410

Histology

Pregnant mice were killed by one of the methods included in Schedule One of the Animals (Scientific Procedures) Act 1986. The uterine horns were removed and placed in ice-cold PBS. Then, in a separate Petri dish containing ice-cold PBS, brains were dissected from the embryos and fixed in Bouin's for 48 hours, then washed five times in 70% EtOH (~30 mins per wash) before being passed to the Histology Section at N.I.M.R. for sectioning and staining with haematoxylin and eosin (H&E) or luxol fast blue.

Immunohistochemistry

Embryonic brains intended for use in immunohistochemistry (IHC) were dissected into PBS on ice, fixed for 1 hour in pre-chilled 4% paraformaldehyde (PFA) in PBS (on a rocking platform at 4°C), washed 3 × 10 mins in 0.1% Triton X-100 in PBS, then embedded in O.C.T. compound. Sections were then cut using a Leica cryostat, to a thickness of 12μm, before being dried at room temperature for >10 mins, and stored at -20°C. The antibodies used are as follows: SOX9 (1:200; non-commercial, purified by

Silvana Guioli), GFAP (conjugated to Cy3; 1:200; Sigma, C9205); NeuN (1:200); PAX6 (1:20; Abcam); TuJ1 (1:1000; Covance, MMS-435P); INSM1 (gift from John Jacob, Briscoe group); TBR1 (1:500, Abcam, ab31940); BRN2 (1:100; Santa Cruz, sc-6029); CTIP2 (1:500; Abcam, ab18465); PDGFRα (1:500; BD Biosciences, 558774); OLIG2 (1:1000; Chemicon, AB9610). Once thawed, the sections were washed for 5 mins in PBS-0.01% Triton X-100, and then blocked for >30 mins with PBS-10% Donkey Serum-0.1% Triton X-100. If the antigen in question was a membrane or cytosolic protein, Tween-20 was substituted for Triton X-100 because it is a milder detergent. After blocking, the antibody was diluted as required in the blocking buffer and incubated overnight in a humidified chamber at 4°C. For unconjugated antibodies, the sections were washed the following day 3 × 10 mins with PBS-0.01% Triton X-100, then incubated for >30 mins with an appropriate secondary antibody (conjugated to a fluorophore) at room temperature. Finally, sections were washed 3 × 10 mins in PBS-0.01% Triton X-100 supplemented with DAPI, mounted with Aqua-Poly/Mount (Polysciences) and coverslipped. Where conjugated antibodies were used, the sections were simply washed in PBS-0.01% Triton X-100 (+ DAPI; 3 × 10 mins), mounted and coverslipped. Images were taken with a Leica SP5 confocal microscope.

In Situ **Hybridisation**

With the exception of the *in situ* hybridisations in Chapter 3 and those for *Rlbp1* and *Hopx* in Chapter 5, for which the sections were prepared in the same way as for IHC, specimens for *in situ* were fixed in modified Carnoy's (60% EtOH, 11.1% formaldehyde, 10% glacial acetic acid) overnight, then embedded in paraffin wax before being sectioned at a thickness of 5μm. *In situ* probes were made by PCR amplification of E16.5 whole telencephalon cDNA using primers specific to the gene of interest that were designed to

produce a single amplicon common to all known transcript variants (primers shown in Table 2.1). At the beginning of the reverse primer, the sequence of the T7 bacteriophage promoter was included so that the amplicon would contain this promoter and could be *in vitro* transcribed using the T7 RNA polymerase (Promega, P207B) in the presence of digoxigenin (DIG)-labelled dNTPs to give a DIG-labelled riboprobe. *In situ* hybridisation was then performed according to the modified Paris protocol (Etchevers et al., 2001), with the exception that proteinase K treatment of slides was omitted and 50% formamide-1X SSC-0.1% Tween 20 used for post-hybridisation washes (the authors used the same recipe but with 2X SSC).

Obtaining RNA from FAC Sorted Cells

Crosses were set between *Sox9*$^{Fl/Fl}$ and *Sox9*$^{Fl/WT;NesCre}$ animals, and the litters harvested at E16.5. All embryos were liberated from extraembryonic tissues, the dorsal telencephalons dissected and each pair placed in a separate 15ml Falcon tube containing 900µl 0.1M Hepes (in PBS). These samples were then transferred to a tissue culture hood and triturated; first using a P1000, then by drawing up and down using a fine polished Pasteur pipette that had been drawn out over a flame to a very fine tip. The cell suspension was then filtered through a 40µm cell strainer (Invitrogen), pelleted and re-suspended in 900µl of Sort/Stain Buffer (PBS-5% foetal calf serum, containing penicillin and streptomycin). A CD133-PE conjugated antibody (eBioscience, 12-1331) was added to each of these cell suspensions (with the exception of a no antibody control) at a dilution of 1:100 and incubated for 20-30 mins (whilst protected from light). Finally, the samples were pelleted and re-suspended in fresh buffer twice to wash, then filtered into a FACS tube via a 40µm cell strainer. The suspensions were then taken to the FACS Facility at N.I.M.R. where they were sorted according to their fluorescence at 594nm. A gate was established to sort

the top quartile of 594nm-fluorescing cells from each sample. Once sorted, the CD133-enriched samples were centrifuged and total RNA extracted from the pellets using an RNeasy Mini Kit Plus (Qiagen). This kit was used in place of the standard RNeasy Mini Kit because contamination with genomic DNA had been a problem in our early attempts to purify RNA from these samples because sheared genomic DNA would obscure the 18 and 28S peaks of ribosomal RNA required for proper evaluation of RNA integrity.

RNA-Seq

cDNA libraries for sequencing were made in accordance with Illumina's Sample Preparation Guide (Revision D), with the exception that poly-A selection and size-selection of cDNA fragments were omitted. The latter, size-selection on a gel, was not performed because the SPRI beads, used later in the DSN normalisation protocol, have a preference for fragments in the 150-300bp range at the cation concentrations used. Library normalisation was performed as set out in the 'DSN normalisation' protocol (Illumina, Revision C). This involved suddenly denaturing the library at 95°C, and then allowing the single-stranded cDNA molecules to slowly re-anneal at 65°C. After 5 hours, a duplex-specific nuclease was added, and then the reaction stopped and the remaining intact cDNAs purified. The expectation was that during the 5 hours of re-annealing time, highly prevalent transcripts, such as ribosomal and mitochondrial RNA would easily find their complementary partners, whereas rarer mRNA molecules would be very unlikely to find theirs. When the duplex-specific nuclease was added, all the common transcripts would be degraded, leaving the rarer mRNAs for sequencing. Finally, the cDNA libraries were briefly amplified in a PCR reaction, and taken forward for cluster generation and sequencing by the High-Throughput Sequencing Facility at N.I.M.R. Sequencing was performed using an Illumina GenomeAnalyser IIx. The raw reads from the sequencing

runs (in FASTQ format) were aligned to the July 2007 (NCBI37/mm9) assembly of the mouse genome with CLC Genomics Workbench, then the number of reads mapping to each CDS ('total exon reads') were extracted and fed into the R/Bioconductor implementation of Anders and Huber's method for calling differential expression in RNA-Seq data (Anders and Huber, 2010).

Affymetrix Arrays

Six Affymetrix GeneChip 430 2.0 arrays were used to analyse gene expression in three *Sox9*$^{\Delta/\Delta}$ and three *Sox9*$^{Fl/Fl}$ controls. The *Sox9*$^{\Delta/\Delta}$ embryos comprised two females and one male, and the controls for each of the *Sox9*$^{\Delta/\Delta}$ were littermates of the same sex. Normalisation was performed using the PLIER+16 algorithm in GeneSpring GX. Probe sets with low expression values (<20% of the maximal expression value) were filtered out, and differentially-expressed probe sets called using a combination of fold-change and the probability of an observed difference being due to chance (determined using Student's t-test).

Bioinformatics

The GO term categorisation, GO term enrichment analyses and KEGG pathway analyses were performed using WebGestalt (http://bioinfo.vanderbilt.edu/webgestalt/). The 'Placental Mammal Basewise Conservation' data and the multiple alignment of the *Kcnj10* and *Dbi* loci in various mammalian species were obtained from University of California's Genome Bioinformatics website (http://genome.ucsc.edu/), and the locations of SOX9 binding sites were taken from the SOX9 ChIP dataset (made available to us by

the Guillemot group at N.I.M.R.). Consensus binding sites in the vicinity of SOX9 binding sites were located using MatInspector (http://www.genomatix.de/).

Quantitative PCR

For the purposes of confirming the targets that were up- or down-regulated in both the RNA-Seq and microarray experiments, cDNA was reverse transcribed from total RNA samples prepared in exactly the same way as for the sequencing or hybridisation to the microarray chips, using Superscript III (Invitrogen) and oligo-dTs. qPCR was performed on an ABI 7500 instrument using ABsolute Blue qPCR Master Mixes (Thermo Scientific). The following PCR program was used:-

95°C 15 mins

95°C 15 secs
60°C 30 secs
72°C 30 secs
} 40 cycles

qPCR primers were designed using an implementation of the Primer3 algorithm on the NCBI website (Primer-BLAST; http://www.ncbi.nlm.nih.gov/tools/primer-blast/). A region of the gene in question common to all known transcript variants as close as possible to the 3' end was selected (since this region is less likely to be affected by truncated reverse transcription). This region supplied to Primer-BLAST with all settings as default except an amplicon of 80-300bp was specified, and the program was set to look for primers separated by at least one intron. The primers used for qPCR are shown in Table 2.2.

Gene Symbol	Forward	Reverse (+T7)
Rlbp1	AGGAGCAGGAGCTCCGAGCA	GGTAATACGACTCACTATAGGGCCTGCTGCCTGCTGCATGGT
Hopx	CCGGAGGCAGCACTTGAGGC	GGTAATACGACTCACTATAGGGCCTTCTGACCGCCGCCACTC
Tnfrsf19	GACGGTGCTCTTCGCTGCCA	GGTAATACGACTCACTATAGGGGCAGAGCTGCGGGCCTCTTC
2810459M11Rik	GGAGTGCTGGTGGCCGACAC	GGTAATACGACTCACTATAGGGCTGGGTTGGCAGCCCTTCGG
5830403L16Rik	CAGCCAGAACCTGCTGCCCA	GGTAATACGACTCACTATAGGGTGGTGGCGAACGCTACGTCG
AI646023	TGCGCTGGCTGCGAGAGATC	GGTAATACGACTCACTATAGGGGGTCCACCCAGGCCAACACG
Arhgef3	TTCCCCGGAGCCGGCTAGTG	GGTAATACGACTCACTATAGGGGCAGTCCGACTCGCTGTCCG
Dbi	CACTTCAAACAAGCTACTGTGGGCG	GGTAATACGACTCACTATAGGGTCATGGCACTTTCCTTGGAAGTCCC
Hs3st1	AACGCCTGCCTGCAAGGTCC	GGTAATACGACTCACTATAGGGCAGCACGCGCTCTGATGGGT
Kcnj10	CCCGCTGCCCCGCGATTTAT	GGTAATACGACTCACTATAGGGGGCATGCTGGCTGAAGCGGA
Mmd2	CGGGATTTGCGATCCGGGAGAC	GGTAATACGACTCACTATAGGGAGGCAGTAGAAAGCCCCTCCTGT
Plce1	TGGTGTCCCAGGTCCAGAGCC	GGTAATACGACTCACTATAGGGTCCCGCACCCTTCCACTTGC
Col2a1	TCCCCGTGGACGCTCAGGAG	GGTAATACGACTCACTATAGGGAACCTGCTGTTGCCCTCGGC
Pdgfra	GAGTGACCATCCGGCCGTGG	GGTAATACGACTCACTATAGGGGCGCGTGTGGGACTCTCACC

Table 2-1 PCR primers used to make DNA templates for *in vitro* transcription into DIG-labelled riboprobes for *in situ* hybridisation.

Reverse Transcription (RT)-PCR

In order to determine if expression of the candidate genes identified in Chapter 5 is maintained in neurosphere cultures, RNA was extracted from neurospheres derived from E14.5 dorsal telencephalon cells, grown in Neural Proliferation Media (NPM; see *Neurosphere assay*) for 7 days, with the media changed every 2-3 days, and intact E14.5 dorsal telencephalons. TRIzol LS (Invitrogen) was used to extract RNA from pelleted neurosphere cultures and an RNeasy Mini kit (Qiagen) for the intact dorsal telencephalons (after homogenisation using a Rotor-Stator). cDNA was made from this RNA using Superscript III (Invitrogen), and PCR performed using the same primers used to amplify those genes by qPCR (Table 2.2; PCR program below).

95°C	5 mins	
95°C	1 min	35 cycles
60°C	1 min	
72°C	1 min	
72°C	5 mins	
4°C	Forever	

Gene Symbol	Forward	Reverse
Rlbp1	TGGGAAACGGTGGGCCTGAGA	GAAAGTGCCCACCCCGTCTGA
Mmd2	TGATGGAACCGCGGCGATGT	TACCTCTTGTGCGCCGGGACT
Tesc	GGGACCAGCCCACCATTCGC	TCGCCCAGGGTGGTGTCGAT
Kcnj10	TCCCGCTGCCCCGCGATTTA	TGCTCCGGCCGTCTTTCGTG
Dbi	GCGCTTTCGGCATCCGTATCAC	CCCACTTGGCTTTGCCCTTGAGG
Arhgef3	CGCGGGGCCTTCAGCAACAA	CGGGACCCTGGACCAGTCCC
AI646023	ACCACCTCACTCCGCACTCC	GAGGCTGGGCAGCAGCAGAT
Heph	GCCTGCCTGGTTGGGCTTCC	TGGGTCTGCCTCAGTGGGGG
Pdpn	GCGTGGGACGAAGCCTCCCT	TCCCTCCGACGAAGCCAATGG
Pla2g16	CGTGATCCACCTGGCTCCTCCA	GTCCTTCCCGGCCACATGGC
Rab40b	TCTCCTTACGGCCACCCGGC	TGCCAGGTGCAGCCGATTTCC
Tnfrsf19	GACGGTGCTCTTCGCTGCCA	TTCCTTGAACCGGTGCGGCC
Hopx	GAGGCGGGTCTCACGGAGGA	GGCAAGCCTTCTGACCGCCG
Plce1	TGGCTGTATTGGGCCAGCTGC	TCCCCTCTTCTCACGGCACTGT
Tbp	ACCACTGCACCGTTGCCAGG	ACGCAGTTGTCCGTGGCTCT
Hs3st1	CGCCTGCCTGCAAGGTCCTC	GCCACACGCGCCTGGATCAT
Col2a1	GGAGACCGGCGAGACTTGCG	TTGCCAGCCGCTTCGTCCAG
Pdgfra	TGGTCCTCAGCTGTCTCCTCACAG	GGCTGCGGAGGCGTTAACCAC
2810459M11Rik	GGGTCCTCGGAGGCAGAGGAA	CAGTCTCCAGTGGGGAATACAGGT

Table 2-2 qPCR primers.

Neurosphere Assay

Neurosphere cultures were prepared using dorsal telencephalons dissected from E14.5 wild-type MF1 embryos using a method modified from that originally described by Reynolds and Weiss (1992). The dorsal half of each telencephalic vesicle was dissected in ice-cold PBS, then mechanically dissociated by three periods of pipetting with a P1000 (15-20 times), interspersed by 3-5 mins of incubation at room temperature. The resulting cell suspension was then filtered through a 40μm filter, and cells seeded to 6cm dishes containing Neural Proliferation Media (NPM; recipe below) that had been pre-warmed in a 5% CO_2 incubator at 37°C (at a density of 5×10^4 cells/ml). Pharmacological agents were then added to the dishes at a range of concentrations (usually two log-dilutions either side of the range in which their IC_{50}/EC_{50} lay). All compounds used in functional studies ($BaCl_2$, fluoxetine, muscimol, SR95531 and bicuculline) were purchased from Sigma-Aldrich. The effect of these agents on proliferation in the context of the neurosphere assay was then determined by counting all neurospheres in each dish >300μm in diameter 6-9 days after plating.

In order to determine if any of these agents affected the differentiative capacity of NPCs, neurospheres were grown in NPM for 7 days and then distributed amongst the wells of a chamber slide (~5/well) that had been pre-coated in Matrigel (BD Biosciences) and containing 0.5ml/well of Neural Differentiation Media (NDM; recipe below). Different agents were then added to the wells and the neurospheres allowed to differentiate (changing the media every other day). After 4 days, the cells that had differentiated and migrated onto the surface of the slide were fixed and stained for markers of neurons, astrocytes and oligodendrocytes.

Neural Proliferation Media (NPM):-

	For 100ml (ml)
DMEM/F-12 (-L Glut)	93.5
40% glucose in DPBS	1.5
Pen/Strep	1
L-Glut	1

The above should be filtered through a 40µm filter unit, then the following added:-

N2	1ml
B27	2ml
bFGF (1µg/µl)	2µl
EGF (1µg/µl)	2µl

Neural Differentiation Media (NDM):-

	For 100ml (ml)
DMEM/F-12 (–L Glut)	93.5
40% glucose in DPBS	1.5
Pen/Strep	1
L-Glut	1

The above should be filtered through a 40µm filter unit, then the following added:-

N2	1ml
B27	2ml

Chapter 3 The Role of *Sox9* in the *In Vivo* Development of the Forebrain

In light of the findings of Scott and colleagues (2010) that *Sox9* is required for the induction of NSC-like cells from the neuroepithelium at the onset of neurogenesis, I performed a phenotypic analysis of the $Sox9^{Flox/Flox}$;NesCre dorsal telencephalon, which will now be referred to as $Sox9^{\Delta/\Delta}$ for simplicity. Since the Cre acts shortly after *Sox9* expression initially arises in the CNS, the cells of the neuroepithelium may have already been exposed to SOX9. However, two findings in Scott and colleagues' paper point to a role of SOX9 in maintaining NSCs; firstly, $Sox9^{\Delta/\Delta}$ dorsal telencephalon cells form radically fewer neurospheres in culture, even at mid-neurogenesis (E14.5), and secondly, the authors report that $Sox9^{\Delta/\Delta}$ embryos die at around the time of birth, exhibiting dilated ventricles into which haemorrhage is occasionally seen. Of particular interest in this phenotypic analysis is the process of corticogenesis, in which cortical progenitors sequentially generate neurons with different properties, a feature that is at least in part intrinsically regulated (Shen et al., 2006). Any perturbation of neural progenitor behaviour, such as premature differentiation, or reduced potential, might result in a disordered cortex, which could inform our understanding of the defect within those progenitors. As the full knockout of *Sox9* leads to death at around E11.5 from defects of heart morphogenesis (Akiyama et al., 2004), I employed the same strategy used by Stolt et al. (2003) and Scott et al. (2010), namely the Nestin Cre (NesCre) and a floxed allele of *Sox9*. The NesCre involves a Cre transgene driven by a Nestin promoter and enhancer that produces specific expression in the progenitors of the CNS (Tronche et al., 1999), and the floxed *Sox9* mice carry an allele of *Sox9* in which the latter two exons of the gene are flanked by LoxP sites (Akiyama et al., 2002; Figure 3-1). Although previous investigators have addressed the role of *Sox9* in the spinal cord (Stolt et al., 2003), to our

knowledge no-one has examined it in the brain, where it is expressed most strongly within the VZ of the dorsal telencephalon.

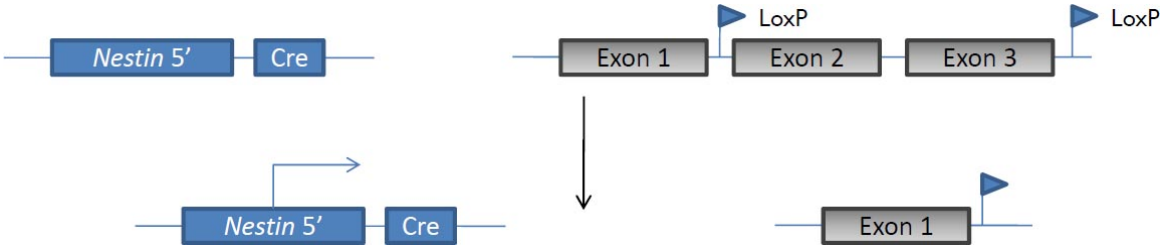

Figure 3-1 Diagram depicting strategy used to delete *Sox9* specifically within the CNS.

Introduction

Formation of the Embryonic Brain

The embryonic brain begins as a flat sheet of neuroepithelial cells specified from dorsal ectoderm, which folds to form a neural tube and, at its anterior end, forms three 'bulges' that give rise to the major subdivisions of the CNS: The prosencephalon, mesencephalon and rombencephalon. The prosencephalon then dilates either side of the midline, giving rise to two telencephalic vesicles. From very early in the development of the brain, there is a clear functional distinction between the dorsal and ventral halves of the telencephalon: the dorsal half generates a variety of projection neurons that eventually form the cortex, and the ventral half gives rise to the striatum and pallidum, which are dominated by a different class of neuron, the medium spiny neuron (Kemp and Powell, 1971).

Progenitors in the Developing CNS

The adult brain is composed of three main lineages of cell: Neurons, astrocytes and oligodendrocytes. In the course of embryonic and early post-natal development, these cell types are generated from a progenitor zone, which is initially the region lining the ventricles, but at later stages, also comprises a second layer of progenitors, known as the subventricular zone (or SVZ). The primary progenitors of the CNS, radial glial cells, were first described by Ramón y Cajal at the end of the 19th century (Ramon y Cajal, 1881). These cells extend one process to the adjacent ventricular (apical) surface and another to the far-off pial (basal) surface. For many years, until Misson and colleagues showed in

the late 80s (Misson et al., 1988) that radial glia are actively dividing cells, radial glia were thought to be merely a scaffold for the radial migration of new neurons. The ability of radial glia to generate neurons was first demonstrated by Noctor (2001) using a retrovirus to trace the immediate progeny of radial glia. However, the position of radial glia as the sole primary progenitor of the mammalian CNS was put beyond doubt by Cre/LoxP lineage tracing. First, Malatesta and colleagues (2003) found, using hGFAP-Cre and a reporter construct activated by the excision of a floxed stop codon, that all the projection neurons of the dorsal telencephalon were derived from radial glia, but not the interneurons of the ventral telencephalon. Under this system, all the progeny of a cell in which Cre has acted will express the reporter. However, the lack of staining of interneurons was later found to be caused by the hGFAP promoter not being active in the rodent ventral telencephalon. When these experiments were repeated with a *Blbp*-Cre, all the cells of the postnatal brain were found to have derived, directly or indirectly, from radial glia (Anthony et al., 2004).

During the expansion of the neuroepithelium that precedes neurogenesis, the neuroepithelial cells divide symmetrically to increase their numbers as the surface area of the telencephalic vesicles increases. However, at around mid-gestation, these progenitors switch to asymmetrical division, generating a new neuron with each turn of the cell cycle (Chenn and McConnell, 1995). This mechanism of neurogenesis is phylogenetically very old, and is the sole mechanism of corticoneurogenesis in reptiles and birds (reviewed in Abdel-Mannan et al., 2008). Concurrent in evolutionary terms with the development of the more complex, six-layered structure of the mammalian cortex, is the generation of intermediate progenitors. Once generated from radial glia, these progenitors immediately translocate to a region above the VZ, which becomes known as the SVZ (Miyata et al., 2004, Noctor et al., 2004). Intermediate progenitor cells (IPCs) usually divide only once,

giving rise to two neurons, although there have been reports of some dividing up to four times. Once formed, new neurons, regardless of which cell type they were generated from, migrate along the processes of radial glia to form, or elaborate, the structure of the cortical plate (CP; Levitt and Rakic, 1980).

Corticogenesis

The adult mammalian cortex is a complex laminated structure, in which neurons residing in each layer share hodological and morphological properties, as well as characteristic gene expression profiles. Neurons destined to form a particular layer are born in the VZ at the same time in a distinct 'wave' of neurogenesis (reviewed in Molyneaux et al., 2007). The first neurons to be formed from these progenitors arise at ~E11.5 and migrate radial out of the VZ to form a layer superficial to it, termed the 'preplate'. A later wave of neurogenesis gives rise to neurons that migrate to form a layer that splits the preplate, forming the first layer of the CP, and dividing the preplate into a superficial layer (the marginal zone) and a deep layer (the subplate). Subsequent waves of neurogenesis, produce ever more superficial layers of the CP. In this way, every new batch of neurons is required to migrate through an existing layer, leading some to describe the CP as being formed in an 'inside-out' fashion. The final wave of corticogenesis occurs at ~E15.5, and gives rise to neurons that will eventually form layers II-IV.

Interestingly, the transcription factor profile of new neurons formed at different stages of neurogenesis is different. For instance, early-born neurons (formed between E12.5 and E13.5), which are destined to become layer V and VI neurons, express the transcription factor *Otx1* from the very point of their birth in the VZ (Inoue et al., 2004), whereas later-born neurons destined for layers II-IV express *Brn2* from the point of their formation and

continue to express it after reaching their destination in the CP. The sequential expression of transcription factors typical of different layers of the CP can be recapitulated *in vitro* (Shen et al., 2006), suggesting that individual cells advance through the program of neurogenesis in a cell-autonomous fashion. However, another series of experiments suggested that extrinsic signalling molecules also have a crucial role to play. As described above, progenitors in the VZ generate deep neurons first, then more superficial layers. McConnell and colleagues (1991) found that progenitors isolated at the beginning of neurogenesis, which would normally give rise to layers V and VI, when transplanted into brains at later stages of development, produce more superficial (layer II-IV) neurons. This shows that cell extrinsic factors are also capable of influencing the outcome of neurogenic divisions, although interestingly McConnell and colleagues showed that this effect is only seen if the progenitors go through their final mitosis in the new environment.

Interneurons

Aside from cortical projection neurons, another neuronal subtype, interneurons, are essential for the proper functioning of the mature cortex. They are characterised by short, spiny axons, which project locally. Stimulation of these neurons exerts an inhibitory effect on the neurons they synapse with, through the release of γ-aminobutyric acid (GABA). Other neurotransmitters employed by interneurons include acetylcholine, calretinin, parvalbumin, somatostatin, neuropeptide Y and nitric oxide (Marin et al., 2000).

During development, interneurons are generated from progenitors in the lateral and medial ganglionic eminences (Anderson et al., 1997, Lavdas et al., 1999), and migrate tangentially into the cortex. Using transplantation techniques, Wichterle and colleagues

(2001) found that interneurons generated from the LGE tended to migrate anteriorly to populate the striatum, whereas those from the MGE migrate tangentially into the dorsal telencephalon to populate the cortex. In *Nkx2.1*$^{-/-}$ mice, which lack an MGE, ~50% fewer interneurons are seen in the cortex after birth (Sussel et al., 1999), strengthening the conclusion that the MGE is the dominant contributor to the cortical interneuron population. Interneurons are a highly heterogeneous population, with most (if not all) secreting other neurotransmitters in addition to GABA. An example of this would be two non-overlapping groups of GABAergic neurons in the cortex, which are characterised by expression of either parvalbumin or somatostatin, together with the GABA-synthesising enzyme, GAD67 (Kubota et al., 1994). Attempts to locate the origins of different subtypes of interneurons have been frustrated by the fact that these cells take many weeks of postnatal development to mature and begin to express the neurotransmitters that define their identity.

Oligodendrogenesis

Oligodendrocytes are the myelin-forming cells of the CNS, and their role is to insulate axons, allowing fast salutatory conduction. Because of their ubiquity in the adult CNS, oligodendrocytes were originally thought to be produced from all regions of the VZ. However, it is now known that they are formed at specific locations. Within the spinal cord, the first region to be identified as being important for oligodendrogenesis was the pMN region of the ventral spinal cord, which also generates motor neurons. The pMN origin of oligodendrocytes is supported by three lines of evidence: First, in mice expressing a hypomorphic allele of *Pax6*, in which the pMN region is shifted dorsally, the region of OPC production is also shifted dorsally (Sun et al., 1998); secondly, genetic ablation of *Olig2*, a bHLH transcription factor expressed in the pMN region, results in the

loss of both motor neurons and oligodendrocytes (Lu et al., 2002, Takebayashi et al., 2002) and finally, Cre/LoxP fate mapping shows that *Olig2*$^{+}$ progenitors give rise to both these cell types (Lu et al., 2002). However, analysis of a mutant in which the pMN region is absent (*Nkx6.1*$^{-/-}$*Nkx6.2*$^{-/-}$) revealed that oligodendrocytes are still formed (Cai et al., 2005, Vallstedt et al., 2005), suggesting that other regions within the developing spinal cord are capable of generating these cells. Later, Cre/LoxP fate mapping revealed that a region dorsal to the pMN zone also produced oligodendrocytes, although at a slightly later time-point (E15.5 vs. E13.5; Fogarty et al., 2005, Kessaris et al., 2008). This ventral-to-dorsal progression of oligodendrogenesis is mirrored in the embryonic brain, with the first OPCs being formed from the MGE and anterior entopeduncular area (AEP) at ~E11.5 (Kessaris et al., 2006). Later, another wave of oligodendrogenesis occurs in the LGEs and caudal ganglionic eminences (CGEs; Kessaris et al., 2006). Then, at around the time of birth a final cohort of OPCs are generated from the progenitors of the dorsal telencephalon (Kessaris et al., 2006).

Unlike neurons, which undergo their terminal division as they are generated in the VZ, oligodendrocytes begin life as migratory precursors, that continue to mature as they move toward their final destinations in the brain. Oligodendrocyte precursors were first identified by Martin Raff in the early 1980s (Raff et al., 1983), when he described cells isolated from the rat optic nerve that, depending on the culture conditions, could differentiate into either oligodendrocytes or a certain type of astrocyte (type-2 astrocytes). This property led to them being named ‘oligodendrocyte-type-2 astrocyte’ (O-2A) precursors. However, cells with the antigenic profile of these precursors were never found *in vivo* (Kessaris et al., 2008). In fact, differentiation into any identifiable type of astrocyte has not been consistently observed, so it may be that these cells are in reality,

oligodendrocyte progenitors, which under 'extra-physiological' conditions can be transformed into astrocytes.

Clearly, Sonic hedgehog (SHH) is important for oligodendrogenesis in certain contexts. SHH signalling is required for the establishment of the pMN zone (Briscoe et al., 2000), and embryos lacking *Shh* do not produce oligodendrocytes from this region of the ventral spinal cord (Cai et al., 2005). Furthermore, the expression of *Olig1* and *2* can be induced by SHH *in vitro* (Lu et al., 2000). However, other authors have also demonstrated SHH-independent routes for oligodendrocyte production (Cai et al., 2005, Chandran et al., 2003). Conversely, BMPs probably have a inhibitory effect on the production of OPCs. This finding stems from the observation in the chick neural tube that over-expression of BMPs ablates oligodendrogenesis, whereas Noggin, an inhibitor of BMP signalling, enhances it (Mekki-Dauriac et al., 2002). Finally, within the pMN domain, Notch signalling is also clearly important: Disruption of Notch signalling gives rise to an excess of motoneurons, at the expense of OPCs, whereas ectopic expression of a constitutively active form of the Notch receptor leads to the opposite, more OPCs at the expense of motoneurons (Appel et al., 2001, Park and Appel, 2003).

Olig2 is probably the most important cell-intrinsic determinant of oligodendrocyte fate, since no oligodendrocytes are formed in the spinal cords of *Olig2*$^{-/-}$ mice (Lu et al., 2002, Takebayashi et al., 2002). However, oligodendrocytes are generated in the hind- and forebrain, indicating functional compensation from *Olig1* in this setting. By contrast, loss of *Olig1*, which is expressed in an identical pattern in the ventral spinal cord, has no effect on OPC number, only a slight slowing of OPC maturation (Lu et al., 2002). Although recent evidence contradicted this finding, with another research group finding that maturation of oligodendrocytes in *Olig1*$^{-/-}$ mice was severely affected, leading to

death in the third postnatal week (Xin et al., 2005). Further to this, absence of *Olig1* prevents re-myelination following experimental ablation of myelin (Arnett et al., 2004), reinforcing its importance in mature oligodendrocytes. In the forebrain, loss of *Mash1* depletes the OPCs generated from the ventral telencephalon (Parras et al., 2007). In the spinal cord, *SoxE* genes have also been shown to be important in the oligodendrocyte lineage. Loss of *Sox9* results in an initial depletion, and then a resurgence of OPC numbers (Stolt et al., 2003), and compound loss of *Sox9* and *Sox8* eliminates all OPCs from the spinal cord (Stolt et al., 2005). OPCs are formed in $Sox10^{-/-}$ embryos, but they fail to mature (Stolt et al., 2002).

Results

In order to further our understanding of the role of *Sox9* in the developing telencephalon, mice carrying a floxed allele of *Sox9* (Akiyama et al., 2002) were crossed with a line carrying a Cre transgene, driven by the Nestin promoter and a neural-specific enhancer (Tronche et al., 1999), to delete *Sox9* specifically in the CNS from ~E10.5. The deletion of *Sox9* was verified by IHC, and the results are shown in Figure 3-2.

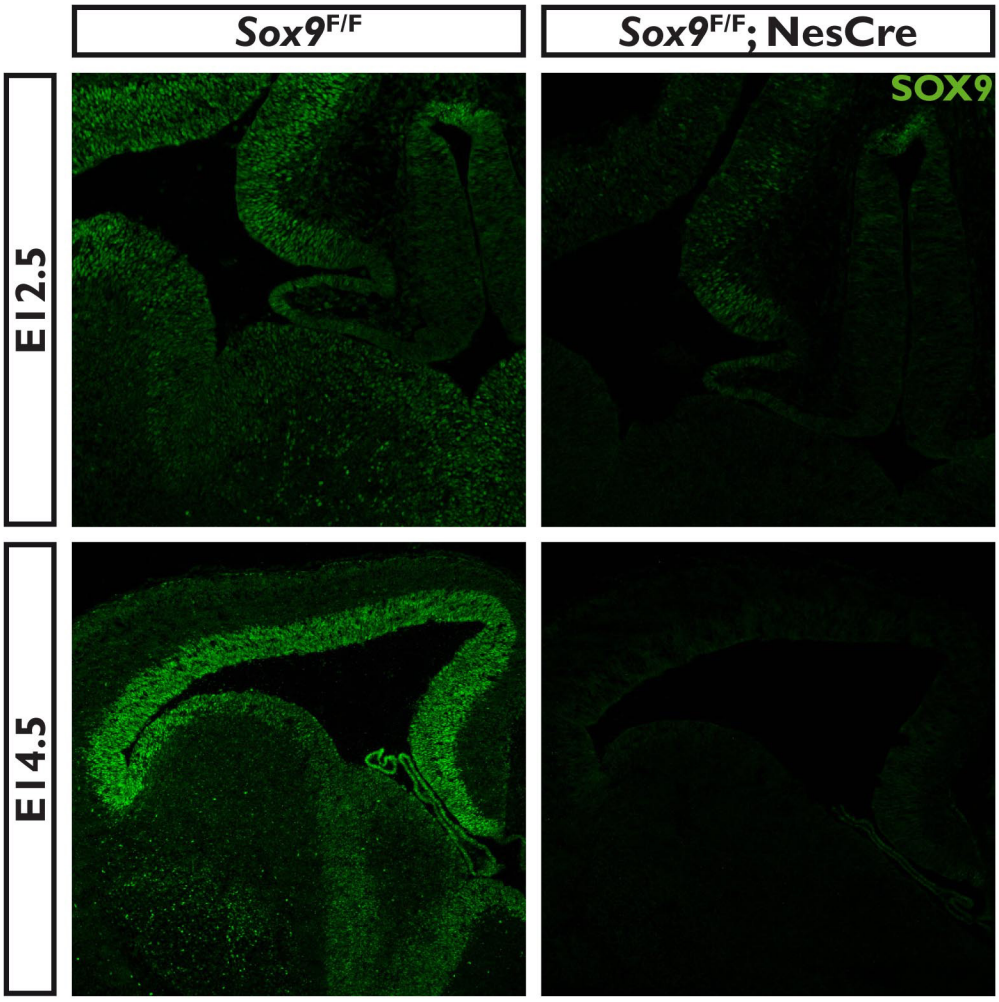

Figure 3-2 SOX9 immunostaining on *Sox9*$^{F/F}$ and *Sox9*$^{F/F}$;NesCre embryonic brains.

Survival of *Sox9*$^{\Delta/\Delta}$ Pups

Among litters harvested at P2, 15.9% were found to be *Sox9*$^{\Delta/\Delta}$, compared to the expected proportion of 25% (Figure 3-3; p=0.28, N=44). However, at the time of weaning (at ~4 weeks of age), only 3% of animals were *Sox9*$^{\Delta/\Delta}$, which is very different to the expect proportion and highly statistically significant (p<0.0001, N=101). These data suggest that the *Sox9*$^{\Delta/\Delta}$ pups are dying at some point between P2 and weaning, although a small proportion of animals (~12%; 3 vs. the expected number of 25.25), do survive to weaning and beyond. The surviving adults lack a corpus callosum (Figure 3-4), suggesting that this is not the reason for the inviability of the majority of *Sox9*$^{\Delta/\Delta}$ pups. The fact that some *Sox9*$^{\Delta/\Delta}$ mice survived into adulthood was surprising since two previous papers that employed the same strategy to delete *Sox9* found that these mice are not viable (Stolt et al., 2003, Scott et al., 2010). However, the fact that surviving adults show agenesis of the corpus callosum, a phenotype seen in all of the *Sox9*$^{\Delta/\Delta}$ embryos and none of the heterozygotes serves as evidence that these mice are not mis-genotyped. The genotypes of *Sox9*$^{\Delta/\Delta}$ adults were also confirmed prior to sectioning for histology.

	WTs/Hets	Homs
P2 (N=44)	84.1%	15.9%
Weaning (N=101)	97.0%	3.0%

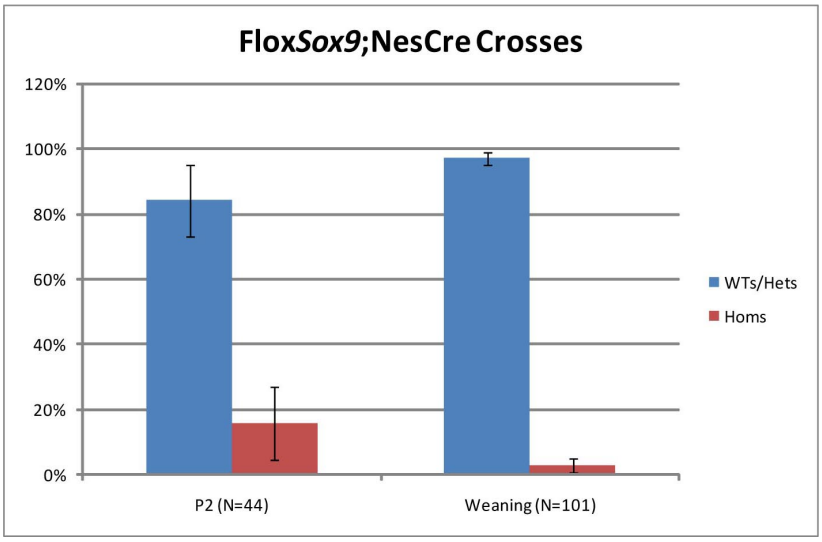

Figure 3-3 Survival of *Sox9*$^{\Delta/\Delta}$ pups at P2 and at weaning (~4 weeks of age).

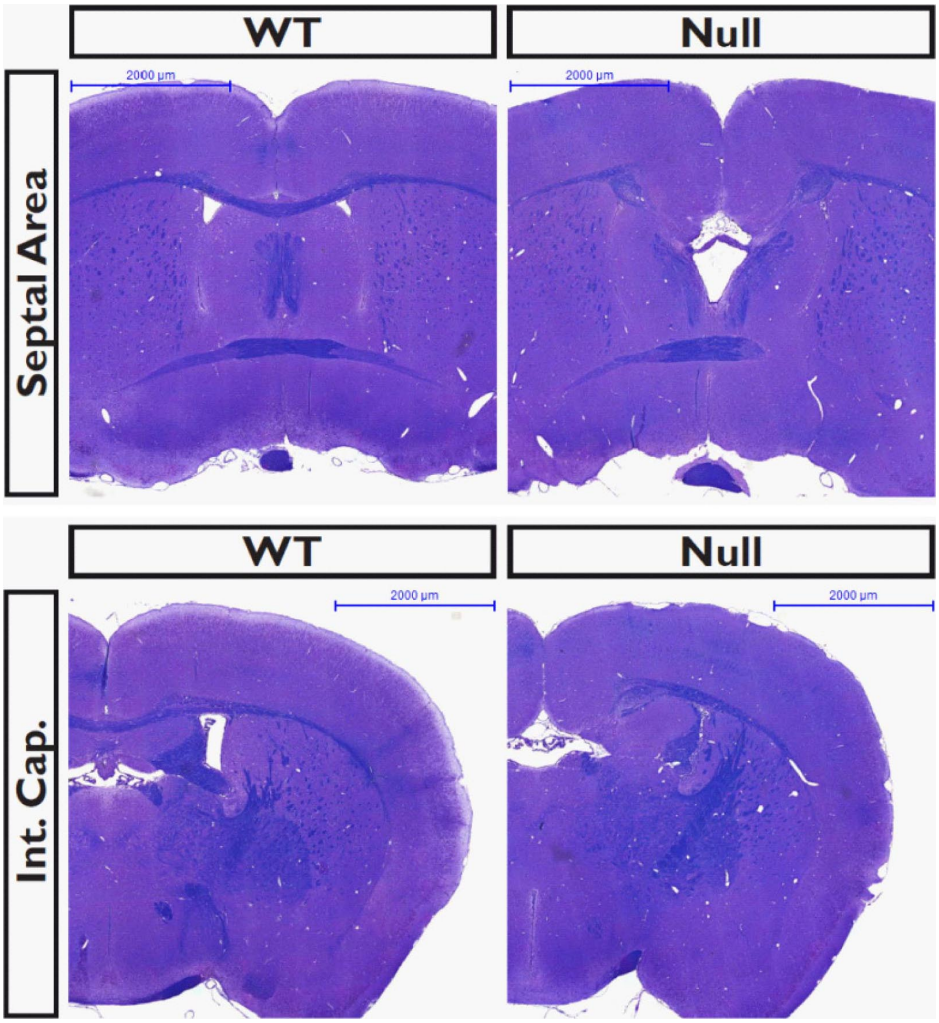

Figure 3-4 Luxol fast blue staining of the brain of a surviving *Sox9*$^{\Delta/\Delta}$ adult and a wild-type littermate (P63).

SOX9 Expression in the Forebrain

In the wild-type situation, SOX9 is expressed in the VZ at all stages examined (Figure 3-5). At E12.5, there are some scattered cells expressing SOX9 in the parenchyma of the MGE, and some are also seen in the LGE at E14.5; in both cases these cells are likely to be OPCs. At E18.5, the VZ is considerably thinner, and there are many $SOX9^{+}$ cells, which are presumably migrating away from their site of generation in the VZ. These are likely to be OPCs, but may also be astrocytes.

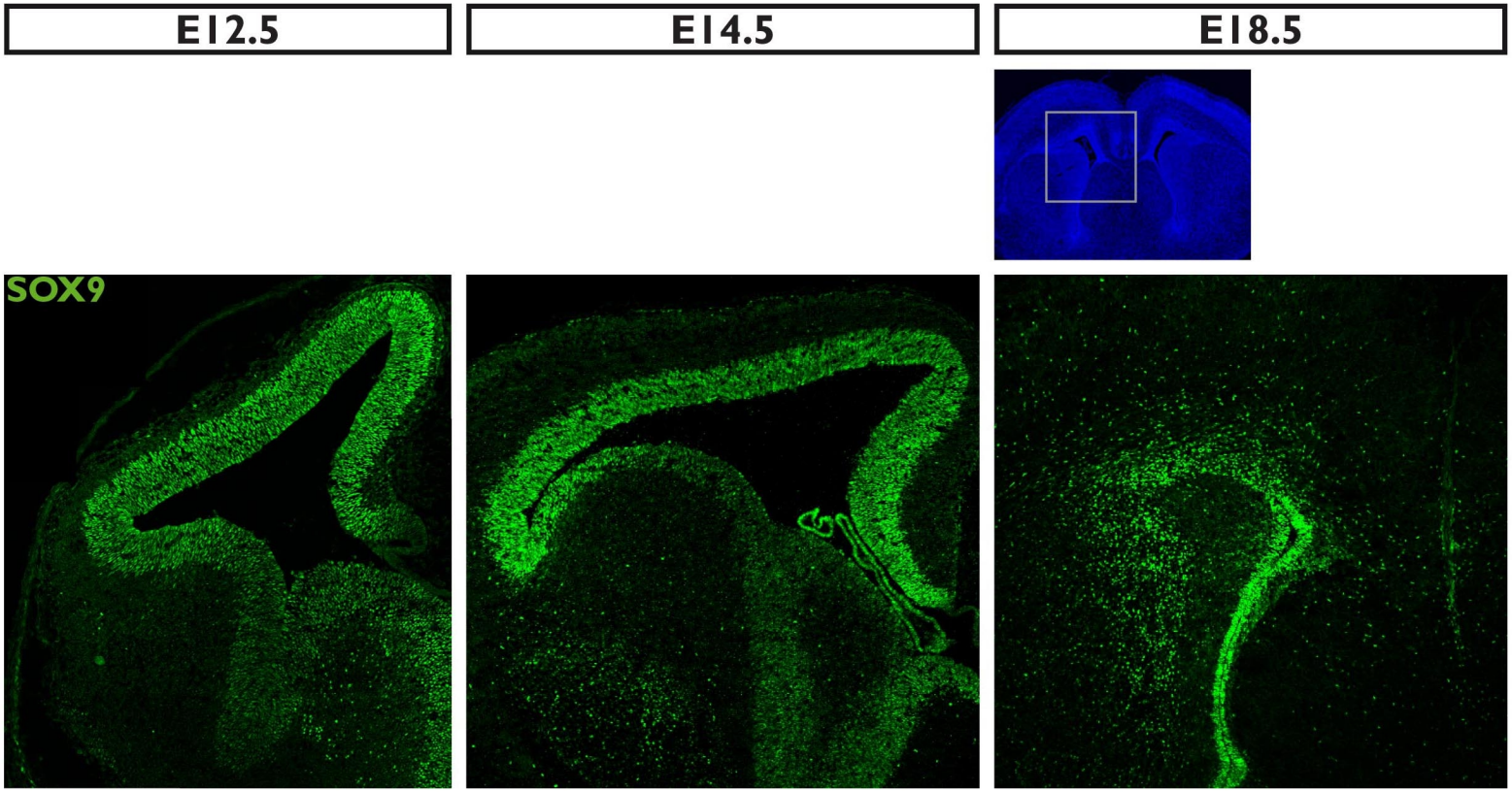

Figure 3-5 SOX9 expression (by immunohistochemistry) at E12.5, E14.5 and E18.5.

Embryonic Analysis

In order to ascertain if there were any gross abnormalities in the anatomy of *Sox9*$^{\Delta/\Delta}$ brains, E18.5 *Sox9*$^{\Delta/\Delta}$ brains were sectioned and stained using hematoxylin and eosin (H&E). Upon examination of these sections, the corpus callosum was noted to be absent, as was the hippocampal commissure, whereas the anterior commissure was unaffected (Figure 3-6). This exact pattern of agenesis of the corpus callosum (known as ACC) and absence of the hippocampal commissure was seen in all 5 *Sox9*$^{\Delta/\Delta}$ brains examined, and although commissural tracts were only examined specifically in 5 cases, I have not encountered a *Sox9*$^{\Delta/\Delta}$ brain in which either of these tracts are present. Instead of projecting into the contralateral hemisphere, callosal axons form 'bundles of Probst' either side of the midline. These were originally described as involving axons curling back on themselves, forming "whorls", instead of crossing the midline (Probst, 1901); however, it is now known that they in fact turn left or right, in a rostral or caudal direction (Lee et al., 2004). One of three heterozygous brains also showed this phenotype, suggesting that this aspect of the phenotype has variable penetrance in the heterozygous situation. Loss of commissural tracts was never observed in any wild-type embryo. In addition to abnormalities of commissural tracts, in one of the 5 *Sox9*$^{\Delta/\Delta}$ brains sectioned, the lateral and third ventricles were dilated and filled with blood.

A

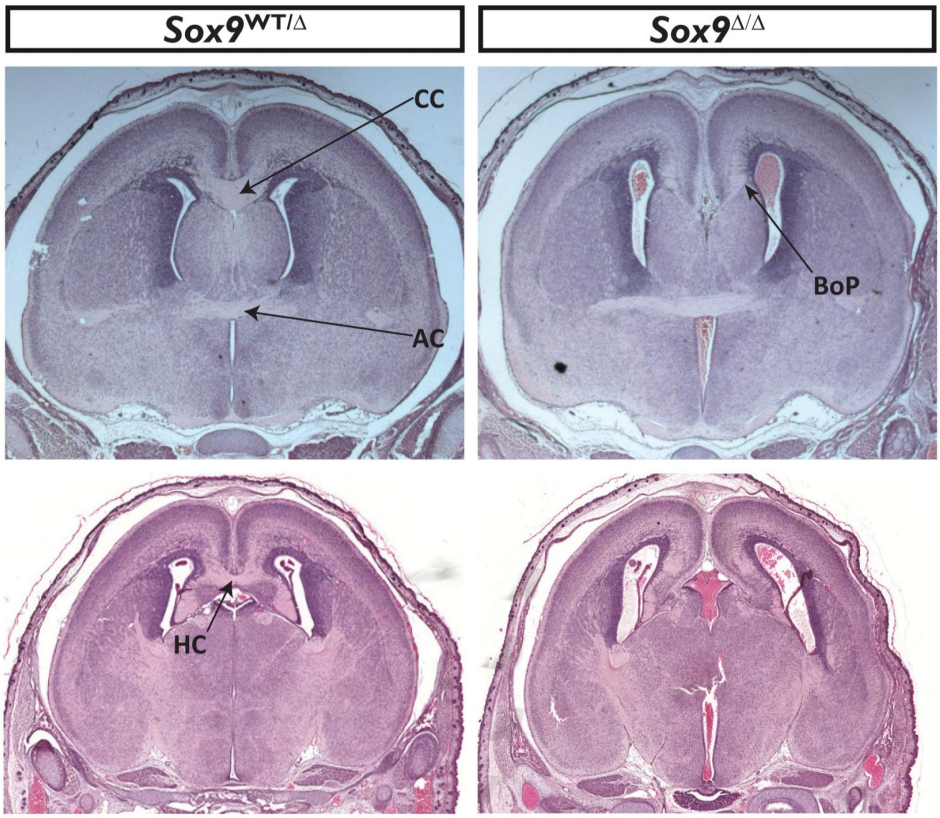

B

	Corpus callosum	Hippocampal commissure	Anterior commissure
D/D (N=5)	0	0	5
D/WT (N=3)	2	2	3
F/F (N=3)	3	3	3

Figure 3-6 A. H&E-stained sections of the anterior cortex of E18.5 embryos. CC = corpus callosum; AC = anterior commissure; HC = hippocampal commissure; BoP = bundle of Probst. B. Number of times a given commissure is present in a given number of brains of each genotype.

In light of the fact that *Sox9* has been previously reported to be essential for the formation of glia in the CNS (Stolt et al., 2003), and the finding of ACC, I examined the formation of the midline glial populations, and the 'glia sling' in the $Sox9^{\Delta/\Delta}$, which are midline features of the developing brain that have been shown to be essential for the formation of the corpus callosum (Smith et al., 2006). Using an antibody against GFAP to identify the glial populations, it was found that in the wild-type, both the indusium griseum and the midline zipper glia have formed by E18.5 (Figure 3-7). In the $Sox9^{\Delta/\Delta}$, neither of these populations form and instead $GFAP^{+}$ cells are dispersed within the bundles of Probst. In addition to $Sox9^{\Delta/\Delta}$ brains lacking midline glial populations, they also lack the 'glial sling'

(Figure 3-7B), which is actually composed of neurons (Shu et al., 2003a) that migrate concurrently with the pioneer axons of the corpus callosum. Due to its neuronal identity, this structure is better known as the 'subcallosal sling'. The characteristic 'U' shape of the subcallosal sling is lost in the *Sox9*$^{\Delta/\Delta}$, and because of the usual anatomy, it is unclear where these neurons have migrated. Some authors have suggested that the subcallosal sling is involved in guiding axons across the midline (Silver and Ogawa, 1983); however, others propose that it may be the initial axons of the corpus callosum that guide the subcallosal neurons in their migration (Donahoo and Richards, 2009).

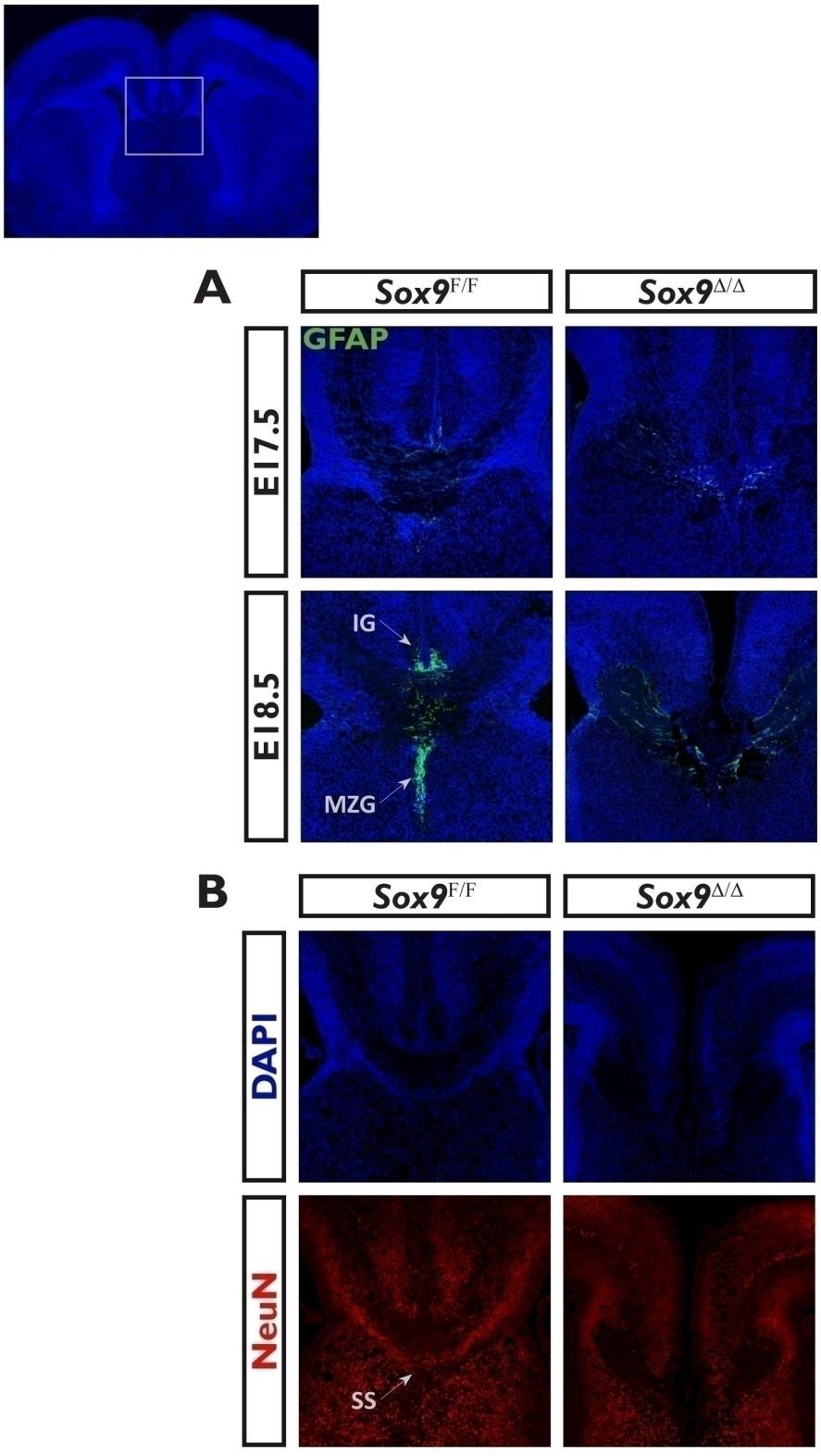

Figure 3-7 A. Midline glial populations in the *Sox9*$^{\Delta/\Delta}$ at E17.5 and E18.5. B. The 'glial' sling fails to form in the *Sox9*$^{\Delta/\Delta}$ (E17.5). IG = indusium griseum, MZG = midline zipper glia, SS = subcallosal sling.

Early Neurogenesis

Since *Sox9* is expressed in the VZ of the CNS from the earliest stages of neurogenesis (~E9.5; Stolt et al., 2003), I asked if there was any defect in the distribution of cortical radial glia, or if there was any delay in the onset of neurogenesis. I find that by PAX6 immunohistochemistry, there is no apparent depletion of cortical radial glia in the $Sox9^{\Delta/\Delta}$ at either E12.5 or E14.5. Additionally, the initial step in corticogenesis, the formation of the preplate, is seen to an identical extent in the $Sox9^{\Delta/\Delta}$ and wild-type littermates (Figure 3-8B, by TuJ1 immunohistochemistry). However, as described in the introduction to this chapter, radial glia are not the only progenitors of the CNS; they also give rise to intermediate progenitors, which usually divide once, generating two neurons, and are particularly important for mammalian neurogenesis. Therefore, the percentage of $DAPI^{+}$ cells that were also positive for a marker of IPCs, INSM1, were counted in $Sox9^{\Delta/\Delta}$ and wild-type sections. The resulting data showed that there are no statistically significant differences in the prevalence of IPCs at E12.5, E14.5 or E18.5 (Figure 3-9).

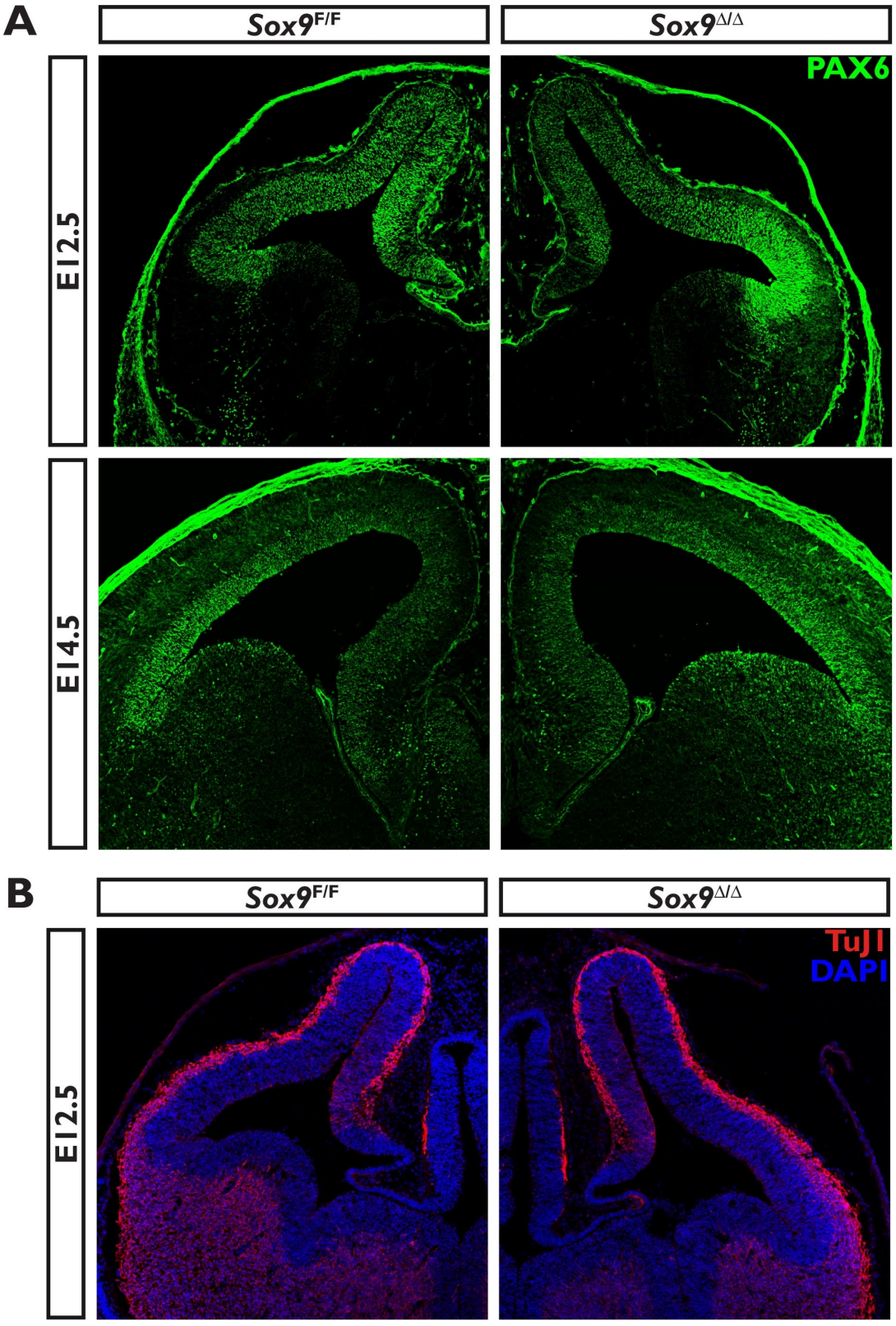

Figure 3-8 A. The distribution of PAX6^{+} cortical radial glia is similar between *Sox9*$^{\Delta/\Delta}$ and wild-type littermates at E12.5 and E14.5. B. The initial phase of neurogenesis, formation of the preplate, is normal in the *Sox9*$^{\Delta/\Delta}$.

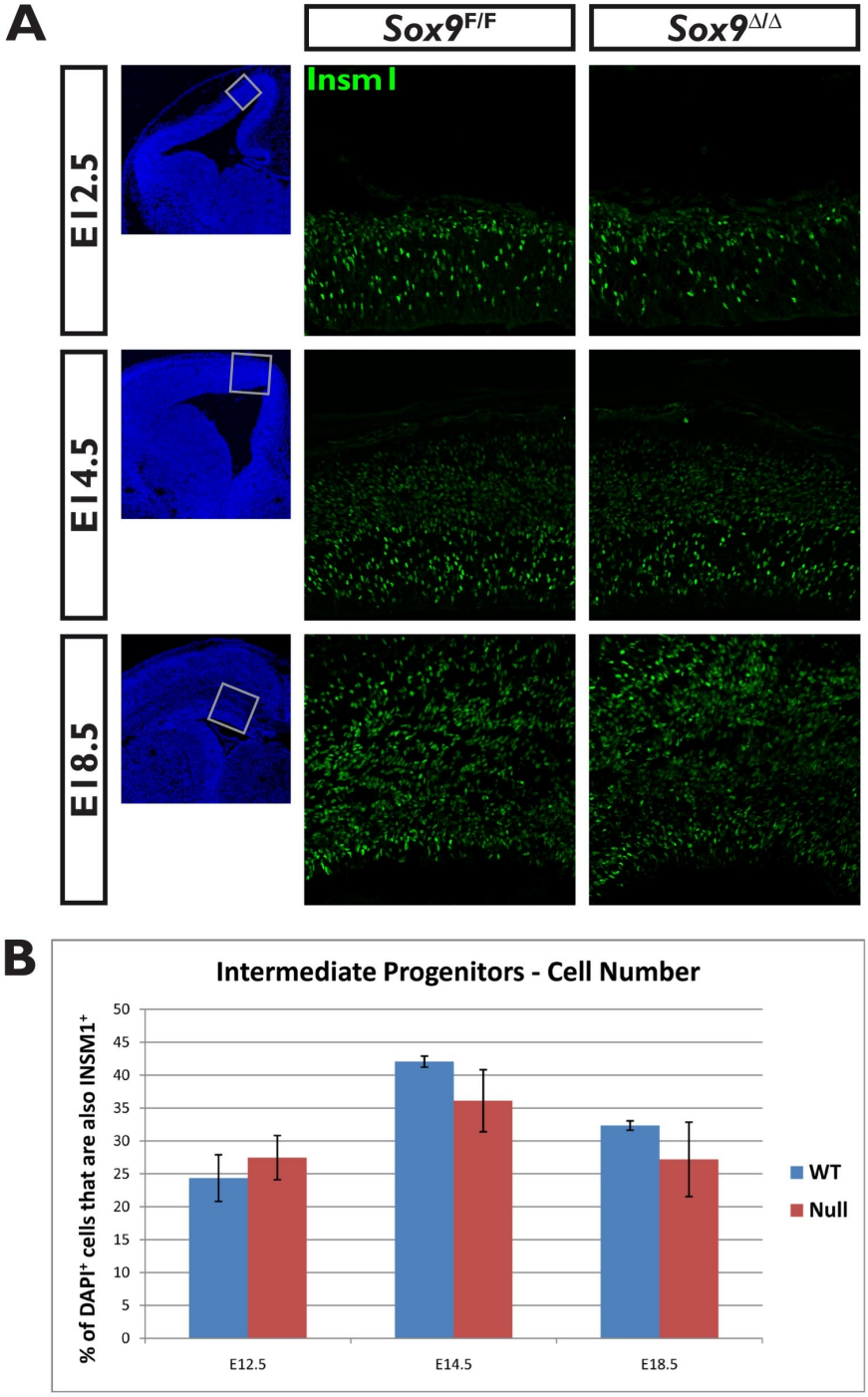

Figure 3-9 A. Immunostaining for INSM1, which is a marker of intermediate progenitor cells (IPCs), at E12.5, E14.5 and E18.5. B. Percentage of $DAPI^{+}$ cells that are also $INSM^{+}$ at these three stages of development.

Corticogenesis

Although radial glia and IPCs are present in apparently normal numbers and preplate formation commences at the expected time in the *Sox9*$^{\Delta/\Delta}$, it is still possible that the complex structure of the cortical plate (CP) fails to form properly. In order to determine if this was the case, IHC was performed using a number of markers specific to particular layers of the emerging CP: CTIP2, which markers layers V and VI, TBR1, which marks only layer VI, and BRN2, which is expressed in layers II-IV but unlike the other two, is also expressed in the newly-formed neurons destined to contribute to these layers as they migrate (shown in Figure 3-10). In order to assess the distribution of neurons positive for these markers, radial segments of the ventricular wall of multiple *Sox9*$^{\Delta/\Delta}$ and wild-type embryos were divided up into 'bins' such that Bin 1 was closest to the pial surface of the brain and Bin 9 to the ventricular surface. The percentages of marker positive cells that fell into each bin were then determined, and the data plotted to give an impression of their distribution (Figure 3-11). No statistically significant differences were observed in any bin for BRN2, showing that there is no defect in the distribution of these cells in the *Sox9*$^{\Delta/\Delta}$. Among the data for CTIP2^{+} neurons, only one bin showed a statistically significant difference (Bin 6; $p = 0.004$); however, a difference in one bin does not amount to an overall trend and in any case, this difference was not mirrored by the TBR1 data, in which no differences reached the necessary level of significance.

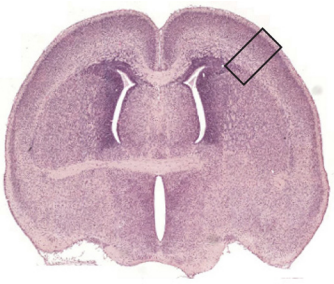

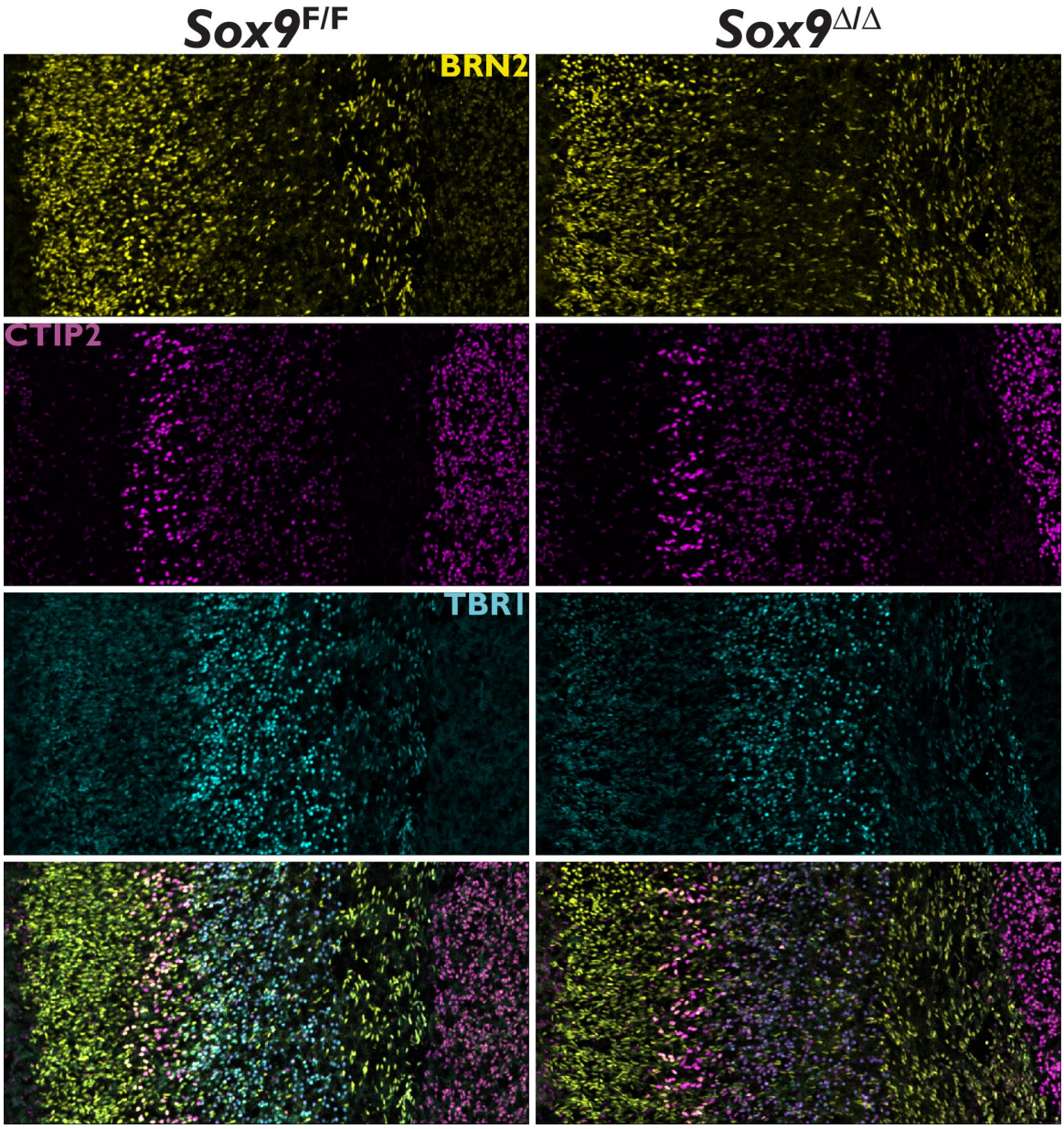

Figure 3-10 Immunohistochemistry showing the distribution of three antigens, each marking a particular subset of cortical plate layers. The ventricular zone is to the right of each image, and the pial surface to the left.

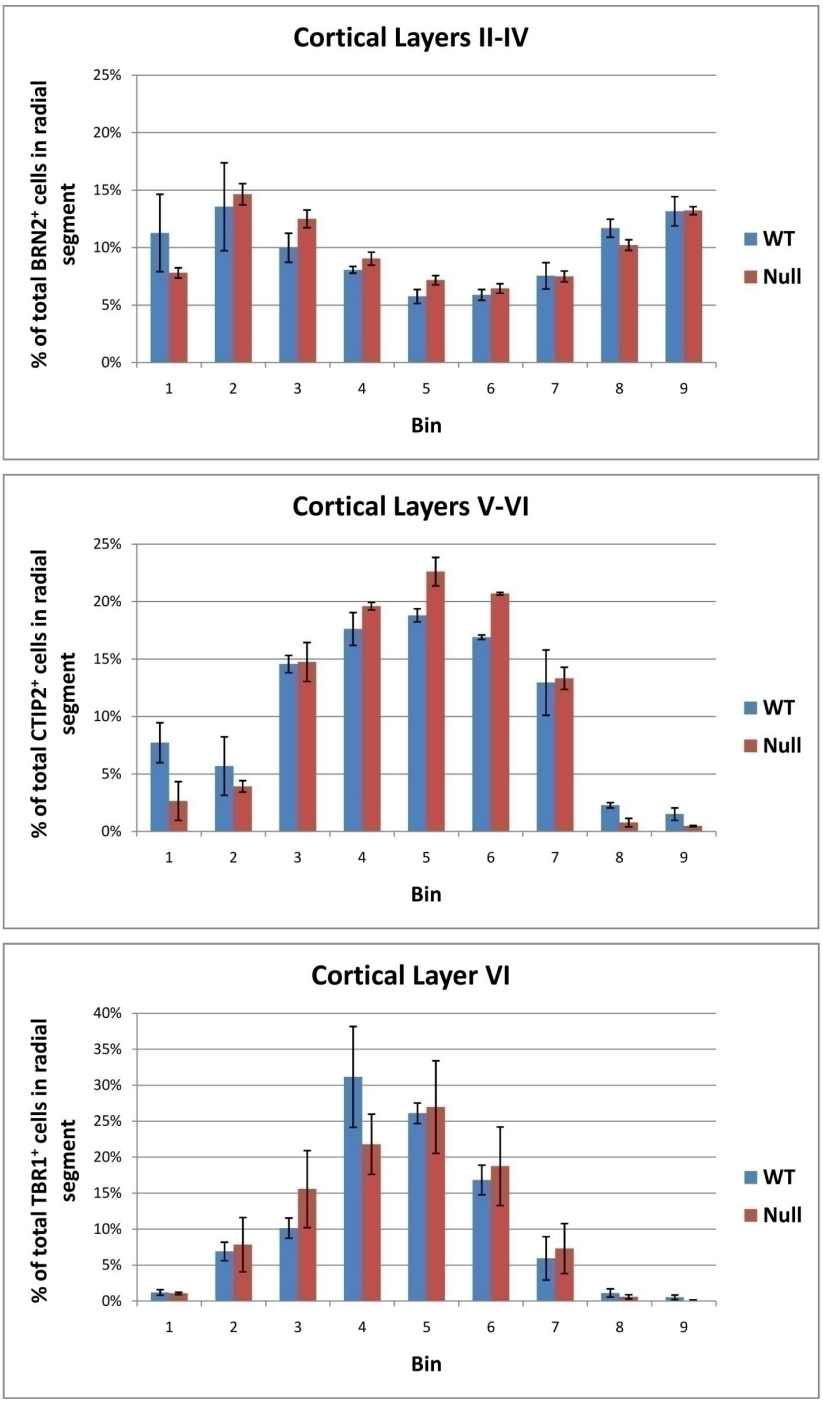

Figure 3-11 Binning on immunostainings for three markers of different cortical layers, BRN2 (marks layers II-IV of the future cortex), CTIP2 (marks layers V and VI) and TBR1 (marks layer VI only). The bars represent the percentage of the total number of marker-positive cells in a radial segment of dorsal telencephalon that reside within the each bin, where Bin 1 is closest to the pial surface, and Bin 9 to the ventricular surface.

Generation of Interneurons in *Sox9*$^{\Delta/\Delta}$ Embryos

Aside from projection neurons, the other neuronal subtype generated during embryogenesis is that of interneurons. In order to screen our *Sox9*$^{\Delta/\Delta}$ embryos for defects of interneuron formation, two markers of different interneuron classes were used: *Lhx6*, which is expressed in all interneurons destined to populate the dorsal telencephalon, and maintained in the parvalbumin- and somatostatin-expressing interneurons of the adult (Liodis et al., 2007), and *Isl1*, which marks the future cholinergic interneurons of the striatum (Fragkouli et al., 2009). No qualitative differences were seen in *Lhx6* expression by *in situ*, with *Lhx6*$^{+}$ interneurons being formed in the medial ganglionic eminences (MGEs) and beginning their migration away from this region in both the *Sox9*$^{\Delta/\Delta}$ and wild-type littermates (Figure 3-12A). Cholinergic (*Isl1*$^{+}$) interneurons are also seen in a similar distribution in *Sox9*$^{\Delta/\Delta}$ and wild-type littermates at E12.5, suggesting that these neurons are normally specified (Figure 3-12B).

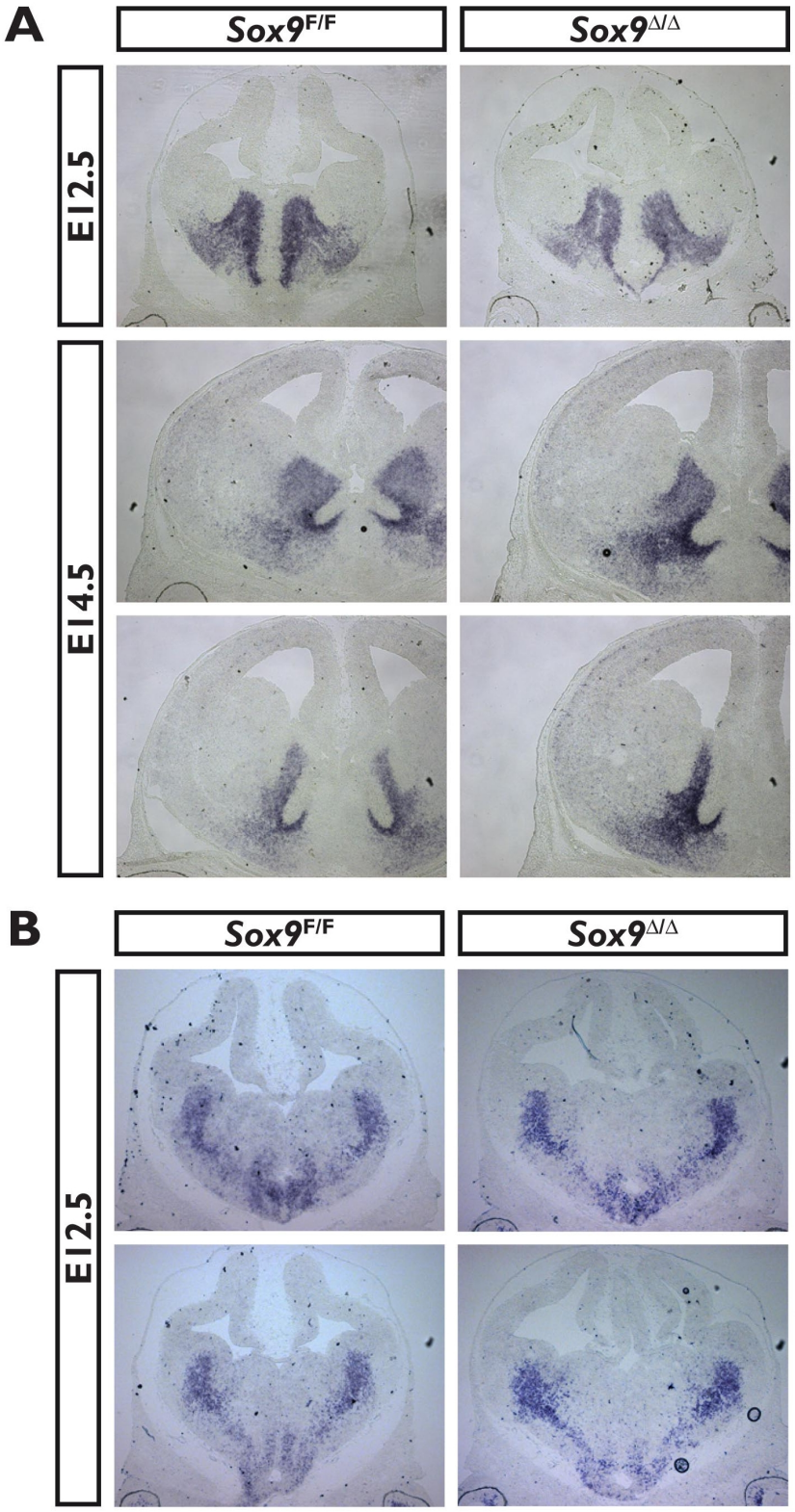

Figure 3-12 A. In situs showing the distribution of *Lhx6* transcripts at E12.5 and E14.5. B. In situs showing the distribution of another marker of interneuons (*Isl1*) at E12.5.

Formation of OPCs in *Sox9*$^{\Delta/\Delta}$ Embryos

As described in the introduction to this chapter, the first OPCs arise deep within the ventral forebrain, in the MGEs, with progressive waves of oligodendrogenesis arising from progressively more dorsal locations, such as the caudal, and lateral ganglionic eminences (LGE and CGE, respectively). The final wave arises from the cortex (Kessaris et al., 2006). The OPCs generated from the MGEs, LGE and CGE are the only ones to arise during embryonic development; only those from the dorsal telencephalon arise postnatally. In order to determine if this initial wave was dependent on *Sox9*, IHC was performed with two antibodies (OLIG2 and PDGFRα), which together identify early OPCs in the ventral telencephalon. It was found that whilst OLIG2 expression is similar between the wild-type and *Sox9*$^{\Delta/\Delta}$ ventral telencephalons, almost all expression of PDGFRα is lost in the *Sox9*$^{\Delta/\Delta}$, suggesting a severe depletion of OPCs (Figure 3-13).

Oligodendrogenesis was also assessed at a later stage (P5), and a depletion of OPCs is again seen (Figure 3-14). In this case, OLIG2/OLIG1 and OLIG2/PDGFRα were counted in a defined region of the medial-most dorsal telencephalon across three adjacent sections, in three *Sox9*$^{\Delta/\Delta}$ brains and three wild-type littermates. The resulting data shows a small (non-statistically significant) reduction in the numbers of OLIG2^{+}/PDGFRα^{+} cells in the *Sox9*$^{\Delta/\Delta}$, and a large and highly significant reduction in OLIG2/OLIG1 double-positive cells (50.5%; $p = 0.005$). Both of these combinations should identify OPCs, although there are fewer PDGFRα^{+} cells compared to OLIG1^{+} cells, perhaps suggesting that expression of OLIG1 is seen across a wider time-window in the oligodendrocyte lineage than is PDGFRα.

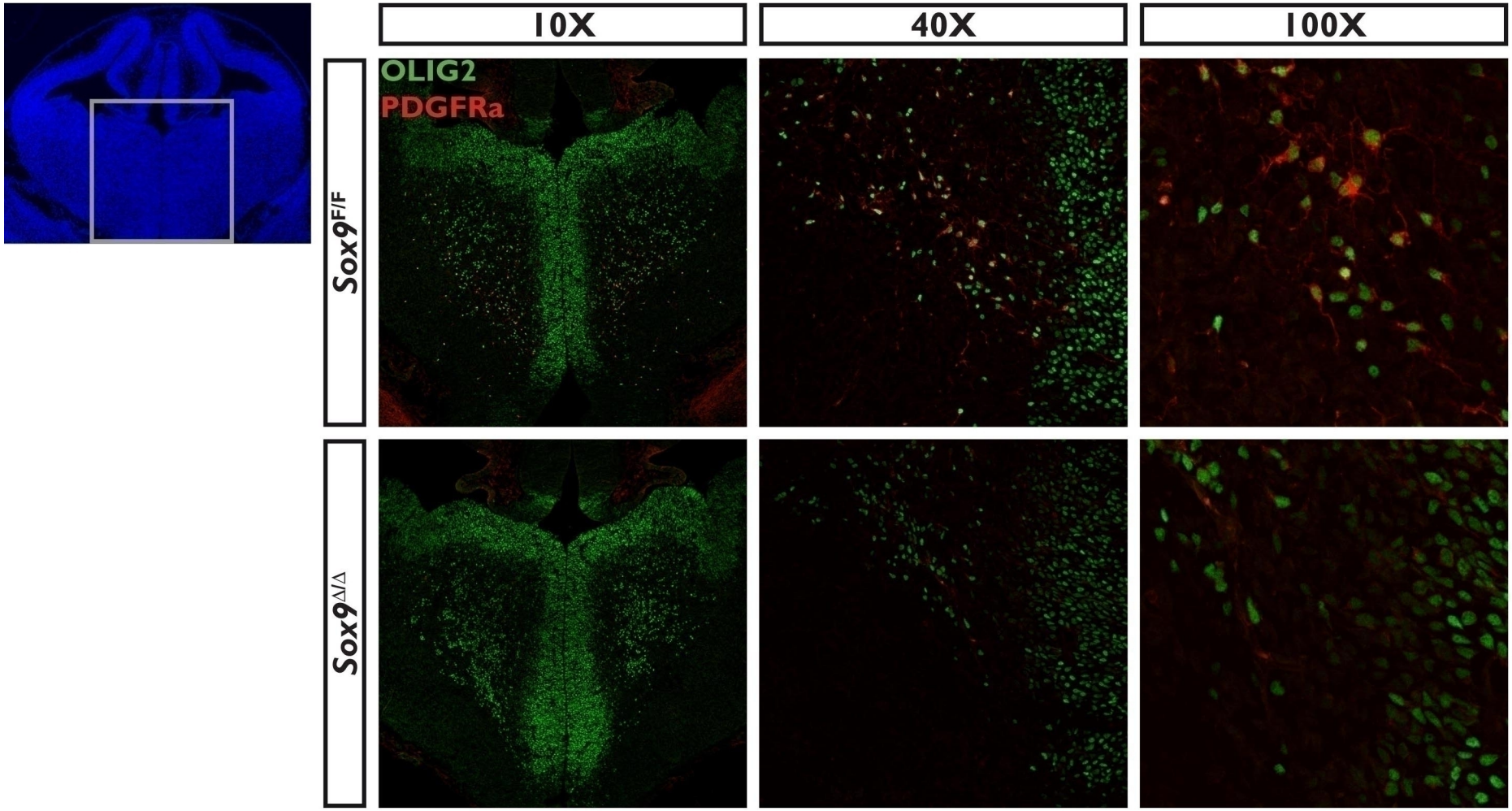

Figure 3-13 Oligodendrocyte progenitors (OPCs) in the ventral telencephalon at E12.5.

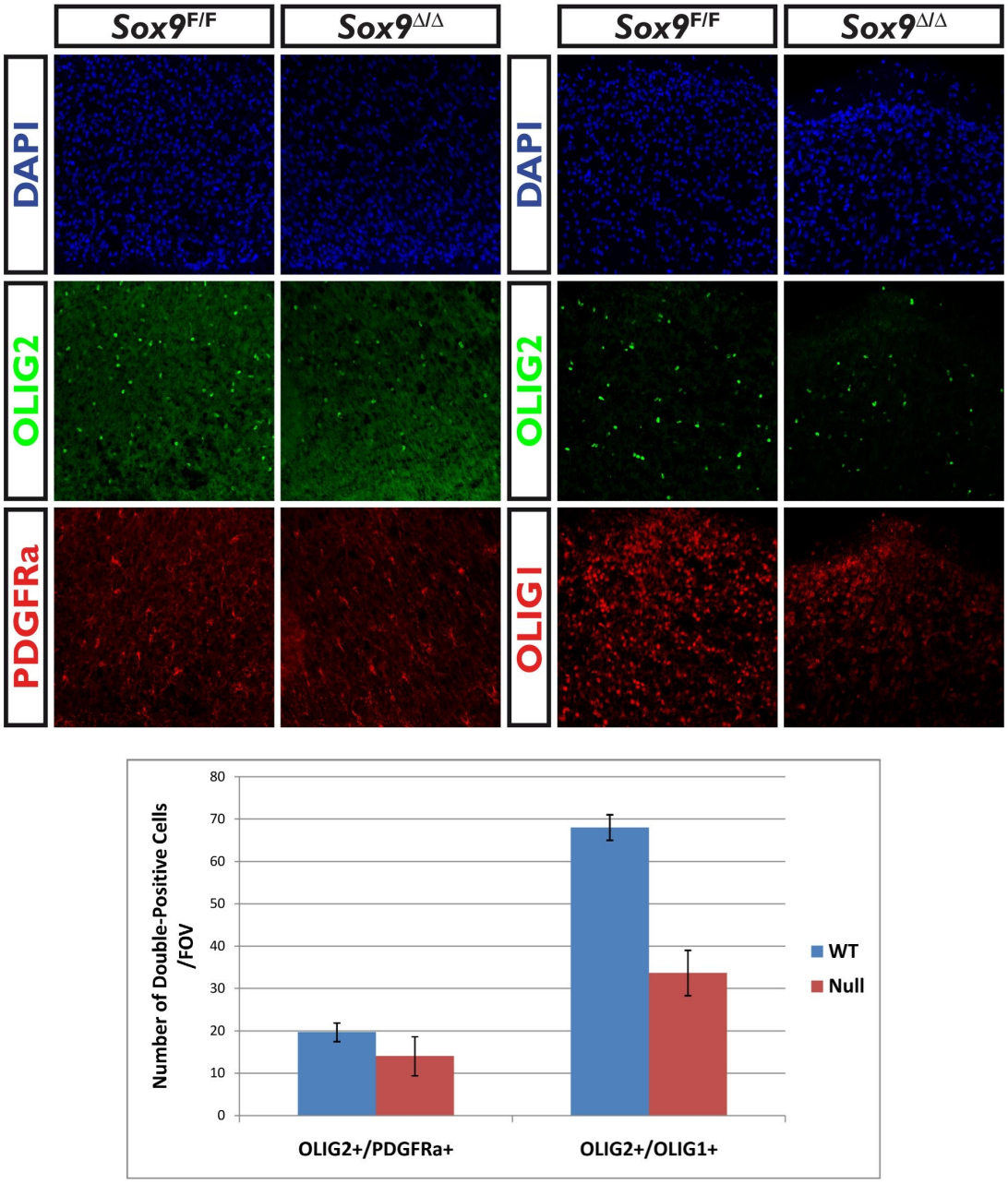

Figure 3-14 Fewer oligodendrocyte progenitor cells (OPCs) are found in the cortex of *Sox9*$^{\Delta/\Delta}$ brains versus wild-type littermates at P5.

Discussion

In light of the strong expression of *Sox9* in the VZ of the developing forebrain from at least E12.5 (our data), and probably earlier, I expected loss of *Sox9* to have a profound effect on the behaviour of progenitors in the forebrain, especially considering the effect of *Sox9* deletion in the neurosphere assay, and its ability to transform neuroepithelial cells into a state that is suggestive of a more radial glia-like phenotype (Scott et al., 2010). However, I have not uncovered any depletion of radial glia (using PAX6 IHC), or premature differentiation into neurons (TuJ1 IHC) in the $Sox9^{\Delta/\Delta}$. Additionally, no change in the tendency of radial glia to generate IPCs was seen at any stage during corticoneurogenesis. Furthermore, and perhaps most convincingly, I see that all the layers of the adult cortex are laid down by the end of gestation in the $Sox9^{\Delta/\Delta}$, and there is no consistent evidence of slowing of this process, or loss of progenitor potential, which would manifest as a lack or reduction of a particular layer.

Having said this, the $Sox9^{\Delta/\Delta}$ mice are not generally viable as adults, with the vast majority dying between P2 and weaning (~4 weeks of age). I initially thought that this was likely to be due to the severe midline defects seen in $Sox9^{\Delta/\Delta}$ brains from E16.5, which involve the failure of the corpus callosum and hippocampal commissure to form, and perhaps the failure of the telencephalic vesicles to fuse, a process that forms the commissural plate, which is a prerequisite for commissural tract formation. However, the few surviving $Sox9^{\Delta/\Delta}$ adults that I have examined show complete agenesis of the corpus callosum, indicating that this defect is not in itself sufficient to explain their deaths. A more likely explanation is the drastic, although not complete, loss of OPCs in the $Sox9^{\Delta/\Delta}$. This affects the earliest source of forebrain OPCs (those arising from the AEP/MGE), and is also evident in the postnatal dorsal telencephalon. The fact that this defect is still seen

at P5 suggests that other sources of forebrain OPCs are also affected, because otherwise, I would expect those OPCs generated from the LGE/CGE or postnatally from the dorsal telencephalon to compensate for the loss of the early population. Indeed, this is what Kessaris and colleagues observe when they ablate early sources of OPCs (Kessaris et al., 2006).

Previous work and our own supports a role for *Sox9* in the specification of OPCs, which are a population of migratory precursors that divide as they migrate, passing through a number of intermediate phenotypes before differentiating as oligodendrocytes. As I alluded to in the *General Introduction*, SOX proteins are known to commonly function in partnership with other transcription factors. High on the list of potential SOX9 binding partners in the oligodendrocyte lineage would have to be other proteins that have been shown to be required for the induction of OPCs, such as OLIG2 or MASH1.

One possible explanation for the failure of corpus callosal and hippocampal commissure formation in the $Sox9^{\Delta/\Delta}$ is the absence of midline glial populations. These midline glial populations are essential for the formation of the corpus callosum, probably through a mechanism involving SLIT/ROBO signalling. This is consistent with the presence of bundles of Probst, which suggest that the defect in $Sox9^{\Delta/\Delta}$ embryos lies in midline crossing, rather than neurite outgrowth or axon guidance in general. However, the fact that axons involved in another commissural tract, the anterior commissure, cross the midline successfully shows that these mice do not have any fundamental defect in the mechanism of midline crossing. One important midline glial population, the indusium griseum, is formed by the delamination of radial glia in the medial VZ, which then migrate to a central region above the future corpus callosum and adopt an astrocytic morphology. In Chapter 5, I show that a number of down-regulated genes in the $Sox9^{\Delta/\Delta}$

are expressed in exactly the pattern that would be expected for radial glia just prior to their delamination, supporting a potential role for *Sox9* in this process. *Sox9* has similarly been shown to be important for specifying neural crest cells, prior to their delamination from the dorsal neural tube (Spokony et al., 2002, Cheung and Briscoe, 2003). The location of these transcripts seem to favour the defect being one of specification of indusium griseum cells or delamination, although it is also possible that there is a generalised failure of the anterior fusion of the telencephalic vesicles, a process which is also thought to be mediated by another migratory population of glia, the midline zipper glia.

The normal architecture of the $Sox9^{\Delta/\Delta}$ CP is surprising because SOX9 is strongly expressed in the VZ of the forebrain long before the onset of gliogenesis, and in fact from the very beginning of neurogenesis. SOX9 must be performing some role in these cells, or the enhancers that maintain its expression in the neurogenic VZ would degenerate as a result of random mutations. One explanation is that the phenotype of *Sox9* deletion is hidden by compensation from other transcription factors. This theory is supported by the finding that a number of *Sox* genes are expressed in the VZ of the dorsal telencephalon (described in more detail in the *General Discussion*, Chapter 8) because, due to the homology of their DNA-binding domains, they are highly likely to exhibit a degree of functional redundancy. For instance, between the HMG Boxes of SOX8 and SOX9, only one of the 79 amino acids are different (Barrionuevo and Scherer, 2010).

Chapter 4 Transcriptional Targets of SOX9 in the Neural Progenitors of the Dorsal Telencephalon

SOX9 is expressed in the VZ of both the spinal cord and the dorsal telencephalon well before the onset of gliogenesis in either region of the CNS. Since our phenotypic analysis has indicated that *Sox9*, at least when deleted with the NesCre, does not appear to have a role in corticogenesis, this leaves the other hypothesis I alluded to in the *General Introduction*; that *Sox9* may set up conditions in neural progenitors prior to gliogenesis that allows them to respond to gliogenic signals when they arise. In order to answer this question, I took $Sox9^{\Delta/\Delta}$ dorsal telencephalons, two days before the expected onset of gliogenesis from this part of the forebrain (at E16.5; Kessaris et al., 2006), and FACS sorted them with the aim of purifying or enriching a population of neural progenitors, and used transcriptional profiling techniques to compare their gene expression profiles with that of similarly-sorted wild-type E16.5 dorsal telencephalon cells. I then used bioinformatics techniques to identify patterns of gene expression changes that might implicate a particular pathway or receptor that could explain the reduction or delay in gliogenesis seen in the $Sox9^{\Delta/\Delta}$.

Introduction

Enriching a Population of NPCs

There are a number of potential strategies for enriching a population of progenitors from the embryonic dorsal telencephalon: The first would be to use a reporter strain in which a fluorescent protein is expressed under the control of an NPC-specific enhancer, such as in the *Sox2*-GFP mice. Another option would be to combine an inducible Cre, expressed in NPCs (such as the *Sox1*-CreER^{T2}), with a reporter transgene such as the ROSA26-EYFP, in which a STOP cassette is flanked by LoxP sites. Then, after activating the Cre by administration of tamoxifen, YFP^{+} cells could be sorted. Alternatively, an antibody that recognises an antigen specific to the cell population of interest could be used for sorting.

The first option (using the *Sox2*-GFP mice) would seem like an excellent strategy for obtaining a pure population of NPCs; however, when GFP expression was assessed by IHC (data not shown), expression was detected in the progeny of NPCs suggesting that GFP is more stable than the SOX2 protein, precluding its use in sorting NPCs. The second option (using a Cre reporter strain) is not feasible because we are already using a Cre transgene (the NesCre) to delete *Sox9* so, since all cells of the CNS arise from *Nestin*$^{+}$ progenitors, they would all have activated expression of YFP. This leaves the option of sorting using a cell-surface marker, of which a handful have been described in the literature: CD133 (Uchida et al., 2000, Panchision et al., 2007), CD15, CD29, CD56, CD146 and FORSEI (Pruszak et al., 2009). I chose CD133 since in the developing human and mouse CNS, it has been shown to mark neurosphere-forming cells (Uchida et al., 2000, Panchision et al., 2007), which are those residing in the VZ; however, IHC demonstrated that, at least in the mouse forebrain, it is not specific to VZ cells and is also

expressed in the IZ, and to a lesser extent, in the SVZ (Figure 4-1). Having said this, since it is not expressed in CP cells, this method could be used to remove contaminating CP cells, thus slightly enriching for VZ cells relative to unsorted samples.

CD133 is a cell-surface receptor present on a variety of progenitor cell types, and also in 'cancer stem cells' which are thought to be responsible for tumour growth in some, if not all, solid tumours (Meregalli et al., 2010, Singh et al., 2004). In the context of the haemopoietic system, CD133 has been used to enrich a subset of haemopoietic stem cells (granulocyte-macrophage progenitors; Yin et al., 1997). In the human and murine foetal CNS, $CD133^{High}$ cells isolated from the brain and spinal cord have been shown to contain a higher proportion of neurosphere-forming cells compared to unsorted cells, and $CD133^{Low}$ cells contain few, if any, cells with this capacity (Uchida et al., 2000, Panchision et al., 2007). Furthermore, a recent study identified that CD133 is strongly (but heterogeneously) expressed in NS cells derived from the embryonic mouse CNS, and the authors found that the strongly expressing NS cells tended to be those in the S, G_2 or M phase of the cell cycle (Sun et al., 2009)

Transcriptional Profiling

Currently, two techniques exist to acquire information about the global transcriptional state of cells, allowing comparisons to be made between different cells or tissues, such as mutant versus wild-type, or diseased versus non-diseased samples. There is the tried-and-tested method of microarray chips, and with recent advances in next-generation sequencing, allowing massively-parallel sequencing of cDNA molecules, 'RNA sequencing' (RNA-Seq) has become possible. Both techniques require that total RNA from cells is converted into cDNA. Microarrays determine the quantity of each transcript

by measuring the fluorescent signal produced by the hybridisation of cDNA molecules to complementary oligonucleotides synthesised on a glass surface. The same information can be acquired from RNA-Seq because, for a given depth of sequencing, the number of times each transcript is sequenced represents its concentration in the original sample. RNA-Seq is also not subject to the vagaries of background fluorescence or cross-hybridisation that afflict microarrays, but does carry the potential for 'mutant' reads (those containing sequencing errors) to falsely align within the genome (Mortazavi et al., 2008).

DNA Microarrays

The first example of a microarray chip was designed and made by Schena and colleagues in 1995, followed swiftly by the production of the first array chip to include probes to all known and predicted genes in yeast (Lashkari et al., 1997), a concept that was then extended to mammalian genomes. The type of microarray used in this chapter involves a glass or silicon surface onto which short oligonucleotides (or 'probes') have been synthesised at known points in a vast array; these points are called 'features'. The array is designed so that each transcript is detected by 10 probes (called 'perfect-match' or PM probes). Each of these PM probes has a corresponding mismatch (MM) probe that is identical to it except that it differs in a few bases in the middle of the sequence, which should prevent it from annealing to the same sequence as the PM probe. Since microarrays rely on fluorescent signal detected at these features, the signal at the MM probe gives a read out of background fluorescence. Collectively, these 20 probes are known as a 'probe set'. In order to obtain expression data, the RNA sample in question is first converted into cDNA, and then labelled with a fluorescent molecule such as Cy3 or Cy5. This labelled cDNA is applied to the surface of the chip, and then the chip is washed

several times to remove non-specifically bound cDNAs, and scanned for fluorescent signal. The intensity of signal is then measured at each feature. Some analysis methods ignore the MM signal and summarise the PM values, such as the Robust Multichip Analysis (RMA) algorithm, whereas others subtract the MM intensity from the PM intensity to give a normalised value for each probe (MAS5 algorithm).

Microarrays are subject to two major sources of error. Firstly, cross-hybridisation of similar sequences leads to a high degree of background fluorescence, which may obscure differences in low-expressed genes. Also, in order to use small quantities of RNA in microarray analysis, several rounds of PCR amplification are required, which may not be linear for all transcripts. There are also limitations inherent to a system based on fluorescence, because the signal can become saturated: If a feature on one chip in an experiment is saturated, and not in another chip, it is impossible to say whether it is 10, 100 or 1000 times more expressed in the former situation. This limitation is not seen in RNA sequencing, where the output variable is the number of times a particular transcript was sequenced, which is a proxy measure of its original concentration.

Second-Generation Sequencing

The majority of new, second-generation sequencing techniques are based on the dye-terminating technology originally performed by Sanger in 1977, which has been the dominant method of sequencing since the early 1980s. The Sanger method involves first cloning the DNA fragment of interest into a vector, and then using a polymerase to extend the 3' end of a sequencing primer in the presence of dNTPs that contain a small percentage of a particular nucleotide (A, T, C or G) that cannot be used for further extension of the strand. This process is carried out in four different reaction mixes, one

containing a small percentage of terminating As, another with a small percentage of terminating Ts, and so on. When each of these reactions is complete and run out on a gel, a variety of bands will be seen and the length of each band will show the positions of that particular nucleotide in the sequence. Sanger sequencing can be used for transcriptional profiling through the production and sequencing of libraries of expressed sequence tags (ESTs), where all the RNA molecules within a sample are converted to cDNA, cloned into vectors and then sequenced. After sequencing all of these clones, highly expressed sequences will be read more often than less prevalent sequences, and the incidence of reading sequences can be compared across samples from different sources, such as wild-type and mutant cells, and differentially-expressed genes detected. The major limitations of this approach are its huge cost, and the rate-limiting step of transforming and picking colonies (Shendure and Ji, 2008). Another problem is the limited parallelisation of Sanger sequencing; a machine will only sequence 96 or 384 clones simultaneously, so many thousands of runs would be required to sequence an entire transcriptome to the required level of depth.

In order to overcome this problem, second-generation sequencers have been developed with the aim of sequencing vast number of cDNAs in parallel, without the need to clone or pick bacterial colonies. These sequencers typically produce short reads ~35bp in length, but may be as long as 100bp (454 sequencing). A number of different approaches to parallelisation have been taken, but the common characteristic is that cDNAs are immobilised on a surface or on beads. The technique that is available at our Institute is that developed by Illumina, and involves reversible dye-terminator chemistry – a development of the Sanger method.

With the availability of the mouse genome sequence, allowing the alignment of short reads to a reference genome, it is now possible to use this technique to look for differentially-expressed genes between samples by comparing the number of reads aligning to a particular locus, which represents the abundance of that transcript in the original sample. The process of RNA-Seq is complex, but essentially it involves the production of double-stranded cDNA from fragmented RNA, followed by its attachment to a solid surface (the flow cell), and sequencing by a reversible dye-terminator chemistry. Sequencing occurs in the presence of nucleotides with a nucleotide-specific fluorophore attached, which, like the terminating nucleotides of Sanger sequencing, halt primer extension; the difference is, an enzyme can be added to remove the fluorophore, and convert the nucleotide into one that is capable of being extended. At the first cycle, one fluorescent dNTP is added to a vast number of sequences extending in parallel, and an image taken. The fluorescent signal at each spot represents the nucleotide at that point in the sequence. Then, a cleavage enzyme is added and the process is repeated, so that the sequence of millions of cDNAs attached to the surface of the flow cell are determined in parallel.

cDNA Normalisation

In order to compare the transcriptomes of two samples, the first step is to fragment the RNA, and to convert it into single-stranded cDNA. Then, following the degrading of the RNA by an RNase, a second strand can be formed, giving double-stranded cDNA fragments. Before proceeding to this step, it is commonplace to remove all RNA species apart from messenger RNAs (mRNAs). This is primarily to ensure that rarer protein-coding transcripts are sequenced to sufficient depth. Without any attempt to remove abundant RNA species such as ribosomal RNA, much of the resources of the sequencing

machine would be consumed in sequencing these transcripts to huge depth, whilst very few rarer transcripts would be sequenced. The drawback of this approach is that interesting non-coding RNAs, such as microRNAs, are also eliminated. Another drawback, which precludes this approach from being used in our case, is the large quantity of starting material that is required for poly-A selection (1μg). In place of poly-A selection, we have used duplex-specific nuclease (DSN) normalisation to remove abundance RNA species. This relies on the principle that once you have denatured a cDNA library, abundant transcripts will find their complementary partners very quickly, whereas rare transcripts will take a very long time to find theirs (Zhulidov et al., 2004). In DSN normalisation, double-stranded cDNA molecules are rapidly denatured, then allowed to re-anneal at 65°C for several hours. After 5 hours, a duplex-specific nuclease, which degrades double-stranded DNA is added to eliminate those denatured cDNA strands that have found complementary partners. The overall effect of this process is to reduce the proportion of the cDNA that represents common transcripts, allowing differential expression amongst low-abundance transcripts to be more readily detected.

Bridge Amplification

Once constructed, the cDNA library must be attached to a solid surface (the 'flow cell') prior to sequencing by the 'sequencing by synthesis' (SBS) method described previously. However, the fluorescence signal from a single nucleotide would be extremely difficult to detect using optics suitable for scanning a large area of flow cell; therefore, an amplification step is required, and this is performed by 'bridge amplification'. The flow cell itself is composed of a solid surface onto which both forward and reverse primers have been covalently bonded by their 5' ends. These primers are complementary to the adaptors ligated to either end of the cDNA molecules during library construction. When the denatured library is added to a lane of the flow cell, one end of each cDNA molecule will anneal to a primer. Because the 3' ends of both primers are protruding, the cDNA molecule cannot, at this stage, anneal to both primers in a 'bridge' fashion. dNTPs and a polymerase are added, and the sequence is extended from the primers to give double-stranded cDNA. Formamide is added to denature the strands, releasing the original cDNA template into solution, which is discarded. The remaining complementary copies of these cDNAs are a continuation of the primers. The trailing end of the attached copy is the 3' end, and so it can 'flop' over and anneal to one of the reverse primers if it is derived from a forward primer, or vice-versa. Extension from this primer results in a complementary strand being extended from the new primer. This bridge can then be denatured with formamide, and the process repeated again. After 35 cycles, each cluster (derived from an individual single-stranded cDNA molecule) has grown to ~1,000 copies, which contains a mixture of both sense and antisense strands, attached to the flow cell by their 5' ends. Finally, an enzyme is used to cleave one of the primers, leaving each cluster composed of a single, identical sequence. As SBS proceeds, the fluorescent signal is read from a vast

number of cDNAs in a particular spot on the flow cell, each having incorporated the same fluorescently-labelled dNTP.

Alignment and Analysis

Once short reads have been obtained from each library, they must be aligned either to a reference genome, or more appropriately for transcriptional profiling, a reference transcriptome. From this alignment, the total number of reads aligning to each transcript can be determined, and once these counts are normalised for the total size of the library (i.e. total number of mapped reads), the expression of each gene can be compared between samples. Naturally, almost all transcripts will show small differences in expression between samples, so the challenge becomes one of finding statistically significant differences between two sets of replicates. Because RNA-Seq data is in the form of count data, it has traditionally been modelled using the Poisson distribution; however, it was found that this tended to underestimate the variance of replicates. A recent paper by Ander and Huber (2010) claims to have overcome this problem of 'over-dispersion' by using a statistical test based on the negative binomial distribution. Hence, we have used their implementation of this method to interpret our own data in R/Bioconductor.

RNA-Seq has many potential advantages over microarrays, such as its huge dynamic range and its ability to more readily distinguish differential expression in low abundance transcripts. However, RNA-Seq is not devoid of errors. For example, because it relies on the alignment of short reads, many problems arise from sequence similarity within the genome. Mortazavi et al. (2008) investigated this problem by segmenting the genome into 25-mers, and found that only 76% of these mapped uniquely within the mouse genome.

The remainder mapped to multiple sites, such as paralogs. Other potential mischief may be caused by occasional wrong base calls. Mortazavi and colleagues suggest that this might be a particular problem in gene families where one member of the family is highly expressed and another is very slightly expressed, or not expressed at all. The highly expressed family member would be expected to generate 'mutant reads' at a certain rate (the error of base calls is ~1% on the Illumina platform; Shendure and Ji, 2008), and some of these might erroneously align to the non-expressed family member.

Results

In order to obtain total RNA from *Sox9*$^{\Delta/\Delta}$ and wild-type dorsal telencephalon cells, crosses were set between *Sox9*$^{Fl/Fl}$ and *Sox9*$^{Fl/WT}$;NesCre animals, and the litters harvested at E16.5. From each embryo, the dorsal half of the telencephalic vesicles were dissected, and triturated to give separate, single cell suspensions. As described in the introduction to this chapter, in order to obtain as pure a population of VZ cells as possible, i.e. those cells which in the wild-type situation are expressing *Sox9*, the CD133 antigen was used to enrich a population of dorsal telencephalon cells for progenitors. In order to confirm that there is no change in CD133 expression in the absence of *Sox9*, and also that CD133 is expressed in VZ cells in both the mutant and wild-type, immunohistochemistry with an antibody against CD133 was performed (shown in Figure 4-1). The results show that in the wild-type, the cells of the VZ co-express SOX9 and CD133 (panels A and D, magnified in B and E; SOX9 is nuclear and in green, CD133 is found in the membrane and is in red). CD133 appears to be strongly expressed in the cells of the VZ, SVZ and IZ, but is significantly less strongly expressed in the CP, which is also consistent with the FACS plots (Figure 4-2) that show that approximately 60% of the cells of the E16.5 dorsal telencephalon fall into the CD133^{High} population. Although an antibody capable of sorting a pure population of VZ cells would have been ideal, using this antibody will have cleansed our original sample of CP cells, and thus marginally enriched our population for those cells (the VZ cells) which, in the wild-type situation, express *Sox9*. Therefore, this method was used to enrich populations of CD133^{High} cells from three *Sox9*$^{\Delta/\Delta}$ dorsal telencephalons and three *Sox9*$^{Fl/Fl}$ controls (such that each control was a 'paired' littermate of the same sex). RNA was then extracted from these samples and subjected to transcriptional profiling by microarray and RNA-Seq.

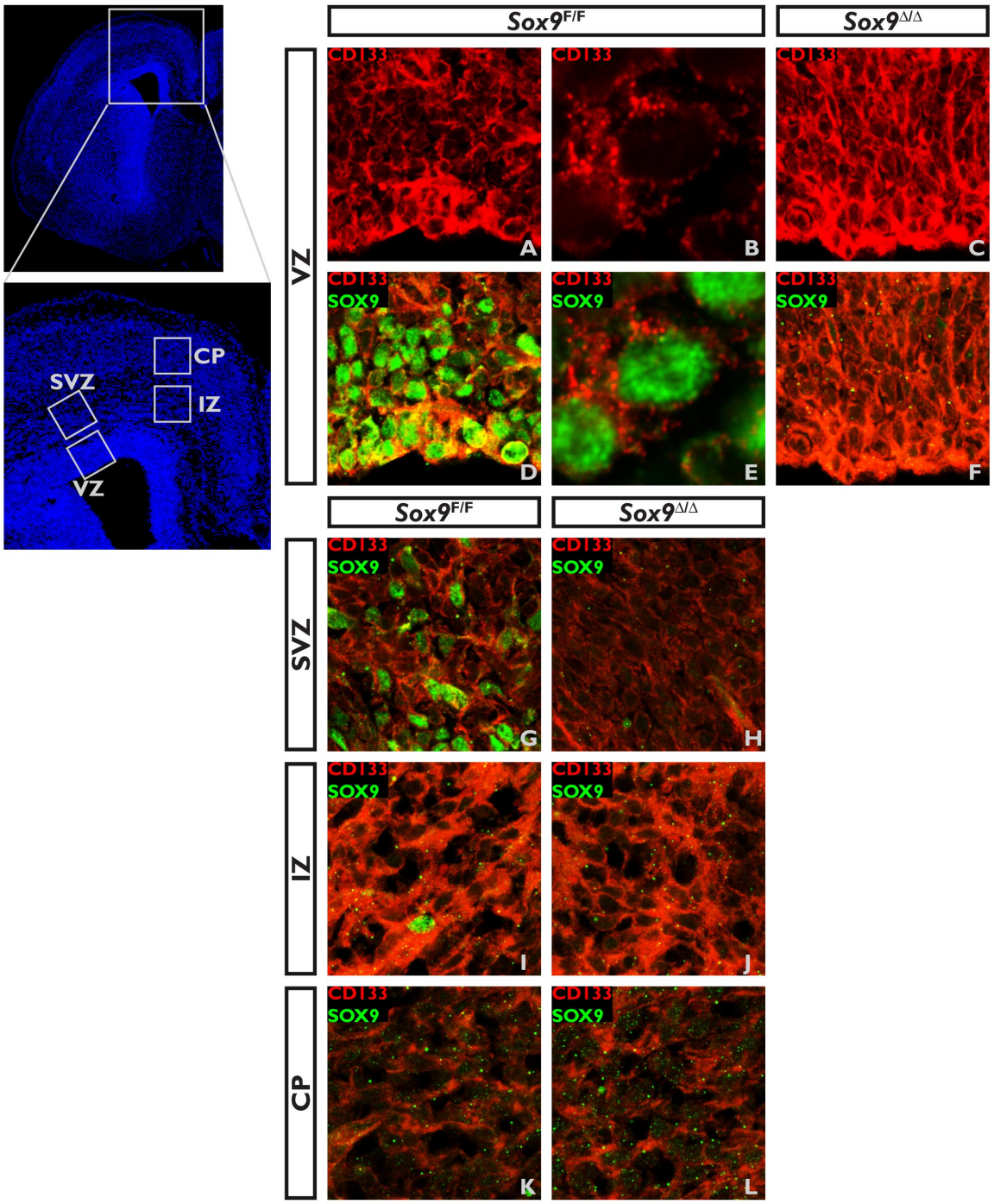

Figure 4-1 CD133/SOX9 immunohistochemistry on sections of the E16.5 forebrain from *Sox9*$^{\Delta/\Delta}$ and wild-type littermates. All images are at 240X, except B and E, which are magnifications of A and D, respectively (at 1200X). VZ – ventricular zone, SVZ – subventricular zone, IZ – intermediate zone, CP – cortical plate.

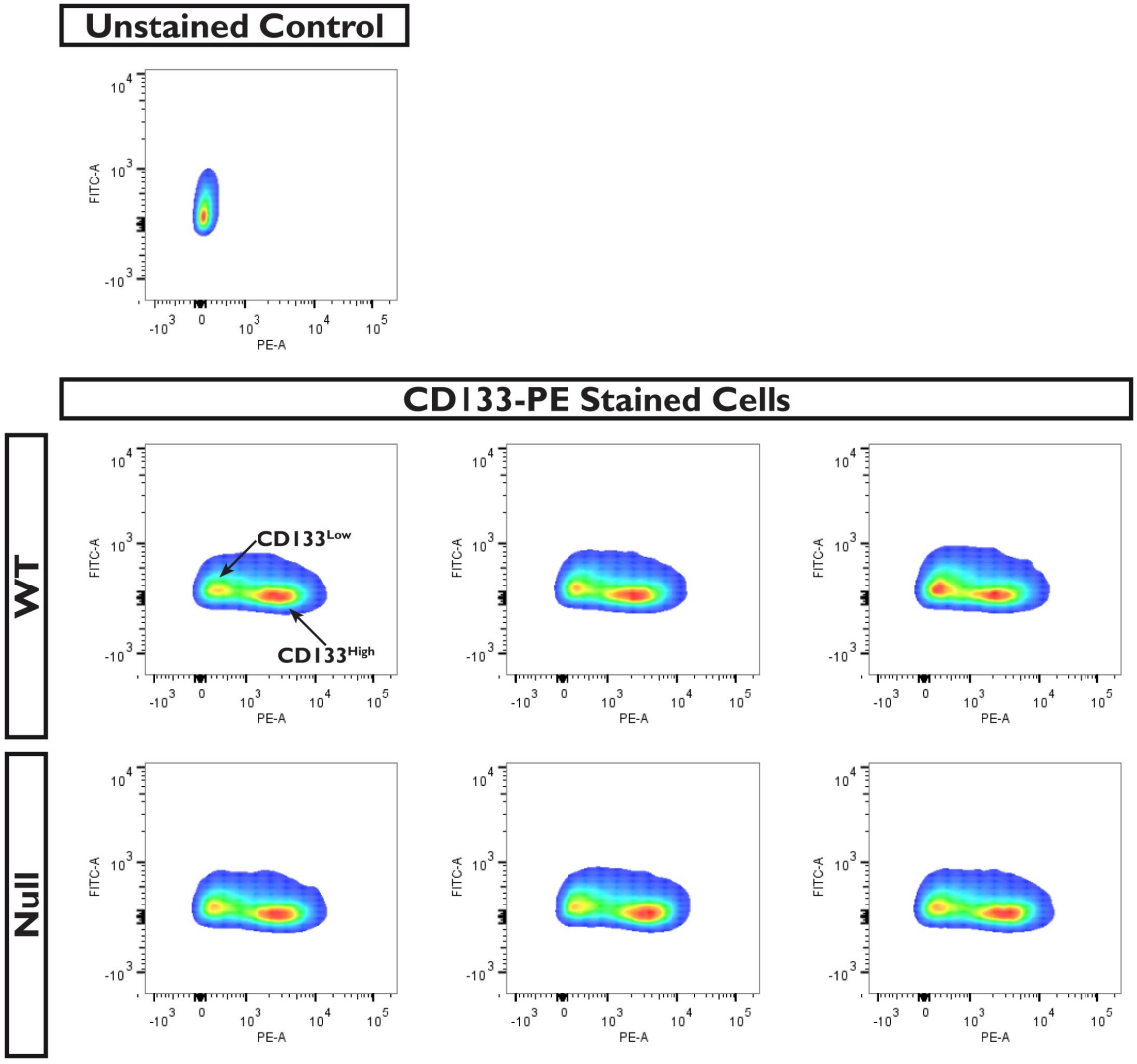

Figure 4-2 FACS plots of CD133-PE- and unstained populations.

RNA-Seq

RNA extraction from each sample yielded about 300-400ng of total RNA. Because this was below the 1μg required for library construction under the standard Illumina protocol, which involves poly-A selection with poly-T attached beads, the decision was taken to make the cDNA libraries directly from total RNA and to reduce the prevalence of highly-abundant transcripts by 'normalising' them after construction using a duplex-specific nuclease from the Kamchatka crab (DSN normalisation; Zhulidov et al., 2004), which requires only 100ng of total RNA as a starting material. Hence, 100ng of each of the RNA samples was used to make cDNA libraries in accordance with Illumina's Sample Preparation Guide (revision D), with the exception of the poly-A selection step, which was omitted, proceeding directly to RNA fragmentation. In brief, library construction involved synthesising first-strand cDNA from the fragmented RNA, and then degrading the RNA and filling in the second strand using DNA polymerase. To these short segments of double-stranded DNA, double-stranded adaptors were ligated, and primers against the adaptors used to amplify the library by PCR. DSN normalisation was then performed as described in the Illumina protocol 'DSN Normalization' (revision C), and the library amplified by a final PCR.

The six normalised libraries were then each seeded to a lane of a flow cell and underwent cluster generation by bridge amplification before being sequenced on the Illumina platform. Each sample produced ~50 million paired reads. The reads from each sample were then separately aligned to the July 2007 (NCBI37/mm9) assembly of the mouse genome. Alignment of reads to the *Sox9* locus is shown in Figure 4-3. Consistent with a *Sox9* floxed allele in which exons 2 and 3 are flanked by loxP sites, reads only aligned to the 5' untranslated region (UTR) and first exon in the $Sox9^{\Delta/\Delta}$; in the wild-type, reads

aligned evenly over the entire gene. From each alignment, total exon reads at all annotated features of the genome were extracted and analysed for differential expression using DESeq, which is an implementation of the method of Anders and Hubel (2010) in R/Bioconductor. The resulting volcano plot is shown in Figure 4-4A. From a list of genes found to be statistically significant (at a p-value cut-off of 0.05), 115 were more than 1.25-fold down-regulated, and 142 were more than 1.25-fold up-regulated (lists shown in Appendix A).

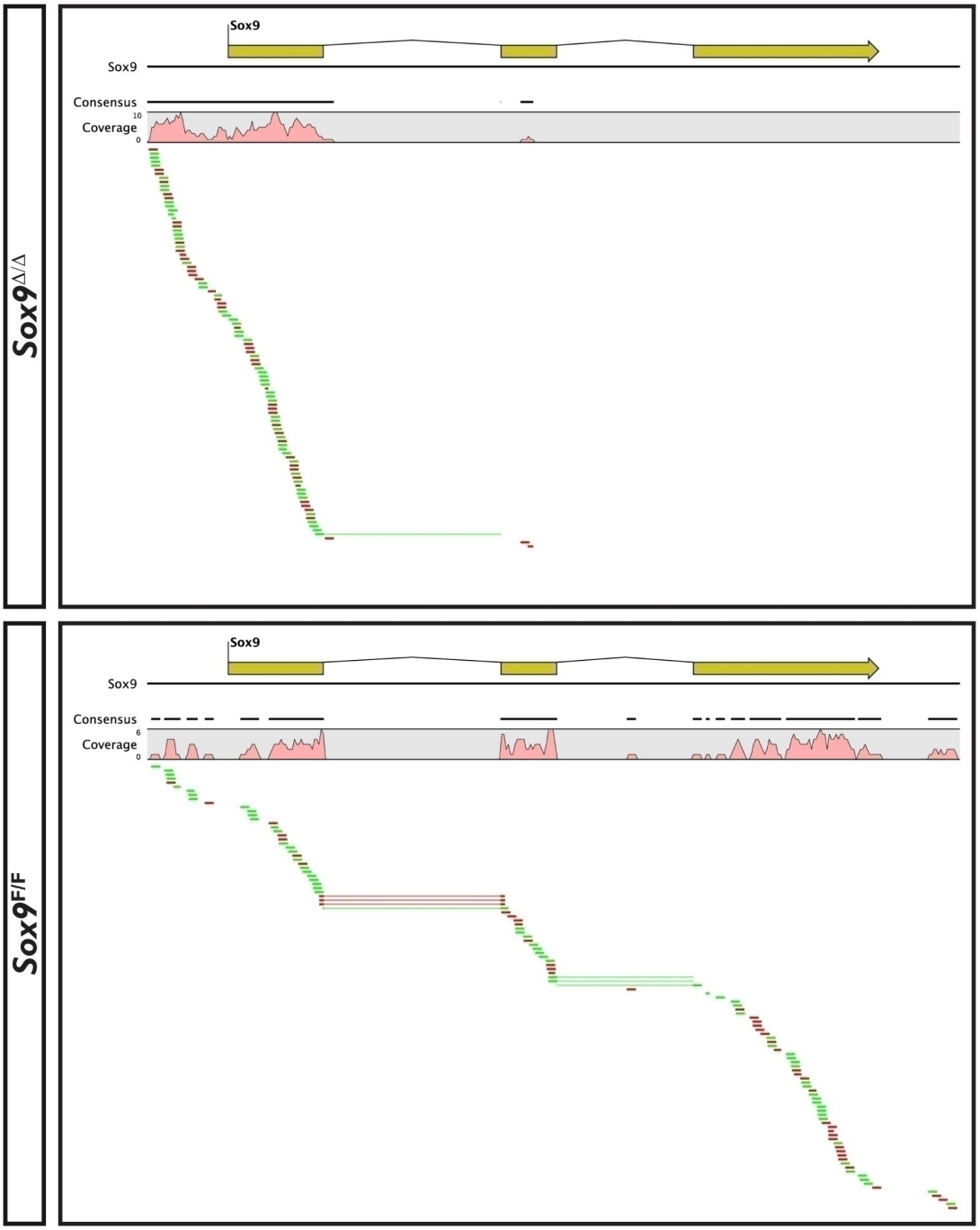

Figure 4-3 Alignment of reads from the sequencing of RNA extracted from CD133^{High} cells to the *Sox9* locus in the *Sox9*$^{\Delta/\Delta}$ and wild-type situation.

Microarray

Because RNA-Seq is a relatively new technique, and we were performing a normalisation step that had never been used at this Institute before, we decided to perform arrays on independent samples for comparison. After filtering out probe sets with low expression, which are thought to be unreliable in a hybridisation-based system, differentially-expressed probe sets were called using a Student's t-test with a p-value cut-off of 0.05. The resulting volcano plot is shown in Figure 4-4B. Probe sets not associated with an NCBI-annotated gene and those that map to multiple genes were removed from the list. Where the list of differentially-expressed genes contained multiple probe sets mapping to the same gene, the entry with the highest fold change was kept and the other entries deleted to ensure that each gene was represented only once in the list. The most differentially-expressed probe set was used instead of averaging the fold change among multiple probe sets to preserve a p-value associated with differential expression of that gene (although the fact that two independent probe sets are present means that the true p-value is much lower). Reassuringly, *Sox9* was the most differentially-expressed gene at 31.8-fold down-regulated. Once this entry was removed, 64 down-regulated and 76 up-regulated genes were differentially-expressed at a fold-change cut-off of 1.25 (lists shown in Appendix B).

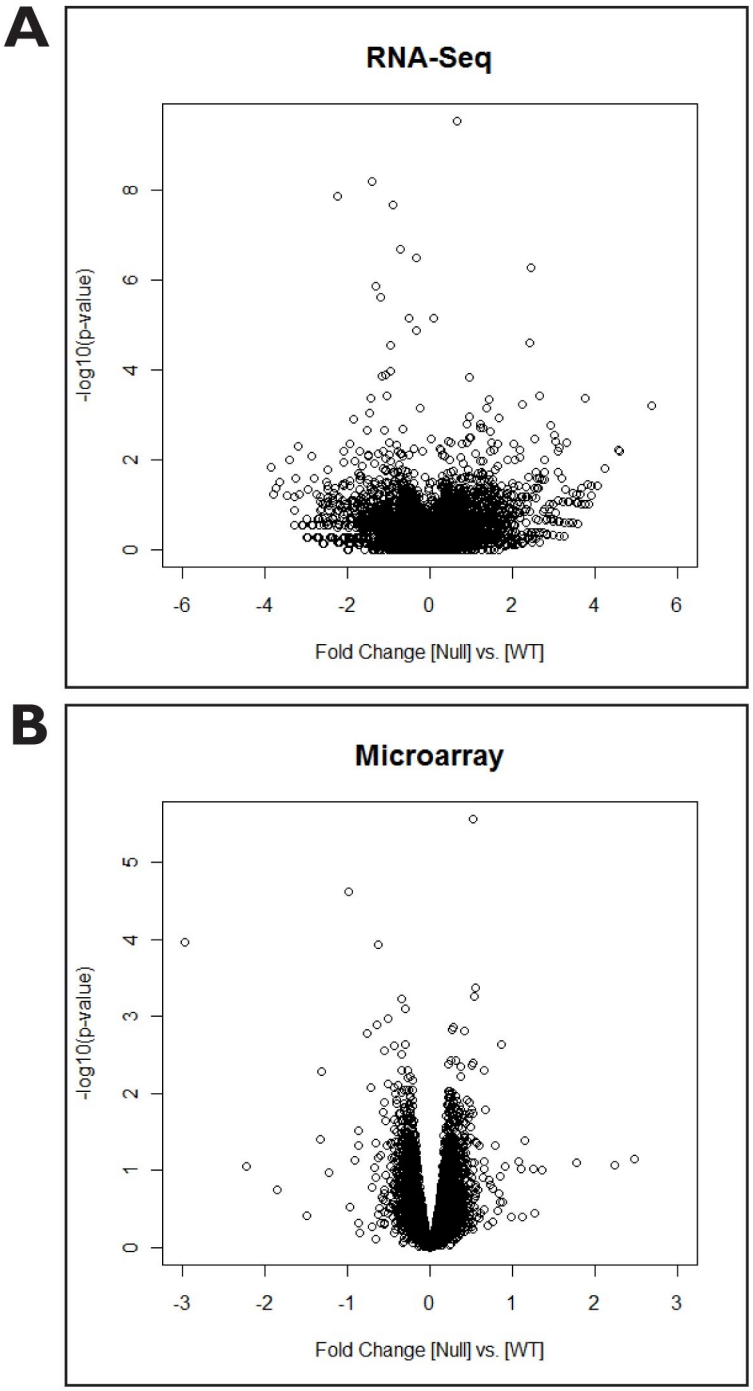

Figure 4-4 Volcano plots for RNA-Seq (A) and microarray data (B).

Gene Ontology Categories

The categories of molecular function into which these genes fall are shown in Figure 4-5 (defined by the Gene Ontology Consortium); however, it is difficult to draw conclusions from this data because certain categories may be highly represented in a gene list simply because a large number of genes in the genome fall into that category. For example, the dominant categories in both the RNA-Seq and Microarray Down-Regulated datasets are 'protein binding' and 'ion binding'. 24.3% of the RNA-Seq Down-Regulated dataset and 31.1% of the Microarray Down-Regulated dataset fall into the protein binding category, compared to 17.4% of genes in the mouse genome as a whole. In the case of ion-binding, this category accounts for 18.9% of the RNA-Seq dataset and 27.0% of the array dataset, compared to 10.4% genome-wide. In terms of the location of the gene products in the cells, the majority in both datasets are located in the cell membrane (27% [RNA-Seq], 41% [microarray]), the next largest category being the nucleus (17% [RNA-Seq], 15% [microarray]). The graphs depicting 'Biological Process' categories are more difficult to interpret. The two largest categories for both datasets are 'Metabolic Process' and 'Biological Regulation'; however, these each comprise 27% of the genome so little can be gleamed from this information. However, in both datasets, 'Localisation', 'Developmental Process', and 'Cell Communication' are enriched above their prevalence in the genome as a whole (11%, 11% and 5%, respectively). In order to determine if these, or any other perceived enrichments of GO categories are statistically significant, we turned to GO Term Enrichment Analysis, which returns a fold enrichment of genes from a particular category in a dataset, relative to the number expected from that category by chance, and a p-value associated with that enrichment.

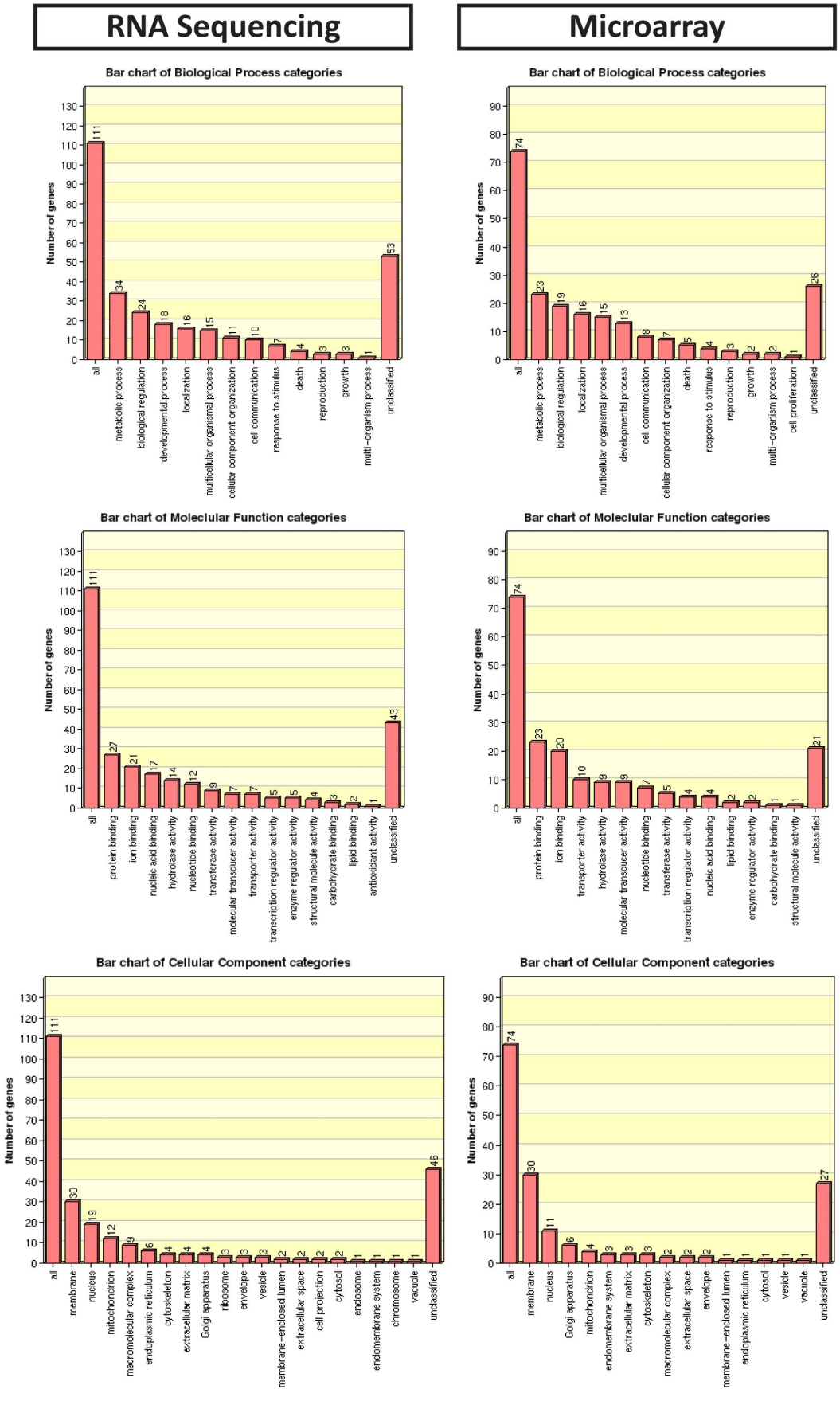

Figure 4-5 The different Gene Ontology categories into which the genes of each gene list fall.

Down-Regulated Gene Lists

Among the down-regulated datasets, only one category, 'Platelet-derived growth factor binding', is enriched in both the RNA-Seq and the array lists (Figure 4-6 and Figure 4-7), and in both cases this enrichment results from the presence of two genes, 'platelet-derived growth factor receptor alpha polypeptide' (*Pdgfra*) and 'collagen type II, alpha 1' (*Col2a1*). *Pdgfra* encodes a tyrosine kinase receptor that is bound primarily by platelet-derived growth factor A (PDGF-A; Betsholtz et al., 2001).

PDGF-A was discovered in the 1980s as a potent mitogen for fibroblasts, smooth muscle cells and glial cells in culture, and is secreted by neurons in the CNS (Yeh et al., 1991). It is essential for the proliferation of $Pdgfra^{+}$ oligodendrocyte progenitor cells (OPCs) *in vivo*, and only 10% of the normal complement of OPCs are seen in PDGF-$A^{-/-}$ mice (Calver et al., 1998, Fruttiger et al., 1999). *Col2a1* encodes a helical protein that is secreted from the cell and, in regions of chondrogenesis, is cleaved and undergoes spontaneous assembly into a triple helix with other COL2A1 polypeptides, forming 'tropocollagen' which is the building block of collagen fibrils. Interestingly, *Col2a1* has already been found to be a transcriptional target of SOX9 in chondrogenic tissue (Bell et al., 1997). The classification of COL2A1 as PDGF-binding stems from the observation that PDGF is bound and immobilised in the extracellular matrix (ECM; Whitby and Ferguson, 1991). Later *in vitro* binding assays showed that PDGF is bound by a variety of collagens, including type-II (Somasundaram and Schuppan, 1996). Although these two genes, *Pdgfra* and *Col2a1*, are interesting individually, the fact that they both bind PDGF (one transducing its signal and the other binding and inactivating it), may be a co-incidence.

One further category that is enriched only in the microarray dataset is 'Transporter Activity' (Figure 4-7). This is a large category with 864 members, although the seven transporters present in our dataset amount to a 4.3 fold-enrichment (adjusted p-value 0.02). These seven include two glucose transporters, *Slc5a2* and *Slc2a13*, a potassium channel, *Kcnj10*, a constituent protein of nuclear pores, nucleoporin 133 (*Nup133*), a retinaldehyde-binding protein (*Rlbp1*), expressed in the VZ but better studied in the context of the retina where it plays an essential role in the replenishment of visual pigments, a Na^{2+}/K^{+} ATPase (*Atp1a2*) and an ATP-binding cassette transporter (*Abcb9*). Using a larger microarray down-regulated dataset with no fold-change cut-off, we see an enrichment of genes encoding proteins with vascular endothelial growth factor (VEGF) receptor activity. In fact, half of all genes known to bind VEGFs (*Flt1*, *Flt4* and *Pdgfra*) are seen in this dataset. VEGFs are best known for their role in lymphangiogenesis. However, in recent years other functions specific to the CNS have emerged, such as in the specification of OPCs (Le Bras et al., 2006) and in guiding their migration (Hayakawa et al., 2011).

Sub-Root	GO Term	GO ID	Number of Genes in Gene Set and Also in Category	Ratio of Enrichment	Adjusted p-value
Molecular Function	Platelet-Derived Growth Factor Binding	0048407	2	92.4	0.011
Molecular Function	Growth Factor Binding	0019838	3	19.2	0.014
Molecular Function	Heparin Binding	0008201	3	15.4	0.019
Molecular Function	Polysaccharide Binding	0030247	3	10.4	0.028
Molecular Function	Glycosaminoglycan Binding	0005539	3	11.7	0.028
Molecular Function	Pattern Binding	0001871	3	10.4	0.028

Molecular Function: Platelet-Derived Growth Factor Binding (GO:0048407)

Col2a1	Collagen, type II, alpha 1
Pdgfra	Platelet derived growth factor receptor, alpha polypeptide

Molecular Function: Growth Factor Binding (GO:0019838)

Kl	Klotho
Col2a1	Collagen, type II, alpha 1
Pdgfra	Platelet derived growth factor receptor, alpha polypeptide

Molecular Function: Heparin Binding (GO:0008201) / Polysaccharide Binding (GO:0030247) / Glycosaminoglycan Binding (GO:0005539) / Pattern Binding (GO:0001871)

Lamc2	Laminin, gamma 2
Gpnmb	Glycoprotein (transmembrane) nmb
Mpo	Myeloperoxidase

Figure 4-6 GO Term Enrichment Analysis (restricted to Molecular Function categories) on RNA-Seq Down-Regulated dataset (p-value ≤ 0.05, fold change ≥ 2 [66 genes]), using Entrez genes as a background list. Statistical test: Hypergeometric. Multiple-testing correction: Benjamini-Hochberg. Cut-off: Adjusted p-value < 0.05.

KEGG Pathway Analysis

In addition to finding categories of gene function that are enriched in these gene lists, it is also possible to look for genes that act in the same pathway, using KEGG pathways. This tool is used to determine if the constituents of a particular metabolic pathway are enriched in a gene list. Using this tool, three pathways were found to be enriched in both the RNA-Seq Down-Regulated and Microarray Down-Regulated datasets. They were: 'Focal adhesions', 'Calcium signalling pathway' and 'Cytokine-cytokine receptor interaction' (Figure 4-8 and Figure 4-9). Focal adhesions are circumscribed regions of the cell membrane that mediate attachment to the basement membrane. When analysing the phenotype of *Sox9*$^{\Delta/\Delta}$ embryos (Chapter 3), we found that midline glial populations are missing, and this might be caused by a failure of the cells that constitute this population to delaminate from the dorsal VZ. If this were the case, one might expect the down-regulated of components of focal adhesions, since if cells are not delaminating and migrating to form these structures, there would be less turn-over of focal adhesion proteins. Perturbations in calcium signalling might also be interesting because changes in intracellular Ca^{2+} concentration ($[Ca^{2+}]_i$) are important in the transduction of a number of extrinsic signals within cells. As described in later chapters, *Sox9* appears to control the expression of a K^+ channel subunit, Kir4.1, and one of the ways that expression of this channel might influence cell behaviour is through an effect on $[Ca^{2+}]_i$. Thus, a change in the Ca^{2+} signalling pathway might be secondary to a change in K^+ currents across the cell membrane.

Molecular Function: Platelet-Derived Growth Factor Binding (GO:0048407)
C=9;O=2;E=0.02;R=117.52;rawP=0.0001;adjP=0.0053

Col2a1	Collagen, type II, alpha 1
Pdgfra	Platelet derived growth factor receptor, alpha polypeptide

Molecular Function: Transporter Activity (GO:0005215)
C=864;O=7;E=1.63;R=4.28;rawP=0.0008;adjP=0.0212

Atp1a2	ATPase, Na+/K+ transporting, alpha 2 polypeptide
Abcb9	ATP-binding cassette, sub-family B (MDR/TAP), member 9
Rlbp1	Retinaldehyde binding protein 1
Kcnj10	Potassium inwardly-rectifying channel, subfamily J, member 10
Slc5a2	Solute carrier family 5 (sodium/glucose cotransporter), member 2
Nup133	Nucleoporin 133
Slc2a13	Solute carrier family 2 (facilitated glucose transporter), member 13

Figure 4-7 GO Term Enrichment Analysis on the 'Microarray Down-Regulated' dataset (p-value ≤ 0.05, fold change ≥ 1.35 [26 genes]), using the genes represented by a probe set on the Affymetrix 430 2.0 GeneChip as a background list. Statistical test: Hypergeometric. Multiple-testing correction: Benjamini-Hochberg. Cut-off: Adjusted p-value<0.05.

KEGG Pathway	Number of Genes in Dataset and Also in Category	Ratio of Enrichment	Adjusted p-value
ECM-receptor interaction	2	13.73	0.0428
Focal adhesion	3	8.36	0.0428
Metabolic pathways	6	2.82	0.0612
Purine metabolism	2	7.08	0.0738
Alzheimer's disease	2	4.35	0.0874
Regulation of actin cytoskeleton	2	5.08	0.0874
Calcium signalling pathway	2	5.68	0.0874
Cytokine-cytokine receptor interaction	2	4.58	0.0874

Figure 4-8 KEGG pathways that are enriched in RNA-Seq Down-Regulated dataset (p-value < 0.05, fold change ≥ 1.4 [106 genes]), using Entrez genes as a background list. Statistical test: Hypergeometric. Multiple-testing correction: Benjamini-Hochberg. Cut-off: Adjusted p-value ≤ 0.1.

KEGG Pathway	Number of Genes in Dataset and Also in Category	Ratio of Enrichment	Adjusted p-value
Taurine and hypotaurine metabolism	2	58.8	0.0050
Focal adhesion	3	4.9	0.0420
Glioma	2	9.6	0.0420
Calcium signalling pathway	3	5.1	0.0420
Phosphatidylinositol signalling system	2	8.2	0.0420
Endocytosis	3	4.8	0.0420
GnRH signalling pathway	2	6.4	0.0499
Cytokine-cytokine receptor interaction	3	3.97	0.0499

Figure 4-9 KEGG pathways that are enriched in Microarray Down-Regulated dataset (p-value < 0.05, fold change ≥ 1.25 [67 genes]), using the gene recognised by probe sets on the Affy GeneChip 430 2.0 array as a background list. Statistical test: Hypergeometric. Multiple-testing correction: Benjamini-Hochberg. Cut-off: Adjusted p-value ≤ 0.1.

Up-Regulated Gene Lists

Within the RNA-Seq Up-Regulated dataset, the GO term category 'regulation of cell proliferation' was enriched (3.7-fold, p-value 0.09), as was one of its descendents, 'negative regulation of cell proliferation' (Figure 4-10). The up-regulation of genes that negatively regulate cell proliferation in the *Sox9*$^{\Delta/\Delta}$ mouse is consistent with the proliferation defect previously noted in *Sox9*$^{\Delta/\Delta}$ cells *in vitro* (Scott et al., 2010). Unfortunately, these categories are not enriched in the Microarray Up-Regulated dataset, although one of the 4 genes present in the RNA-Seq dataset, 'runt-related transcription factor 3' (*Runx3*), is also up-regulated in the array dataset (fold change 1.3). It is interesting to note that *Runx3* is also down-regulated in glioblastomas, a cancer of the brain originating from glial cells (mediated by promoter methylation; Mueller et al., 2007), in which *Sox9* is strongly expressed (Kordes and Hagel, 2006). This lends support to the idea that *Runx3* might be repressed by SOX9.

The picture for the Microarray Up-Regulated dataset is more complex, and so we have displayed it in the form of a directed acyclic graph (Figure 4-11). Taking only those categories that are enriched in our dataset at an adjusted p-value < 0.05, we see that 12 categories are enriched, although some of these are the parents of more specific GO terms, such as in the relationship of 'central nervous system development' to 'brain development'. Ignoring the parent categories, we are left with 5 'pinnacle' terms: 'Regulation of cell shape' (3 genes); 'negative regulation of neuron differentiation' (3 genes); 'gliogenesis' (3 genes); 'brain development' (6 genes); 'organ morphogenesis' (10 genes); and 'pattern specification process' (6 genes). 'Negative regulation of neuron differentiation' and 'gliogenesis' seem the most interesting categories for a gene that has

been postulated to be part of the 'gliogenic switch', that is, the transition to gliogenesis at the end of neurogenesis (Stolt et al., 2003).

The constituents of these two categories are shown in Figure 4-12, and contain one common member, *Nr2e1*, which is more commonly referred to in the literature as '*Tlx*'. In the context of adult NSCs, *Tlx* strongly represses the expression of two well-characterised markers of astrocyte identity, S100β and GFAP, and when transfected into NSCs *in vitro*, astrocyte differentiation (driven by the addition of LIF to the culture medium) is markedly reduced (Shi et al., 2004). Since *Sox9* is expressed in early astrocytes, it makes sense that it should repress a repressor of astrocyte identity, making *Tlx* an attractive candidate for transcriptional repression by SOX9. However, the fact that *Tlx* and *Sox9* are expressed in similiar patterns at E12.5 (Stenman et al., 2003b) seems to argue against such a relationship. *Tlx* expression begins earlier than *Sox9* expression, peaks at E12.5 and then rapidly dissipates (Monaghan et al., 1995), whilst *Sox9*, having arisen at ~E9.5, continues to be expressed throughout embryogenesis (Stolt et al., 2003, Scott et al., 2010). However, it is possible that increasing levels of SOX9 in the period E9-E12 might gradually extinguish *Tlx* expression, or that another factor is required for SOX9-mediated repression. Reports of *Tlx* repressing neuronal differentiation appear to be restricted to findings in the retina, where reduced numbers of neurons are formed in each of the three neuronal layers of the retina of the $Tlx^{-/-}$ mouse (Miyawaki et al., 2004), a phenotype not seen in other parts of the CNS.

GO ID	Sub-Root	GO Term	Total Number of Genes in Category	Number of Genes in Gene Set and Also in Category	Ratio of Enrichment	Adjusted p-value
0009266	Biological Process	Response to temperature stimulus	45	3	18.9	0.030
0008285	Biological Process	Negative regulation of cell proliferation	181	4	6.3	0.080
0042127	Biological Process	Regulation of cell proliferation	462	6	3.7	0.094
0055114	Biological Process	Oxidation reduction	634	7	3.1	0.098
0008283	Biological Process	Cell proliferation	629	7	3.2	0.098

Figure 4-10 GO Term Enrichment Analysis on RNA-Seq Up-Regulated dataset (p-value ≤ 0.05, fold change ≥ 2.5 [81 genes]), using Entrez genes as a background list. Statistical test: Hypergeometric. Multiple-testing correction: Benjamini-Hochberg. Cut-off: Adjusted p-value < 0.1. Categories represented by fewer than 3 genes in the gene set were ignored.

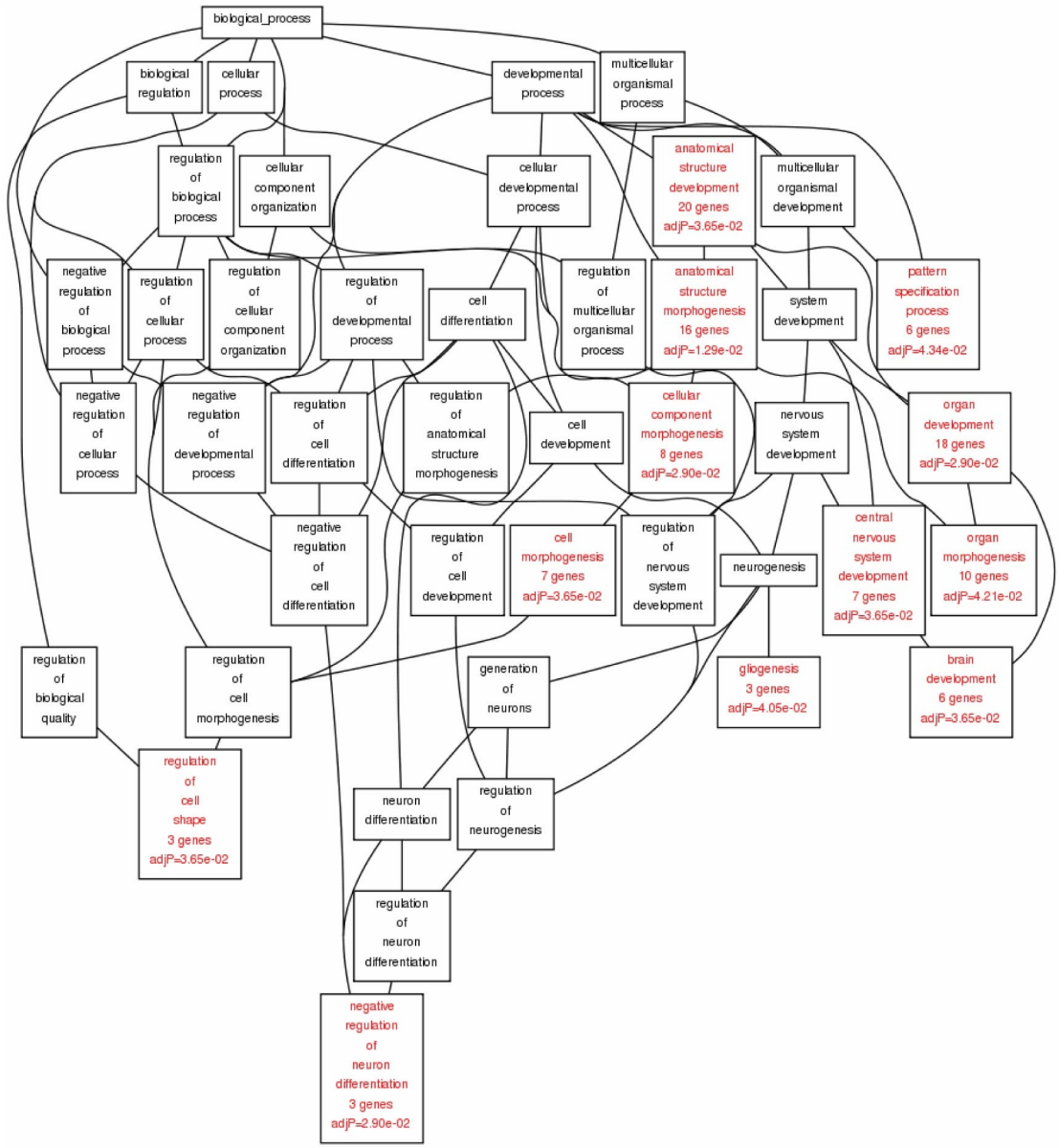

Figure 4-11 GO Term Enrichment Analysis on the 'Microarray Up-Regulated' dataset (p-value ≤ 0.05, fold change ≥ 1.25 [89 genes]) , using the gene represented by a probe set on the Affymetrix 430 2.0 GeneChip as a background list. Statistical test: Hypergeometric. Multiple-testing correction: Benjamini-Hochberg. Cut-off: Adjusted p-value < 0.05. Minimum: 3.

Biological Process: Negative Regulation of Neuron Differentiation (GO:0045665)
C=29;O=3;E=0.15;R=19.87;rawP=0.0004;adjP=0.0290

Nr2e1	Nuclear receptor subfamily 2, group E, member 1
Hes1	Hairy and enhancer of split 1 (Drosophila)
Notch3	Notch gene homolog 3 (Drosophila)

Biological Process: Gliogenesis (GO:0042063)
C=49;O=3;E=0.26;R=11.76;rawP=0.0021;adjP=0.0405

Nr2e1	Nuclear receptor subfamily 2, group E, member 1
Nab2	Ngfi-A binding protein 2
Ercc2	Excision repair cross-complementing rodent repair deficiency, complementation group 2

Figure 4-12 The members of two GO term categories enriched in our Microarray Up-Regulated dataset.

Discussion

In this chapter, a bioinformatics approach was used to determine if any categories of gene function or metabolic pathway was enriched in either or both of the down-regulated lists (from microarray and RNA-Seq), or up-regulated lists. No categories containing more than two constituents were common to both the down-regulated lists or both the up-regulated lists. Individually, however, the datasets do provide useful information.

My original rationale for performing these transcriptional profiling experiments was to identify receptors or second messengers that might be down-regulated in the *Sox9*$^{\Delta/\Delta}$ and could explain why the effect of *Sox9* loss on NPCs does not manifest *in vivo* until gliogenesis commences. The finding that three of the six known VEGF receptor genes (*Flt1*, *Flt4* and *Pdgfra*) were down-regulated in the *Sox9*$^{\Delta/\Delta}$ (microarray data) appeared to support this hypothesis. *Flt1*, *Flt4* and *Pdgfra* encode VEGFR-1, VEGFR-3 and PDGFRα, respectively. Two of these receptors have been shown to be important for OPC specification/proliferation (VEGFR-3 and PDGFRα): Mice lacking the VEGF ligand VEGF-C, which is transduced via VEGFR-3, are profoundly deficient in oligodendrocyte progenitor cells (OPCs; Le Bras et al., 2006), as are mice lacking *Pdgfa*, which encodes PDGF-A, the main ligand of PDGFRα (Fruttiger et al., 1999, Betsholtz et al., 2001). Therefore, consistent with our initial hypothesis, it appears that *Sox9*$^{\Delta/\Delta}$ CD133^{High} cells lack two receptors that are important in the initial specification or proliferation of OPCs. Some may argue, however, that down-regulation of these receptors could reflect a loss of OPCs in the *Sox9*$^{\Delta/\Delta}$, and this is possible since our CD133^{High} cells are not a pure population of progenitors and may be contaminated in the wild-type sample with OPCs that were not present in the *Sox9*$^{\Delta/\Delta}$ sample.

Although I originally set out to identify receptors or second messengers that might transduce a gliogenic signal, in the process I have also come across two transcription factors, *Nr2e1* and *Runx3*, which may be important in the *Sox9*$^{\Delta/\Delta}$ phenotype. Within the RNA-Seq Up-Regulated dataset, one category relevant to the observed phenotype jumps out: Negative regulation of cell proliferation, and one of the four genes enriched in this category, *Runx3*, is also in the Microarray Up-Regulated dataset. *Runx3* is expressed exclusively in post-mitotic neurons in the CNS, which do not express *Sox9*. This is consistent with a situation in which SOX9 represses *Runx3* transcription in glia and in progenitors. Analysis of the Microarray Up-Regulated dataset also yields a promising finding. Two of the enriched categories are 'Negative regulation of neuronal differentiation' and 'Gliogenesis', which fits with the previous observation that *Sox9* is important in the gliogenic switch in the CNS. Moreover, these two categories contain a common member, *Nr2e1* (better known as *Tlx*). *Tlx* is up-regulated in the absence of *Sox9* (1.42-fold), and represses two markers of astrocyte identity (S100β and GFAP) in differentiating neural stem cells (Shi et al., 2004). Unfortunately, the negative effect of *Tlx* on neuronal differentiation appears only to have been seen in the retina, and not in the CNS (Miyawaki et al., 2004). *Tlx* remains, however, a good candidate for a gene that might be repressed by SOX9 and mediate the failure of midline glial cells (which resemble astrocytes and express GFAP) to differentiate in the *Sox9*$^{\Delta/\Delta}$. Also, *Plce1* has been shown to be repressed by TLX (Zhang et al., 2006), and since *Plce1* is robustly down-regulated in the *Sox9*$^{\Delta/\Delta}$, this would fit with the de-repression of *Tlx* down-regulating *Plce1* in these mice.

KEGG pathway analysis identified 'Focal Adhesions', 'Cytokine-cytokine interactions' and 'Ca^{2+} signalling', although in all three cases this was based on the enrichment of only two genes. The idea that the proteins involved in Ca^{2+} signalling might be altered in the

Sox9$^{\Delta/\Delta}$ was of interest because Ca^{2+} signalling is very important in the transduction of extracellular signals (mediated by calmodulin), and activates the MAP kinase pathway (Rosen et al., 1994). However, this enrichment was based on the presence of two genes, *Plce1* and *Pdgfra*. When activated, PLCE1 hydrolyses phosphatidylinositol bisphosphate (PIP2), releasing inositol 1,4,5-triphosphate (IP3) and diacyl glycerol (DAG). IP3 then stimulates the release of Ca^{2+} from intracellular stores. Focal adhesions may also warrant further investigation since the down-regulation of proteins required for their formation might represent a defect of delamination in the *Sox9*$^{\Delta/\Delta}$, which may be the cause of the failure of midline glial populations to arise from the medial VZ.

In conclusion, amongst these datasets, the most convincingly enriched gene set is that of the VEGF receptors, since three of the six known receptors are down-regulated in the Microarray Down-Regulated dataset. In addition to this, gene set enrichment analysis has also highlighted two potential repressive targets of SOX9, one that inhibits astrocyte differentiation (*Tlx*), and another, *Runx3*, that exerts a negative effect on cell proliferation, supporting the theory that *Sox9* is important both for astrocyte differentiation and progenitor identity, which is by definition a proliferative cell population.

Chapter 5 Identifying Candidate SOX9 Primary Targets

Previous work in our laboratory has shown that *Sox9*$^{\Delta/\Delta}$ neural progenitors, derived from the spinal cord and dorsal telencephalon, form radically fewer neurospheres than wild type cells when cultured in the presence of basic fibroblast growth factor (bFGF) and epidermal growth factor (EGF; Scott et al., 2010). It was felt that the data obtained from the transcriptional profiling experiments in the previous chapter might shed light on the mechanisms involved in this phenotype. To this end, a list of targets that were robustly up- or down-regulated in both the microarray and RNA-Seq datasets was generated and subsequently confirmed by qPCR. In order to find direct targets of *Sox9* that might also be involved in the behaviour of neural progenitors, *in situ* hybridisation was performed using probes against all the candidate down-regulated targets. Subsequently, three of these candidates were found to be expressed to a similar extent in neurospheres as they were in E14.5 dorsal telencephalons, and thus represent good candidates for factors that might mediate the *Sox9*$^{\Delta/\Delta}$ neurosphere phenotype.

Introduction

Neurosphere Assay

The neurosphere assay is a system for determining the proliferative and differentiative capacity of neural progenitors, originally devised by Reynolds and Weiss (1992). It involves the dissection of a particular region of the CNS, which is triturated and cultured in the presence of EGF and bFGF, which are both mitogenic factors important for the proliferation of neural progenitors. Over the course of 6-10 days, large spherical colonies of cells arise, measuring up to 300-400μm in diameter. Although originally thought to be composed of homogeneous $Nestin^{+}$ progenitors, it is now known that neurospheres contain a heterogeneous population including progenitors, as well as more differentiated progeny (reviewed in Pastrana et al., 2011). Historically, the neurosphere assay has been used to identify neural stem cells, although in this thesis we use it to investigate the effect of loss of *Sox9* on neurosphere growth rates, which may represent an impairment of proliferation, a reduction in the size of the neurosphere-forming population, or indeed another sphere-forming population, such as early OPCs. Another aspect to the neurosphere assay is its ability to assess the differentiative capacity of the neurosphere-forming cells, which involves culturing them on a three dimensional matrix (*Matrigel*) in media in which growth factors have been removed, followed by fixation and staining for markers of differentiated cells.

Results

Having obtained detailed information about the genes differentially expressed in the *Sox9*$^{\Delta/\Delta}$ embryonic CNS, and therefore potential direct targets of SOX9, we decided to use this to look for candidates that might mediate the poor proliferation and reduced potential of neural progenitors observed in *Sox9*$^{\Delta/\Delta}$ mice (Scott et al., 2010). We began this analysis by looking for genes that were either up-regulated in both the RNA-Seq and microarray experiments, or down-regulated in both.

Generating Candidate Lists

Since the RNA-Seq and microarray datasets were produced from independent, consecutive experiments, any gene that reaches significance at the traditional cut-off of 0.05 in both datasets is extremely significant, because each p-value (representing the probability that that difference is due to chance) is specific to its experiment. With overlapping datasets, a p-value of 0.22 ($\sqrt{0.05}$) is more appropriate because the genes identified as meeting this criterion in both datasets can be considered to be significant at $p < 0.05$. The number of genes common to both the RNA-Seq and array datasets at a range of p-value cut-offs are shown as Venn diagrams in Figure 5-1. Taking a p-value cut-off of 0.22 in each dataset, 33 down-regulated and 22 up-regulated candidates are common to both datasets. The size of this overlap in the down-regulated datasets increases as the stringencies of the respective statistical tests are increased, with 9.9% of the genes down-regulated by RNA-Seq being present in the down-regulated array dataset at $p < 0.22$, increasing to 19.2% at $p < 0.05$, indicating that 'noise' in the two experiments is being removed, leaving we hope, the majority of the 'true' signal. This is not seen in the Venn diagrams for the up-regulated candidates, with the percentage overlap remaining largely

constant at ~5%. The robustness of the overlap in the down-regulated datasets, even at very high stringency (0.05^2), makes us very confident of these genes being down-regulated, and the poor concordance between the up-regulated datasets make us less confident about these targets, an observation supported by qPCR analysis of the common up- and down-regulated candidates shown in the next section. Although the 33 down-regulated and 22 up-regulated targets at a p-value cut-off of 0.22 (in each dataset) meet the conventional p-value cut-off of 0.05 overall, we decided to prioritise those genes that were differentially expressed at $p<0.05$ ($p<0.05^2$ overall), because we can be more confident that these genes are true signal, and also at this level we have a list of manageable size for downstream analyses.

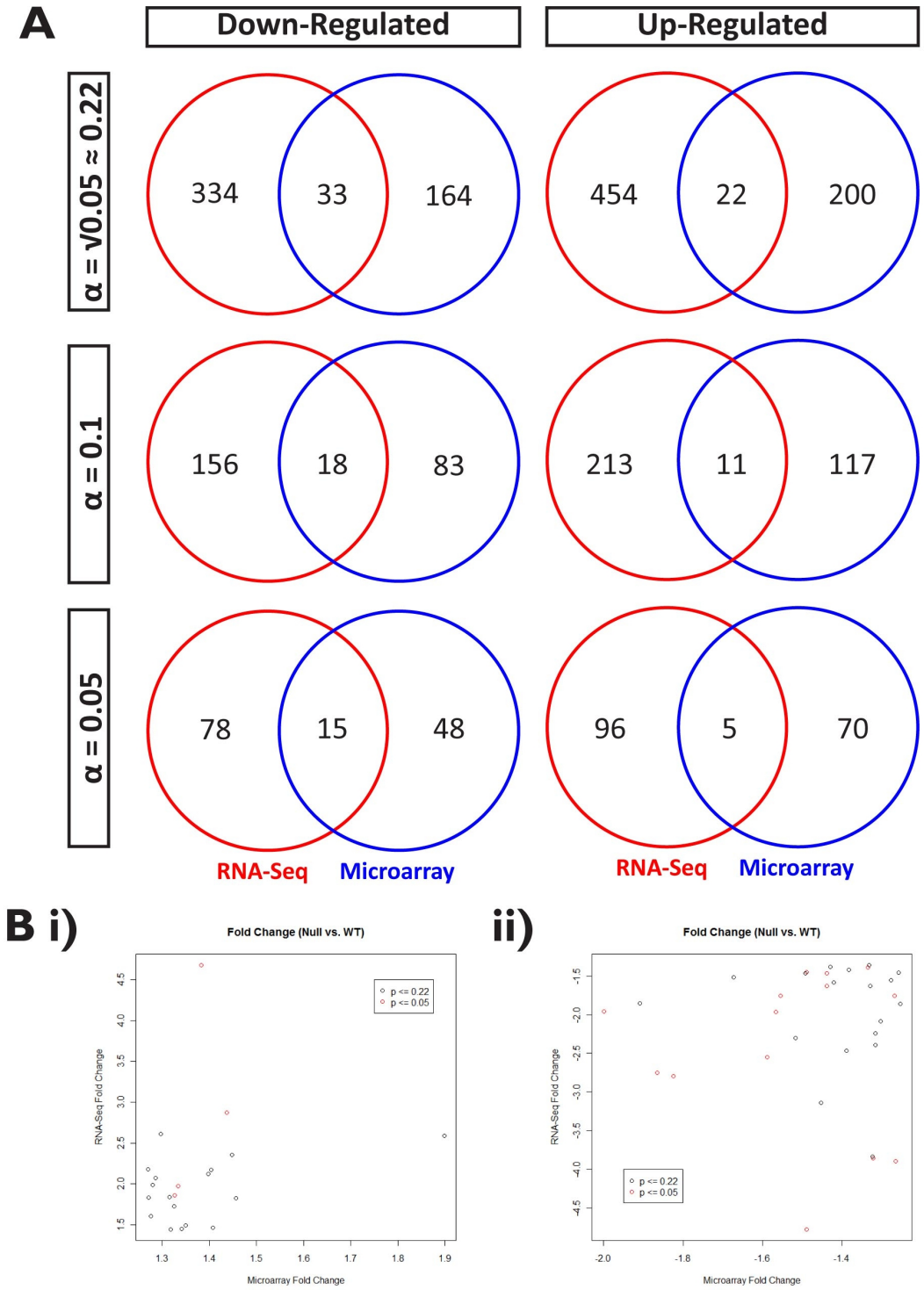

Figure 5-1 A – Venn diagrams showing the overlap between the RNA-Seq and microarray datasets at a variety of p-value cut-off levels (α). B – Correlation between the fold change derived from the RNA-Seq and microarrays for i) the up-regulated genes and ii) the down-regulated genes.

Validation of Candidates by qPCR

Differential expression in both overlapping datasets (which will be referred to as 'Combined Up-Regulated' and 'Combined Down-Regulated') was confirmed by RT-qPCR, using primers designed to produce the same amplicon across all known transcript variants. Ensembl was used as the source for transcript variant information. In cases where it was not possible to amplify all Ensembl transcripts with one set of primers, it was ensured that at least all RefSeq transcripts were included. In order to validate our primers, which were designed using the Primer3 algorithm, we performed qPCR on serial dilutions of E16.5 telencephalon cDNA, and verified that a single product was formed (by melt curve analysis) and that primer efficiency was in the range 95-105%.

Of the 14 genes[1] found to be down-regulated in both the RNA-Seq and array datasets, 13 were confirmed to be down-regulated by qPCR, although two were not statistically significant (*Arhgef3* and *Hs3st1*), and 7 candidates were more than two-fold down-regulated: *2810459M11Rik*, *Col2a1*, *Dbi*, *Hopx*, *Kcnj10*, *Pdgfra* and *Rlbp1* (Figure 5-2A). One down-regulated candidate, *5830403L16Rik*, was particularly problematic because no reliable transcript information was available, and this gene could not be satisfactorily amplified despite three different sets of qPCR primers being tried. Of the 5 candidate up-regulated targets, 3 were confirmed to be up-regulated by qPCR (Figure 5-2B), although only two met the requirements of statistically significance. These were *Heph*, and *Tesc*, and only the latter was more than two-fold up-regulated.

[1] The 15th gene, *Lhb*, was only identified as being common to both datasets when the data was recently re-analysed, so this was not included.

Reassuringly, ChIP-Seq[2] using chromatin extracted from NS cells, which are an *in vitro* model of radial glial cells (Conti et al., 2005), and an antibody against SOX9, identified SOX9 binding sites within 20kb of the transcriptional start sites (TSSs) of 11 out of our 14 candidates in the Common Down-Regulated list (Figure 5-3), compared to a genome-wide incidence of SOX9 binding within 20kb of TSSs of 14.5% (personal communication from B. Martynoga). The three lacking a SOX9 binding site within this range are *5830403L16Rik*, *Hs3st1* and *Pdgfra*.

[2] Kindly made available to us by the Guillemot group at the N.I.M.R.

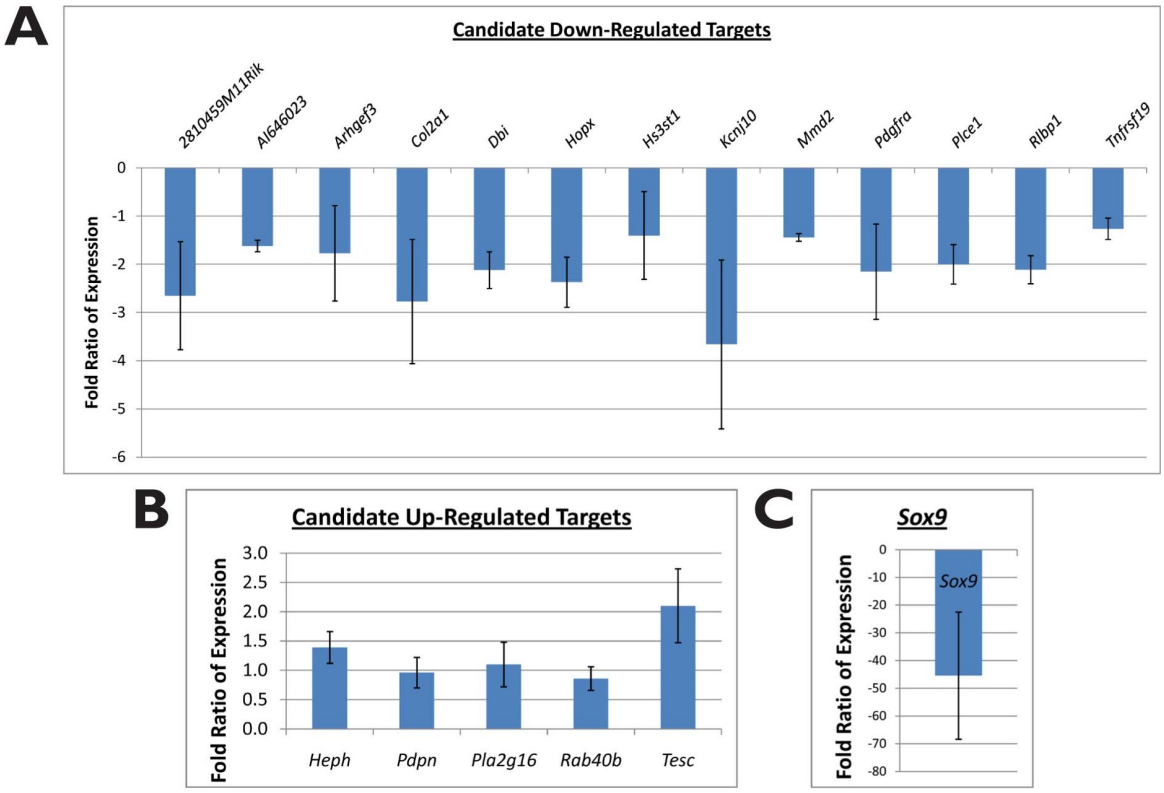

Figure 5-2 qPCR expression data for Common Down-Regulated dataset (A), Common Up-Regulated dataset (B) and *Sox9* (C).

A

Name	No. of *Sox9* Peaks
2810459M11Rik	2
5830403L16Rik	0
AI646023	2
Arhgef3	1
Col2a1	1
Dbi	1
Hopx	1
Hs3st1	0
Kcnj10	2
Mmd2	1
Pdgfra	0
Plce1	1
Rlbp1	1
Tnfrsf19	1

B

Name	No. of *Sox9* Peaks
Heph	0
Pdpn	1
Pla2g16	1
Rab40b	1
Tesc	0

Figure 5-3 Number of SOX9 binding sites identified by ChIP-Seq within 20kb of the transcriptional start sites of the candidate targets.

Spatial Expression Patterns of Candidates at Mid-Neurogenesis by *In Situ* Hybridisation

The down-regulation of a particular mRNA in a sample of total RNA might represent the reduction of the absolute levels of that transcript in a cell that is expressing SOX9 (a direct target) or the loss or reduction of a specific cell population induced or maintained by *Sox9*. Determining the spatial distribution of the candidate down-stream targets at a time of peak neurogenesis in the telencephalon (E14.5) allows us to distinguish between these two causes of differential expression and to refine our list to a smaller number of, hopefully, primary targets that might feasibly mediate the aberrant behaviour of $Sox9^{\Delta/\Delta}$ neural progenitors in the neurosphere assay. In this section, the down-regulated candidate genes will be referred to simply as the 'candidate genes'.

In order to assess the spatial expression pattern of the candidate genes, we made *in situ* probes by a method that involves PCR amplification from cDNA with PCR primers specific to the transcript of interest that include the T7 bacteriophage promoter, such that the resulting amplicon can be used as a template for T7 RNA polymerase. When *in vitro* transcription is performed in the presence of a certain concentration of DIG-labelled nucleotides, a DIG-labelled riboprobe specific to that transcript is produced.

These riboprobes were used to detect the mRNA of the candidates in sections of $Sox9^{\Delta/\Delta}$ and wild-type littermate brains at mid-neurogenesis (E14.5). This was done with two objectives in mind: Firstly, to see if there was any change in the distribution of the candidate genes in the $Sox9^{\Delta/\Delta}$ that might be indicative of the loss of a particular cell population, or indeed differential expression in terms of transcript level. The distribution of these transcripts in the wild-type situation is also of interest since any target expected

to influence the behaviour of progenitors would have to be expressed within those progenitors, i.e. within the VZ. The resulting in situs are shown in Figures 5.4-5.8.

Heparan sulfate (glucosamine) 3-O-sulfotransferase 1 (*Hs3st1*; Figure 5-4A) is expressed moderately in the ventral VZ, and strongly in the subventricular zone (SVZ) of the dorsal telencephalon, where intermediate progenitor cells (IPCs) reside (Noctor et al., 2004). There is also some expression in the emerging cortical plate (CP). Consistent with the qPCR data, the intensity of signal from this transcript is not noticeably reduced in the null. *Mmd2* is also expressed specifically within the SVZ, although more weakly than *Hs3st1*. Again, expression of this transcript does not appear to be reduced in the null, although it is only mildly down-regulated by qPCR (1.44-fold). *Pdgfra* and *Plce1* also follow the same expression pattern, although *Pdgfra* expression is more convincingly down-regulated than *Plce1* in these images, consistent with it being the most down-regulated of the four (2.2-fold by qPCR).

HOP homeobox (*Hopx*; Figure 5-5A) is expressed diffusely in the dorsal VZ, but particularly strongly in the region of the dorsal VZ closest to the septum. Interestingly, this is the region from which radial glia delaminate and migrate to form midline glial structures (Shu et al., 2003b, Smith et al., 2006), which are absent in the $Sox9^{\Delta/\Delta}$. This expression pattern is almost entirely lost in the absence of *Sox9*. Tumor necrosis factor receptor superfamily, member 19 (*Tnfrsf19*; Figure 5-5B), often referred to as *Troy* in the literature, is also expressed most strongly in the region of the dorsal VZ adjacent to the septum, suggesting it may also play a role in mediating this aspect of the $Sox9^{\Delta/\Delta}$ phenotype. Evidence of differential expression is weak, although this is to be expected with a gene that is down-regulated only 1.26-fold by qPCR. Interestingly, we have detected tumour necrosis factor (TNF) in conditioned media from both neurospheres

(after 6 days of culture) and NS cells (1480pg/ml and 2478pg/ml, respectively)[3], suggesting that this cytokine is produced by NPCs. However, researchers disagree as to whether TNF is in fact a ligand for TNFRSF19, and it is currently regarded as an orphan receptor (Bossen et al., 2006).

Retinaldehyde binding protein 1 (*Rlbp1*; Figure 5-6) is expressed strongly in the medial, and dorsolateral VZ, with expression bleeding into the most lateral part of the ventral VZ, and rapidly fading out in the lateral-to-medial direction. This expression pattern is reminiscent of that of *Pax6*, which defines the pallial region of the VZ (Stenman et al., 2003b), destined to give rise to the glutamatergic projection neurons of the CP. Expression of this transcript is dramatically weaker in the VZ of the $Sox9^{\Delta/\Delta}$, most pronounced caudally, but also rostrally.

Diazepam-binding inhibitor (*Dbi*; Figure 5-7B*)* is strongly expressed in the VZ, both in the dorsal and ventral regions, and also in diffuse cells within the parenchyma of the telencephalon. The dorsal VZ expression is selectively lost in the $Sox9^{\Delta/\Delta}$. Like *Dbi*, the inwardly-rectifying potassium channel, *Kcnj10* (Figure 5-7C), is also expressed strongly and uniformly throughout the dorsal and ventral VZ, although with considerably less expression in the parenchyma. Again, expression of this gene is lost specifically in the dorsal VZ of the $Sox9^{\Delta/\Delta}$, leaving the ventral expression almost untouched.

A similar pattern is seen for *Col2a1*, which is again expressed uniformly throughout the VZ at this rostrocaudal position, although the expression pattern does appear to involve a greater thickness of the ventricular wall, perhaps encroaching into the intermediate zone (IZ). In the case of *Col2a1*, expression is lost in all regions of the VZ in the $Sox9^{\Delta/\Delta}$ (note

[3] Assay performed by Gavin Sewell, Department of Medicine, U.C.L.

that the expression in the chondrogenic field of the future skull base is similar in both the wild-type and *Sox9*$^{\Delta/\Delta}$). Although it is perhaps surprising for a procollagen to be expressed in the progenitor zone of the embryonic brain, we are not the first to note this expression pattern: Ng and colleagues refer to the VZ expression of *Col2a1* in their 1997 paper, and VZ expression is clearly visible in the Allen Brain Atlas entry for *Col2a1*[4]. A similar expression pattern is seen for three other transcripts: *Arhgef3*, *2810459M11Rik* and *AI646023*, involving uniform expression in the dorsal and ventral VZs, and probable expression in the SVZ/IZ. Reduced expression in the *Sox9*$^{\Delta/\Delta}$ is seen in the first two, *Arhgef3* and *2810459M11Rik*, but not for *AI646023*.

Finally, at the rostrocaudal level shown, 5830403L16Rik is expressed most strongly in the SVZ of the lateral ganglionic eminences (Figure 5-8), which comprise a population of neural precursors, which express GAD67, and are destined to give rise to either pyramidal neurons of the basal ganglia, or interneurons (Stenman et al., 2003a). 5830403L16Rik is also diffusely expressed within the dorsal ventricular wall; this might be thought of as being consistent with the tangential migration of interneurons from the SVZ of the LGE, however, if this were the case, expression would be expected to either be within the marginal zone and IZ (early born interneurons) or in the VZ (late born interneurons), when in fact it seems present in all layers of the dorsal ventricular wall (Jovanovic and Thomson, 2011). Once again, expression is lost selectively in the dorsal VZ.

In conclusion, the expression patterns of the 14 genes identified as being down-regulated in the *Sox9*$^{\Delta/\Delta}$ have highlighted six targets that are robustly down-regulated, and expressed specifically and uniformly throughout the VZ of the telencephalon. Therefore, these genes are excellent candidates for mediating the progenitor defects seen in the

[4] Allen Developing Mouse Brain Atlas [Internet]. Seattle (WA): Allen Institute for Brain Science. ©2009. Available from: http://developingmouse.brain-map.org.

Sox9$^{\Delta/\Delta}$, namely reduced neurosphere-forming ability, and loss of potential to form glia. However, before proceeding to functional analyses of these genes, we first attempted to confirm their expression in neurospheres.

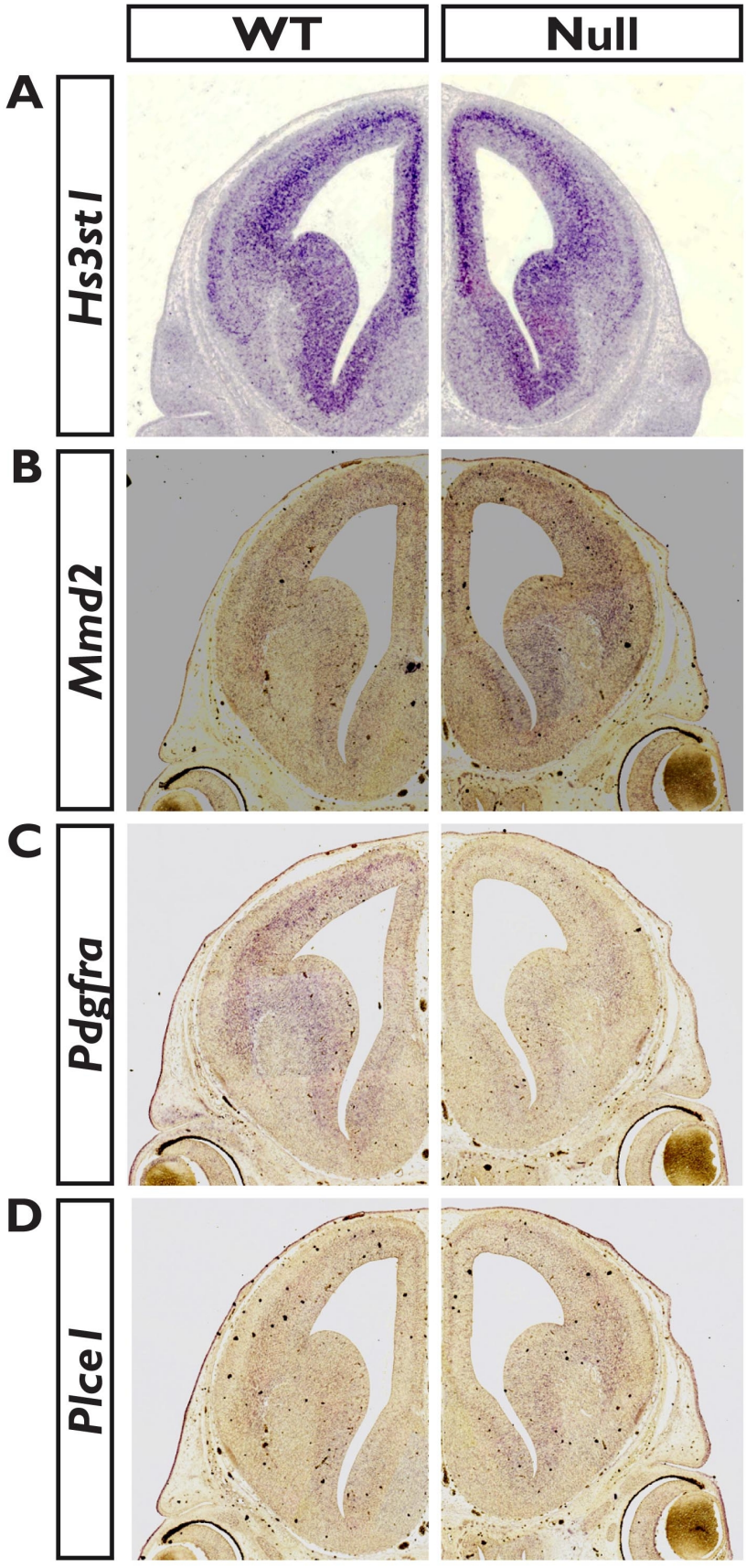

Figure 5-4 The expression patterns (by *in situ* hybridisation) of those candidates whose dominant expression was deemed to be in the subventricular zone of the dorsal telencephalon.

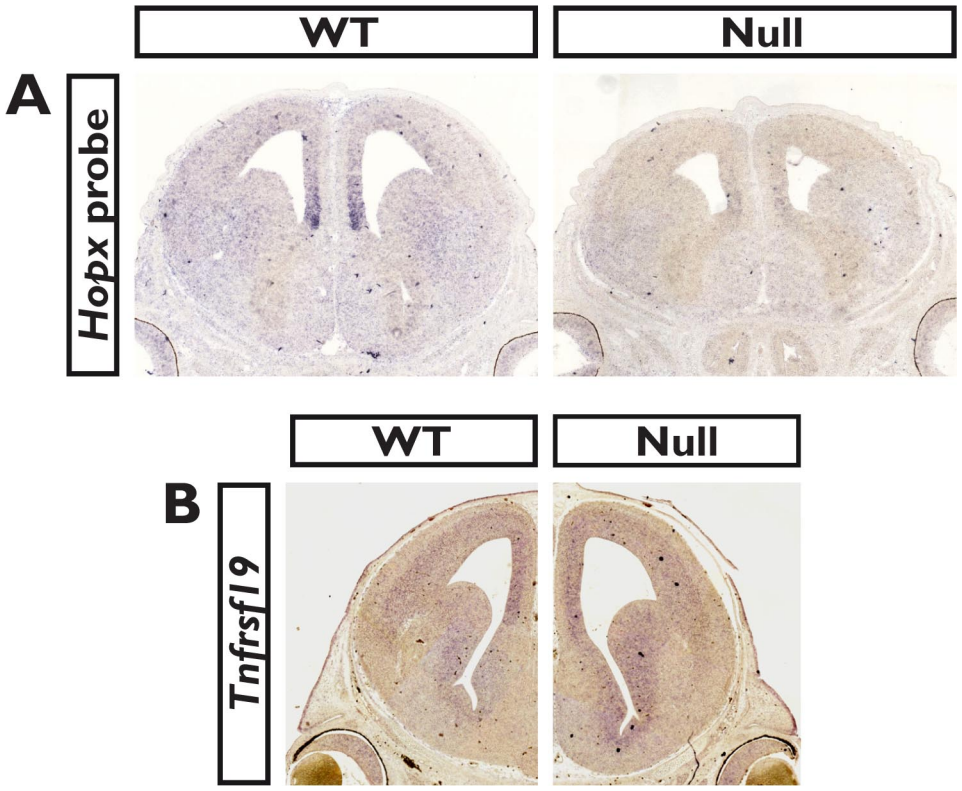

Figure 5-5 Expression (by *in situ* hybridisation) of *Hopx* (A) and *Tnfrsf19* (B).

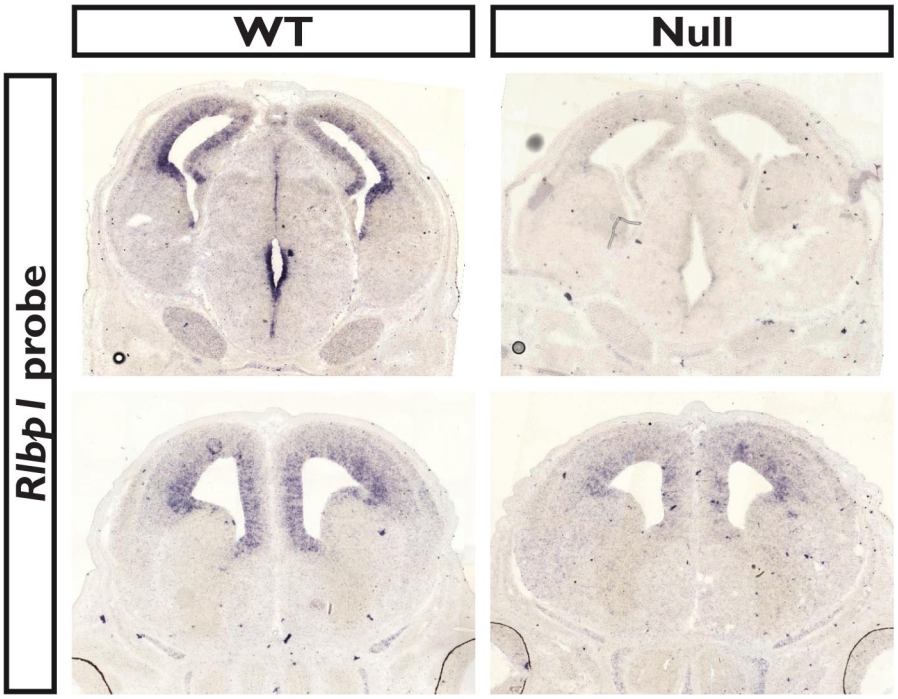

Figure 5-6 Expression (by *in situ* hybridisation) of *Rlbp1*.

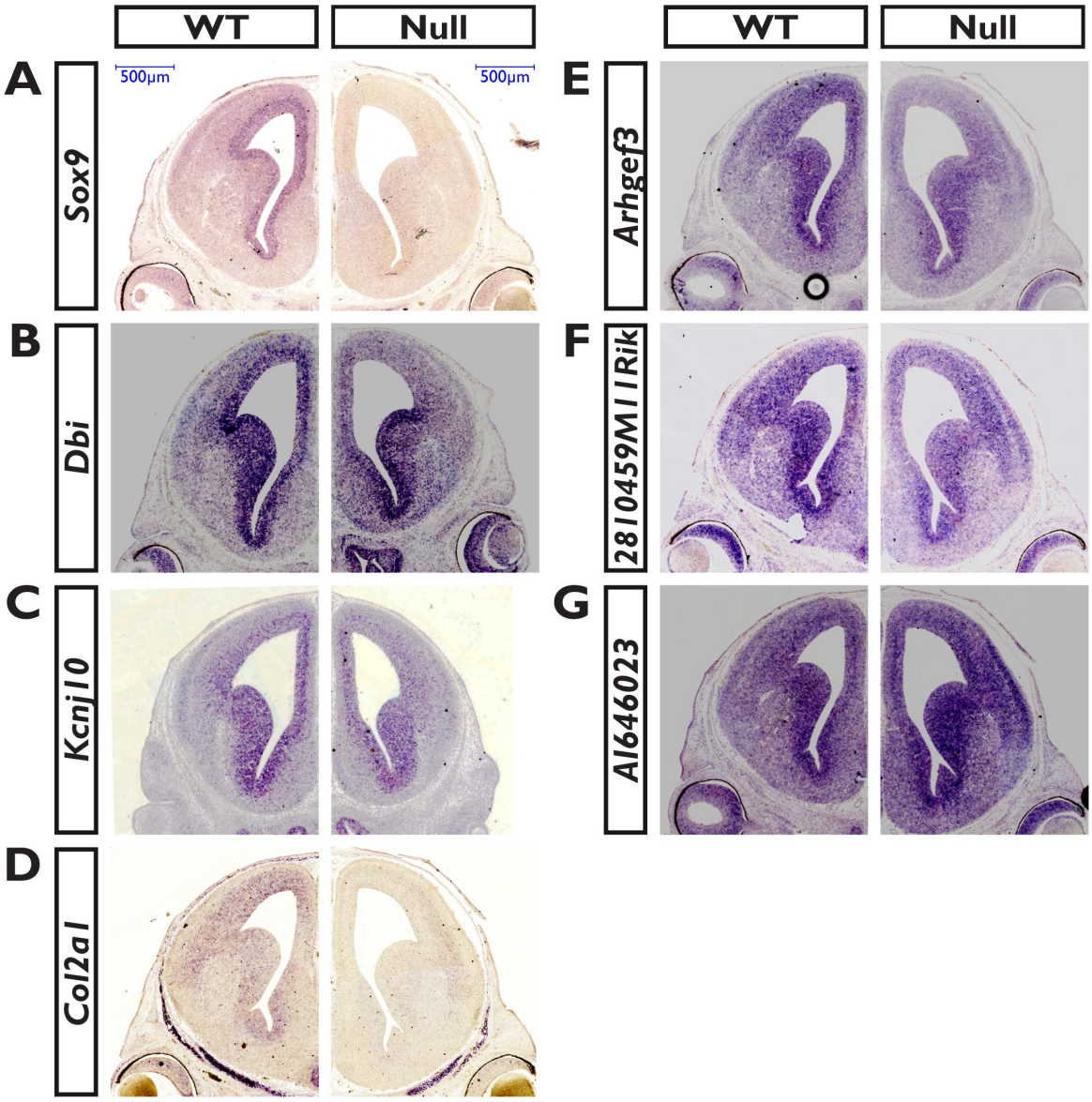

Figure 5-7 The expression patterns (by *in situ* hybridisation) of those candidates that appear to be expressed specifically within the VZ of the developing telencephalon. A *Sox9 in situ* is included for comparison.

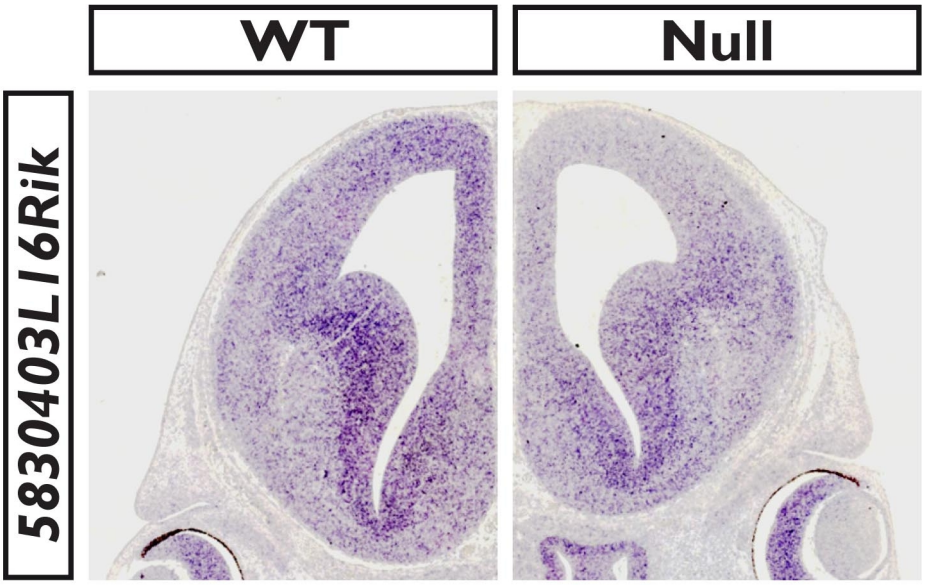

Figure 5-8 The expression pattern (by *in situ* hybridisation) of *5830403L16Rik*.

Expression of Candidate Genes in Neurospheres

Following the analysis of the expression patterns of these 14 down-regulated candidates, the list has been reduced to six genes that are felt likely to be primary targets of SOX9 since they are expressed in the same pattern, namely *Dbi*, *Kcnj10*, *Arhgef3*, *2810459M11Rik*, *AI646023* and *Col2a1*, with the first two being of particular interest because the others appear also to be expressed in the SVZ/IZ. The next logical step was to ask if any of these genes are expressed in neurosphere cultures. To this end, RT-PCR for the candidates was performed using total RNA extracted from E14.5 dorsal telencephalons from two embryos, and on two independently established neurosphere cultures, derived from E14.5 dorsal telencephalons, harvesting and extracting RNA after 7 days in culture. The results are shown in Figure 5-9. Unfortunately, only those primers against *Kcnj10*, *Dbi*, *Arhgef3* and *AI646023* worked in the reaction mix used, however, these results do show that the first three, *Kcnj10*, *Dbi* and *Arhgef3* are strongly expressed in neurospheres, whereas *AI646023*, whilst being moderately expressed in E14.5 dorsal telencephalons, is down-regulated in neurosphere cultures, ruling it out as a mediator of

the progenitor defects seen in the *Sox9*$^{\Delta/\Delta}$. The PCRs for *Col2a1* and *2810459M11Rik* did not work; however, in any case, we decided to take forward only *Kcnj10* and *Dbi*, because these were the genes for which the *in situ* data suggested expression specifically within the VZ, and not in the SVZ/IZ.

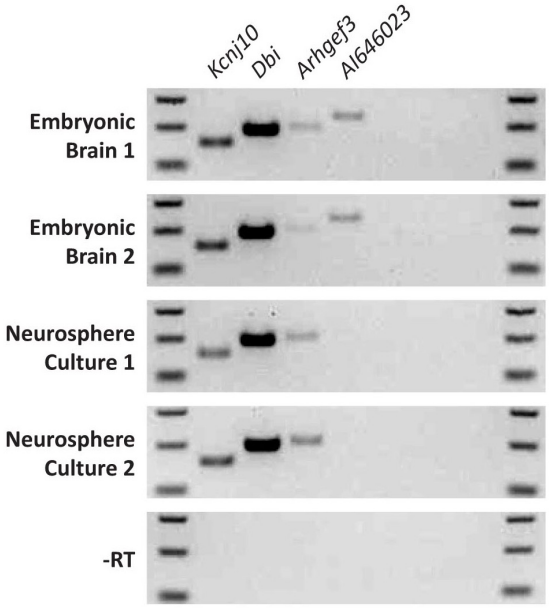

Figure 5-9 The expression (by RT-PCR) of *Kcnj10*, *Dbi*, *Arhgef3* and *AI646023* in neurosphere cultures and embryonic brains (E14.5).

Discussion

In this chapter, I have taken the transcriptional profiling data from our CD133^{High} cells, originally obtained to aid in our understand of the *Sox9*$^{\Delta/\Delta}$ phenotype, and used this information to refine a list of potential candidates that might mediate the poor proliferation of *Sox9*$^{\Delta/\Delta}$ progenitors in the neurosphere assay (Scott et al., 2010). Scott and colleagues also note that in the context of the neurosphere assay, *Sox9*$^{\Delta/\Delta}$ VZ cells exhibit a narrowed developmental potential upon growth factor withdrawal (only neurons are formed), and therefore any targets may have relevance to this aspect as well.

I began by overlapping both the down- and up-regulated lists from the RNA-Seq and array experiments to find genes that were differentially regulated in the same direction in both experiments. Since a p-value cut-off of 0.05 was chosen in each experiment, the likelihood of a gene appearing on one of the two overlapped datasets by chance is 0.0025. As expected, all of the down-regulated candidates were down-regulated by qPCR, although two of them, *Arhgef3* and *Hs3st1*, did not meet statistical significance. Using an external ChIP-Seq dataset, performed using genomic DNA from NS cells, 11 of the 14 down-regulated candidates were found to have at least one region bound by SOX9 within 20kb of their TSSs, and many (*2810459M11Rik*, *AI646023* and *Kcnj10*) had 2 such regions. Three genes, *5830403L16Rik*, *Hs3st1* and *Pdgfra*, did not have binding sites within the 20kb range, although it is possible that their transcription is activated by enhancers outside this range; it is also possible that they are indirect targets, with one or more intermediate transcription factors involved in their activation. Alternatively, these genes might be down-regulated because a cellular population fails to be generated in the *Sox9*$^{\Delta/\Delta}$. This is particularly likely in the case of *Pdgfra*, which is one of the earliest markers of oligodendrocyte progenitor cells (OPCs), and a marker that is found to be

lacking in the ventral telencephalons of *Sox9*$^{\Delta/\Delta}$ embryos in Chapter 3. *Pdgfra* (along with three other candidates *Hs3st1*, *Mmd2* and *Plce1*) appears to be expressed in the SVZ of the dorsal telencephalon. The fact that *Pdgfra* is a marker of OPCs, and they may be populating the embryonic cortex at this stage, leads us to speculate that loss of these markers might represent the depletion of an early population of OPCs, however, we have no direct evidence for this. Intermediate progenitor cells also reside in the SVZ of the dorsal telencephalon, although our investigation of these in Chapter 3 did not show any difference in their numbers. *5830403L16Rik* is also expressed most strongly in regions that lie outside the domain of *Sox9* expression, the ventral SVZ, from which interneurons are generated, raising the possibility that a population of interneurons might be depleted in the *Sox9*$^{\Delta/\Delta}$. Interestingly, in many cases, the expression of candidate genes was lost specifically in the dorsal telencephalon, suggesting that in the ventral telencephalon, other compensating factors might maintain the expression of these genes. Three of the down-regulated genes are found to be expressed to a similar degree in neurospheres as they are in the dorsal telencephalon *in vivo*, suggesting that these (*Kcnj10*, *Dbi* and *Arhgef3*) may be important in mediating the defect of NPC maintenance/proliferation seen in the neurosphere assay.

Hopx **and** ***Tnfrsf19*** **May Mediate the Failure of Midline Glial Populations to Form in** ***Sox9***$^{\Delta/\Delta}$ **Embryos**

As was seen in Chapter 3, two major commissural tracts, the corpus callosum and hippocampal commissure, fail to form in the anterior forebrain of *Sox9*$^{\Delta/\Delta}$ embryos. The fact that the anterior commissure forms normally suggests that there is no generalised defect of neurite outgrowth or axonal extension. Furthermore, the presence of bundles of Probst, which are aberrant tangles of axons either side of the midline at the rostrocaudal

level where the corpus callosum would be expected to form, suggests that it is the final step in commissural formation, midline crossing, that is lacking.

In humans and in mice, the corpus callosum is the major fibre tract that connects the neurons of the two hemispheres. Axonal outgrowth from newly-formed neurons begins early, within a few hours of their arrival at their final position in the CP. These axons extend in a reverse-radial fashion towards the ventricle, in close proximity to the fibres of radial glia, before executing a 90° turn and travelling medially, in a tangential fashion towards the midline (reviewed in Donahoo and Richards, 2009). Once at the midline, permissive and repulsive signals, some of which are released by a specialised region of glial cells, the indusium griseum, ensure the successful completion of their passage into the contralateral hemisphere.

Three populations of astrocytes make up the midline glial structures: The midline zipper glia, which populate the 'seam' formed after the fusion of the telencephalic vesicles, thus creating the substrate through which callosal axons can migrate (Silver et al., 1993); the glial wedges, which extend from the medial corners of the lateral ventricles towards the midline; and the indusium griseum, which lies at the dorsal-most extent of the commissural plate. The midline zipper glia are thought to participate in the process of midline fusion of the telencephalic vesicles on the basis of their expression in the trajectory of this fusion, which occurs in a ventral to dorsal direction (Silver et al., 1993). The glial wedges are thought to prevent callosal axons from projecting into the septum; they do this not only by forming a physical boundary, but also by expressing SLIT2 (Shu et al., 2003c), a secreted signalling molecule that serves to repel axon growth cones through an interaction with ROBO receptors expressed on their surfaces. The third structure, the so-called 'glia sling', is actually a population of neurons. Pioneer axons

from the cingulate cortex migrate over it, and immediately below the indusium griseum. These midline populations of glia are composed of astrocytes, and are born significantly earlier than the mainstay of forebrain astrocytes, which are generated postnatally. GFAP, a well-known marker of astrocytes is expressed in these populations at E16.5, and GFAP is not up-regulated in astrocytic precursors until ~2 days after their specification, so this is several days in advance of the majority of astrocytes, which are thought to arise from the transdifferentiation of radial glia cells (Kessaris et al., 2008).

Hopx and *Tnfrsf19* are both expressed in a similar distribution to that of *Fgfr1* in the rostral forebrain at E14.5, and this gene has been shown to be essential for the development of midline glia populations (Smith et al., 2006). The authors of this paper showed that in the absence of *Fgfr1*, radial glia in the ventromedial aspect of the dorsal telencephalon fail to retract their endfeet and delaminate from the VZ, thus preventing them from migrating to form the indusium griseum. This raises the possibility that there may be some genetic interaction between FGFR1 and SOX9, such as co-operative binding between SOX9 and an effector of FGF signalling in regulatory regions of genes important for radial glial delamination. An alternative explanation is that *Fgfr1* might lie downstream of *Sox9*, although no evidence of this is seen in our transcriptional profiling data. The reverse is unlikely to be true because *Fgfr1* is expressed in only a small portion of the *Sox9* expression domain. In order to ascertain if SOX9 and FGFR1 are acting in the same pathway to either specify, or trigger the delamination of, midline glial populations, it would be interesting to generate compound heterozygotes ($Sox9^{F/WT}$;$Fgfr1^{F/WT}$;NesCre) to see if midline glia are absent in these mutants (individually the heterozygotes are unaffected). However, before commencing any investigation of such a genetic interaction, I would want to confirm that *Hopx* and *Tnfrsf19* are in fact important for the generation of midline glia by examining tissue from null mice. A $Tnfrsf19^{-/-}$ has been produced (Shao et

al., 2005), but to date, no *Hopx*$^{-/-}$ has been generated. Also, if SOX9 and an effector of FGFR1 signalling were to bind co-operatively to activate the transcription of *Hopx* and/or *Tnfrsf19*, one might expect these genes to be absent or more weakly expressed in the *Fgfr1*$^{F/F;NesCre}$. One would also expect to find binding sites for potential effectors of FGF signalling in the vicinity of the SOX9 binding site identified in the SOX9 ChIP-Seq.

In addition to investigating a possible interaction between SOX9 and FGFR1, part of my further work would be to see if it is possible to rescue the callosal agenesis phenotype with either *Hopx* or *Tnfrsf19*. This could be done in slice culture with *Sox9*$^{\Delta/\Delta}$ brains by electroporating these factors individually, or in combination, into the ventromedial part of the dorsal telencephalon to see if radial glial delamination and midline glial population formation was restored. Co-electroporation of a radial glial reporter construct, such as the *Blbp*-GFP used by Smith and colleagues (2006), would enable the process of delamination to be observed by time-lapse confocal microscopy.

Chapter 6 KCNJ10 as a Candidate SOX9 Target Involved in Mediating the Impaired Neurosphere-Forming Ability of *Sox9*$^{\Delta/\Delta}$ Neural Progenitors

Through the refining of our candidate list in Chapter 5, we have identified a gene, *Kcnj10*, that has a number of characteristics that suggest it as a potential mediator of the *Sox9*$^{\Delta/\Delta}$ neurosphere phenotype. Firstly, it is the most down-regulated gene (by qPCR) among the targets that were down-regulated ($p < 0.05$) in both our RNA-Seq and microarray datasets. Additionally, it has two SOX9 binding peaks within 20kb of its transcriptional start site (TSS), and it is expressed in the same distribution as *Sox9* within the developing telencephalon (Figure 5-7C). Furthermore, *Kcnj10* is expressed specifically and uniformly in the ventricular zone (VZ) suggesting that it may be important in some way for the function of radial glia. The combination of these two lines of evidence make *Kcnj10* a promising candidate to explain the effect that deleting *Sox9* has on the behaviour of progenitors, i.e. impaired neurosphere-forming ability and loss of glial potential in differentiation assays.

Kcnj10 encodes an inwardly-rectifying potassium channel subunit, Kir4.1. In order to see if modulation of the expression of this potassium channel might be involved in the *Sox9*$^{\Delta/\Delta}$ neurosphere phenotype, I investigated the effect of blocking both inwardly-rectifying channels in general and also Kir4.1 in particular, on the proliferation and differentiative capacity of neural progenitor cells (NPCs).

Introduction

The Resting Membrane Potential

The membranes of cells are composed of a bilipid membrane, which is innately permeable to gases and lipid-soluble molecules. Artificial bilipid membranes are not permeable to charged molecules (such as glucose) and ions; these must be transported across the membrane by ion channels or carriers. Although transporters exist for many molecules in vertebrate cells, the gradients of three ions, Na^+, K^+ and Cl^- are of paramount importance. In all cells, the concentrations of these ions are radically different between the inside and outside of the cell: K^+ is ~40 times more concentrated within the cell than outside it, and a similar concentration gradient, but with opposite polarity, exists for Na^+ and Cl^- ions, which have very low intracellular concentrations. The enormous concentration gradients of Na^+ and K^+ ions are established by the action of an integral membrane protein called the Na^+/K^+ ATPase (or Na^+/K^+ pump). With every action of this pump, two K^+ ions are introduced into the cell, and three Na^+ ions extruded. A consequence of segregating ions across the cell membrane is that a potential difference develops across it, which is known as the 'resting membrane potential' (RMP) and is always negative within the cell (relative to the outside). However, it is the relative 'leakiness' of the cell membrane to K^+ compared to Na^+ (between 10- and 100-fold depending on the cell type) that is responsible for the large RMPs seen in many cells (such as glia and muscle cells). As a result of this difference in permeability, K^+ ions can flow out of the cell along their concentration gradient, but Na^+ ions cannot flow into the cell along theirs. Consequently, the cell becomes progressively more negative with respect to the outside. At some point, the electrical attraction of K^+ ions to the interior of the cell equals its tendency to flow out along its concentration gradient, and the voltage at

which this happens is called the potassium equilibrium potential (E_K), and it is very negative (~-90mV). In reality the cell membrane is permeable to other ions, which complicates the situation, so that the RMP never quite reaches this theoretical value.

Almost all cells segregate ions across their membrane – this is important for their function for a number of reasons. Primarily, the establishment of resting gradients of certain ubiquitous ions, such as Na^+ and K^+, can be used to drive desired molecules, such as the substrates of chemical reactions important to the cell, into its interior. Another important consequence of resting membrane potentials in multicellular organisms is in transmitting signals over long distances, such as in motor neurons or the specialised cardiomyocytes that co-ordinate the contraction of the heart. This is achieved through ion channels that transiently disrupt (or depolarise) the RMP, which spreads over the membrane of the cell and can induce cellular events (such as exocytosis of signalling molecules) at distant processes.

Potassium Channels

Over 100 different K^+ channel subunits have been identified to date, which assemble into four different classes of K^+ channel: Voltage-gated, Ca^{2+}-activated, 'leak', and inwardly-rectifying K^+ channels (Coetzee et al., 1999). All potassium channels are formed from the assembly of four subunits, some are homotetramers, others are heteromers, composed of compatible subunits from the same K^+ channel class. One striking property of K^+ channels is their selectivity: They are permeable to K^+ ions, but not to smaller cations such as Na^+ ions. The basis of this selectivity is the 'pore' of the K^+ channel. Although both K^+ and Na^+ ions are attracted to the negatively charged interior of the channel, the diameter of the pore is perfect to strip the water molecules from the surface of K^+ ions,

allowing them to pass into the cell, but not Na^+ ions, which are repelled (Doyle et al., 1998). Once the RMP is established, K^+ ions are in dynamic equilibrium across the membrane of the cell, such that the rate of K^+ ion entry equals K^+ ion exit. The number, and precise properties of these channels modulate the extent of K^+ entry, and hence the RMP.

This raises the question, why would it be beneficial for a particular cell to have a high or low RMP? This is easily answered for many differentiated cell types: Neurons with low RMPs will be more excitable, cells that store charged ions or molecules will be more efficient at importing them at higher RMPs, such as in the case of iodine import into the follicle cells of the thyroid gland via the I^-/Na^+ symporter. The latter process couples the 'downhill' movement of Na^+ ions along their electrochemical gradient with the 'uphill' movement of I^- against its electrochemical gradient (Levy et al., 1998). The ion conductance properties of excitable cells not only determines their threshold for depolarisation, but also the ensuing electrical events, such as the length of the period of depolarisation, and the refractory period of hyperpolarisation afterwards in which a second depolarisation cannot occur.

Kcnj10

The *Kcnj10* gene encodes a subunit of the inwardly-rectifying potassium channel, Kir4.1, which is expressed in astrocytes and oligodendrocytes in the adult brain (Kalsi et al., 2004), and in the VZ of the developing mouse brain (our own data). Outside of the cerebrum, it is expressed in the Bergmann glia of the cerebellum and the Müller glia of the retina (Takumi et al., 1995, Ishii et al., 2003), which are cell types also noted for their expression of *Sox9* (Pompolo and Harley, 2001, Poche et al., 2008). The fact that *Kcnj10*

is expressed in the Müller glia of the retina is interesting, because it has been shown that these glia are capable of neurogenesis (Fischer and Bongini, 2010). This complements our finding in the previous chapter that *Kcnj10* is also expressed in radial glia cells, further strengthening the argument that *Kcnj10* is important in some way for the identity of progenitors.

In physiology, the term 'rectification' refers to the direction of greatest ease for ion flow. Almost all channels, by their nature, allow ions to move in both directions (inwards and outwards) – 'inwardly rectifying' channels allow greater flow in the inward direction than in the outward direction at all membrane potentials. The KCNJ10 subunit can either be assembled as a homotetramer with three other KCNJ10 proteins, or as a heteromer with other inwardly-rectifying K^+ (Kir) channel subunits, of which about 20 are known. To date, KCNJ10 has been reported to form heteromers with two other Kir subunits: Kir5.1 (Tucker et al., 2000) and Kir2.1 (Fakler et al., 1996); in both cases, the resulting channel is more strongly rectifying than the Kir4.1 homotetramer, which is considered weakly rectifying. The *Kcnj10*$^{-/-}$ mouse shows a 'dysmyelinating' phenotype, that is, very little myelin is formed around the axons of either the central or peripheral nervous systems in these mice (Neusch et al., 2001). Disruption of the *Kcnj10* gene is one of very few cases in which a gene not directly involved in the production or export of myelin components exhibits a dysmyelinating phenotype, suggesting a role for *Kcnj10* in the specification of oligodendrocytes and Schwann cells.

Kir Channels and Their Role in Glia

One of the textbook properties of glial cells is their highly negative RMP (close to the E_K, and much greater than that of neurons), which was originally observed by Kuffler in

amphibians, and his predecessors working on the leech (1966; references therein). Modern electrophysiological techniques have shown that the RMP of glial cells, especially astrocytes is heterogeneous, however, the principle still holds true. One key benefit for astrocytes and oligodendrocytes of having a steep electrical gradient across their membranes is that it aids in one of their principal functions in the CNS, that of K^+ uptake and K^+ spatial buffering/siphoning. These are mechanisms by which K^+ ions, released by neurons during periods of intense activity, are absorbed by glia or re-distributed through the glia syncytium. Mounting evidence suggests that Kir channels are the major contributors to K^+ removal/re-distribution in the CNS. For instance, when isolated toad retinas are bathed in a solution of Ba^{2+}, a specific inhibitor of Kir channels, and stimulated with light, they fail to properly buffer K^+ (Oakley et al., 1992). Additionally, there is evidence that the Kir channel we are interested in is of special importance for this process, since the genetic ablation of *Kcnj10* results in the membrane potential of Müller glia, which perform the mainstay of K^+ siphoning in the retina, being reduced by 10-fold (Kofuji et al., 2000). Kir channels are the main source of K^+ conductance in glial membranes, and as such have a central role in setting the glial RMP (Butt and Kalsi, 2006).

A Role for K^+ Channels in Neural Progenitors?

Striking evidence for the importance of K^+ channels in neural progenitor proliferation comes from the phenotype of a mouse deficient in a voltage-gated K^+ channel, Kv1.1. These mice exhibit megencephaly (excessive growth of the brain) affecting principally the hippocampi and ventral cortex, which was found to have resulted from increased proliferation in the subgranular zone (SGZ) of the adult hippocampus, which is a well-characterised neural stem cell niche (Almgren et al., 2007). However, over-expression

studies have presented a more complex picture for the role of these outward, voltage-gated channels. Vautier and colleagues (2004) over-expressed three voltage-gated K^+ channels in oligodendrocyte progenitors and found that two of them, Kv1.3 and Kv1.4, increased proliferation (which is surprising in the context of the Kv1.1 phenotype), whereas a third, Kv1.6, decreased proliferation. In another study linking K^+ currents and NPC behaviour, the antidepressant Spadin, which blocks a two pore domain K^+ channel, TREK-1, was also shown to increase neurogenesis in the adult SGZ (Mazella et al., 2010).

Kir Channels and the Neural Stem Cells of the Adult SVZ

In addition to Kv channels, Kir channels may also have a role to play in the behaviour of neural progenitors. A number of authors have shown that Kir4.1 is expressed in the slowly-proliferating ($GFAP^+Nestin^+$) astrocytes of the adult subventricular zone in mice, but not in the differentiating migratory (DCX^+) cells of the rostral migratory stream (RMS; Pruss et al., 2011, Liu et al., 2006, Yasuda et al., 2008). Furthermore, Kir channels are expressed in a cyclical fashion in line with cell-cycle progression in cultured astrocytes, and their inhibition leads to cell cycle arrest (MacFarlane and Sontheimer, 2000, Pappas et al., 1994). These findings support the idea that Kir channels are important for the cycling state of progenitors, and that their loss may in some way be necessary for differentiation, possibility through a depolarisation-based mechanism. An alternative mechanism by which altering the permeability of a cell to K^+ might affect its physiology comes from potential effects on intracellular Ca^{2+} concentration ($[Ca^{2+}]_i$). Changing the conductance of the membrane to K^+ is likely to affect the distribution of other ions as they attempt to compensate, and restore electrochemical balance. Shi and colleagues (2007) showed that depolarising hippocampal neural progenitors using KCl did in fact increase

$[Ca^{2+}]_i$, and that the Ca^{2+} influx was coming from the extracellular environment, not the endoplasmic reticulum, which often serves as an intracellular reservoir for Ca^{2+}. $[Ca^{2+}]_i$ is known to have a number of effects on cellular physiology, which are brought about by the interaction of Ca^{2+} ions with a protein called calmodulin (CalM). CalM is a 'dumbbell' shaped molecule that can interact with a number of proteins in its unbound state. Binding of CalM to Ca^{2+} ions changes its conformation and thus its protein targets. A third possibility is that regulation of K^+ conductance might exert its effects through modulation of cell volume, which is known to influence the cell cycle (Rouzaire-Dubois and Dubois, 1998). Rouzaire-Dubois and Dubois noted that there was a concomitant increase in cell volume that accompanied the decrease in proliferation brought about by K^+ channel blockers in neuroblastoma/glioma hybrid cells. They then asked if simply changing the volume of a cell by altering the culture medium osmolarity would have a similar effect on proliferation; and they found that it did: An increase in cell volume was associated with a decrease in proliferation rate. Thus, they proposed that the effect of K^+ channel blockers on proliferation could be explained by consequent changes in cell volume.

A Potential Role for K^+ Channels in the Maturation of Oligodendrocytes

Two lines of evidence point to a specific role for Kir4.1 in the differentiation of oligodendrocytes. Firstly, Kir channels are strongly up-regulated in terminally differentiated oligodendrocytes resulting in hyperpolarisation (Knutson et al., 1997), and secondly, the genetic ablation of Kir4.1 leads to depolarised, morphologically immature oligodendrocytes (Neusch et al., 2001). Interestingly, a normal number of oligodendrocytes are observed in the $Kir4.1^{-/-}$ spinal cord, indicating that in the absence of Kir4.1, oligodendrocytes can advance in their differentiation program. However, the oligodendrocytes that form fail to produce myelin both *in vitro* and *in vivo*. The authors

describe these ‘immature’ oligodendrocytes as being round, showing greater somatic area, and forming fewer connections with other cells of the CNS.

Results

A number of lines of evidence support *Kcnj10* as a potential transcriptional target of SOX9. Firstly, it has been shown to be down-regulated in the neural progenitors of the telencephalon in the absence of *Sox9* by microarray, RNA-Seq and RT-qPCR (~3-fold [qPCR data]). We can also further define the nature of this down-regulation as affecting the NPCs of the dorsal telencephalon more than the ventral telencephalon (*in situ* data, Chapter 5). Our suspicion that this K^+ channel subunit may be a direct target of SOX9 is increased by the finding that SOX9 binds two regions within the only intron of *Kcnj10* (marked A and B in Figure 6-1). Both of these sites are highly conserved in mammals, as shown by the 'Placental Mammal Basewise Conservation' and the multiple alignment of this region in a number of mammalian species (Figure 6-1). Since SOX transcription factors are known to commonly bind DNA in concert with other transcription factors, the 40bp either side of each SOX9 binding site was examined to see if there might be a binding site for a potential binding partner using MatInspector (part of the Genomatix suite of bioinformatics tools; http://www.genomatix.de/). The consensus binding sites found are shown in Figure 6-2. In both SOX9 binding regions, a ZFP263 binding site (V$ZNF263 matrix; Frietze et al., 2010) is located very close to the SOX9 binding site, but on the opposite strand (15bp upstream at Site A; overlapping with the region bound by SOX9 at Site B). Very little is known about this transcription factor, except that its homolog is widely expressed in human tissues (Yokoyama et al., 1997).

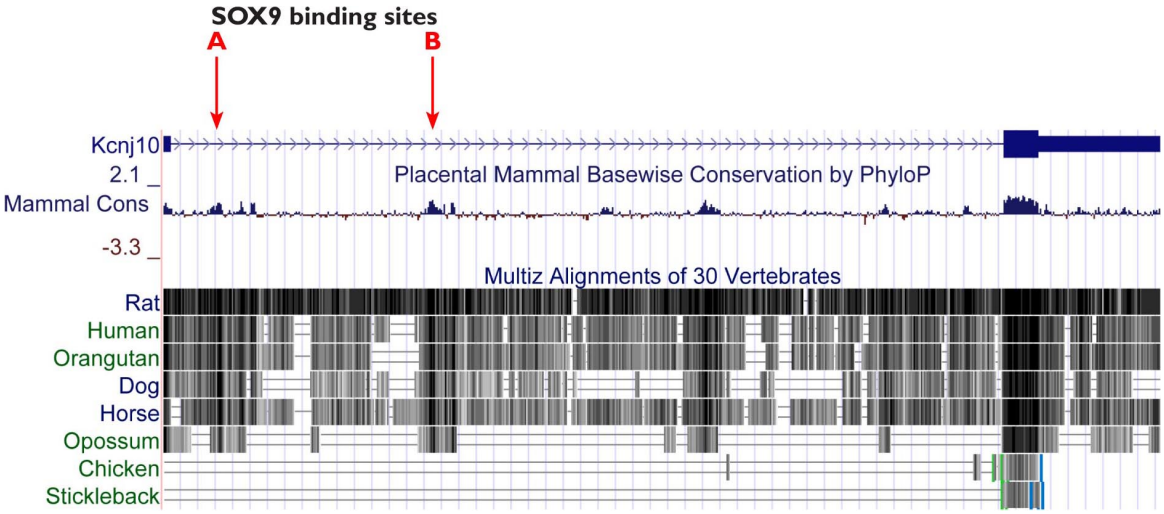

Figure 6-1 Both of the SOX9 binding sites in the first intron of the *Kcnj10* gene are highly conserved across mammalian species.

±40bp of SOX9 Binding Site A

Matrix Family	Family Information	Matrix	Start Position	End Position	Strand
V$GLIF	GLI zinc finger family	V$ZIC2.01	15	29	+
V$SPZ1	Testis-specific bHLH-Zip transcription factors	V$SPZ1.01	18	28	-
V$EGRF	EGR/nerve growth factor induced protein C & related factors	V$CKROX.01	18	34	-
V$BARB	Barbiturate-inducible element box from pro+eukaryotic genes	V$BARBIE.01	56	70	+
V$ZF07	C2H2 zinc finger transcription factors 7	V$ZNF263.01	57	71	-
V$EGRF	EGR/nerve growth factor induced protein C & related factors	V$EGR1.03	60	76	+
V$GLIF	GLI zinc finger family	V$ZIC2.01	62	76	-
V$SPZ1	Testis-specific bHLH-Zip transcription factors	V$SPZ1.01	66	76	+
V$BCDF	Bicoid-like homeodomain transcription factors	V$PTX1.01	64	80	-
V$RREB	Ras-responsive element binding protein	V$RREB1.01	65	79	-
V$PLAG	Pleomorphic adenoma gene	V$PLAG1.01	62	84	+
V$PLAG	Pleomorphic adenoma gene	V$PLAG1.02	64	86	+
V$GLIF	GLI zinc finger family	V$GLIS2.01	70	84	-
V$GLIF	GLI zinc finger family	V$ZIC2.01	73	87	-
V$RREB	Ras-responsive element binding protein	V$RREB1.01	76	90	-

±40bp of SOX9 Binding Site B

Matrix Family	Family Information	Matrix	Start Position	End Position	Strand
V$SORY	SOX/SRY-sex/testis determinig and related HMG box factors	V$HBP1.02	11	35	-
V$HDBP	Huntington's disease gene regulatory region binding proteins	V$HDBP1_2.01	29	47	-
V$NOLF	Neuron-specific olfactory factor	V$EBF1.01	28	50	-
V$PLAG	Pleomorphic adenoma gene	V$PLAG1.01	30	52	+
V$ZF07	C2H2 zinc finger transcription factors 7	V$ZNF263.01	36	50	-
V$SORY	SOX/SRY-sex/testis determinig and related HMG box factors	V$SOX9.02	44	68	+
V$PLAG	Pleomorphic adenoma gene	V$PLAGL1.02	58	80	-
V$RREB	Ras-responsive element binding protein	V$RREB1.01	64	78	+
V$HOXH	HOX - MEIS1 heterodimers	V$MEIS1A_HOXA9.01	72	86	-
V$RREB	Ras-responsive element binding protein	V$RREB1.01	74	88	+

Figure 6-2 Transcription factor binding sites within 40bp of each SOX9 binding site (limited to those transcription factors expressed in the CNS).

In addition to the evidence of SOX9 binding to a conserved non-coding region of the *Kcnj10* locus, and an effect of SOX9 on the expression of *Kcnj10*, this candidate is also expressed in the expected distribution for radial glia cells – strongly and uniformly in the VZ (*in situ* data; Chapter 5). These two lines of evidence, combined with the fact that modulation of K^+ channel expression has been shown to affect proliferation in a number of contexts, lead us to the hypothesis that *Kcnj10* may mediate the reduced proliferation of $Sox9^{\Delta/\Delta}$ NPCs in the neurosphere assay. We therefore asked if inhibiting K^+ currents through these channels could re-capitulate this aspect of the $Sox9^{\Delta/\Delta}$ phenotype. For this we used two Kir channel blockers, one that is widely-used in the literature, and believed to be specific to Kir channels (as opposed to other K^+ channels), Ba^{2+} ions, and another, fluoxetine, which has been reported to be specific to Kir4.1 (Ohno et al., 2007). In order to better interpret these studies, it was felt that it would be useful to know which Kir subunits are expressed on $CD133^{High}$ cells, and since we have RNA-Seq data from wild-type $CD133^{High}$ cells as part of a previous experiment, the data was utilised to answer this question.

Expression of Kir Subunits in $CD133^{High}$ Cells

The expression of all Kir subunits with >1 read aligning per kilobase of CDS are shown in Figure 6-3. Three Kir channels subunits are expressed in our sorted cell population: Kir3.1, Kir6.2 and our subunit of interest, Kir4.1. As was mentioned in the introduction to this chapter, Kir4.1 has only been reported to form heteromers with Kirs 2.1 and 5.1, neither of which are expressed in our $CD133^{High}$ cells, which leads us to the conclusion that Kir4.1 subunits are assembled as homotetrameric channels on the surfaces of radial glia. There have been no reports of heteromeric channels being formed from Kirs 3.1 and 6.2, so these are also likely to be in the form of homotetrameric channels. It is important

to bear in mind that although three channels may be present on the surfaces of progenitors in the VZ of the embryonic forebrain, not all may be open and influencing the electrochemical gradient of K^+; for instance, Kir6.2 is 'ATP-dependent' and is thus closed at physiological ATP concentrations, and the opening of Kir3.1 is controlled by interactions with G-proteins. This leaves open the possibility that Kir4.1 might be the dominant inwardly-rectifying potassium channel in radial glia, as is the case in Müller glia, which also express other subunits (Kofuji et al., 2000, Raap et al., 2002). Kir4.1 is also the dominant inwardly-rectifying K^+ channel in oligodendrocytes, demonstrated by the lack of Kir currents in the oligodendrocytes of Kir4.1$^{-/-}$ mice (Neusch et al., 2001). These oligodendrocytes are also depolarised, suggesting that Kir4.1 is the dominant K^+ channel responsible for setting their RMP.

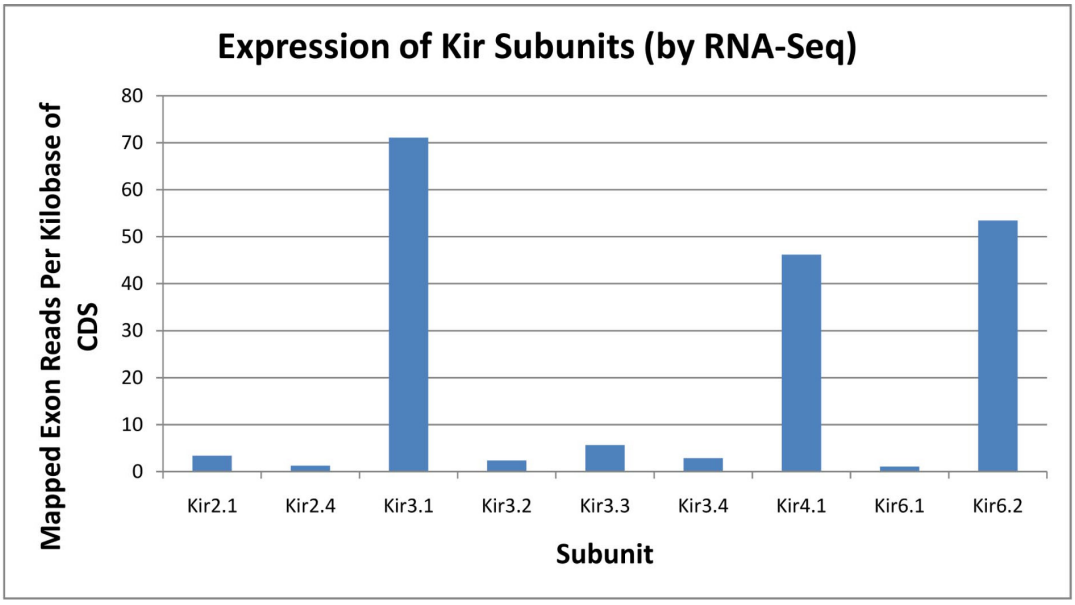

Figure 6-3 The expression of Kir subunits in CD133^{High} cells from the embryonic VZ. Only those subunits with >1 read aligning per 1kb of CDS were included.

The Effect of Kir Channel Blockade on the Proliferation of NPCs

Ba^{2+} ions are thought to inhibit all Kir currents, whereas fluoxetine was found in a recent report to be a specific inhibitor of Kir4.1 (Ohno et al., 2007). Subsequent studies have shown the precise residues responsible for the specific inhibition of Kir4.1 by fluoxetine (Furutani et al., 2009). Fluoxetine is better known as a treatment for depression in human patients that is believed to work by preventing re-uptake of serotonin (5-HT) via an interaction with the serotonin transporter, SLC6A4 (Sangkuhl et al., 2009, Stahl, 1998). Therefore, Ba^{2+} ions would be expected to block all Kir currents in NPCs, whereas fluoxetine would be expected to show the contribution of Kir4.1 currents specifically. One potential complicating factor is that fluoxetine may be a more effective inhibitor of Kir4.1 than Ba^{2+} ions, which only reduce astrocytic Kir currents by 63% (Liu et al., 2006).

In order to see if these two agents could mimic the loss of *Sox9 in vitro*, we harvested and dissociated dorsal telencephalons from E14.5 WT embryos and cultured them in the presence of bFGF and EGF. We assayed a diverse range of Ba^{2+} concentrations (Figure 6-4), and found that although slight reductions in the rate of neurosphere formation were seen at concentrations in the range 1-100μM, only at 1mM did we seen a statistically significant reduction (65% reduction in neurospheres over 300μm in diameter; $p = 0.039$). Although one author claims that Kir channels are sensitive to 100μM Ba^{2+} and that higher concentrations affect other K^+ channels (Liu et al., 2006), many other authors have used concentrations of 1mM and above to block Kir currents (Neusch et al., 2001).

A more pronounced effect on NPC proliferation is seen with fluoxetine (Figure 6-5), which would not be expected to impair the function of the other two Kir channels

expressed in $CD133^{High}$ cells. With this inhibitor, formation of neurospheres is completely ablated at 10μM. However, we suspect that fluoxetine may be interacting with other receptors on the surfaces of E14.5 neural progenitors at these concentrations since this loss of neurosphere-forming ability is seen below the IC_{50} of fluoxetine on Kir4.1 (15.2μM; Ohno et al., 2007). Additional suspicions are raised by the initial proliferation-enhancing effects of fluoxetine at concentrations distant from its IC_{50} (1nM and 10nM). In its clinical application in treatment of depression, fluoxetine, a selective serotonin reuptake inhibitor, is thought to exert its effects via negative allosteric modulation of the serotonin transporter, SLC6A4 (Sangkuhl et al., 2009, Stahl, 1998). However, an effect on SLC6A4 could not have affected our results since interrogation of our $CD133^{High}$ RNA-Seq data reveals no expression of the gene encoding this transporter. Having said this, it is possible that fluoxetine interacts with other receptors, and pharmacogenomic studies have implicated a number of targets, including other receptors involved in serotonergic neurotransmission such as the $5\text{-}HT_{2A}$ receptor (Serretti and Artioli, 2004).

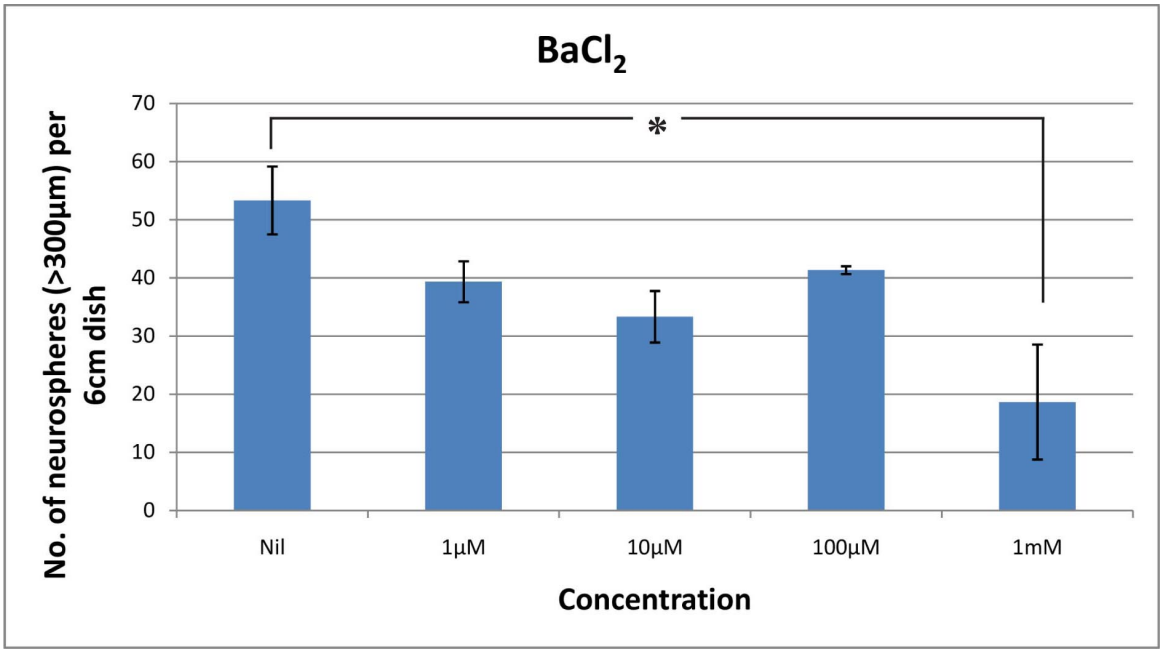

Figure 6-4 The effect of Ba^{2+} ion concentration on the rate of neurosphere formation (assayed at 7DIV).

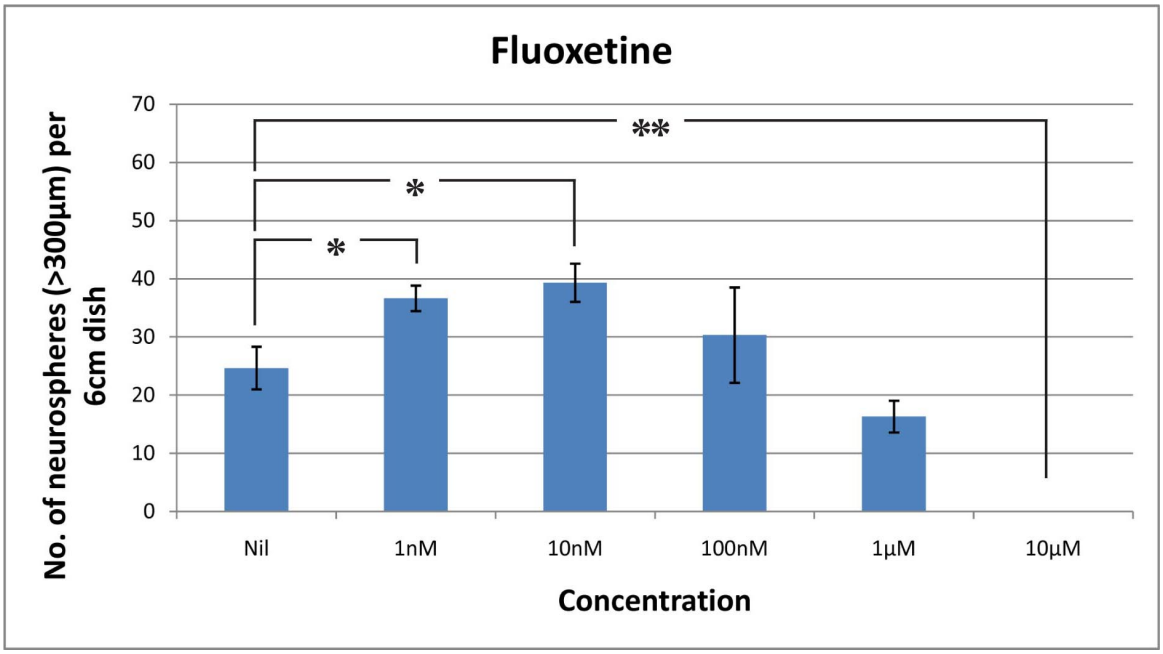

Figure 6-5 The effect of fluoxetine concentration on the rate of neurosphere formation (assayed at 9DIV).

Although these experiments support a role for Kir4.1 in actively proliferating cells, we cannot be certain in either case that these inhibitors are not exerting non-specific effects on other channels or receptors. To overcome this limitation, we decided to knock-down expression of *Kcnj10* by RNA interference (RNAi). The difficulty of doing this in a culture-based system is introducing the vector carrying the short-hairpin RNA (shRNA) into a majority of the cells in order to assess the phenotype produced. The strategy we adopted for this was electroporation with a plasmid containing both the shRNA against *Kcnj10* and the puromycin-resistance gene, and then a period of enrichment with puromycin after transfection. Despite various attempts at this experiment, involving exhaustive combinations of different *Kcnj10* shRNA clones, concentrations of puromycin and length (as well as timing) of puromycin exposure, I was unable to get significant knockdown of *Kcnj10* (by RT-qPCR). The extent of knock-down was always assayed at the end of the enrichment process, so there should not have been time for the selection against shRNA-expressing cells. In hindsight, rather than attempt to obtain a cell population in which all cells are expressing a plasmid, I would have used an shRNA plasmid containing GFP. Two populations of E14.5 dorsal telencephalons could be transfected, one with a scrambled shRNA linked to GFP, and one with the *Kcnj10* shRNA linked to GFP. After allowing these cells to form neurospheres, the number of GFP^+ spheres as a proportion of all spheres could be counted. I would then expect a proportion of the neurospheres formed from the control-transfected cells to be GFP^+, whereas those transfected with a plasmid containing the *Kcnj10* shRNA together with GFP I would expect to be all (or mainly) GFP^-, showing that only untransfected cells in the latter cultures could form neurospheres.

Another aspect of the $Sox9^{\Delta/\Delta}$ phenotype, recently published by our lab, is the fact that $Sox9^{\Delta/\Delta}$ neurospheres fail to generate astrocytes or oligodendrocytes upon removal of

growth factors (Scott et al., 2010). Therefore, I asked if ablation of Kir currents might affect the differentiation of NPCs. It was found that, in the presence of 1mM Ba^{2+} ions or 1μM fluoxetine (the highest concentration that permitted neurosphere formation), only astrocytes (marked by GFAP expression) or neurons were formed normally (Figure 6-6). Markedly fewer oligodendrocytes were formed (by PDGFRα immunohistochemistry), and those cells that did appear to express PDGFRα did so to a much lesser degree than untreated cells, or those treated with an inhibitor of a different type of channel ($GABA_A$ in this case). This finding suggests either that a change in the K^+ gradient across the membrane, or an initially hyperpolarised state is required for oligodendrocyte differentiation. This could be clarified by asking if Cs^+ ions (which block Kir channels, without depolarisation) or KCl (which would depolarise NPCs) could re-capitulate this effect.

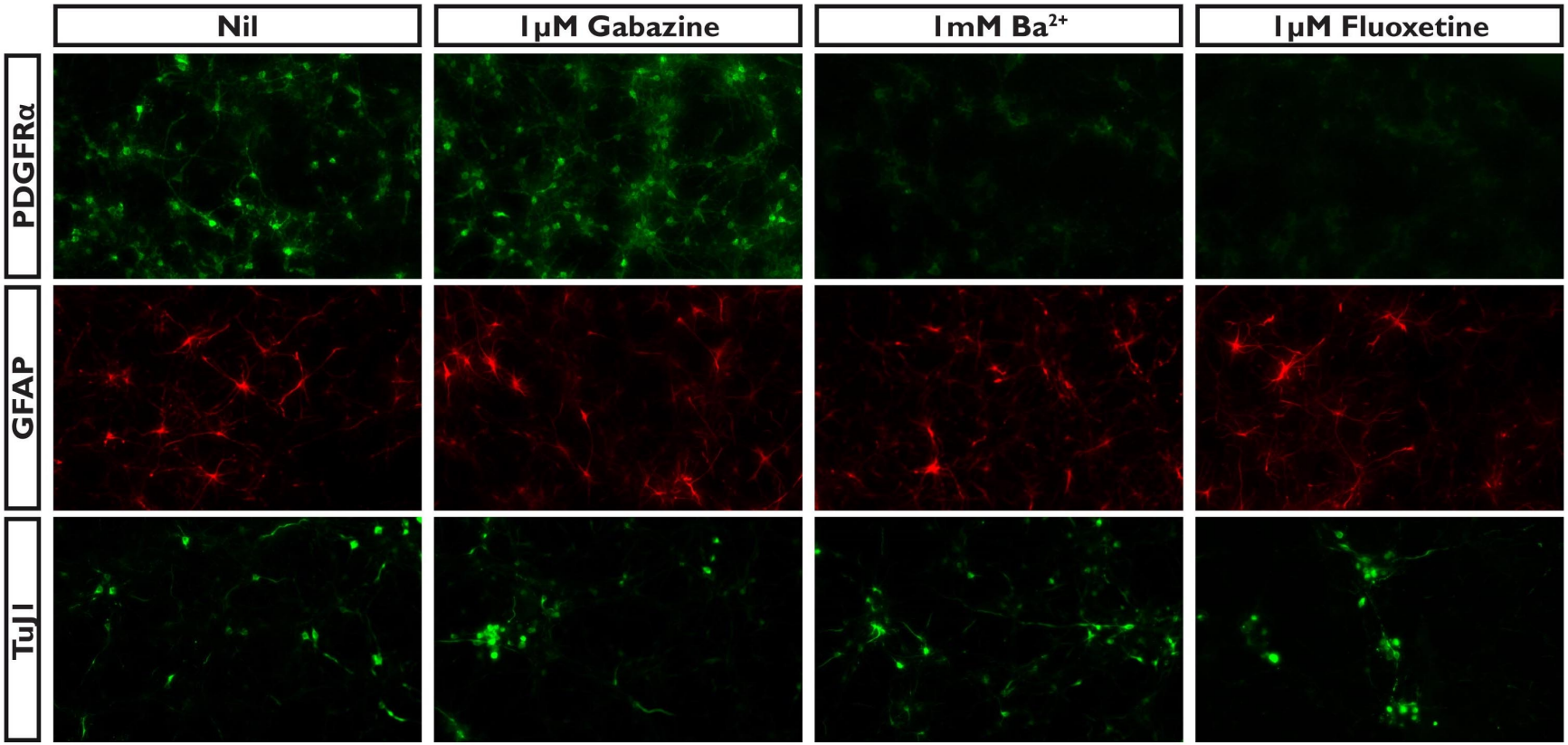

Figure 6-6 The effect of two inhibitors of Kir currents on the differentiation of neural progenitor cells. Ba^{2+} ions are regarded as a general inhibitor of Kir channels; fluoxetine has been reported to be a specific inhibitor of Kir4.1. The $GABA_A$ channel antagonist, gabazine, was used as a control in this experiment.

Discussion

The fact that *Kcnj10* is expressed in neurospheres (Figure 5-9), and may be a transcriptional target of SOX9, raised the possibility that this K^+ channel subunit might be involved in mediating the poor proliferation of $Sox9^{\Delta/\Delta}$ NPCs in the neurosphere assay. Supporting an important functional role for Kir4.1, I find that it is one of only three Kir channels expressed in wild-type $CD133^{High}$ cells. Since Kir channels have been shown to make a substantial contribution to the RMP of adult NPCs (Yasuda et al., 2008), this suggests that loss of Kir4.1 might have a dramatic effect on the RMP of radial glia, and hence diverse physiological processes within them.

The functional studies set out in this chapter also support a role for Kir4.1 in the ability of NPCs to form neurospheres in culture. Generalised blockade of Kir currents with Ba^{2+} ions reduced the proliferation of NPCs in the neurosphere assay at 1mM, a concentration commonly used for this purpose (e.g. Neusch et al., 2001). However, the situation for an inhibitor reported to be specific to Kir4.1, fluoxetine (Furutani et al., 2009, Ohno et al., 2007), was more complex. At low concentrations (1-10nM), fluoxetine appeared to increase the proliferation of NPCs through a mechanism that is unknown, but which cannot be mediated by the serotonin transporter SLC6A4, since expression of this protein is not seen in $CD133^{High}$ cells. However, at 1μM, a reduction is seen, and at 10μM, no neurospheres at all were formed. Since the IC_{50} of fluoxetine has been reported to be 15.2μM, this effect would appear to have occurred at too low a concentration for us to be confident that the effect is mediated by Kir4.1. Unfortunately, RNAi experiments intended to show definitively that *Kcnj10* is required for neurosphere formation have not so far been successful. However, *Kcnj10* remains an attractive candidate for a gene that

may be involved in mediating the reduced growth rates of neurospheres formed from *Sox9*$^{\Delta/\Delta}$ NPCs.

There are a number of mechanisms by which a change in the K^+ permeability of a cell might affect cellular processes, such as proliferation/cell-cycle progression. One possible mechanism is cell swelling, which often accompanies Kir channel blockade. Rouzaire-Dubois and Dubois (1998) showed that manipulating cell volume using hypo- or hypertonic culture medium mimicked the changes in proliferation brought about by K^+ channel modulation. Another mechanism might involve changes in intracellular Ca^{2+} concentration as a result of cell depolarisation since intracellular Ca^{2+} ions are known to influence many cellular processes through binding to Calmodulin. A third way might be through an effect resulting from changes in intracellular pH (Pappas et al., 1994), or finally, some other consequence of depolarisation of the cell.

Other authors have reached a different conclusion about the effect of Kir channels on the proliferation of NPCs, but this could be explained either by methodological differences or differences in the electrochemical gradients of adult versus embryonic NPCs. Yasuda and colleagues (2008) investigated the K^+ channel subunits expressed in adult NPCs (using dissociated neurospheres, formed from the SVZ) and found that two types, Kv and Kir, predominated. They found that the Kv blocker tetra-ethyl-ammonium (TEA) reduced the proliferation of these cells, whereas Ba^{2+}, which inhibits Kir channels, enhanced proliferation. However, on closer inspection, we find that they have used the number of cells obtained from dissociating neurosphere cultures as a measure of proliferation, and there is only a very modest increase in sphere number, and actually a decrease at 1mM. However, the spheres themselves are larger, accounting for the increase in total cell number post-dissociation.

Effect of Ba^{2+} and Fluoxetine on NPC Differentiation

Surprisingly, I find that inhibition of Kir currents with both Ba^{2+} ions and fluoxetine leads to abnormal morphology of oligodendrocytes and significantly reduced expression of PDGFRα, which suggests that Kir currents are necessary for the specification, differentiation or maturation of OPCs. However, the phenotype of the Kir4.1$^{-/-}$ mouse reveals that *Kcnj10* is not required for the formation of OPCs, but is required for their maturation (Neusch et al., 2001). Thus, loss of *Kcnj10* expression could not explain the depletion of OPCs observed in the *Sox9*$^{\Delta/\Delta}$ spinal cord (Stolt et al., 2003) or the postnatal cortex (our own data). However, this observation might reveal a role for *Sox9* in the later stages of oligodendrocyte maturation, in addition to its requirement for their initial generation.

A Role for *Kcnj10* in Establishing the Conditions for Gliogenesis?

I have raised the hypothesis that *Sox9* might set up a state in neural progenitors that creates the conditions for gliogenesis a number of times in this thesis; *Sox9* is expressed from the earliest stages of neurogenesis in the dorsal telencephalon (from ~E10.5; Scott et al., 2010), yet gliogenesis does not occur in this region of the CNS until after birth. Perhaps hyperpolarisation, brought about by expression of *Kcnj10*, is a pre-requisite for the transduction of some other stimulus that induces gliogenesis? One possible mechanism for this relates to the likely effects of a change in the RMP on the concentration of other ions within the cell that might affect the functioning of ligand-gated channels.

Further Work

In order to strengthen the evidence for a direct transcriptional relationship between *Sox9* and *Kcnj10*, it is essential to know more about the relative timing of onset of *Kcnj10* and *Sox9* expression in the developing CNS. Is it, for example, that *Kcnj10* is expressed from the first instance of *Sox9* expression (~E9.5 in the mouse) or does it arise later, suggesting the requirement of a co-factor, or a less direct relationship, perhaps mediated by an intermediate transcription factor?

I would also like to confirm that *Sox9* loss affects the RMP of NPCs in culture, which could be done by comparing the RMP of $Sox9^{Flox/Flox}$ NS cells with or without Cre-adenovirus. In the course of these experiments, we could also ask if *Sox9* deletion leads to changes in intracellular Ca^{2+} or pH, or to cell swelling, that might illuminate its role in NPC physiology. It is also important to show what effect *Kcnj10* knock-down has on NPC behaviour in the neurosphere assay. Rather than attempting to obtain a homogenous population of transfected cells, I would use plasmids that co-expressed GFP with the *Kcnj10* shRNA and ask if spheres were formed from these GFP^{+} cells, and if they were, how their sizes and relative frequencies compared to those expressing a construct containing GFP and a scrambled shRNA. It would also be important to ask whether electroporation with a *Kcnj10* expression construct could rescue proliferation in $Sox9^{\Delta/\Delta}$ neurospheres.

Chapter 7 DBI as a Candidate SOX9 Target Involved in Mediating the Impaired Neurosphere-Forming Ability of *Sox9*$^{\Delta/\Delta}$ Neural Progenitors

Apart from *Kcnj10*, the other candidate that was felt highly likely to be implicated in the *Sox9*$^{\Delta/\Delta}$ neurosphere phenotype was diazepam-binding inhibitor, DBI. This was based on two lines of evidence: Firstly, from our transcriptional profiling experiments and subsequent confirmation by qPCR, we know that *Dbi* expression is reduced in *Sox9*$^{\Delta/\Delta}$ CD133^{High} cells (2.1-fold by qPCR). It is also clear that *Dbi* is expressed in the same pattern as *Sox9* within the rostral forebrain (Figure 5-7). These observations, together with the finding that a region of the first intron of *Dbi* is bound by SOX9, make it likely that *Dbi* is a transcriptional target of SOX9. Unlike other potential targets identified in Chapter 5, *Dbi* is expressed uniformly in the VZ, and not significantly in other regions of the embryonic brain, making it a good candidate for a gene regulated by SOX9 that might influence the behaviour of progenitors. There is considerable evidence that a proteolytic product of the DBI protein is an endogenous antagonist of $GABA_A$ receptors, which are cell-surface Cl^- channels. In order to test the hypothesis that SOX9 might influence progenitor behaviour through an indirect effect on $GABA_A$ channels, I have used pharmacological manipulation to establish if modulation of GABA signalling might recapitulate the effect of SOX9 on NPC behaviour in the neurosphere assay.

Introduction

GABA and the $GABA_A$ Receptor

Gamma-aminobutyric acid (GABA) is widely known as the major inhibitory neurotransmitter of the adult brain, where it induces hyperpolarisation of post-synaptic membranes and thus increases the threshold for an action potential in the post-synaptic neuron. GABA achieves this by increasing the permeability of the cell to Cl^- ions, which are many times more concentrated outside the cell than inside it. The transient influx of Cl^- ions results in hyperpolarisation, which lessens the likelihood of future action potentials in that neuron. This effect is mediated by binding of GABA to one of three classes of GABA receptor, $GABA_A$, $GABA_B$ or $GABA_C$. $GABA_A$ and $GABA_C$ are ionotropic receptors, that is, they are themselves ion channels and binding of GABA increases the likelihood of the channel being in an open state. The $GABA_B$ receptor is a metabotropic receptor, which is not itself an ion channel, but is instead linked to a G-protein which, via second messengers, influences the opening of Cl^- channels elsewhere in the membrane. $GABA_C$ receptors are a variant of the $GABA_A$ channel, defined functionally by their insensitivity to bicuculline.

Seventeen different $GABA_A$ subunits have been described to date, which can be grouped by sequence homology into 6α, 4β, 4γ, 1δ and 2ρ subunits (Möhler et al., 1997). The $GABA_A$ receptor is a pentameric channel that is usually composed of a combination of two α-, one β- and two γ-subunits. The potential combinations of these subunits, and splice variants thereof, give rise to a formidable array of receptor subtypes, which may have slightly different pharmacological profiles. DBI, which is the focus of this chapter, is an allosteric antagonist of $GABA_A$ channels. This means, DBI, or a proteolytic

fragment of it, binds to a site separate from the sites of GABA-binding, of which there are two. Aside from the GABA binding sites, there are also three other important modulatory sites that affect the probability of channel opening: The barbiturate site, the benzodiazepine/β-carboline site, and the neurosteroid site (Upton and Blackburn, 1997).

The adoption of GABA as a neurotransmitter has been a relatively recent innovation in evolution; although it has an ancient origin: GABA is synthesised by plants, and GABA receptors, resembling the $GABA_B$ type, are expressed by the earliest phylum of Metazoa, the Porifera sponges (Shelp et al., 1999, Perovic et al., 1999). This leaves open the possibility that GABA may have other roles, possibly as a signalling molecule in a more general sense. There is mounting evidence that this may be the case in the developing mammalian CNS, where both the enzymes required for GABA synthesis and receptors equipped to respond to it are expressed in distinct regions of the progenitor zones of the forebrain (Lo Turco and Kriegstein, 1991, LoTurco et al., 1995, Ma and Barker, 1995).

GABA Signalling in CNS development

LoTurco and colleagues showed in 1995 that GABA has a strong inhibitory effect on the proliferation of neural progenitor cells (NPCs) in culture. This effect was found to be mediated by $GABA_A$ receptors, and binding of GABA to its receptor in this context was shown to bring about membrane depolarisation. This is counter-intuitive, since opening of a membrane Cl^- channel usually results in hyperpolarisation. However, it was found that in NPCs, the gradient of Cl^- is reversed, with a high intracellular concentration of Cl^- ions. This led another group to investigate the expression of GAD67, an enzyme required for the biosynthesis of GABA, and a number of $GABA_A$ subunits in the embryonic brain and spinal cord. They found that GAD67 is expressed in the SVZ of the dorsal telencephalon,

and that the α4-, β1- and γ1-subunits of the $GABA_A$ receptors are expressed in the VZ. Other subunits (α3, β3 and γ2) where confined to the cortical plate (CP), suggesting that they were destined to form the GABA receptors conventionally found in synapses. It is interesting to note that the pattern of subunit expression in both the embryonic VZ and CP is different to that commonly observed in the adult brain (two α-, one β- and two γ2-subunits; Möhler et al., 1997). These findings raise the possibility that in the dorsal telencephalon, GABA, secreted by the cells of the SVZ, might be signalling back to the progenitors of the VZ, stimulating their proliferation. Other authors have assayed GABA concentration in the embryonic brain directly and found that GABA is by far the most highly expressed neurotransmitter in both the developing cerebellum (assayed from E15) and the developing olfactory bulbs (assayed from E13; Miranda-Contreras et al., 1999, Miranda-Contreras et al., 2000).

In addition to expression in the embryo, a recent paper has shown that both GAD and $GABA_A$ subunits are expressed in neurospheres derived from the SVZ neural stem cell niche of the adult brain (Nguyen et al., 2003). There is also evidence that neurospheres derived from the embryonic brain maintain their responsiveness to GABA over several passages (Sah et al., 1997).

How Might GABA Affect the Proliferation of NPCs?

Most importantly from our perspective, GABA has been found to depolarise NPCs from the dorsal telencephalon of the rat brain (Lo Turco and Kriegstein, 1991). This effect was abolished by pre-treatment with bicuculline, a specific antagonist of $GABA_A$ channels, and enhanced by diazepam, a positive allosteric modulator of $GABA_A$ channels (LoTurco et al., 1995). To the surprise of the investigators, it was found that GABA induces Cl^-

efflux from the cell, and infusion of the cell with a solution that did not contain Cl^- ions prevented GABA-induced depolarisation. Changes in intracellular Ca^{2+} concentration were also noted, and the shifts in Ca^{2+} ions resulting from GABA application resembled to the authors those seen with voltage-gated Ca^{2+} channels. This was confirmed by blockade of the Ca^{2+} channels with La^{3+} ions. Thus, the authors showed elegantly that Cl^- efflux mediated by GABA binding to $GABA_A$ receptors led to membrane depolarisation, which through the activation of voltage-gated Ca^{2+} channels, inhibited DNA synthesis (using [^{3}H]-thymidine and bromodeoxyuridine (BrdU) assays). Using slice cultures, they showed that this is in fact a physiological mechanism by which proliferation is regulated, by demonstrating that addition of $GABA_A$ channel antagonists to cortical slices significantly increases proliferation in the VZ.

Diazepam-Binding Inhibitor

DBI was first identified in 1983 by Guidotti and colleagues as the first endogenous ligand of the benzodiazepine/β-carboline recognition site of the $GABA_A$ receptor. Many years previously, it had been discovered that the anxiolytic/hypnotic drug, diazepam, exerted its effects by modulation of GABAergic transmission (Polc and Haefely, 1976). This began a search for an endogenous compound that might interact with this site. Guidotti and colleagues showed that DBI is at least one endogenous ligand of the benzodiazepine/β-carboline site by demonstrating its ability to displace both diazepam and its antagonist, β-carboline, from this site on crude synaptic membranes, but not GABA, which binds at a separate site. They also elegantly demonstrated the *in vivo* relevance of this effect by showing that intraventicular infusion of DBI abrogated the anti-conflict effect of diazepam in thirsty rats (Vogel test). Shortly after Guidotti et al. identified DBI and described its function, the benzodiazepine/β-carboline recognition site was found to be located on the γ_2-subunit of the $GABA_A$ receptor (Pritchett et al., 1989). However, inverse agonists such as DBI can exert weak effects on receptors that include the γ1-subunit but not the γ2, showing that the benzodiazepine/β-carboline site is not wholly dependent on the presence of a γ2-subunit (Puia et al., 1991). In addition to $GABA_A$ receptors, DBI is known to bind 'peripheral-type' benzodiazepine sites, which are located on mitochondrial membranes in secretory tissues (Parola et al., 1993, Upton and Blackburn, 1997).

However, DBI's status as a neurotransmitter was quickly challenged on two counts: First, it is expressed in many tissues, not just the brain, and secondly, it carries no 'export signal' from the cell, and so it was not thought to be secreted (Shen et al., 2006). On the basis of its high expression in the liver, and its lack of a signal sequence, Knudsen and Nielsen (1990) asserted their view that DBI was more likely to be an acyl-CoA binding

protein, involved in lipid biosynthesis. However, the authors of the original paper re-asserted their findings that DBI is able to displace [^{3}H]diazepam, and that intraventricular administration of DBI abrogates the anti-conflict effects of diazepam. They suggested that although full-length DBI lacks a signal sequence, proteolytic derivatives of the protein might be secreted from the cell. For instance, Slobodyansky and colleagues (1989) identified a secreted polypeptide thought to be formed from proteolysis of DBI (triakontatetraneuropeptide [TTN]); however, they find that this protein does bind to 'central' type benzodiazepine/β-carboline sites, so would not modulate the activity of $GABA_A$ channels.

Genetic ablation of the *Dbi* locus has yielded conflicting results. Landrock and colleagues (2010) find that deletion of the *Dbi* gene is embryonic lethal, whereas Neess and colleagues (2011) find a much milder phenotype involving delayed activation of lipo- and cholesterogenic gene expression programs following weaning, although the latter result seems the most likely in light of the fact that a naturally-occurring deletion that includes the *Dbi* locus gives rise a mild phenotype limited to sparse, greasy hair (Lee et al., 2007).

Results

Surprisingly, the site identified by ChIP-Seq as being bound by SOX9 lies in intron 3-4 (the last intron) of *Dbi*. However, due to the small size of the gene, and the relative shortness of the two preceding introns, this site is only 5.2kb upstream of the transcriptional start site. Like the two regions identified in *Kcnj10*, this SOX9 binding site lies within a region that is highly conserved within mammalian species (in metatherians as well as eutherians; Figure 7-1). Other parts of the same intron show no conservation at all with non-rodent species, suggesting that there is a role for this region in the regulation of *Dbi* transcription. Unlike the two SOX9 binding sites identified in *Kcnj10*, this binding site is not associated with a ZFP263 binding site. However, there are similarities between the factors binding close to SOX9 in the *Kcnj10* locus and at this site. The site in *Dbi* is close to a 'Barbie box', which is shared by many barbiturate-inducible genes. This site is also present in the vicinity of Binding Site A in *Kcnj10* (Figure 6-1). In addition, two binding sites for a MEIS1A/HOXA9 heterodimer are present in the vicinity of the SOX9 binding site in *Dbi*, and Binding Site B in *Kcnj10* is also close to a MEIS1A/HOXA9 binding site.

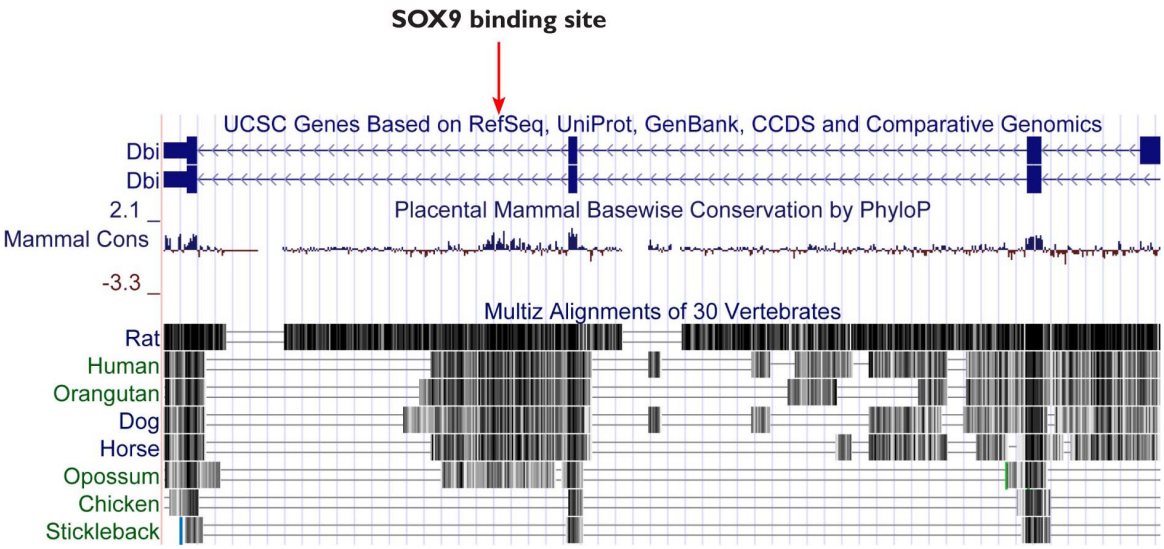

Figure 7-1 The SOX9 binding site identified by ChIP-Seq is highly conserved across mammalian species.

Matrix Family	Family Information	Matrix	Start Position	End Position	Strand
V$MYBL	Cellular and viral myb-like transcriptional regulators	V$CMYB.02	9	23	+
V$HOXH	HOX - MEIS1 heterodimers	V$MEIS1A_HOXA9.01	28	42	-
V$MYT1	MYT1 C2HC zinc finger protein	V$MYT1L.01	31	43	+
V$TALE	TALE homeodomain class recognizing TG motifs	V$MEIS1.02	31	47	+
V$MYBL	Cellular and viral myb-like transcriptional regulators	V$VMYB.02	38	52	+
V$BARB	Barbiturate-inducible element box from pro+eukaryotic genes	V$BARBIE.01	40	54	-
V$NF1F	Nuclear factor 1	V$NF1.04	41	61	+
V$E2FF	E2F-myc activator/cell cycle regulator	V$E2F.02	44	60	-
V$CTCF	CTCF and BORIS gene family, transcriptional regulators with 11 highly conserved zinc finger domains	V$CTCF.04	47	73	-
V$MYT1	MYT1 C2HC zinc finger protein	V$MYT1L.01	52	64	-
V$HOXH	HOX - MEIS1 heterodimers	V$MEIS1A_HOXA9.01	53	67	+
V$DEAF	Homolog to deformed epidermal autoregulatory factor-1 from D. melanogaster	V$NUDR.01	59	77	+

Figure 7-2 Transcription factor binding sites within 40bp of the SOX9 binding site.

In order to ascertain if DBI might mediate the effect of loss of *Sox9* on the formation of neurospheres, cell suspensions from E14.5 dorsal telencephalons of wild-type MF1 mice were cultured in the presence of a variety of concentrations of i) an agonist of the $GABA_A$ receptor (muscimol), and ii) two specific antagonists of $GABA_A$ channels, SR-95531 and bicuculline (Figure 7-3). Since there is a lack of an antagonist of $GABA_A$ channels in the $Sox9^{\Delta/\Delta}$ (DBI), it might be expected that an agonist of $GABA_A$ receptors such as muscimol would at least partially recapitulate the $Sox9^{\Delta/\Delta}$ phenotype and hence reduce the rate of neurosphere formation. This is in fact what was seen: At 100nM, there was a small reduction in neurosphere number after 6 days *in vitro* (15% relative to untreated NPCs, which is not statistically significant); however, between 100nM and 1μM, there was a significant drop in neurosphere number (to 59% of the untreated level; $p = 0.03$), and this change occurs close to the EC_{50} of muscimol (1.7μM). Conversely, one might expect treatment with an antagonist to produce the reverse effect, an increase in the rate of neurosphere formation, and again this is what was seen with the $GABA_A$ antagonist, SR-95531. This result is particularly striking, with a 3-fold increase in the number of neurospheres from 100nM to 1μM, which is the range in which the IC_{50} for this antagonist lies. Unfortunately, the same effect is not seen with bicuculline, which is also a specific antagonist of $GABA_A$ receptors, although it is possible that the subunit composition of embryonic $GABA_A$ receptors differs from that of adult $GABA_A$ receptors. However, LoTurco and colleagues (1995) were able to antagonise the depolarisation elicited by GABA using bicuculline, although this was in NPCs from a slightly later time in development (E16.5).

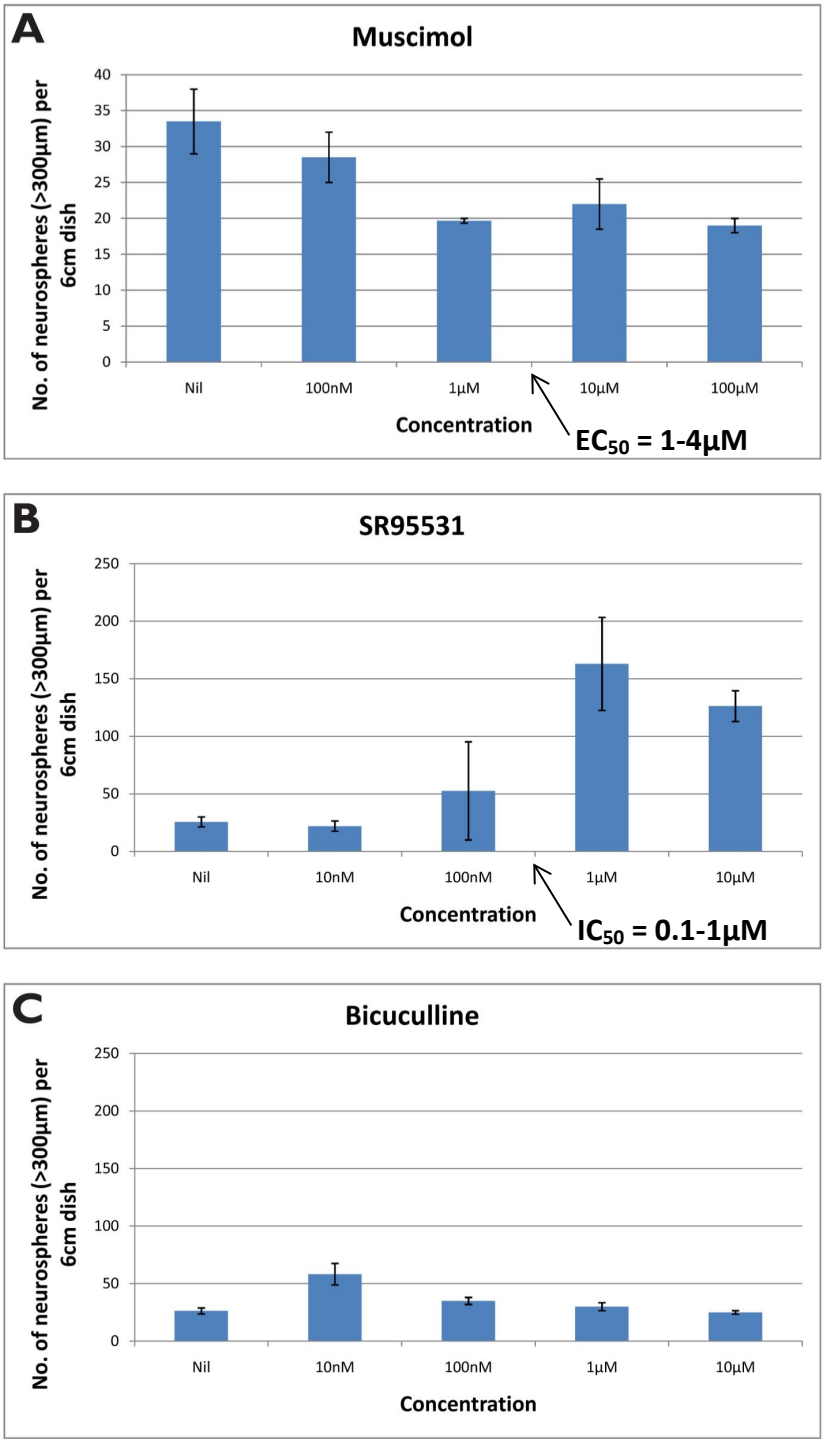

Figure 7-3 The effect of various concentrations of two antagonists, SR95531 and bicuculline, and one agonist of $GABA_A$ channels, muscimol, on the proliferation of NPCs in the neurosphere assay (N=3).

Rescue

Although these *in vitro* results are consistent with previous findings that the activation of $GABA_A$ channels can inhibit cell-cycle progression, and thus might be a mechanism by which loss of *Sox9* could impair neurosphere formation, we have not proven this link. In order to show this, I attempted to rescue the $Sox9^{\Delta/\Delta}$ phenotype using SR-95531. I reasoned that, if the major reason why $Sox9^{\Delta/\Delta}$ NPCs were proliferating poorly was the unrestrained activity of $GABA_A$ channels, leading to depolarisation and cell-cycle arrest, restoring normal inhibition would eliminate this restraint on proliferation, and result in similar rates of neurosphere formation between SR-95531-treated $Sox9^{\Delta/\Delta}$ NPCs and SR-95531-treated $Sox9^{F/F}$ NPCs. If, however, another mechanism was mediating the defect, SR-95531 might increase proliferation in $Sox9^{\Delta/\Delta}$ NPCs, but not to wild-type (+ SR-95531) levels. To distinguish these two possibilities, I cultured E14.5 NPCs from $Sox9^{F/F}$ embryos containing a ROSA26 reporter transgene, to which a Cre adenovirus was added. To control dishes, a GFP adenovirus was added in place of the Cre adenovirus. Both Cre-treated and control dishes showed high transduction rates, close to 100%. However, in these experimental conditions, no reduction in neurosphere numbers was seen after *Sox9* deletion. One explanation for this might be that by E14.5, several days of *Sox9* expression has set in motion genetic programs which are then resistant to its removal. Were I to repeat this experiment, I would use $Sox9^{F/F;NesCre}$ cells, and compare them to $Sox9^{F/F}$ cells, with and without SR-95531. This would allow us to ask, in cells never exposed to *Sox9*, if an antagonist of $GABA_A$ channels could achieve maximal rates of neurosphere formation (equivalent to wild-type cells + SR-95531), and thus determine if the loss of $GABA_A$ channel inhibition is the major cause of the $Sox9^{\Delta/\Delta}$ neurosphere phenotype.

Discussion

Dbi appears to be a good candidate for a direct target of SOX9 that might influence the proliferation of neural progenitors. It is down-regulated in the absence of *Sox9*, expressed in the same domain as *Sox9*, and its final intron contains a highly conserved region that includes a SOX9 binding site. Previous work has demonstrated that GABA strongly inhibits proliferation (LoTurco et al., 1995), and our own data shows that activation of GABA receptors reduces neurosphere-forming ability. Moreover, inhibition of GABA signalling in cortical slices (LoTurco et al., 1995), and in neurospheres (our own data), substantially increases proliferation/neurosphere formation, demonstrating a role for endogenously secreted GABA in controlling proliferation. In the context of the neurosphere assay, these findings suggest a model in which GABA released within neurospheres, but probably not by NPCs (since GAD is expressed in the SVZ of the embryonic brain), depolarises NPCs. A potential model for how DBI might mediate the poor proliferation of $Sox9^{\Delta/\Delta}$ NPCs in the neurosphere assay is shown in Figure 7-4. In the wild-type situation, a fragment of DBI (such as octadecaneuropeptide, ODN) might be secreted by NPCs, and may, in an autocrine or paracrine fashion, dampen down the activation of GABA receptors, allowing cell-cycle progression. However, in the absence of SOX9, *Dbi* transcription would be radically reduced, meaning that there would be no opposition to the action of GABA with the result that the majority of $Sox9^{\Delta/\Delta}$ NPCs would fail to form neurospheres of substantial size.

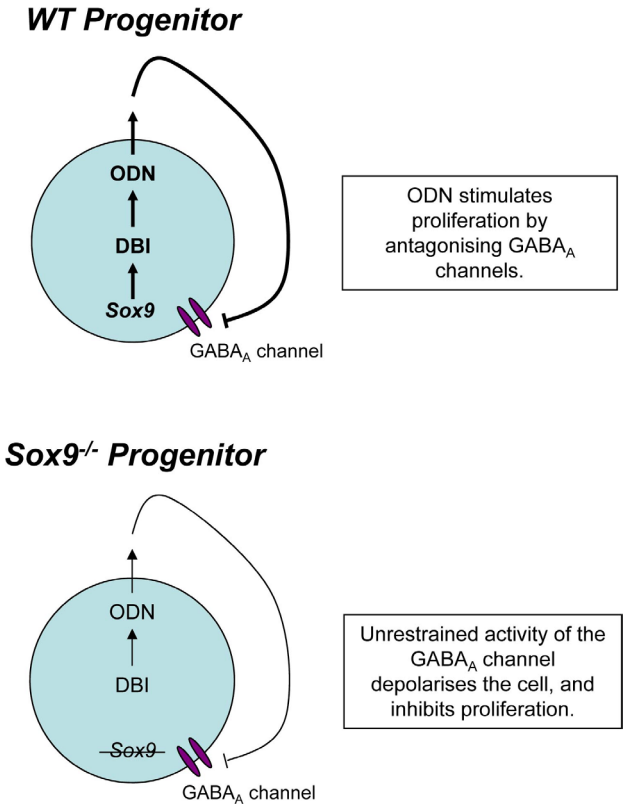

Figure 7-4 Potential model illustrating how reduced expression of DBI might contribute to the poor growth rates of *Sox9*-deficient neurospheres. ODN – octadecaneuropeptide.

In the developing embryo, GABA appears to be secreted by the cells of the SVZ, whereas the $GABA_A$ receptor subunits are confined to the VZ (Ma and Barker, 1995). This is interesting in the context of the increasing size of the SVZ, relative to the VZ, during corticogenesis. It is conceivable that as the number of GABA-secreting SVZ cells increases, this has an inhibitory effect on proliferation within the VZ. It is not yet clear to what extent this mechanism is important in controlling neurogenesis, although it is interesting to note that the $GABA_A$ receptor, with its multiple modulatory sites, would be capable of integrating a number of pro- and anti-proliferative signals. The effect of $GABA_A$ channel activation on proliferation is thought to be mediated by an increase in cytosolic Ca^{2+} (Ma et al., 1998a), although it is also possible that other mechanisms, such as cell swelling, or altered intracellular pH might be the cause.

$GABA_A$ or $GABA_C$?

The findings of this chapter suggest that the effect of GABA on NPCs is mediated by bicuculline-insensitive channels. This is not in agreement with the work of LoTurco and colleagues (1995), who showed that bicuculline could prevent the depolarisation of NPCs by GABA, although this was at a later time-point (E16.5). The bicuculline-insensitivity of these GABA channels suggests that a definition of $GABA_C$ may be more appropriate. It is possible that subunit expression in the embryonic VZ is dynamic, and that the subunit or units that render $GABA_A$ channels susceptible to bicuculline might not be expressed until after E14.5.

Potential SOX9 Binding Partners?

Binding sites for the MEIS1A/HOXA9 heterodimer, which is believed to participate in *Gata1* transactivation (Pillay et al., 2010), were found both at the 'B' binding site of *Kcnj10* (Figures 6–1 and 6–2), and at the site in the final intron of *Dbi*. However, an initial inspection of the entries for these genes in the Allen Brain Atlas does not show any significant expression in the embryonic forebrain. If this were confirmed by my own in situs, it would rule out these factors as potential binding partners for SOX9 in the developing CNS. Barbiturate-inducible elements ('Barbie boxes') are also present in both *Kcnj10* Site A and the *Dbi* site. The Barbie box is thought to be bound by a repressor (Bm3R1) in most instances, but can be displaced by an activator (Bm1P1) when this is expressed (reviewed in Sueyoshi and Negishi, 2001).

Further Work

Our existing data on the pharmacological manipulation of $GABA_A$ channels shows the effect of modulation of GABA by antagonists that act on the GABA binding site. This does not show that an effect on proliferation can be brought about by DBI itself. Since recombinant DBI is now available commercially, it would obviously strengthen our argument to show that DBI itself can enhance proliferation. Furthermore, showing that this effect can be blocked by flumazenil, which binds to the benzodiazepine/β-carboline site, would show that this effect was mediated by $GABA_A$ channels and not other DBI receptors, such as the peripheral-type found on the surface membranes of mitochondria (Upton and Blackburn, 1997). Ultimately, only a rescue experiment could provide direct evidence that *Sox9* is affecting proliferation through this mechanism. In addition to proliferation, it would be interesting to see if $GABA_A$/$GABA_C$ activation by muscimol or GABA could affect the differentiation capacity of NPCs upon growth factor withdrawal, because this is another aspect to the abnormal behaviour of $Sox9^{\Delta/\Delta}$ NPCs noted in Scott and colleagues' paper (2010).

Chapter 8 General Discussion

The phenotype of the *Sox9*$^{\Delta/\Delta}$ embryo reveals that in the absence of *Sox9*, radial glia are specified, begin to produce neurons at the expected time, and give rise to normal numbers of intermediate progenitors during corticoneurogenesis. Further to this, neurons of different layer-fates are generated and migrate to their intended positions in the developing cortical plate. However, *Sox9*$^{\Delta/\Delta}$ mice do show a profound deficit of oligodendrogenesis in the MGE during embryonic development and in the postnatal cortex. This is consistent with the findings of Stolt et al. (2003) and Scott et al. (2010), who both saw defects of oligodendrogenesis in *Sox9*$^{Flox/Flox}$;NesCre mice. This dramatic reduction in OPC numbers supports a requirement for *Sox9* in the specification of OPCs.

It is surprising, however, that a gene expressed throughout corticogenesis (from E10.5; Scott et al., 2010), should have no apparent effect on this process when it is removed. There are several possible explanations for this: First, because the Nestin-Cre becomes active fractionally after *Sox9* is first expressed, the NPCs of the dorsal telencephalon will have already been exposed to SOX9, and this brief exposure may have been sufficient to set in motion genetic programs, for instance, specifying NPC identity, which are then refractory to its removal. However, it has been shown that fewer neurospheres are formed at E14.5 using the same strategy to delete *Sox9* (the Nestin-Cre), showing that this initial exposure to SOX9 is not sufficient for normal neurosphere generation later in embryonic development (Scott et al., 2010).

Another possible explanation for the lack of a cortical phenotype is that another transcription factor, expressed in the embryonic VZ, but down-regulated in neurospheres, might be compensating for SOX9 loss by binding to the same regions within the genome.

Since there is a high degree of homology between different SOX proteins, particularly in their HMG boxes, the most likely candidates to compensate for SOX9 are other SOX proteins expressed in NPCs. Re-analysis of the RNA-Seq data from E16.5 dorsal telencephalons reveals that *Sox* genes of the *SoxC* subfamily, *Sox4*, *Sox11* and *Sox12* are the most strongly expressed *Sox* genes in cells enriched for CD133 expression ($CD133^{High}$ cells), with between 692 and 13,033 reads mapping to these loci per kilobase of their CDS (Figure 8-1). However, *Sox4* and *Sox11* are expressed only in newly-formed neurons arising in the VZ (Bergsland et al., 2006), and *Sox12* is expressed in both mature neurons and NPCs, but more intensely in the former (Hoser et al., 2008). Also highly expressed in $CD133^{High}$ cells are *Sox5* and *Sox6*. These transcription factors are known to be expressed throughout the VZ of the developing spinal cord, which supports a compensatory role in progenitor identity. However, recent evidence suggests that they antagonise SOX9 binding during neurogenesis (Stolt et al., 2006). *Sox21* is also found in the $CD133^{High}$ cells; however, in the spinal cord its expression was found to be restricted to newly-formed neurons, and ectopic expression causes progenitors to differentiate and up-regulate neuronal markers (Sandberg et al., 2005), suggesting that its role is antagonistic to *Sox9*.

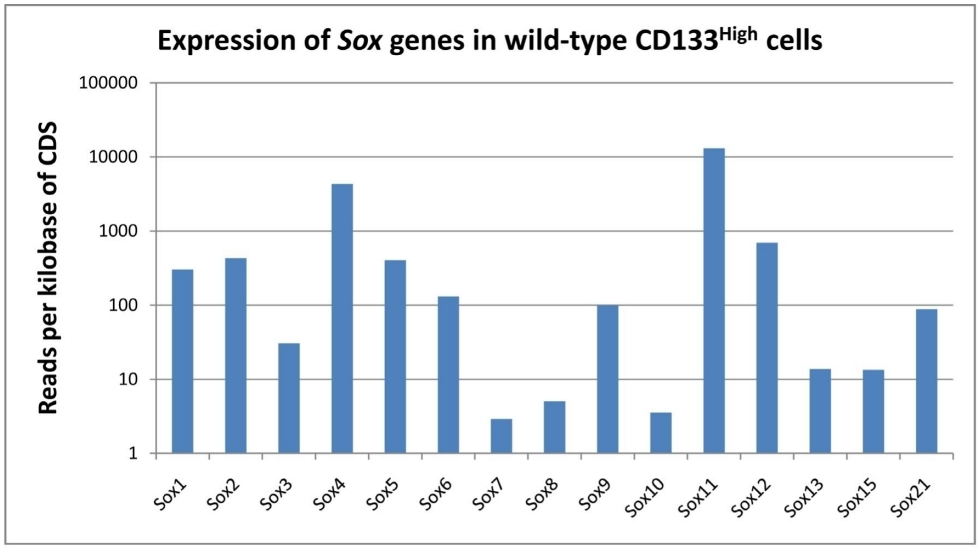

Figure 8-1 Expression of *Sox* genes in wild-type $CD133^{High}$ cells. Those genes with <1 read mapping per kilobase of CDS were omitted.

Because of the close homology between SOX9 and the other two members of the SOXE subfamily, SOX8 and SOX10, both within and outside their HMG boxes, several authors have suggested that these two proteins are the best candidates to compensate for SOX9 (Stolt et al., 2003, Scott et al., 2010). This is supported by the finding that these two transcription factors show functional redundancy with SOX9 in the oligodendrocyte lineage (Finzsch et al., 2008, Stolt et al., 2005). However, neither *Sox8* or *Sox10* are significantly expressed in the $CD133^{High}$ cells, and evidence from the literature shows that *Sox10* is only expressed in a restricted region of the VZ in the spinal cord (the pMN region; Stolt et al., 2002, Stolt et al., 2005, Kellerer et al., 2006, Finzsch et al., 2008) and *Sox8* expression is also restricted to the ventral spinal cord (Stolt et al., 2005, Kellerer et al., 2006), suggesting that these two factors could not compensate for a function of *Sox9* in NPCs as a whole. This leaves *Sox1* and *Sox2*, which are relatively highly expressed in $CD133^{High}$ cells (302 and 432 reads mapping per kilobase, respectively), and are restricted to the progenitors of the VZ (Bylund et al., 2003, Graham et al., 2003).

One final possibility is that SOX9 provides added stability to a complex of transcription factors that will still bind and transactivate in its absence, but less reliably, and such a phenotype may be highly dependent on genetic background. This is analogous to the synergistic effects of SOX5, SOX6 and SOX9 in the transactivation of the *Col2a1* gene in 10T1/2 cells, in which SOX5 and SOX6 will enhance transcription, but when SOX9 is also present, transactivation is considerably more efficient (Lefebvre et al., 1998).

This leaves two possible scenarios for functional compensation by SOX proteins in NPCs of the embryonic VZ: Either one of the SOXB1 proteins are able to compensate for SOX9 loss (probably SOX1 or SOX2 as these are the most strongly expressed; Figure 8-1), or SOX5/SOX6 act synergistically with SOX9 to transactivate genes important for

progenitor identity and multipotency, but antagonistically at sites important for transactivation of genes required for oligodendrocyte differentiation (as shown by Stolt et al., 2006). The former possibility would be amenable to compound deletion by examining the phenotype of *Sox1*$^{F/F}$;*Sox9*$^{F/F}$;NesCre and *Sox2*$^{F/F}$;*Sox9*$^{F/F}$;NesCre mice for premature differentiation of NPCs or disordered corticogenesis.

Transcriptional Profiling

As I alluded to in the *General Introduction*, *Sox9* expression long precedes the onset of gliogenesis in all regions of the CNS, which is the sole abnormality of the *Sox9*$^{\Delta/\Delta}$ mutants observed in our phenotypic analysis (Chapter 3). This led us to hypothesise that *Sox9* may establish the conditions, perhaps expression of a receptor (or receptors), that are responsible for initiating gliogenesis. In order to answer this question, I performed transcriptional profiling experiments on E16.5 CD133^{High} cells from the dorsal telencephalon, to identify differentially expressed genes that may account for an altered ability of *Sox9*$^{\Delta/\Delta}$ NPCs to respond to a gliogenic signal. The rationale for choosing E16.5 dorsal telencephalons is that this is a time-point just before the onset of gliogenesis in this region, which would occur around the time of birth (Kessaris et al., 2006). This experiment highlighted one category of molecular function, the VEGF receptors, whose members were consistently down-regulated in the absence of SOX9. Since VEGF receptors are known to be important for the initial specification of OPCs (Le Bras et al., 2006), this might explain the reduction in OPC numbers seen in the *Sox9*$^{\Delta/\Delta}$ CNS. Analysis of the categories of molecular function affected by *Sox9* loss also revealed the up-regulation of a transcription factor (*Tlx*) that inhibits astrocyte differentiation, which might explain the delayed transition from glio- to neurogenesis in the spinal cords of *Sox9*$^{\Delta/\Delta}$ mice observed by Stolt et al. (2003). Another potential repressive target of SOX9,

Runx3, is expressed in newly-formed neurons and is known to negatively regulate proliferation in other contexts (Li et al., 2002), suggesting that suppression of this factor may be important in progenitor identity.

Candidate Downstream Targets of SOX9

Since I now had a dataset of *Sox9* targets, albeit from a late time-point in neurogenesis, I decided to use these target lists to try to identify an individual target or group of targets that might explain the observation in the paper of Scott and colleagues (2010) that, even late in neurogenesis, $Sox9^{Flox/Flox}$;NesCre NPCs exhibit poor neurosphere-forming ability within the neurosphere assay. By overlapping the target lists from the RNA-Seq and microarray experiments, two lists were refined, one of consistently up-regulated genes across the two experiments, and one of consistently down-regulated genes. Because the members of these lists had met the criterion for statistical significance in two independent experiments, the probability of them appearing on this list by chance was very slim. Consequently, all of the 13 putative down-regulated genes tested were confirmed by qPCR, as were 3 of the 5 up-regulated targets. Furthermore, using a ChIP-Seq dataset generated by another group at our Institute, I found that 11 of the 13 had a SOX9-bound region within 20kb of their transcriptional start site, and 3 had two such sites. In order to look for primary targets of SOX9, *in situ* probes were made against all 13 down-regulated candidates; unfortunately time did not allow the expression patterns of the up-regulated genes to be explored. When the resulting expression patterns were examined, it was found that six of the 13 candidates were expressed in the same distribution as *Sox9*, which would be consistent with these genes being primary targets of SOX9. Of the remaining seven, a proportion were expressed in the SVZ, and interestingly, two (*Hopx* and *Tnfrsf19*) were expressed in the medial VZ, the region from which radial glia would be

about to migrate to form the indusium griseum. This observation suggests that *Hopx* and *Tnfrsf19* might lie downstream of *Sox9* in specifying future indusium griseum (IG) cells. However, since these cells are only induced in a defined region of the *Sox9* expression domain, the involvement of a co-factor would be required, and in light of recent observations that FGFR1 is important for the specification or delamination of these cells, I think that an effector of FGF signalling might be this co-factor, perhaps by synergistically activating genes required for IG specification/delamination.

Since loss of *Sox9* produces a proliferation defect in NPCs in the neurosphere assay, any target of SOX9 involved in mediating this effect would have to be expressed in neurospheres derived from wild-type tissue. Consequently, RT-PCR was performed to compare the expression of the six remaining candidates in wild-type neurosphere cultures and E14.5 dorsal telencephalons. Expression of three genes, *Kcnj10*, *Dbi* and *Arhgef3*, was found to be maintained after 7 days *in vitro*, and since one of these is an ion channel and another a modulator of GABA signalling, we asked if pharmacological manipulation of these cell-surface proteins could re-capitulate the impaired neurosphere-forming ability of $Sox9^{\Delta/\Delta}$ NPCs.

Functional Studies

Two of the candidates, *Kcnj10* and *Dbi*, were chosen for further investigation to establish if their down-regulation might be the cause of the proliferation defect or the lack of multipotentiality exhibited by $Sox9^{\Delta/\Delta}$ NPCs. It was found that an analogue of GABA, muscimol, reduced the growth rates of neurospheres in a dose-dependent fashion, and that inhibition of GABA signalling using SR95531 radically enhanced neurosphere formation. This supports a role for DBI in the proliferation defect observed in $Sox9^{\Delta/\Delta}$ neurospheres.

In the wild-type situation, opening of $GABA_A$ channels in response to GABA would be dampened by the action of DBI or a fragment thereof. However, in *Sox9*$^{\Delta/\Delta}$ neurospheres, significantly lower levels of DBI would be unable to prevent the opening of the $GABA_A$ channels, resulting in depolarisation of the NPCs, and cell-cycle arrest (a phenomenon demonstrated by LoTurco et al., 1995). Down-regulation of *Kcnj10* may also affect proliferation of NPCs, since blockade of inwardly-rectifying channels by Ba^{2+} ions reduces neurosphere numbers, as does fluoxetine, which is believed to block the specific Kir channel formed by homotetramers of KCNJ10, Kir4.1. In addition to an effect on proliferation, down-regulation of *Kcnj10* may also explain or contribute to the loss of OPCs in the *Sox9*$^{\Delta/\Delta}$ since in differentiation assays of neurospheres, those exposed to either Ba^{2+} ions or fluoxetine exhibit a specific defect of oligodendrocyte differentiation. Neurospheres differentiated in the presence of either of these two inhibitors give rise to morphologically normal neurons and astrocytes, but the oligodendrocytes formed show fewer processes, a less differentiated morphology, and lower expression of PDGFRα.

In conclusion, I have identified two potential mechanisms for the impaired proliferation of *Sox9*$^{\Delta/\Delta}$ NPCs in the neurosphere assay: The first is that loss of SOX9 results in the reduced secretion of a negative modulator of GABA, causing NPCs to become depolarised and undergo cell cycle arrest. However, the loss of the inwardly-rectifying K^+ channel, Kir4.1, also appears to affect their proliferation. Further studies attempting to rescue the *Sox9*$^{\Delta/\Delta}$ phenotype will be required to determine which of these mechanisms is the most important in producing the observed phenotype. Surprisingly, corticogenesis proceeds normally in the *Sox9*$^{\Delta/\Delta}$ despite SOX9 being expressed in the progenitors that give rise to these neurons, and this may be because the Nestin-Cre acts too late (after NPC specification) or because another SOX protein compensates for its loss by binding to the same sites within the genome. The best candidates to fulfil this compensatory role are

proteins of the SOXB1 subfamily because these are expressed within the VZ during corticoneurogenesis. I also find that VEGF receptors are down-regulated in the absence of *Sox9*, which may explain the dramatic reduction in OPCs seen in the $Sox9^{\Delta/\Delta}$ CNS, and screening of down-regulated targets by examining their expression patterns revealed two genes (*Hopx* and *Tnfrsf19*) that might be responsible for the failure of midline glia populations, necessary for formation of the corpus callosum, to be specified and migrate to the correct location in the developing brain.

Appendix A

RNA-Seq Up-Regulated Gene List ($p \leq 0.05$, fold change ≤ -1.25)

Rank	Gene Symbol	Fold Change	p-value
1	*1700028P14Rik*	Inf	0.033
2	*5830416P10Rik*	Inf	0.022
3	*A330049M08Rik*	Inf	0.036
4	*Aass*	Inf	0.003
5	*Aire*	Inf	0.039
6	*AL596181.1*	Inf	0.013
7	*AL929524.1*	Inf	0.013
8	*Bbox1*	Inf	0.034
9	*Cdkl1*	Inf	0.021
10	*Cyp4f14*	Inf	0.019
11	*Gm10103*	Inf	0.033
12	*Gm10109*	Inf	0.039
13	*Gm10609*	Inf	0.036
14	*Gm6756*	Inf	0.022
15	*Gm9793*	Inf	0.021
16	*Grb7*	Inf	0.033
17	*Grem2*	Inf	0.004
18	*Hal*	Inf	0.039
19	*Hoxc11*	Inf	0.036
20	*Hsf4*	Inf	0.039

Rank	Gene Symbol	Fold Change	p-value
21	*Kcna5*	Inf	0.033
22	*Kdm4d*	Inf	0.033
23	*Lbp*	Inf	0.036
24	*Lefty2*	Inf	0.041
25	*Lrrc34*	Inf	0.034
26	*Mlph*	Inf	0.039
27	*Mthfr-ps1*	Inf	0.034
28	*Myof*	Inf	0.021
29	*Naif1*	Inf	0.017
30	*Runx3*	Inf	0.033
31	*Slc35d3*	Inf	0.045
32	*Slc9a3*	Inf	0.041
33	*Spn*	Inf	0.007
34	*Tlr5*	Inf	0.033
35	*Tmem139*	Inf	0.033
36	*Ttc36*	Inf	0.033
37	*Zdhhc19*	Inf	0.034
38	*Si*	41.27	0.001
39	*Palm2-Akap2*	24.37	0.006
40	*Lama3*	23.52	0.006
41	*Lipt1*	18.88	0.015
42	*Runx2*	16.57	0.040
43	*Gm5048*	14.89	0.038
44	*Gm5423*	14.11	0.037

Rank	Gene Symbol	Fold Change	p-value
45	*Thnsl2*	12.67	0.044
46	*Sfn*	9.79	0.046
47	*Lxn*	9.08	0.027
48	*Cnpy1*	8.80	0.006
49	*Xdh*	8.60	0.007
50	*Mybph*	8.29	0.004
51	*Ttr*	7.99	0.003
52	*AL845463.1*	7.54	0.002
53	*Gm10335*	6.90	0.028
54	*D17H6S56E-3*	6.78	0.010
55	*Gm10751*	6.77	0.019
56	*Gm12500*	6.34	0.000
57	*Gm10197*	6.29	0.027
58	*Npsr1*	6.10	0.043
59	*Gm6043*	6.07	0.043
60	*Sh3tc1*	6.05	0.027
61	*Tspan1*	5.96	0.020
62	*Fam122a*	5.82	0.042
63	*Zfp566*	5.75	0.003
64	*5430435G22Rik*	5.19	0.025
65	*Adrb2*	5.03	0.041
66	*Slc2a5*	4.68	0.001
67	*Abcc6*	4.52	0.006
68	*Gm10480*	4.07	0.040

Rank	Gene Symbol	Fold Change	p-value
69	*Itgax*	4.07	0.004
70	*Ccdc78*	3.96	0.034
71	*Gpd1*	3.69	0.010
72	*Rab40b*	3.67	0.045
73	*Hfm1*	3.15	0.001
74	*Gm6790*	3.09	0.004
75	*Adamts8*	3.07	0.048
76	*a*	2.92	0.046
77	*Trim13*	2.89	0.006
78	*Heph*	2.87	0.028
79	*Pla2g16*	2.87	0.035
80	*Ttpal*	2.79	0.042
81	*Greb1l*	2.79	0.004
82	*Tcfl5*	2.77	0.002
83	*Gm5160*	2.76	0.006
84	*Thsd1*	2.68	0.028
85	*Ifitm3*	2.59	0.038
86	*Tspyl4*	2.47	0.030
87	*Itgae*	2.46	0.044
88	*Glcci1*	2.44	0.011
89	*Lgals1*	2.42	0.020
90	*Otx2*	2.41	0.045
91	*Mxra8*	2.41	0.021
92	*Prokr1*	2.36	0.019

Rank	Gene Symbol	Fold Change	p-value
93	*Mppe1*	2.35	0.043
94	*Gm5239*	2.34	0.002
95	*Ampd2*	2.33	0.002
96	*Pdzd7*	2.33	0.031
97	*1700022I11Rik*	2.33	0.023
98	*Gm10252*	2.33	0.011
99	*Tesc*	2.25	0.020
100	*Bhlhe41*	2.23	0.046
101	*Sstr2*	2.19	0.028
102	*Rhoc*	2.18	0.042
103	*Gadl1*	2.13	0.007
104	*Pdpn*	1.97	0.003
105	*Calb2*	1.96	0.047
106	*2810417H13Rik*	1.94	0.023
107	*Dmp1*	1.94	0.003
108	*Slc7a8*	1.93	0.000
109	*Rfpl4*	1.91	0.001
110	*Nup62*	1.91	0.017
111	*C1galt1*	1.87	0.050
112	*Asb4*	1.86	0.002
113	*Eln*	1.84	0.004
114	*F8a*	1.80	0.042
115	*Hist2h4*	1.79	0.043
116	*Has1*	1.77	0.025

Rank	Gene Symbol	Fold Change	p-value
117	*Ablim3*	1.74	0.012
118	*Egfr*	1.72	0.004
119	*Arap1*	1.70	0.027
120	*Golga7b*	1.68	0.026
121	*Serf2*	1.67	0.009
122	*U2af1l4*	1.66	0.043
123	*Cdh22*	1.61	0.046
124	*Lrdd*	1.59	0.044
125	*Xist*	1.56	0.000
126	*Ppp1r3e*	1.52	0.027
127	*Slc25a13*	1.47	0.039
128	*Aurkb*	1.46	0.032
129	*Fbxo44*	1.43	0.019
130	*Pcna*	1.42	0.004
131	*St8sia3*	1.39	0.010
132	*Nanos1*	1.38	0.031
133	*Ier5l*	1.37	0.042
134	*Zic1*	1.36	0.037
135	*Vps25*	1.33	0.021
136	*Hbb-b1*	1.33	0.035
137	*Atrip*	1.32	0.047
138	*Hes5*	1.31	0.047
139	*Hsd17b7*	1.31	0.028
140	*Tnc*	1.29	0.034

Rank	Gene Symbol	Fold Change	p-value
141	*Lama5*	1.28	0.041
142	*Pla2g4b*	1.27	0.008

RNA-Seq Down-Regulated Gene List ($p \leq 0.05$, fold change ≥ 1.25)

Rank	Gene Symbol	Fold Change	p-value
1	*4930578I07Rik*	-Inf	0.022
2	*Ccdc103*	-Inf	0.014
3	*Cdnf*	-Inf	0.031
4	*Gm10643*	-Inf	0.031
5	*Gm13225*	-Inf	0.017
6	*Gm5431*	-Inf	0.021
7	*Lhb*	-Inf	0.036
8	*Mpo*	-Inf	0.008
9	*Prss33*	-Inf	0.027
10	*Slc38a5*	-Inf	0.027
11	*Tmem220*	-Inf	0.027
12	*Creg2*	-14.36	0.015
13	*Edn2*	-13.29	0.044
14	*Fam43b*	-12.63	0.032
15	*Ankrd55*	-10.70	0.010
16	*Ttll9*	-9.57	0.026
17	*Oit3*	-9.27	0.005
18	*Kirrel2*	-7.76	0.045
19	*Ccdc162*	-7.34	0.009
20	*Tmsb15b1*	-6.96	0.027
21	*Enpp3*	-5.73	0.032
22	*Ankrd29*	-5.64	0.017

Rank	Gene Symbol	Fold Change	p-value
23	*Barhl2*	-5.55	0.038
24	*Gm5464*	-4.97	0.043
25	*Col2a1*	-4.78	0.000
26	*Calhm2*	-4.32	0.036
27	*C2cd4b*	-4.31	0.038
28	*Zfp322a*	-4.30	0.007
29	*Rasgef1a*	-4.23	0.011
30	*Lamc2*	-4.16	0.033
31	*5830403L16Rik*	-3.89	0.004
32	*Arhgef3*	-3.85	0.037
33	*Prelp*	-3.83	0.030
34	*Ttc30a2*	-3.30	0.023
35	*4930420K17Rik*	-3.30	0.027
36	*Ephx3*	-3.25	0.046
37	*Rbm12*	-3.24	0.006
38	*Fam82a1*	-3.15	0.014
39	*Alas2*	-2.91	0.033
40	*Ism1*	-2.90	0.002
41	*Xlr3b*	-2.82	0.008
42	*Abca8b*	-2.81	0.028
43	*Hopx*	-2.80	0.008
44	*Pdgfra*	-2.75	0.001
45	*Spata1*	-2.74	0.046
46	*Stambpl1*	-2.72	0.041

Rank	Gene Symbol	Fold Change	p-value
47	*Six2*	-2.65	0.000
48	*Sdf2*	-2.57	0.036
49	*Gm8923*	-2.55	0.032
50	*2810459M11Rik*	-2.55	0.012
51	*Metrnl*	-2.53	0.036
52	*Mtcp1*	-2.52	0.000
53	*Micalcl*	-2.38	0.008
54	*Nme3*	-2.36	0.027
55	*Sipa1*	-2.31	0.000
56	*Ccdc28a*	-2.29	0.047
57	*40603*	-2.25	0.000
58	*Gpnmb*	-2.24	0.037
59	*Il31ra*	-2.20	0.007
60	*L2hgdh*	-2.19	0.016
61	*Kl*	-2.16	0.002
62	*Mrpl33*	-2.14	0.000
63	*Sft2d2*	-2.13	0.019
64	*Gfra1*	-2.12	0.016
65	*Psenen*	-2.11	0.010
66	*Myh14*	-2.06	0.032
67	*Gm10174*	-2.05	0.000
68	*Pappa*	-2.02	0.033
69	*Mrpl17*	-2.00	0.046
70	*Zbtb7c*	-1.97	0.008

Rank	Gene Symbol	Fold Change	p-value
71	*Plce1*	-1.97	0.004
72	*Syde2*	-1.97	0.016
73	*Insm2*	-1.96	0.000
74	*Rlbp1*	-1.96	0.000
75	*Slc25a44*	-1.93	0.011
76	*Uty*	-1.88	0.000
77	*Col9a3*	-1.86	0.019
78	*Slc38a3*	-1.85	0.036
79	*Ppm1m*	-1.84	0.030
80	*Hist2h2aa2*	-1.82	0.019
81	*Hmga1-rs1*	-1.82	0.036
82	*1700069B07Rik*	-1.80	0.029
83	*Slc35e4*	-1.77	0.039
84	*AI646023*	-1.76	0.005
85	*Kcnj10*	-1.76	0.043
86	*Ubiad1*	-1.73	0.020
87	*Dynlt1c*	-1.71	0.006
88	*Ntn4*	-1.69	0.048
89	*Dedd2*	-1.67	0.026
90	*Rgs4*	-1.67	0.013
91	*Eif2s3y*	-1.66	0.000
92	*Stim2*	-1.64	0.007
93	*Eif2ak3*	-1.63	0.017
94	*Hs3st1*	-1.63	0.007

Rank	Gene Symbol	Fold Change	p-value
95	*Dct*	-1.63	0.046
96	*Trex1*	-1.58	0.002
97	*Dalrd3*	-1.58	0.035
98	*Hba-a2*	-1.58	0.009
99	*Poli*	-1.54	0.046
100	*Zfp277*	-1.52	0.044
101	*Lypd6*	-1.51	0.039
102	*Naa16*	-1.51	0.018
103	*Zcchc14*	-1.47	0.045
104	*Tnfrsf19*	-1.47	0.025
105	*Mmd2*	-1.45	0.019
106	*Dpm1*	-1.43	0.000
107	*3110035E14Rik*	-1.42	0.045
108	*Neurog2*	-1.41	0.008
109	*Kcnn1*	-1.41	0.043
110	*Dbi*	-1.39	0.045
111	*Ptp4a1*	-1.37	0.043
112	*Ccdc41*	-1.32	0.034
113	*Rnasel*	-1.31	0.020
114	*Ddx3y*	-1.26	0.000
115	*Kdm5d*	-1.26	0.000

Appendix B

Microarray Up-Regulated Gene List ($p \leq 0.05$, fold change ≥ 1.25)

Rank	Gene Symbol	Fold Change	p-value
1	*Slc16a14*	2.36	0.010
2	*B3galt6*	1.82	0.045
3	*Fes*	1.61	0.030
4	*Kcnc2*	1.60	0.046
5	*Snord123*	1.59	0.000
6	*Fam173b*	1.54	0.000
7	*Gsta4*	1.53	0.032
8	*Zbtb38*	1.49	0.045
9	*Mrc2*	1.48	0.017
10	*Htra1*	1.46	0.028
11	*Wnt5b*	1.46	0.013
12	*Fam167a*	1.45	0.003
13	*Heph*	1.44	0.020
14	*1110032F04Rik*	1.41	0.004
15	*Myl9*	1.40	0.047
16	*Npy2r*	1.40	0.014
17	*Ino80d*	1.39	0.037
18	*Gkn2*	1.39	0.031
19	*Sdad1*	1.39	0.033
20	*Ercc2*	1.39	0.005

Rank	Gene Symbol	Fold Change	p-value
21	*ENSMUSG00000074303*	1.39	0.024
22	*Slc2a5*	1.38	0.037
23	*Tmem67*	1.38	0.048
24	*Fam59a*	1.37	0.012
25	*Mafb*	1.36	0.030
26	*Apobec1*	1.36	0.025
27	*Csprs*	1.35	0.043
28	*Panx2*	1.35	0.012
29	*Cldn23*	1.34	0.042
30	*Lfng*	1.34	0.019
31	*Spinlw1*	1.34	0.023
32	*Egln3*	1.34	0.023
33	*Notch3*	1.34	0.004
34	*Paqr7*	1.34	0.013
35	*Bnc2*	1.34	0.020
36	*Arhgef19*	1.33	0.012
37	*Pdpn*	1.33	0.013
38	*Tada1l*	1.33	0.015
39	*C1galt1*	1.33	0.043
40	*Doc2a*	1.33	0.033
41	*Paqr6*	1.32	0.012
42	*Runx3*	1.31	0.011
43	*Wwc2*	1.31	0.003
44	*Epb4.1l2*	1.31	0.035

Rank	Gene Symbol	Fold Change	p-value
45	*Chek2*	1.31	0.049
46	*Mia1*	1.31	0.021
47	*Icos*	1.30	0.034
48	*Sema5a*	1.30	0.006
49	*2600010E01Rik*	1.30	0.001
50	*Tmem121*	1.30	0.028
51	*Chd6*	1.30	0.017
52	*Clip1*	1.29	0.041
53	*Depdc6*	1.29	0.006
54	*Mapk12*	1.29	0.034
55	*Rpa3*	1.29	0.016
56	*Gpc3*	1.29	0.018
57	*1810014F10Rik*	1.29	0.013
58	*4930579J09Rik*	1.28	0.014
59	*Clspn*	1.28	0.018
60	*Adam5*	1.28	0.015
61	*Ccbp2*	1.28	0.030
62	*Pcdh8*	1.28	0.037
63	*Nab2*	1.27	0.042
64	*Arap3*	1.27	0.007
65	*Mybphl*	1.27	0.027
66	*4833438C02Rik*	1.27	0.017
67	*C79595*	1.26	0.031
68	*Rad9b*	1.26	0.049

Rank	Gene Symbol	Fold Change	p-value
69	*Napepld*	1.26	0.015
70	*Hoxb2*	1.26	0.018
71	*Hes1*	1.26	0.017
72	*Intu*	1.26	0.016
73	*Fzd10*	1.25	0.010
74	*Bcan*	1.25	0.014
75	*Csn2*	1.25	0.045
76	*Sord*	1.25	0.034

Microarray Down-Regulated Gene List ($p \leq 0.05$, fold change ≤ -1.25)

Rank	Gene Symbol	Fold Change	p-value
1	*Atp1a2*	-2.37	0.038
2	*Matn2*	-2.19	0.011
3	*Rlbp1*	-2.00	0.000
4	*Pdgfra*	-1.87	0.028
5	*Hopx*	-1.82	0.002
6	*Abhd1*	-1.79	0.041
7	*2810459M11Rik*	-1.59	0.003
8	*Plce1*	-1.57	0.001
9	*Kcnj10*	-1.55	0.048
10	*Abcb9*	-1.55	0.019
11	*Nup133*	-1.54	0.001
12	*Pdlim4*	-1.49	0.011
13	*Col2a1*	-1.49	0.014
14	*Mmd2*	-1.49	0.007
15	*Foxn3*	-1.48	0.010
16	*Hs3st1*	-1.44	0.032
17	*Tnfrsf19*	-1.44	0.002
18	*Tceb3*	-1.41	0.013
19	*Ssu72*	-1.41	0.004
20	*Cyp2j9*	-1.39	0.037
21	*Scrg1*	-1.39	0.032
22	*Slc5a2*	-1.38	0.023

Rank	Gene Symbol	Fold Change	p-value
23	*Dio2*	-1.36	0.046
24	*Slc2a13*	-1.35	0.018
25	*1700029I01Rik*	-1.35	0.008
26	*Sdf4*	-1.34	0.006
27	*Dbi*	-1.34	0.040
28	*Slc39a14*	-1.33	0.011
29	*Cdo1*	-1.33	0.012
30	*Arhgef3*	-1.32	0.004
31	*4930404N11Rik*	-1.32	0.029
32	*Pja1*	-1.32	0.042
33	*Asrgl1*	-1.31	0.018
34	*Gm9*	-1.30	0.048
35	*Vdr*	-1.29	0.036
36	*Madcam1*	-1.29	0.004
37	*100042016*	-1.29	0.004
38	*Aif1l*	-1.29	0.045
39	*B930068K11Rik*	-1.28	0.025
40	*Sgms2*	-1.28	0.039
41	*Ado*	-1.28	0.035
42	*Pcdh10*	-1.27	0.029
43	*Lhb*	-1.27	0.008
44	*Prss23*	-1.27	0.025
45	*AI646023*	-1.27	0.017
46	*Wdr92*	-1.26	0.026

Rank	Gene Symbol	Fold Change	p-value
47	*5830403L16Rik*	-1.26	0.037
48	*Nedd9*	-1.26	0.005
49	*Calm1*	-1.26	0.040
50	*Stk39*	-1.26	0.008
51	*Fbxo36*	-1.26	0.009
52	*Tspan8*	-1.26	0.041
53	*Tacc1*	-1.26	0.010
54	*Tctex1d1*	-1.26	0.037
55	*F3*	-1.26	0.044
56	*Flt1*	-1.26	0.004
57	*Pard6b*	-1.26	0.004
58	*2610028D06Rik*	-1.26	0.038
59	*Bnip2*	-1.25	0.043
60	*2900024I21Rik*	-1.25	0.045
61	*Ptprz1*	-1.25	0.027
62	*Stx11*	-1.25	0.034
63	*Acss1*	-1.25	0.015
64	*Cdh6*	-1.25	0.007

Acknowledgements

I would like to acknowledge my supervisors Robin Lovell-Badge and James Briscoe, the members of the Lovell-Badge Lab in which I worked, and everyone in the Division of Stem Cell Biology and Developmental Genetics.

I would like to thank especially James Turner and Donald Bell for their advice and camaraderie, which kept me sane during this process, and without whom I fear I wouldn't have made it.

References

ABDEL-MANNAN, O., CHEUNG, A. F. & MOLNAR, Z. 2008. Evolution of cortical neurogenesis. *Brain Res Bull,* 75**,** 398-404.

AKIYAMA, H., CHABOISSIER, M. C., BEHRINGER, R. R., ROWITCH, D. H., SCHEDL, A., EPSTEIN, J. A. & DE CROMBRUGGHE, B. 2004. Essential role of Sox9 in the pathway that controls formation of cardiac valves and septa. *Proc Natl Acad Sci U S A,* 101**,** 6502-7.

AKIYAMA, H., CHABOISSIER, M. C., MARTIN, J. F., SCHEDL, A. & DE CROMBRUGGHE, B. 2002. The transcription factor Sox9 has essential roles in successive steps of the chondrocyte differentiation pathway and is required for expression of Sox5 and Sox6. *Genes Dev,* 16**,** 2813-28.

ALMGREN, M., PERSSON, A. S., FENGHUA, C., WITGEN, B. M., SCHALLING, M., NYENGAARD, J. R. & LAVEBRATT, C. 2007. Lack of potassium channel induces proliferation and survival causing increased neurogenesis and two-fold hippocampus enlargement. *Hippocampus,* 17**,** 292-304.

AMBROSETTI, D. C., BASILICO, C. & DAILEY, L. 1997. Synergistic activation of the fibroblast growth factor 4 enhancer by Sox2 and Oct-3 depends on protein-protein interactions facilitated by a specific spatial arrangement of factor binding sites. *Mol Cell Biol,* 17**,** 6321-9.

ANDERS, S. & HUBER, W. 2010. Differential expression analysis for sequence count data. *Genome Biol,* 11**,** R106.

ANDERSON, S. A., EISENSTAT, D. D., SHI, L. & RUBENSTEIN, J. L. 1997. Interneuron migration from basal forebrain to neocortex: dependence on Dlx genes. *Science,* 278**,** 474-6.

ANTHONY, T. E., KLEIN, C., FISHELL, G. & HEINTZ, N. 2004. Radial glia serve as neuronal progenitors in all regions of the central nervous system. *Neuron,* 41**,** 881-90.

APPEL, B., GIVAN, L. A. & EISEN, J. S. 2001. Delta-Notch signaling and lateral inhibition in zebrafish spinal cord development. *BMC Dev Biol,* 1**,** 13.

ARNETT, H. A., FANCY, S. P., ALBERTA, J. A., ZHAO, C., PLANT, S. R., KAING, S., RAINE, C. S., ROWITCH, D. H., FRANKLIN, R. J. & STILES, C. D. 2004. bHLH transcription factor Olig1 is required to repair demyelinated lesions in the CNS. *Science,* 306**,** 2111-5.

AVILION, A. A., NICOLIS, S. K., PEVNY, L. H., PEREZ, L., VIVIAN, N. & LOVELL-BADGE, R. 2003. Multipotent cell lineages in early mouse development depend on SOX2 function. *Genes & Development,* 17**,** 126-40.

BAALA, L., BRIAULT, S., ETCHEVERS, H. C., LAUMONNIER, F., NATIQ, A., AMIEL, J., BODDAERT, N., PICARD, C., SBITI, A., ASERMOUH, A., ATTIE-BITACH, T., ENCHA-RAZAVI, F., MUNNICH, A., SEFIANI, A. & LYONNET, S. 2007. Homozygous silencing of T-box transcription factor EOMES leads to microcephaly with polymicrogyria and corpus callosum agenesis. *Nat Genet,* 39**,** 454-6.

BARRIONUEVO, F., GEORG, I., SCHERTHAN, H., LECUREUIL, C., GUILLOU, F., WEGNER, M. & SCHERER, G. 2009. Testis cord differentiation after the sex determination stage is independent of Sox9 but fails in the combined absence of Sox9 and Sox8. *Dev Biol,* 327**,** 301-12.

BARRIONUEVO, F. & SCHERER, G. 2010. SOX E genes: SOX9 and SOX8 in mammalian testis development. *Int J Biochem Cell Biol,* 42**,** 433-6.

BELL, D. M., LEUNG, K. K., WHEATLEY, S. C., NG, L. J., ZHOU, S., LING, K. W., SHAM, M. H., KOOPMAN, P., TAM, P. P. & CHEAH, K. S. 1997. SOX9 directly regulates the type-II collagen gene. *Nat Genet,* 16**,** 174-8.

BERGSLAND, M., WERME, M., MALEWICZ, M., PERLMANN, T. & MUHR, J. 2006. The establishment of neuronal properties is controlled by Sox4 and Sox11. *Genes Dev,* 20**,** 3475-86.

BETSHOLTZ, C., KARLSSON, L. & LINDAHL, P. 2001. Developmental roles of platelet-derived growth factors. *Bioessays,* 23**,** 494-507.

BI, W., HUANG, W., WHITWORTH, D. J., DENG, J. M., ZHANG, Z., BEHRINGER, R. R. & DE CROMBRUGGHE, B. 2001. Haploinsufficiency of Sox9 results in defective cartilage primordia and premature skeletal mineralization. *Proc Natl Acad Sci U S A,* 98**,** 6698-703.

BLACHE, P., VAN DE WETERING, M., DULUC, I., DOMON, C., BERTA, P., FREUND, J. N., CLEVERS, H. & JAY, P. 2004. SOX9 is an intestine crypt transcription factor, is regulated by the Wnt pathway, and represses the CDX2 and MUC2 genes. *The Journal of cell biology,* 166**,** 37-47.

BOSSEN, C., INGOLD, K., TARDIVEL, A., BODMER, J. L., GAIDE, O., HERTIG, S., AMBROSE, C., TSCHOPP, J. & SCHNEIDER, P. 2006. Interactions of tumor necrosis factor (TNF) and TNF receptor family members in the mouse and human. *J Biol Chem,* 281**,** 13964-71.

BOTQUIN, V., HESS, H., FUHRMANN, G., ANASTASSIADIS, C., GROSS, M. K., VRIEND, G. & SCHOLER, H. R. 1998. New POU dimer configuration mediates antagonistic control of an osteopontin preimplantation enhancer by Oct-4 and Sox-2. *Genes Dev,* 12**,** 2073-90.

BRISCOE, J. & ERICSON, J. 2001. Specification of neuronal fates in the ventral neural tube. *Curr Opin Neurobiol,* 11**,** 43-9.

BRISCOE, J., PIERANI, A., JESSELL, T. M. & ERICSON, J. 2000. A homeodomain protein code specifies progenitor cell identity and neuronal fate in the ventral neural tube. *Cell,* 101**,** 435-45.

BUTT, A. M. & KALSI, A. 2006. Inwardly rectifying potassium channels (Kir) in central nervous system glia: a special role for Kir4.1 in glial functions. *J Cell Mol Med,* 10**,** 33-44.

BYLUND, M., ANDERSSON, E., NOVITCH, B. G. & MUHR, J. 2003. Vertebrate neurogenesis is counteracted by Sox1-3 activity. *Nat Neurosci,* 6**,** 1162-8.

CAI, J., QI, Y., HU, X., TAN, M., LIU, Z., ZHANG, J., LI, Q., SANDER, M. & QIU, M. 2005. Generation of oligodendrocyte precursor cells from mouse dorsal spinal cord independent of Nkx6 regulation and Shh signaling. *Neuron,* 45**,** 41-53.

CALVER, A. R., HALL, A. C., YU, W. P., WALSH, F. S., HEATH, J. K., BETSHOLTZ, C. & RICHARDSON, W. D. 1998. Oligodendrocyte population dynamics and the role of PDGF in vivo. *Neuron,* 20**,** 869-82.

CHANDRAN, S., KATO, H., GERRELI, D., COMPSTON, A., SVENDSEN, C. N. & ALLEN, N. D. 2003. FGF-dependent generation of oligodendrocytes by a hedgehog-independent pathway. *Development,* 130**,** 6599-609.

CHENN, A. & MCCONNELL, S. K. 1995. Cleavage orientation and the asymmetric inheritance of Notch1 immunoreactivity in mammalian neurogenesis. *Cell,* 82**,** 631-41.

CHEUNG, M. & BRISCOE, J. 2003. Neural crest development is regulated by the transcription factor Sox9. *Development,* 130**,** 5681-93.

CHOI, B. H. & LAPHAM, L. W. 1978. Radial glia in the human fetal cerebrum: a combined Golgi, immunofluorescent and electron microscopic study. *Brain Res,* 148**,** 295-311.

COETZEE, W. A., AMARILLO, Y., CHIU, J., CHOW, A., LAU, D., MCCORMACK, T., MORENO, H., NADAL, M. S., OZAITA, A., POUNTNEY, D., SAGANICH, M., VEGA-SAENZ DE MIERA, E. & RUDY, B. 1999. Molecular diversity of K+ channels. *Ann N Y Acad Sci,* 868**,** 233-85.

CONTI, L., POLLARD, S. M., GORBA, T., REITANO, E., TOSELLI, M., BIELLA, G., SUN, Y., SANZONE, S., YING, Q. L., CATTANEO, E. & SMITH, A. 2005. Niche-independent symmetrical self-renewal of a mammalian tissue stem cell. *PLoS Biol,* 3**,** e283.

COPP, A. J., GREENE, N. D. & MURDOCH, J. N. 2003. The genetic basis of mammalian neurulation. *Nat Rev Genet,* 4**,** 784-93.

CROSNIER, C., STAMATAKI, D. & LEWIS, J. 2006. Organizing cell renewal in the intestine: stem cells, signals and combinatorial control. *Nature reviews. Genetics,* 7**,** 349-59.

DENNY, P., SWIFT, S., CONNOR, F. & ASHWORTH, A. 1992. An SRY-related gene expressed during spermatogenesis in the mouse encodes a sequence-specific DNA-binding protein. *EMBO J,* 11**,** 3705-12.

DOETSCH, F. 2003. The glial identity of neural stem cells. *Nat Neurosci,* 6**,** 1127-34.

DOETSCH, F., CAILLE, I., LIM, D. A., GARCIA-VERDUGO, J. M. & ALVAREZ-BUYLLA, A. 1999. Subventricular zone astrocytes are neural stem cells in the adult mammalian brain. *Cell,* 97**,** 703-16.

DONAHOO, A. L. & RICHARDS, L. J. 2009. Understanding the mechanisms of callosal development through the use of transgenic mouse models. *Semin Pediatr Neurol,* 16**,** 127-42.

DOYLE, D. A., MORAIS CABRAL, J., PFUETZNER, R. A., KUO, A., GULBIS, J. M., COHEN, S. L., CHAIT, B. T. & MACKINNON, R. 1998. The structure of the

potassium channel: molecular basis of K+ conduction and selectivity. *Science,* 280**,** 69-77.

ETCHEVERS, H. C., VINCENT, C., LE DOUARIN, N. M. & COULY, G. F. 2001. The cephalic neural crest provides pericytes and smooth muscle cells to all blood vessels of the face and forebrain. *Development,* 128**,** 1059-68.

FAKLER, B., BOND, C. T., ADELMAN, J. P. & RUPPERSBERG, J. P. 1996. Heterooligomeric assembly of inward-rectifier K+ channels from subunits of different subfamilies: Kir2.1 (IRK1) and Kir4.1 (BIR10). *Pflugers Arch,* 433**,** 77-83.

FENG, L., HATTEN, M. E. & HEINTZ, N. 1994. Brain lipid-binding protein (BLBP): a novel signaling system in the developing mammalian CNS. *Neuron,* 12**,** 895-908.

FINZSCH, M., STOLT, C. C., LOMMES, P. & WEGNER, M. 2008. Sox9 and Sox10 influence survival and migration of oligodendrocyte precursors in the spinal cord by regulating PDGF receptor alpha expression. *Development,* 135**,** 637-46.

FISCHER, A. J. & BONGINI, R. 2010. Turning Muller glia into neural progenitors in the retina. *Mol Neurobiol,* 42**,** 199-209.

FOGARTY, M., RICHARDSON, W. D. & KESSARIS, N. 2005. A subset of oligodendrocytes generated from radial glia in the dorsal spinal cord. *Development,* 132**,** 1951-9.

FOSTER, J. W., DOMINGUEZ-STEGLICH, M. A., GUIOLI, S., KWOK, C., WELLER, P. A., STEVANOVIC, M., WEISSENBACH, J., MANSOUR, S., YOUNG, I. D., GOODFELLOW, P. N. & ET AL. 1994. Campomelic dysplasia and autosomal sex reversal caused by mutations in an SRY-related gene. *Nature,* 372**,** 525-30.

FRAGKOULI, A., VAN WIJK, N. V., LOPES, R., KESSARIS, N. & PACHNIS, V. 2009. LIM homeodomain transcription factor-dependent specification of

bipotential MGE progenitors into cholinergic and GABAergic striatal interneurons. *Development,* 136**,** 3841-51.

FRIETZE, S., LAN, X., JIN, V. X. & FARNHAM, P. J. 2010. Genomic targets of the KRAB and SCAN domain-containing zinc finger protein 263. *J Biol Chem,* 285**,** 1393-403.

FRUTTIGER, M., KARLSSON, L., HALL, A. C., ABRAMSSON, A., CALVER, A. R., BOSTROM, H., WILLETTS, K., BERTOLD, C. H., HEATH, J. K., BETSHOLTZ, C. & RICHARDSON, W. D. 1999. Defective oligodendrocyte development and severe hypomyelination in PDGF-A knockout mice. *Development,* 126**,** 457-67.

FUCHS, E., MERRILL, B. J., JAMORA, C. & DASGUPTA, R. 2001. At the roots of a never-ending cycle. *Developmental cell,* 1**,** 13-25.

FURUTANI, K., OHNO, Y., INANOBE, A., HIBINO, H. & KURACHI, Y. 2009. Mutational and in silico analyses for antidepressant block of astroglial inward-rectifier Kir4.1 channel. *Mol Pharmacol,* 75**,** 1287-95.

GLASER, T., JEPEAL, L., EDWARDS, J. G., YOUNG, S. R., FAVOR, J. & MAAS, R. L. 1994. PAX6 gene dosage effect in a family with congenital cataracts, aniridia, anophthalmia and central nervous system defects. *Nat Genet,* 7**,** 463-71.

GRAHAM, V., KHUDYAKOV, J., ELLIS, P. & PEVNY, L. 2003. SOX2 functions to maintain neural progenitor identity. *Neuron,* 39**,** 749-65.

GU, G., DUBAUSKAITE, J. & MELTON, D. A. 2002. Direct evidence for the pancreatic lineage: NGN3+ cells are islet progenitors and are distinct from duct progenitors. *Development,* 129**,** 2447-57.

GUIDOTTI, A., FORCHETTI, C. M., CORDA, M. G., KONKEL, D., BENNETT, C. D. & COSTA, E. 1983. Isolation, characterization, and purification to homogeneity

of an endogenous polypeptide with agonistic action on benzodiazepine receptors. *Proc Natl Acad Sci U S A,* 80**,** 3531-5.

GUO, W., KECKESOVA, Z., DONAHER, J. L., SHIBUE, T., TISCHLER, V., REINHARDT, F., ITZKOVITZ, S., NOSKE, A., ZURRER-HARDI, U., BELL, G., TAM, W. L., MANI, S. A., VAN OUDENAARDEN, A. & WEINBERG, R. A. 2012. Slug and Sox9 cooperatively determine the mammary stem cell state. *Cell,* 148**,** 1015-28.

GUPTA, A., TSAI, L. H. & WYNSHAW-BORIS, A. 2002. Life is a journey: a genetic look at neocortical development. *Nature reviews. Genetics,* 3**,** 342-55.

HARLAND, R. 2000. Neural induction. *Curr Opin Genet Dev,* 10**,** 357-62.

HARLEY, V. R., LOVELL-BADGE, R. & GOODFELLOW, P. N. 1994. Definition of a consensus DNA binding site for SRY. *Nucleic Acids Res,* 22**,** 1500-1.

HAYAKAWA, K., PHAM, L. D., SOM, A. T., LEE, B. J., GUO, S., LO, E. H. & ARAI, K. 2011. Vascular endothelial growth factor regulates the migration of oligodendrocyte precursor cells. *J Neurosci,* 31**,** 10666-70.

HOSER, M., POTZNER, M. R., KOCH, J. M., BOSL, M. R., WEGNER, M. & SOCK, E. 2008. Sox12 deletion in the mouse reveals nonreciprocal redundancy with the related Sox4 and Sox11 transcription factors. *Mol Cell Biol,* 28**,** 4675-87.

HOSKING, B. M., MUSCAT, G. E., KOOPMAN, P. A., DOWHAN, D. H. & DUNN, T. L. 1995. Trans-activation and DNA-binding properties of the transcription factor, Sox-18. *Nucleic Acids Res,* 23**,** 2626-8.

INOUE, K., TERASHIMA, T., NISHIKAWA, T. & TAKUMI, T. 2004. Fez1 is layer-specifically expressed in the adult mouse neocortex. *Eur J Neurosci,* 20**,** 2909-16.

ISHII, M., FUJITA, A., IWAI, K., KUSAKA, S., HIGASHI, K., INANOBE, A., HIBINO, H. & KURACHI, Y. 2003. Differential expression and distribution of

Kir5.1 and Kir4.1 inwardly rectifying K+ channels in retina. *Am J Physiol Cell Physiol,* 285**,** C260-7.

JOHANSSON, C. B., MOMMA, S., CLARKE, D. L., RISLING, M., LENDAHL, U. & FRISEN, J. 1999. Identification of a neural stem cell in the adult mammalian central nervous system. *Cell,* 96**,** 25-34.

JOVANOVIC, J. N. & THOMSON, A. M. 2011. Development of cortical GABAergic innervation. *Front Cell Neurosci,* 5**,** 14.

KALSI, A. S., GREENWOOD, K., WILKIN, G. & BUTT, A. M. 2004. Kir4.1 expression by astrocytes and oligodendrocytes in CNS white matter: a developmental study in the rat optic nerve. *J Anat,* 204**,** 475-85.

KAMACHI, Y., UCHIKAWA, M., TANOUCHI, A., SEKIDO, R. & KONDOH, H. 2001. Pax6 and SOX2 form a co-DNA-binding partner complex that regulates initiation of lens development. *Genes Dev,* 15**,** 1272-86.

KANDEL, E. R., SCHWARTZ, J. H. & JESSELL, T. M. 2000. *Principles of Neural Science*, McGraw-Hill.

KANG, P., LEE, H. K., GLASGOW, S. M., FINLEY, M., DONTI, T., GABER, Z. B., GRAHAM, B. H., FOSTER, A. E., NOVITCH, B. G., GRONOSTAJSKI, R. M. & DENEEN, B. 2012. Sox9 and NFIA coordinate a transcriptional regulatory cascade during the initiation of gliogenesis. *Neuron,* 74**,** 79-94.

KELLERER, S., SCHREINER, S., STOLT, C. C., SCHOLZ, S., BOSL, M. R. & WEGNER, M. 2006. Replacement of the Sox10 transcription factor by Sox8 reveals incomplete functional equivalence. *Development,* 133**,** 2875-86.

KEMP, J. M. & POWELL, T. P. 1971. The structure of the caudate nucleus of the cat: light and electron microscopy. *Philos Trans R Soc Lond B Biol Sci,* 262**,** 383-401.

KESSARIS, N., FOGARTY, M., IANNARELLI, P., GRIST, M., WEGNER, M. & RICHARDSON, W. D. 2006. Competing waves of oligodendrocytes in the

forebrain and postnatal elimination of an embryonic lineage. *Nat Neurosci,* 9**,** 173-9.

KESSARIS, N., PRINGLE, N. & RICHARDSON, W. D. 2008. Specification of CNS glia from neural stem cells in the embryonic neuroepithelium. *Philos Trans R Soc Lond B Biol Sci,* 363**,** 71-85.

KIM, J., LO, L., DORMAND, E. & ANDERSON, D. J. 2003. SOX10 maintains multipotency and inhibits neuronal differentiation of neural crest stem cells. *Neuron,* 38**,** 17-31.

KNUDSEN, J. & NIELSEN, M. 1990. Diazepam-binding inhibitor: a neuropeptide and/or an acyl-CoA ester binding protein? *Biochem J,* 265**,** 927-9.

KNUTSON, P., GHIANI, C. A., ZHOU, J. M., GALLO, V. & MCBAIN, C. J. 1997. K+ channel expression and cell proliferation are regulated by intracellular sodium and membrane depolarization in oligodendrocyte progenitor cells. *J Neurosci,* 17**,** 2669-82.

KOFUJI, P., CEELEN, P., ZAHS, K. R., SURBECK, L. W., LESTER, H. A. & NEWMAN, E. A. 2000. Genetic inactivation of an inwardly rectifying potassium channel (Kir4.1 subunit) in mice: phenotypic impact in retina. *J Neurosci,* 20**,** 5733-40.

KORDES, U. & HAGEL, C. 2006. Expression of SOX9 and SOX10 in central neuroepithelial tumor. *J Neurooncol,* 80**,** 151-5.

KUBOTA, Y., HATTORI, R. & YUI, Y. 1994. Three distinct subpopulations of GABAergic neurons in rat frontal agranular cortex. *Brain research,* 649**,** 159-73.

KUFFLER, S. W., NICHOLLS, J. G. & ORKAND, R. K. 1966. Physiological properties of glial cells in the central nervous system of amphibia. *J Neurophysiol,* 29**,** 768-87.

LANDROCK, D., ATSHAVES, B. P., MCINTOSH, A. L., LANDROCK, K. K., SCHROEDER, F. & KIER, A. B. 2010. Acyl-CoA binding protein gene ablation induces pre-implantation embryonic lethality in mice. *Lipids,* 45**,** 567-80.

LASHKARI, D. A., DERISI, J. L., MCCUSKER, J. H., NAMATH, A. F., GENTILE, C., HWANG, S. Y., BROWN, P. O. & DAVIS, R. W. 1997. Yeast microarrays for genome wide parallel genetic and gene expression analysis. *Proc Natl Acad Sci U S A,* 94**,** 13057-62.

LAVDAS, A. A., GRIGORIOU, M., PACHNIS, V. & PARNAVELAS, J. G. 1999. The medial ganglionic eminence gives rise to a population of early neurons in the developing cerebral cortex. *J Neurosci,* 19**,** 7881-8.

LE BRAS, B., BARALLOBRE, M. J., HOMMAN-LUDIYE, J., NY, A., WYNS, S., TAMMELA, T., HAIKO, P., KARKKAINEN, M. J., YUAN, L., MURIEL, M. P., CHATZOPOULOU, E., BREANT, C., ZALC, B., CARMELIET, P., ALITALO, K., EICHMANN, A. & THOMAS, J. L. 2006. VEGF-C is a trophic factor for neural progenitors in the vertebrate embryonic brain. *Nat Neurosci,* 9**,** 340-8.

LEE, L., DEBONO, C. A., CAMPAGNA, D. R., YOUNG, D. C., MOODY, D. B. & FLEMING, M. D. 2007. Loss of the acyl-CoA binding protein (Acbp) results in fatty acid metabolism abnormalities in mouse hair and skin. *J Invest Dermatol,* 127**,** 16-23.

LEE, S. K., MORI, S., KIM, D. J., KIM, S. Y. & KIM, D. I. 2004. Diffusion tensor MR imaging visualizes the altered hemispheric fiber connection in callosal dysgenesis. *AJNR Am J Neuroradiol,* 25**,** 25-8.

LEFEBVRE, V., LI, P. & DE CROMBRUGGHE, B. 1998. A new long form of Sox5 (L-Sox5), Sox6 and Sox9 are coexpressed in chondrogenesis and cooperatively activate the type II collagen gene. *EMBO J,* 17**,** 5718-33.

LEVITT, P. & RAKIC, P. 1980. Immunoperoxidase localization of glial fibrillary acidic protein in radial glial cells and astrocytes of the developing rhesus monkey brain. *J Comp Neurol,* 193**,** 815-40.

LEVY, O., DE LA VIEJA, A. & CARRASCO, N. 1998. The Na+/I- symporter (NIS): recent advances. *J Bioenerg Biomembr,* 30**,** 195-206.

LI, Q. L., ITO, K., SAKAKURA, C., FUKAMACHI, H., INOUE, K., CHI, X. Z., LEE, K. Y., NOMURA, S., LEE, C. W., HAN, S. B., KIM, H. M., KIM, W. J., YAMAMOTO, H., YAMASHITA, N., YANO, T., IKEDA, T., ITOHARA, S., INAZAWA, J., ABE, T., HAGIWARA, A., YAMAGISHI, H., OOE, A., KANEDA, A., SUGIMURA, T., USHIJIMA, T., BAE, S. C. & ITO, Y. 2002. Causal relationship between the loss of RUNX3 expression and gastric cancer. *Cell,* 109**,** 113-24.

LIODIS, P., DENAXA, M., GRIGORIOU, M., AKUFO-ADDO, C., YANAGAWA, Y. & PACHNIS, V. 2007. Lhx6 activity is required for the normal migration and specification of cortical interneuron subtypes. *J Neurosci,* 27**,** 3078-89.

LIU, X., BOLTEUS, A. J., BALKIN, D. M., HENSCHEL, O. & BORDEY, A. 2006. GFAP-expressing cells in the postnatal subventricular zone display a unique glial phenotype intermediate between radial glia and astrocytes. *Glia,* 54**,** 394-410.

LO TURCO, J. J. & KRIEGSTEIN, A. R. 1991. Clusters of coupled neuroblasts in embryonic neocortex. *Science,* 252**,** 563-6.

LOTURCO, J. J., OWENS, D. F., HEATH, M. J., DAVIS, M. B. & KRIEGSTEIN, A. R. 1995. GABA and glutamate depolarize cortical progenitor cells and inhibit DNA synthesis. *Neuron,* 15**,** 1287-98.

LU, Q. R., SUN, T., ZHU, Z., MA, N., GARCIA, M., STILES, C. D. & ROWITCH, D. H. 2002. Common developmental requirement for Olig function indicates a motor neuron/oligodendrocyte connection. *Cell,* 109**,** 75-86.

LU, Q. R., YUK, D., ALBERTA, J. A., ZHU, Z., PAWLITZKY, I., CHAN, J., MCMAHON, A. P., STILES, C. D. & ROWITCH, D. H. 2000. Sonic hedgehog--regulated oligodendrocyte lineage genes encoding bHLH proteins in the mammalian central nervous system. *Neuron,* 25**,** 317-29.

LYNN, F. C., SMITH, S. B., WILSON, M. E., YANG, K. Y., NEKREP, N. & GERMAN, M. S. 2007. Sox9 coordinates a transcriptional network in pancreatic progenitor cells. *Proceedings of the National Academy of Sciences of the United States of America,* 104**,** 10500-5.

MA, W. & BARKER, J. L. 1995. Complementary expressions of transcripts encoding GAD67 and GABAA receptor alpha 4, beta 1, and gamma 1 subunits in the proliferative zone of the embryonic rat central nervous system. *J Neurosci,* 15**,** 2547-60.

MA, W., LIU, Q. Y., MARIC, D., SATHANOORI, R., CHANG, Y. H. & BARKER, J. L. 1998a. Basic FGF-responsive telencephalic precursor cells express functional GABA(A) receptor/Cl-channels in vitro. *J Neurobiol,* 35**,** 277-86.

MA, Y., CERTEL, K., GAO, Y., NIEMITZ, E., MOSHER, J., MUKHERJEE, A., MUTSUDDI, M., HUSEINOVIC, N., CREWS, S. T., JOHNSON, W. A. & NAMBU, J. R. 2000. Functional interactions between Drosophila bHLH/PAS, Sox, and POU transcription factors regulate CNS midline expression of the slit gene. *J Neurosci,* 20**,** 4596-605.

MA, Y., NIEMITZ, E. L., NAMBU, P. A., SHAN, X., SACKERSON, C., FUJIOKA, M., GOTO, T. & NAMBU, J. R. 1998b. Gene regulatory functions of Drosophila fish-hook, a high mobility group domain Sox protein. *Mech Dev,* 73**,** 169-82.

MACFARLANE, S. N. & SONTHEIMER, H. 2000. Changes in ion channel expression accompany cell cycle progression of spinal cord astrocytes. *Glia,* 30**,** 39-48.

MALATESTA, P., HACK, M. A., HARTFUSS, E., KETTENMANN, H., KLINKERT, W., KIRCHHOFF, F. & GOTZ, M. 2003. Neuronal or glial progeny: regional differences in radial glia fate. *Neuron,* 37**,** 751-64.

MARIN, O., ANDERSON, S. A. & RUBENSTEIN, J. L. 2000. Origin and molecular specification of striatal interneurons. *The Journal of neuroscience : the official journal of the Society for Neuroscience,* 20**,** 6063-76.

MAROTEAUX, P., SPRANGER, J., OPITZ, J. M., KUCERA, J., LOWRY, R. B., SCHIMKE, R. N. & KAGAN, S. M. 1971. [The campomelic syndrome]. *La Presse medicale,* 79**,** 1157-62.

MAZELLA, J., PETRAULT, O., LUCAS, G., DEVAL, E., BERAUD-DUFOUR, S., GANDIN, C., EL-YACOUBI, M., WIDMANN, C., GUYON, A., CHEVET, E., TAOUJI, S., CONDUCTIER, G., CORINUS, A., COPPOLA, T., GOBBI, G., NAHON, J. L., HEURTEAUX, C. & BORSOTTO, M. 2010. Spadin, a sortilin-derived peptide, targeting rodent TREK-1 channels: a new concept in the antidepressant drug design. *PLoS Biol,* 8**,** e1000355.

MCCONNELL, S. K. & KAZNOWSKI, C. E. 1991. Cell cycle dependence of laminar determination in developing neocortex. *Science,* 254**,** 282-5.

MEKKI-DAURIAC, S., AGIUS, E., KAN, P. & COCHARD, P. 2002. Bone morphogenetic proteins negatively control oligodendrocyte precursor specification in the chick spinal cord. *Development,* 129**,** 5117-30.

MEREGALLI, M., FARINI, A., BELICCHI, M. & TORRENTE, Y. 2010. CD133(+) cells isolated from various sources and their role in future clinical perspectives. *Expert Opin Biol Ther,* 10**,** 1521-8.

MIRANDA-CONTRERAS, L., BENITEZ-DIAZ, P. R., MENDOZA-BRICENO, R. V., DELGADO-SAEZ, M. C. & PALACIOS-PRU, E. L. 1999. Levels of amino acid

neurotransmitters during mouse cerebellar neurogenesis and in histotypic cerebellar cultures. *Dev Neurosci,* 21**,** 147-58.

MIRANDA-CONTRERAS, L., RAMIREZ-MARTENS, L. M., BENITEZ-DIAZ, P. R., PENA-CONTRERAS, Z. C., MENDOZA-BRICENO, R. V. & PALACIOS-PRU, E. L. 2000. Levels of amino acid neurotransmitters during mouse olfactory bulb neurogenesis and in histotypic olfactory bulb cultures. *Int J Dev Neurosci,* 18**,** 83-91.

MISSON, J. P., EDWARDS, M. A., YAMAMOTO, M. & CAVINESS, V. S., JR. 1988. Mitotic cycling of radial glial cells of the fetal murine cerebral wall: a combined autoradiographic and immunohistochemical study. *Brain Res,* 466**,** 183-90.

MIYATA, T., KAWAGUCHI, A., SAITO, K., KAWANO, M., MUTO, T. & OGAWA, M. 2004. Asymmetric production of surface-dividing and non-surface-dividing cortical progenitor cells. *Development,* 131**,** 3133-45.

MIYAWAKI, T., UEMURA, A., DEZAWA, M., YU, R. T., IDE, C., NISHIKAWA, S., HONDA, Y., TANABE, Y. & TANABE, T. 2004. Tlx, an orphan nuclear receptor, regulates cell numbers and astrocyte development in the developing retina. *J Neurosci,* 24**,** 8124-34.

MÖHLER, H., BENKE, D., BENSON, J., LÜSCHER, B., RUDOLPH, U. & FRITSCHY, J. M. 1997. Diversity in Structure, Pharmacology and Regulation of GABA(A) Receptors. *In:* ENNA, S. J. & BOWERY, N. G. (eds.) *The GABA Receptors.* Totowa, NJ: Humana Press Inc.

MOLYNEAUX, B. J., ARLOTTA, P., MENEZES, J. R. & MACKLIS, J. D. 2007. Neuronal subtype specification in the cerebral cortex. *Nat Rev Neurosci,* 8**,** 427-37.

MONAGHAN, A. P., GRAU, E., BOCK, D. & SCHUTZ, G. 1995. The mouse homolog of the orphan nuclear receptor tailless is expressed in the developing forebrain. *Development,* 121**,** 839-53.

MORAIS DA SILVA, S., HACKER, A., HARLEY, V., GOODFELLOW, P., SWAIN, A. & LOVELL-BADGE, R. 1996. Sox9 expression during gonadal development implies a conserved role for the gene in testis differentiation in mammals and birds. *Nat Genet,* 14**,** 62-8.

MORTAZAVI, A., WILLIAMS, B. A., MCCUE, K., SCHAEFFER, L. & WOLD, B. 2008. Mapping and quantifying mammalian transcriptomes by RNA-Seq. *Nat Methods,* 5**,** 621-8.

MUELLER, W., NUTT, C. L., EHRICH, M., RIEMENSCHNEIDER, M. J., VON DEIMLING, A., VAN DEN BOOM, D. & LOUIS, D. N. 2007. Downregulation of RUNX3 and TES by hypermethylation in glioblastoma. *Oncogene,* 26**,** 583-93.

MURAKAMI, A., ISHIDA, S., THURLOW, J., REVEST, J. M. & DICKSON, C. 2001. SOX6 binds CtBP2 to repress transcription from the Fgf-3 promoter. *Nucleic Acids Res,* 29**,** 3347-55.

NEESS, D., BLOKSGAARD, M., BEK, S., MARCHER, A. B., ELLE, I. C., HELLEDIE, T., DUE, M., PAGMANTIDIS, V., FINSEN, B., WILBERTZ, J., KRUHOFFER, M., FAERGEMAN, N. & MANDRUP, S. 2011. Disruption of the acyl-CoA-binding protein gene delays hepatic adaptation to metabolic changes at weaning. *J Biol Chem,* 286**,** 3460-72.

NEUSCH, C., ROZENGURT, N., JACOBS, R. E., LESTER, H. A. & KOFUJI, P. 2001. Kir4.1 potassium channel subunit is crucial for oligodendrocyte development and in vivo myelination. *J Neurosci,* 21**,** 5429-38.

NG, L. J., WHEATLEY, S., MUSCAT, G. E., CONWAY-CAMPBELL, J., BOWLES, J., WRIGHT, E., BELL, D. M., TAM, P. P., CHEAH, K. S. & KOOPMAN, P.

1997. SOX9 binds DNA, activates transcription, and coexpresses with type II collagen during chondrogenesis in the mouse. *Dev Biol,* 183**,** 108-21.

NGUYEN, L., MALGRANGE, B., BREUSKIN, I., BETTENDORFF, L., MOONEN, G., BELACHEW, S. & RIGO, J. M. 2003. Autocrine/paracrine activation of the GABA(A) receptor inhibits the proliferation of neurogenic polysialylated neural cell adhesion molecule-positive (PSA-NCAM+) precursor cells from postnatal striatum. *J Neurosci,* 23**,** 3278-94.

NOCTOR, S. C., FLINT, A. C., WEISSMAN, T. A., DAMMERMAN, R. S. & KRIEGSTEIN, A. R. 2001. Neurons derived from radial glial cells establish radial units in neocortex. *Nature,* 409**,** 714-20.

NOCTOR, S. C., MARTINEZ-CERDENO, V., IVIC, L. & KRIEGSTEIN, A. R. 2004. Cortical neurons arise in symmetric and asymmetric division zones and migrate through specific phases. *Nat Neurosci,* 7**,** 136-44.

OAKLEY, B., 2ND, KATZ, B. J., XU, Z. & ZHENG, J. 1992. Spatial buffering of extracellular potassium by Muller (glial) cells in the toad retina. *Exp Eye Res,* 55**,** 539-50.

OHNO, Y., HIBINO, H., LOSSIN, C., INANOBE, A. & KURACHI, Y. 2007. Inhibition of astroglial Kir4.1 channels by selective serotonin reuptake inhibitors. *Brain Res,* 1178**,** 44-51.

PANCHISION, D. M., CHEN, H. L., PISTOLLATO, F., PAPINI, D., NI, H. T. & HAWLEY, T. S. 2007. Optimized flow cytometric analysis of central nervous system tissue reveals novel functional relationships among cells expressing CD133, CD15, and CD24. *Stem Cells,* 25**,** 1560-70.

PAPPAS, C. A., ULLRICH, N. & SONTHEIMER, H. 1994. Reduction of glial proliferation by K+ channel blockers is mediated by changes in pHi. *Neuroreport,* 6**,** 193-6.

PARK, H. C. & APPEL, B. 2003. Delta-Notch signaling regulates oligodendrocyte specification. *Development,* 130**,** 3747-55.

PAROLA, A. L., YAMAMURA, H. I. & LAIRD, H. E., 3RD 1993. Peripheral-type benzodiazepine receptors. *Life Sci,* 52**,** 1329-42.

PARRAS, C. M., HUNT, C., SUGIMORI, M., NAKAFUKU, M., ROWITCH, D. & GUILLEMOT, F. 2007. The proneural gene Mash1 specifies an early population of telencephalic oligodendrocytes. *J Neurosci,* 27**,** 4233-42.

PASTRANA, E., SILVA-VARGAS, V. & DOETSCH, F. 2011. Eyes wide open: a critical review of sphere-formation as an assay for stem cells. *Cell Stem Cell,* 8**,** 486-98.

PEROVIC, S., KRASKO, A., PROKIC, I., MULLER, I. M. & MULLER, W. E. 1999. Origin of neuronal-like receptors in Metazoa: cloning of a metabotropic glutamate/GABA-like receptor from the marine sponge Geodia cydonium. *Cell Tissue Res,* 296**,** 395-404.

PEVNY, L. H. & LOVELL-BADGE, R. 1997. Sox genes find their feet. *Curr Opin Genet Dev,* 7**,** 338-44.

PILLAY, L. M., FORRESTER, A. M., ERICKSON, T., BERMAN, J. N. & WASKIEWICZ, A. J. 2010. The Hox cofactors Meis1 and Pbx act upstream of gata1 to regulate primitive hematopoiesis. *Dev Biol,* 340**,** 306-17.

POCHE, R. A., FURUTA, Y., CHABOISSIER, M. C., SCHEDL, A. & BEHRINGER, R. R. 2008. Sox9 is expressed in mouse multipotent retinal progenitor cells and functions in Muller glial cell development. *J Comp Neurol,* 510**,** 237-50.

POLC, P. & HAEFELY, W. 1976. Effects of two benzodiazepines, phenobarbitone, and baclofen on synaptic transmission in the cat cuneate nucleus. *Naunyn Schmiedebergs Arch Pharmacol,* 294**,** 121-31.

POMPOLO, S. & HARLEY, V. R. 2001. Localisation of the SRY-related HMG box protein, SOX9, in rodent brain. *Brain Res,* 906**,** 143-8.

PONTIGGIA, A., RIMINI, R., HARLEY, V. R., GOODFELLOW, P. N., LOVELL-BADGE, R. & BIANCHI, M. E. 1994. Sex-reversing mutations affect the architecture of SRY-DNA complexes. *EMBO J,* 13**,** 6115-24.

PONTIOUS, A., KOWALCZYK, T., ENGLUND, C. & HEVNER, R. F. 2008. Role of intermediate progenitor cells in cerebral cortex development. *Dev Neurosci,* 30**,** 24-32.

PRINGLE, N. P., YU, W. P., HOWELL, M., COLVIN, J. S., ORNITZ, D. M. & RICHARDSON, W. D. 2003. Fgfr3 expression by astrocytes and their precursors: evidence that astrocytes and oligodendrocytes originate in distinct neuroepithelial domains. *Development,* 130**,** 93-102.

PRITCHETT, D. B., SONTHEIMER, H., SHIVERS, B. D., YMER, S., KETTENMANN, H., SCHOFIELD, P. R. & SEEBURG, P. H. 1989. Importance of a novel GABAA receptor subunit for benzodiazepine pharmacology. *Nature,* 338**,** 582-5.

PROBST, M. 1901. The structure of complete dissolving corpus callosum of the cerebrum and also the microgyry and heterotropy of the grey substance. *Archiv Fur Psychiatrie Nervenkrankheiten,* 34**,** 709-786.

PRUSS, H., DEWES, M., DERST, C., FERNANDEZ-KLETT, F., VEH, R. W. & PRILLER, J. 2011. Potassium channel expression in adult murine neural progenitor cells. *Neuroscience,* 180**,** 19-29.

PRUSZAK, J., LUDWIG, W., BLAK, A., ALAVIAN, K. & ISACSON, O. 2009. CD15, CD24, and CD29 define a surface biomarker code for neural lineage differentiation of stem cells. *Stem Cells,* 27**,** 2928-40.

PUIA, G., VICINI, S., SEEBURG, P. H. & COSTA, E. 1991. Influence of recombinant gamma-aminobutyric acid-A receptor subunit composition on the action of allosteric modulators of gamma-aminobutyric acid-gated Cl- currents. *Mol Pharmacol,* 39**,** 691-6.

RAAP, M., BIEDERMANN, B., BRAUN, P., MILENKOVIC, I., SKATCHKOV, S. N., BRINGMANN, A. & REICHENBACH, A. 2002. Diversity of Kir channel subunit mRNA expressed by retinal glial cells of the guinea-pig. *Neuroreport,* 13**,** 1037-40.

RAFF, M. C., MILLER, R. H. & NOBLE, M. 1983. A glial progenitor cell that develops in vitro into an astrocyte or an oligodendrocyte depending on culture medium. *Nature,* 303**,** 390-6.

RAMON Y CAJAL, S. 1881. Sur la structure de l'ecorce cerebrale de quelques mammiferes. *Cellule,* 7**,** 125-176.

REYNOLDS, B. A. & WEISS, S. 1992. Generation of neurons and astrocytes from isolated cells of the adult mammalian central nervous system. *Science,* 255**,** 1707-10.

ROSEN, L. B., GINTY, D. D., WEBER, M. J. & GREENBERG, M. E. 1994. Membrane depolarization and calcium influx stimulate MEK and MAP kinase via activation of Ras. *Neuron,* 12**,** 1207-21.

ROUZAIRE-DUBOIS, B. & DUBOIS, J. M. 1998. K+ channel block-induced mammalian neuroblastoma cell swelling: a possible mechanism to influence proliferation. *J Physiol,* 510 (Pt 1)**,** 93-102.

SAH, D. W., RAY, J. & GAGE, F. H. 1997. Regulation of voltage- and ligand-gated currents in rat hippocampal progenitor cells in vitro. *J Neurobiol,* 32**,** 95-110.

SANDBERG, M., KALLSTROM, M. & MUHR, J. 2005. Sox21 promotes the progression of vertebrate neurogenesis. *Nat Neurosci,* 8**,** 995-1001.

SANGKUHL, K., KLEIN, T. E. & ALTMAN, R. B. 2009. Selective serotonin reuptake inhibitors pathway. *Pharmacogenetics and genomics,* 19**,** 907-9.

SCHENA, M., SHALON, D., DAVIS, R. W. & BROWN, P. O. 1995. Quantitative monitoring of gene expression patterns with a complementary DNA microarray. *Science,* 270**,** 467-70.

SCOTT, C. E., WYNN, S. L., SESAY, A., CRUZ, C., CHEUNG, M., GOMEZ GAVIRO, M. V., BOOTH, S., GAO, B., CHEAH, K. S., LOVELL-BADGE, R. & BRISCOE, J. 2010. SOX9 induces and maintains neural stem cells. *Nat Neurosci,* 13**,** 1181-9.

SEKIDO, R., BAR, I., NARVAEZ, V., PENNY, G. & LOVELL-BADGE, R. 2004. SOX9 is up-regulated by the transient expression of SRY specifically in Sertoli cell precursors. *Dev Biol,* 274**,** 271-9.

SEKIDO, R. & LOVELL-BADGE, R. 2008. Sex determination involves synergistic action of SRY and SF1 on a specific Sox9 enhancer. *Nature,* 453**,** 930-4.

SERRETTI, A. & ARTIOLI, P. 2004. The pharmacogenomics of selective serotonin reuptake inhibitors. *The pharmacogenomics journal,* 4**,** 233-44.

SEYMOUR, P. A., FREUDE, K. K., TRAN, M. N., MAYES, E. E., JENSEN, J., KIST, R., SCHERER, G. & SANDER, M. 2007. SOX9 is required for maintenance of the pancreatic progenitor cell pool. *Proceedings of the National Academy of Sciences of the United States of America,* 104**,** 1865-70.

SHAO, Z., BROWNING, J. L., LEE, X., SCOTT, M. L., SHULGA-MORSKAYA, S., ALLAIRE, N., THILL, G., LEVESQUE, M., SAH, D., MCCOY, J. M., MURRAY, B., JUNG, V., PEPINSKY, R. B. & MI, S. 2005. TAJ/TROY, an orphan TNF receptor family member, binds Nogo-66 receptor 1 and regulates axonal regeneration. *Neuron,* 45**,** 353-9.

SHELP, B. J., BOWN, A. W. & MCLEAN, M. D. 1999. Metabolism and functions of gamma-aminobutyric acid. *Trends Plant Sci,* 4**,** 446-452.

SHEN, Q., WANG, Y., DIMOS, J. T., FASANO, C. A., PHOENIX, T. N., LEMISCHKA, I. R., IVANOVA, N. B., STIFANI, S., MORRISEY, E. E. & TEMPLE, S. 2006. The timing of cortical neurogenesis is encoded within lineages of individual progenitor cells. *Nat Neurosci,* 9**,** 743-51.

SHENDURE, J. & JI, H. 2008. Next-generation DNA sequencing. *Nat Biotechnol,* 26**,** 1135-45.

SHI, J., MILES, D. K., ORR, B. A., MASSA, S. M. & KERNIE, S. G. 2007. Injury-induced neurogenesis in Bax-deficient mice: evidence for regulation by voltage-gated potassium channels. *Eur J Neurosci,* 25**,** 3499-512.

SHI, Y., CHICHUNG LIE, D., TAUPIN, P., NAKASHIMA, K., RAY, J., YU, R. T., GAGE, F. H. & EVANS, R. M. 2004. Expression and function of orphan nuclear receptor TLX in adult neural stem cells. *Nature,* 427**,** 78-83.

SHIBATA, T., YAMADA, K., WATANABE, M., IKENAKA, K., WADA, K., TANAKA, K. & INOUE, Y. 1997. Glutamate transporter GLAST is expressed in the radial glia-astrocyte lineage of developing mouse spinal cord. *J Neurosci,* 17**,** 9212-9.

SHU, T., LI, Y., KELLER, A. & RICHARDS, L. J. 2003a. The glial sling is a migratory population of developing neurons. *Development,* 130**,** 2929-37.

SHU, T., PUCHE, A. C. & RICHARDS, L. J. 2003b. Development of midline glial populations at the corticoseptal boundary. *J Neurobiol,* 57**,** 81-94.

SHU, T., SUNDARESAN, V., MCCARTHY, M. M. & RICHARDS, L. J. 2003c. Slit2 guides both precrossing and postcrossing callosal axons at the midline in vivo. *J Neurosci,* 23**,** 8176-84.

SILVER, J., EDWARDS, M. A. & LEVITT, P. 1993. Immunocytochemical demonstration of early appearing astroglial structures that form boundaries and pathways along axon tracts in the fetal brain. *J Comp Neurol,* 328**,** 415-36.

SILVER, J. & OGAWA, M. Y. 1983. Postnatally induced formation of the corpus callosum in acallosal mice on glia-coated cellulose bridges. *Science,* 220**,** 1067-9.

SINGH, S. K., HAWKINS, C., CLARKE, I. D., SQUIRE, J. A., BAYANI, J., HIDE, T., HENKELMAN, R. M., CUSIMANO, M. D. & DIRKS, P. B. 2004. Identification of human brain tumour initiating cells. *Nature,* 432**,** 396-401.

SLOBODYANSKY, E., GUIDOTTI, A., WAMBEBE, C., BERKOVICH, A. & COSTA, E. 1989. Isolation and characterization of a rat brain triakontatetraneuropeptide, a posttranslational product of diazepam binding inhibitor: specific action at the Ro 5-4864 recognition site. *J Neurochem,* 53**,** 1276-84.

SMITH, K. M., OHKUBO, Y., MARAGNOLI, M. E., RASIN, M. R., SCHWARTZ, M. L., SESTAN, N. & VACCARINO, F. M. 2006. Midline radial glia translocation and corpus callosum formation require FGF signaling. *Nat Neurosci,* 9**,** 787-97.

SOMASUNDARAM, R. & SCHUPPAN, D. 1996. Type I, II, III, IV, V, and VI collagens serve as extracellular ligands for the isoforms of platelet-derived growth factor (AA, BB, and AB). *J Biol Chem,* 271**,** 26884-91.

SPOKONY, R. F., AOKI, Y., SAINT-GERMAIN, N., MAGNER-FINK, E. & SAINT-JEANNET, J. P. 2002. The transcription factor Sox9 is required for cranial neural crest development in Xenopus. *Development,* 129**,** 421-32.

STAHL, S. M. 1998. Mechanism of action of serotonin selective reuptake inhibitors. Serotonin receptors and pathways mediate therapeutic effects and side effects. *Journal of affective disorders,* 51**,** 215-35.

STENMAN, J., TORESSON, H. & CAMPBELL, K. 2003a. Identification of two distinct progenitor populations in the lateral ganglionic eminence: implications for striatal and olfactory bulb neurogenesis. *J Neurosci,* 23**,** 167-74.

STENMAN, J., YU, R. T., EVANS, R. M. & CAMPBELL, K. 2003b. Tlx and Pax6 co-operate genetically to establish the pallio-subpallial boundary in the embryonic mouse telencephalon. *Development,* 130**,** 1113-22.

STOLT, C. C., LOMMES, P., SOCK, E., CHABOISSIER, M. C., SCHEDL, A. & WEGNER, M. 2003. The Sox9 transcription factor determines glial fate choice in the developing spinal cord. *Genes Dev,* 17**,** 1677-89.

STOLT, C. C., REHBERG, S., ADER, M., LOMMES, P., RIETHMACHER, D., SCHACHNER, M., BARTSCH, U. & WEGNER, M. 2002. Terminal differentiation of myelin-forming oligodendrocytes depends on the transcription factor Sox10. *Genes Dev,* 16**,** 165-70.

STOLT, C. C., SCHLIERF, A., LOMMES, P., HILLGARTNER, S., WERNER, T., KOSIAN, T., SOCK, E., KESSARIS, N., RICHARDSON, W. D., LEFEBVRE, V. & WEGNER, M. 2006. SoxD proteins influence multiple stages of oligodendrocyte development and modulate SoxE protein function. *Dev Cell,* 11**,** 697-709.

STOLT, C. C., SCHMITT, S., LOMMES, P., SOCK, E. & WEGNER, M. 2005. Impact of transcription factor Sox8 on oligodendrocyte specification in the mouse embryonic spinal cord. *Dev Biol,* 281**,** 309-17.

SUDBECK, P., SCHMITZ, M. L., BAEUERLE, P. A. & SCHERER, G. 1996. Sex reversal by loss of the C-terminal transactivation domain of human SOX9. *Nat Genet,* 13**,** 230-2.

SUEYOSHI, T. & NEGISHI, M. 2001. Phenobarbital response elements of cytochrome P450 genes and nuclear receptors. *Annu Rev Pharmacol Toxicol,* 41**,** 123-43.

SUN, T., PRINGLE, N. P., HARDY, A. P., RICHARDSON, W. D. & SMITH, H. K. 1998. Pax6 influences the time and site of origin of glial precursors in the ventral neural tube. *Mol Cell Neurosci,* 12**,** 228-39.

SUN, Y., KONG, W., FALK, A., HU, J., ZHOU, L., POLLARD, S. & SMITH, A. 2009. CD133 (Prominin) negative human neural stem cells are clonogenic and tripotent. *PLoS One,* 4**,** e5498.

SUSSEL, L., MARIN, O., KIMURA, S. & RUBENSTEIN, J. L. 1999. Loss of Nkx2.1 homeobox gene function results in a ventral to dorsal molecular respecification within the basal telencephalon: evidence for a transformation of the pallidum into the striatum. *Development,* 126**,** 3359-70.

TAKEBAYASHI, H., NABESHIMA, Y., YOSHIDA, S., CHISAKA, O. & IKENAKA, K. 2002. The basic helix-loop-helix factor olig2 is essential for the development of motoneuron and oligodendrocyte lineages. *Curr Biol,* 12**,** 1157-63.

TAKUMI, T., ISHII, T., HORIO, Y., MORISHIGE, K., TAKAHASHI, N., YAMADA, M., YAMASHITA, T., KIYAMA, H., SOHMIYA, K., NAKANISHI, S. & ET AL. 1995. A novel ATP-dependent inward rectifier potassium channel expressed predominantly in glial cells. *J Biol Chem,* 270**,** 16339-46.

TRONCHE, F., KELLENDONK, C., KRETZ, O., GASS, P., ANLAG, K., ORBAN, P. C., BOCK, R., KLEIN, R. & SCHUTZ, G. 1999. Disruption of the glucocorticoid receptor gene in the nervous system results in reduced anxiety. *Nat Genet,* 23**,** 99-103.

TUCKER, P. K. & LUNDRIGAN, B. L. 1993. Rapid evolution of the sex determining locus in Old World mice and rats. *Nature,* 364**,** 715-7.

TUCKER, S. J., IMBRICI, P., SALVATORE, L., D'ADAMO, M. C. & PESSIA, M. 2000. pH dependence of the inwardly rectifying potassium channel, Kir5.1, and localization in renal tubular epithelia. *J Biol Chem,* 275**,** 16404-7.

UCHIDA, N., BUCK, D. W., HE, D., REITSMA, M. J., MASEK, M., PHAN, T. V., TSUKAMOTO, A. S., GAGE, F. H. & WEISSMAN, I. L. 2000. Direct isolation of human central nervous system stem cells. *Proc Natl Acad Sci U S A,* 97**,** 14720-5.

UPTON, N. & BLACKBURN, T. 1997. Pharmacology of Mammalian GABA(A) Receptors. *In:* ENNA, S. J. & BOWERY, N. G. (eds.) *The GABA Receptors.* Totowa, NJ: Humana Press Inc.

VALLSTEDT, A., KLOS, J. M. & ERICSON, J. 2005. Multiple dorsoventral origins of oligodendrocyte generation in the spinal cord and hindbrain. *Neuron,* 45**,** 55-67.

VAN DE WETERING, M., OOSTERWEGEL, M., VAN NORREN, K. & CLEVERS, H. 1993. Sox-4, an Sry-like HMG box protein, is a transcriptional activator in lymphocytes. *EMBO J,* 12**,** 3847-54.

VAN DE WETERING, M., SANCHO, E., VERWEIJ, C., DE LAU, W., OVING, I., HURLSTONE, A., VAN DER HORN, K., BATLLE, E., COUDREUSE, D., HARAMIS, A. P., TJON-PON-FONG, M., MOERER, P., VAN DEN BORN, M., SOETE, G., PALS, S., EILERS, M., MEDEMA, R. & CLEVERS, H. 2002. The beta-catenin/TCF-4 complex imposes a crypt progenitor phenotype on colorectal cancer cells. *Cell,* 111**,** 241-50.

VAUTIER, F., BELACHEW, S., CHITTAJALLU, R. & GALLO, V. 2004. Shaker-type potassium channel subunits differentially control oligodendrocyte progenitor proliferation. *Glia,* 48**,** 337-45.

VIDAL, V. P., CHABOISSIER, M. C., LUTZKENDORF, S., COTSARELIS, G., MILL, P., HUI, C. C., ORTONNE, N., ORTONNE, J. P. & SCHEDL, A. 2005. Sox9 is essential for outer root sheath differentiation and the formation of the hair stem cell compartment. *Curr Biol,* 15**,** 1340-51.

WAGNER, T., WIRTH, J., MEYER, J., ZABEL, B., HELD, M., ZIMMER, J., PASANTES, J., BRICARELLI, F. D., KEUTEL, J., HUSTERT, E., WOLF, U., TOMMERUP, N., SCHEMPP, W. & SCHERER, G. 1994. Autosomal sex reversal and campomelic dysplasia are caused by mutations in and around the SRY-related gene SOX9. *Cell,* 79**,** 1111-20.

WHITBY, D. J. & FERGUSON, M. W. 1991. Immunohistochemical localization of growth factors in fetal wound healing. *Dev Biol,* 147**,** 207-15.

WHITFIELD, L. S., LOVELL-BADGE, R. & GOODFELLOW, P. N. 1993. Rapid sequence evolution of the mammalian sex-determining gene SRY. *Nature,* 364**,** 713-5.

WICHTERLE, H., TURNBULL, D. H., NERY, S., FISHELL, G. & ALVAREZ-BUYLLA, A. 2001. In utero fate mapping reveals distinct migratory pathways and fates of neurons born in the mammalian basal forebrain. *Development,* 128**,** 3759-71.

WILSON, M. & KOOPMAN, P. 2002. Matching SOX: partner proteins and co-factors of the SOX family of transcriptional regulators. *Curr Opin Genet Dev,* 12**,** 441-6.

XIN, M., YUE, T., MA, Z., WU, F. F., GOW, A. & LU, Q. R. 2005. Myelinogenesis and axonal recognition by oligodendrocytes in brain are uncoupled in Olig1-null mice. *J Neurosci,* 25**,** 1354-65.

YASUDA, T., BARTLETT, P. F. & ADAMS, D. J. 2008. K(ir) and K(v) channels regulate electrical properties and proliferation of adult neural precursor cells. *Mol Cell Neurosci,* 37**,** 284-97.

YEH, H. J., RUIT, K. G., WANG, Y. X., PARKS, W. C., SNIDER, W. D. & DEUEL, T. F. 1991. PDGF A-chain gene is expressed by mammalian neurons during development and in maturity. *Cell,* 64**,** 209-16.

YIN, A. H., MIRAGLIA, S., ZANJANI, E. D., ALMEIDA-PORADA, G., OGAWA, M., LEARY, A. G., OLWEUS, J., KEARNEY, J. & BUCK, D. W. 1997. AC133, a novel marker for human hematopoietic stem and progenitor cells. *Blood,* 90**,** 5002-12.

YOKOYAMA, M., NAKAMURA, M., OKUBO, K., MATSUBARA, K., NISHI, Y., MATSUMOTO, T. & FUKUSHIMA, A. 1997. Isolation of a cDNA encoding a widely expressed novel zinc finger protein with the LeR and KRAB-A domains. *Biochim Biophys Acta,* 1353**,** 13-7.

YUAN, H., CORBI, N., BASILICO, C. & DAILEY, L. 1995. Developmental-specific activity of the FGF-4 enhancer requires the synergistic action of Sox2 and Oct-3. *Genes Dev,* 9**,** 2635-45.

YUASA, S. 2001. Development of astrocytes in the mouse embryonic cerebrum tracked by tenascin-C gene expression. *Arch Histol Cytol,* 64**,** 119-26.

ZHANG, C. L., ZOU, Y., YU, R. T., GAGE, F. H. & EVANS, R. M. 2006. Nuclear receptor TLX prevents retinal dystrophy and recruits the corepressor atrophin1. *Genes Dev,* 20**,** 1308-20.

ZHONG, W. & CHIA, W. 2008. Neurogenesis and asymmetric cell division. *Curr Opin Neurobiol,* 18**,** 4-11.

ZHULIDOV, P. A., BOGDANOVA, E. A., SHCHEGLOV, A. S., VAGNER, L. L., KHASPEKOV, G. L., KOZHEMYAKO, V. B., MATZ, M. V., MELESHKEVITCH, E., MOROZ, L. L., LUKYANOV, S. A. & SHAGIN, D. A. 2004. Simple cDNA normalization using kamchatka crab duplex-specific nuclease. *Nucleic Acids Res,* 32**,** e37.